

**ÉCOLE DOCTORALE DE LA VIE ET DE LA SANTÉ**

**U1118 Mécanismes centraux et périphériques de la neurodégénérescence**

**THÈSE** présentée par :

**Lavinia PALAMIUC**

soutenue le : **10 Septembre 2014**

pour obtenir le grade de : **Docteur de l'Université de Strasbourg**  
Discipline/ Spécialité : Aspect Moléculaire et Cellulaire de la Biologie  
Mention Neuroscience

**ÉTUDES DES ALTÉRATIONS MÉTABOLIQUES MUSCULAIRES AU  
COURS DE LA  
SCLÉROSE LATÉRALE AMYOTROPHIQUE : RÔLE DANS LE  
DÉVELOPPEMENT DE LA PATHOLOGIE**

**THÈSE dirigée par :**

**Mme RENÉ Frédérique**

Dr., Université de Strasbourg

**RAPPORTEURS :**

**M ANDRES Christian**

Prof., Université de Tours

**M CHARBONNIER Frédéric**

Prof., Université de Paris Descartes

---

**AUTRES MEMBRES DU JURY :**

**Mme FLORENTZ Catherine**

Prof., Université de Strasbourg

**M GENY Bernard**

Prof., Université de Strasbourg

**M WEYDT Patrick**

Dr., Université de Ulm



---

# ACKNOWLEDGEMENTS

My studentship in the lab of **CENTRAL AND PERIPHERAL MECHANISMS OF NEURODEGENERATION** shaped my development, and for that i have to thank all my colleagues from whom i learned so much over these years. I would like to express my gratitude to **Dr. Jean-Philippe LOEFFLER**, the director of the lab, who kindly welcomed me in this great team. With care and patience, he ensures a great atmosphere for doing research.

I will forever be indebted to my advisor, **Dr. Frédérique RENÉ**. It was a great pleasure to work by her side on developing this scientific project. With dedication she passed on to me invaluable skills and knowledge. I would have never achieved my goals without her excellent guidance.

I owe special thanks and appreciation to **Dr. Jose-Luis GONZALEZ DE AGUILAR**, who always had for me great advise and ideas, but also very useful criticism. I want to thank also **Dr. Luc DUPUIS** who has been for me an example of dynamism and perseverance. To **Dr. Caroline ROUAUX** and **Dr. Alexandre HENRIQUES** I am most grateful not only for their scientific input, but also for their mentorship as young scientists. In this line of great mentors i have to include **Dr. Christian GAIDON** who believed in me when i was still a novice with little experience and encouraged and helped me to pursue an academic career. **Jose, Caroline, Alex, Luc** and **Christian** gave me invaluable lessons that will help me make my first steps in the tough world of science.

I would also like to thank **Prof. Maria Teresa CARRI** who kindly welcomed me in her lab at the University of Rome for a short visit and a fruitful collaboration. For this extraordinary „roman“ experience i also have to thank **Dr. Cristiana VALLE**, a wonderful host.

As a PhD student, i could never thank enough the technical team that was there with me on the battle field. Through troubleshooting, organizing, incredibly useful tips and suggestions, our work at the bench is so much easier thanks to you **Annie, Sylvie, Michèle** and **Marie-Jo**. For the efficient logistic organization I want to thank **Brigitte**. Our lab would simply not function without her prompt assistance!

I want to thank all my colleagues, current and former members of the lab. Thanks to **Judith, Yannick, Hus, Florent, Jérôme, Thiebault** and **Vania** i quickly felt as part of the team. **Aurélia** and **Jelena**, I found in you not only respected peers but also invaluable friends. I have to thank you for all the support you showed me, especially through these last months that have been particularly difficult. **Hajer, Pauline, Laura, Christine, Gina** and **Steph**, you make our lab lively and colorful, not to mention sweet (thanks for all the cookies and cakes). I learned something from each of you and for that I am grateful and and really proud of having been your colleague!

Finally I would like to thank all the members of the jury, who took the time to read and thoroughly evaluate this work.

---

# TABLE OF CONTENTS

<b>ABBREVIATIONS</b>	<b>2</b>
<b>INTRODUCTION</b>	<b>6</b>
<b>1 AMYOTROPHIC LATERAL SCLEROSIS – A CLINICALLY AND GENETICALLY DIVERS SYNDROME</b>	<b>7</b>
1.1 Clinical diveristy	7
1.2 Genetic diversity	8
<b>2 PATHOGENESIS: SUPPOSED MECHANISMS AND KEY PLAYERS</b>	<b>14</b>
2.1 Oxidative stress	15
2.2 Protein aggregates	17
2.3 Mitochondrial pathology	20
2.4 Glutamate excitotoxicity	22
<b>3 MULTICELLULAR PATHOLOGY IN ALS</b>	<b>25</b>
3.1 Astrocytes	27
3.2 Microglia	28
3.3 Muscle	29
<b>4 MUSCLE, METABOLISM AND ALS</b>	<b>33</b>
4.1 Muscle structure and physiology	33
4.2 Metabolic regulators of muscle function and fiber type	37
4.3 Muscle metabolism in aging and disease	43
4.4 Metabolic alterations in ALS	46
<b>OBJECTIVES</b>	<b>52</b>
<b>RESULTS I</b>	<b>55</b>
<b>RESULTS II</b>	<b>58</b>
<b>RESULTS III</b>	<b>61</b>
<b>CONCLUSIONS AND PERSPECTIVES</b>	<b>64</b>
<b>SUMMARY IN FRENCH</b>	<b>69</b>
<b>BIBLIOGRAPHY</b>	<b>68</b>

---

## ABBREVIATIONS

AD	Alzheimer's disease
Akt/PKB	Akt/protein kinase B
ALS	Amyotrophic Lateral Sclerosis
AMP	Adenosine monophosphate
AMPA	$\alpha$ -amino-3-hydroxy-4-isoxazole propionic acid
AMPK	AMP-activated kinase
Atg-1	atrogen 1
ATP	Adenosine triphosphate
Bcl2	B-cell lymphoma 2
CaMK	calmodulin-dependent protein kinase
CNS	Central Nervous System
COX	cytochrome oxidase
CPT 1	Carnitine palmitoyltransferase I
CSF	cerebrospinal fluid
DRP1	dynamin related protein 1
ERR	estrogen related receptor
FA	Fatty acid
FALS	Familial Amyotrophic Lateral Sclerosis
FAT/CD36	Fatty acid transporter CD36
FG	fast glycolytic
FOG	fast oxidative glycolytic
FoxO	forkhead transcription factor, O box subfamily
FTD	frontotemporal dementia
FUS	fused in sarcoma
GLT-1/EAAT2	glutamate transporter/excitatory amino-acid transporter 2
GluR 1-4	glutamate receptors (AMPA) subunits 1-4

GLUT4	glucose transporter 4
HDAC	histone de-acetylase
HK	Hexokinase
HRE	hexanucleotide repeat expansion
Hsc	heat shock cognate
Hsp	heat shock protein
IGF1	insulin-like growth factor 1
IGFR	insulin-like growth factor receptor
iPSC	induced pluripotent stem cells
iPSCs	induced pluripotent stem cells
MEF 2	Myocyte enhancer factor 2
MND	motor neuron disease
mSOD1	mutant Cu/Zn superoxide dismutase
mtDNA	mitochondrial DNA
mTOR	mammalian target of Rapamycin
MuRF 1	Muscle RING-finger protein 1
MyHC	myosin heavy chain
MyLC	myosin light chain
NAD <sup>+</sup>	nicotinamide adenine dinucleotide oxidized
NADH	nicotinamide adenine dinucleotide reduced
NMDA	N-methyl-D-aspartate
NMJ	neuromuscular junction
NRF	nuclear respiratory factor
PDH	pyruvate dehydrogenase
PDK	pyruvate dehydrogenase kinase
PFK1	phosphofructokinase

PGC-1 $\alpha$	peroxisome proliferator-activated receptor $\gamma$ coactivator $\alpha$
PI3K	phosphoinositide 3 kinase
PKB	protein kinase B
PLS	Primary Lateral Sclerosis
PMA	Progressive Muscular Atrophy
PPAR $\alpha$ , $\gamma$ , $\beta/\delta$	peroxisome proliferator-activated receptor $\alpha$ , $\gamma$ , $\beta/\delta$
ROS	reactive oxygen species
SALS	Sporadic Amyotrophic Lateral Sclerosis
SDH	succinate dehydrogenase
Sirt	Sirtuin
SO	slow oxidative
SOD1	Cu/Zn superoxide dismutase
TDP-43	transactive response DNA-binding protein 43
UCP	uncoupling protein
WT	wild type

---

# INTRODUCTION

# 1 AMYOTROPHIC LATERAL SCLEROSIS – A CLINICALLY AND GENETICALLY DIVERS SYNDROME

Neurodegenerative disorders are devastating fatal diseases that continue to challenge the scientific community to find adapted cures, with little breakthroughs so far. This endeavor has a tremendous urgency considering the increasing incidence of these diseases within the current aging population.

## 1.1 CLINICAL DIVERISTY

In this category, motor neuron diseases (MND) reached an incidence of 2.16/100,000 people in Europe to date (Logroscino et al., 2010). This group of diseases is characterized by progressive degeneration of upper and/or lower motor neurons accompanied by muscle atrophy. Amyotrophic lateral sclerosis (ALS) is the most common adult MND and presents with degeneration of both upper and lower motor neurons. The site of onset can be either spinal, with symptoms usually appearing first in limbs (65% of all cases) or bulbar affecting first the swallowing muscles (30% of all cases). Denervation and atrophy of respiratory muscles lead to respiratory failure, which is the main cause of death (Kiernan et al., 2011). For the majority of patients age of onset is around 50 years of age and death occurs within 3-5 years from diagnosis. A better prognosis is given for those patients with only upper or lower motor neuron involvement, referred to as primary lateral sclerosis (PLS) and progressive muscular atrophy (PMA) respectively (Hardiman et al., 2011). A small percentage of ALS cases do not fall precisely within these characteristics. Cases of juvenile ALS have been reported, with time of onset before the age of 20. Juvenile ALS has a slow disease progression extending over decades (Ben Hamida et al., 1990), but some aggressive forms have also been reported (Conte et al., 2012). The clinical heterogeneity of ALS is complicated by the association with several other syndromes and

neurodegenerative disorders (Table 1), amongst which frontotemporal dementia (FTD) is the most common (Ling et al., 2013).

## 1.2 GENETIC DIVERSITY

About 10% of patients have a familial history (familial ALS or FALS), the remaining 90% being sporadic (sporadic ALS or SALS) with unknown aetiology but clinically indistinguishable from FALS. It is believed however that FALS incidence is underestimated due to flaws in patient history and reduced genetic penetrance of certain mutations. So far more than 20 genes have been implicated in or associated with ALS pathogenesis, most of them discovered within the last 5 years (Table 1). Mutations of all these genes only account for 68% of FALS and 11% of SALS patients (Renton et al., 2014) (Figure 1). These genes have different functions in the cell, which makes the identification of a common pathogenic mechanism, leading to the same disease, laborious. Moreover, the genetic variation introduces some heterogeneity in the clinical characteristics of ALS regarding time of onset, duration of disease and association with other diseases (Table 1). Some mutations can lead to slow developing ALS, juvenile ALS and ALS cases associated with other diseases (FTD, Parkinson, etc). For this reason, more and more often, ALS is defined as a “syndrome” regrouping complex and diverse pathophysiological manifestations (Hardiman et al., 2011).

The first mutated gene identified in ALS patients was the Cu/Zn superoxide dismutase 1 (SOD1) (Rosen et al., 1993), an enzyme involved in superoxide scavenging and protection from oxidative stress. This discovery enabled the development of the only animal model for ALS that we have today, which recapitulates most of the clinical and pathological aspects of the human disease including neuronal degeneration and paralysis. Many point mutations (177 according to alsod.org) of the SOD1 gene have been described since 1993, representing 12% of FALS and 1% of SALS cases

**Table 1. Main genes involved in ALS pathogenesis**

Gene	Location	Inheritance	Putative protein function	Clinical features
<b>SOD1</b>	21q22	AD	Superoxide metabolism	ALS, cerebellar ataxia
<b>ALS 2</b>	2q33	AR	Vesicle trafficking	Juvenile PLS, infantile HSP
<b>SETX</b>	9q34	AD	RNA metabolism	Juvenile ALS, ataxia, oculomotor apraxia, motor neuropathy
<b>FUS</b>	16p11	AR and AD	RNA metabolism	ALS, ALS-FTD, FTD, parkinsonism
<b>VAPB</b>	20q13	AD	Vesicle trafficking	PMA, FALS
<b>ANG</b>	14q11	AD	Angiogenesis	FALS, SALS, PBP, ALS-FTD, parkinsonism
<b>TARDBP</b>	1p36	AD	RNA metabolism	ALS, ALS-FTD, PSP, PD, FTD, Chorea
<b>FIG4</b>	6q21	AD and AR	Vesicle trafficking	FALS, CMT, cognitive impairments
<b>OPTN</b>	10p13	AR and AD	Vesicle trafficking	ALS
<b>ATXN2</b>	12q23		Endocytosis, RNA translation	SALS, ataxia
<b>VCP</b>	9p13	AD	Proteasome; vesicle trafficking	FALS, IBMPFD syndrome
<b>UBQLN2</b>	Xp11	XD	Proteasome	ALS, ALS-FTD
<b>PFN1</b>	17p13	AD	Cytoskeletal dynamics	ALS, FTD
<b>C9orf72</b>	9p21	AD	DENN protein	ALS-FTD
<b>CHMP2B</b>	3p11	AD	Vesicle trafficking	FALS, SALS, FTD
<b>DCTN1</b>	2p13	AD	Axonal transport	PMA, Perry syndrome
<b>SQSTM1</b>	5q35	AD	Ubiquitination, autophagy	ALS, Paget's bone disease

Adapted from Andersen &amp; Al-Chalabi, 2011

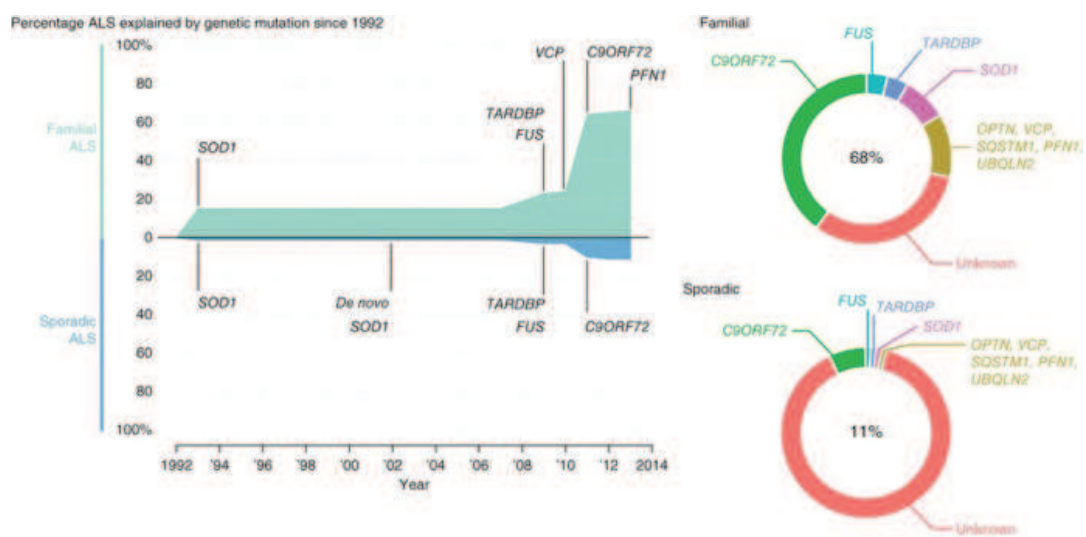


**Figure 1.1. ALS-related genes** (from Renton et al., 2014). More than 20 genes have been implicated in or associated with ALS pathogenesis, most of them discovered within the last 5 years. Mutations of all these genes only account for 68% of FALS and 11% of SALS patients. Some of the most important are represented here with the percentage of ALS patients that present with these mutations in FALS and SALS.

(Renton et al., 2014). Using the SOD1 transgenic animals several putative pathogenic mechanisms that may participate to the progressive degeneration of motor neurons have been described. Among them, oxidative stress, protein aggregates, mitochondrial defects, and glutamate excitotoxicity are the most documented. However after 20 years of research, we still do not have the one critical pathogenic mechanism for ALS. The problematic of SOD1-related pathogenesis and the controversies around it will be detailed in the next section.

In 2006, the seminal discovery that Transactive Response DNA-binding protein (TDP-43) is the major component of the ubiquitinated protein inclusions in degenerating motor neurons opened a new path towards understanding ALS pathogenic mechanisms (Neumann et al., 2006). TDP-43 is part of a family of RNA binding proteins, involved in RNA splicing and transport (Buratti et al., 2001; Wang et al., 2004). Subsequently, TDP-43 mutations have also been described, but only in 4% of FALS cases and approximately 1% of SALS (Renton et al., 2014). TDP-43 binds to a myriad of mRNA targets and for this reason the pathogenicity of its mutation is little understood. Recent evidence seems to indicate that mutation of TDP 43 impairs its function of anterograde transport of essential mRNA species from soma to distal neuronal compartments, including the nerve terminals at the neuromuscular junction (NMJ) (Alami et al., 2014). Alterations of RNA metabolism are now thought to be a key player in ALS pathogenesis, as well as other neurodegenerative diseases. In support of this new paradigm, mutations of other genes involved in RNA processing have been identified in ALS patients. Fused in sarcoma (*Fus*) mutations are localized in the gene's RNA-binding region and represent 4% of FALS and 1% of SALS (Renton et al., 2014). Hexanucleotide repeat expansion (HRE) in C9ORF72 gene represents today the majority of patients, with incidence in 40% of FALS and 7% of SALS cases. Interestingly, all of these mutations are common feature for both ALS and FTD, one of the most common syndromes associated with ALS.

Developing new models for these newly identified mutations has been a difficult challenge. Some TDP-43 rodent lines were described so far. Transgenic lines expressing human mutant TDP-43 showed an extremely short life span (between 14 and 49 days), motor neuron degeneration and astrogliosis associated with a severe motor phenotype and weight loss (Stallings et al., 2010). These pathological characteristics underline the specificity of TDP-43 toxicity for the motor system and are congruent with an early-onset severe ALS. However, transgenic animals expressing human WT TDP-43 presented a similar phenotype. In view of this observation it was argued that human TDP-43, WT or mutant, is toxic in a mouse background. Nevertheless overexpressing mouse TDP-43 in cortex, hippocampus and striatum induced neuronal pathology and led to a neurological phenotype remembering FTD (Tsai et al., 2010). Equally partial ubiquitous loss of TDP-43 led to progressive loss of neurons (specifically layer V and ventral horn motor neurons), motor dysfunction, paralysis and death (Yang et al., 2014).

ALS-linked *Fus* mutants affect the ability of mutant FUS to bind RNA and cause mislocalization in the cytoplasm (Daigle et al., 2013). Such mutations in mouse models induce a so-called fusopathy characterized by motor axon degeneration, severe motor phenotype and death (Shelkovnikova et al., 2013). In a zebra fish (*Danio rerio*) model both mutant FUS and FUS knockdown induced neuromuscular junction abnormalities (Armstrong and Drapeau, 2013). But, like for TDP-43, overexpressing WT human FUS in mice induced an aggressive phenotype with degeneration of spinal cord motor neurons, denervation associated with muscle atrophy and death at 12 weeks of age (Mitchell et al., 2013).

Both loss and gain of function mechanisms have been proposed for C9ORF72. The lack of animal or cellular models expressing mutant C9ORF72 has been a serious drawback in understanding the C9ORF72 pathogenicity. The HREs pose specific technical problems due to their instability, but some advances have been made using the induced pluripotent stem cell (iPSCs) technology (Almeida et al., 2013). Recent reports clearly attest for a gain of

toxic function. Using iPSCs from ALS patients, it was shown that C9ORF72 expression is not particularly modified, and inactivating it rescues the associated phenotype in motor neurons (Sareen et al., 2013). HREs in the C9ORF72 sequence induce the formation of RNA foci, such as G-quadruplexes and RNA-DNA hybrids (Haeusler et al., 2014). This leads to abortive transcription, sequestration of specific HRE-binding proteins and nucleolar stress.

Epidemiological studies have also showed that the incidence of disease and the particularity of the mutations can differ from one geographical area to the other, from one ethnic group to the other, suggesting an important role for environmental factors (Andersen & Al-Chalabi, 2011; Sabatelli et al., 2013). One of the most cited environmental risk factor is physical activity. An active sports-oriented life style has been associated with ALS patients (Scarmeas et al., 2002) and increased incidence amongst professional athletes has also been reported (Chiò et al., 2005). Other factors include diet (Nelson et al., 2000; Okamoto et al., 2007) and toxic substances (e.g. heavy metals, pesticides).

This genetic, clinical and epidemiological diversity of ALS undoubtedly hampered all efforts to find therapeutic targets and design efficient therapeutic approaches. Moreover, the insidious pathology and the limited diagnostic tools lead to a late diagnosis, when therapeutic interventions may no longer be effective. Therefore future lines of research have to concentrate on finding early diagnostic markers on one hand. On the other hand, a big challenge is the development of new animal models that will reflect this genetic diversity and therefore contribute to a better understanding of the complex pathogenicity in ALS.

## 2 PATHOGENESIS: SUPPOSED MECHANISMS AND KEY PLAYERS

Several mechanisms are suspected to intervene in the pathogenesis of ALS. A multitude of pathologic alterations have been described and they appear intricately linked at different levels, making it quite difficult to discern between cause and consequence. For this reason their respective participation to the pathogenesis of ALS remains little understood and for most, a matter of controversy.

Since the first mutated gene identified in ALS patients was the SOD1 gene, one of the first causes investigated was the oxidative stress related to the supposed SOD1 loss of function. However, compelling arguments quickly dismissed this possibility. An anecdotal experiment showed that human mutated SOD1 rescues SOD1 knockout *Saccharomyces cerevisiae* just as effectively as the human WT SOD1, to the point where the two strains are phenotypically undistinguishable (Rabizadeh et al., 1995). Moreover, knockout mouse models for SOD1 do not present ALS-like symptoms (Reaume et al., 1996), and the phenotype of transgenic SOD1 mice cannot be rescued with the WT SOD1. On the contrary, overexpressing human WT SOD1 aggravates disease progression in ALS animal models (Jaarsma et al., 2000). The expression of a murine mutant SOD1 that does not have dismutase activity (G86R) leads to the development of an ALS in mice, even if the endogenous SOD1 is still active (Morrison et al., 1998). Therefore the hypothesis of a toxic gain of function has been investigated and a plethora of potential mechanisms have been described.

## 2.1 OXIDATIVE STRESS

Considering oxidative stress as a causative factor of ALS was a reasonable assumption, since the main function of SOD1 is superoxide scavenging (Figure 2.1-a). Initially it was believed that a decrease in SOD1 activity facilitates the reaction between superoxide and nitric oxide producing peroxynitrite (-ONOO). Peroxynitrite was one of the first “non-physiological” substrates thought to bind to mutant SOD1 (mSOD1) (Figure 2.1-c) inducing deleterious nitration of tyrosine protein residues (Beckman et al., 1993). However, as it was mentioned earlier, it became quickly clear that things are not that simple, since several mSOD1 maintain their scavenging activity. This theory was developed and modified over the years, revealing mechanisms that are a lot more complex than the original simplistic idea of “just” oxidative stress (Beckman et al., 2001; Cleveland & Rothstein, 2001).

The discovery that some mutations induce a looser folding of SOD1 protein (Deng et al., 1993) led to the hypothesis that this is the basis of the SOD1 toxicity. The improper folding of mSOD1 affects the binding specificity for the metal ions essential for its activity ( $\text{Cu}^{2+}$  and  $\text{Zn}^{2+}$ ), the misfolded mutant SOD1 showing low copper-to-zinc ratios (Goto et al., 2000). Copper ions seem to facilitate the toxic activity of mSOD1 augmenting the catalytic oxidation of substrates by peroxide  $\text{H}_2\text{O}_2$  (Fig. 2.1-b) and copper-chelators efficiently inhibit apoptosis in neurons expressing mSOD1 (Wiedau-Pazos et al., 1996). In the same time,  $\text{Zn}^{2+}$  ion deficiency is toxic selectively to motor neurons increasing tyrosine nitration (Crow et al., 1997). In favor of the low metal binding capacity, when replete with both  $\text{Cu}^{2+}$  and  $\text{Zn}^{2+}$  mSOD1 protects neurons even in the absence of trophic factors and does not induce apoptosis (Estévez et al., 1999). Estévez and colleagues showed that Zn-deficient SOD facilitates the production of peroxynitrite through the intermediary of nitric oxide (Figure 2.1-d).

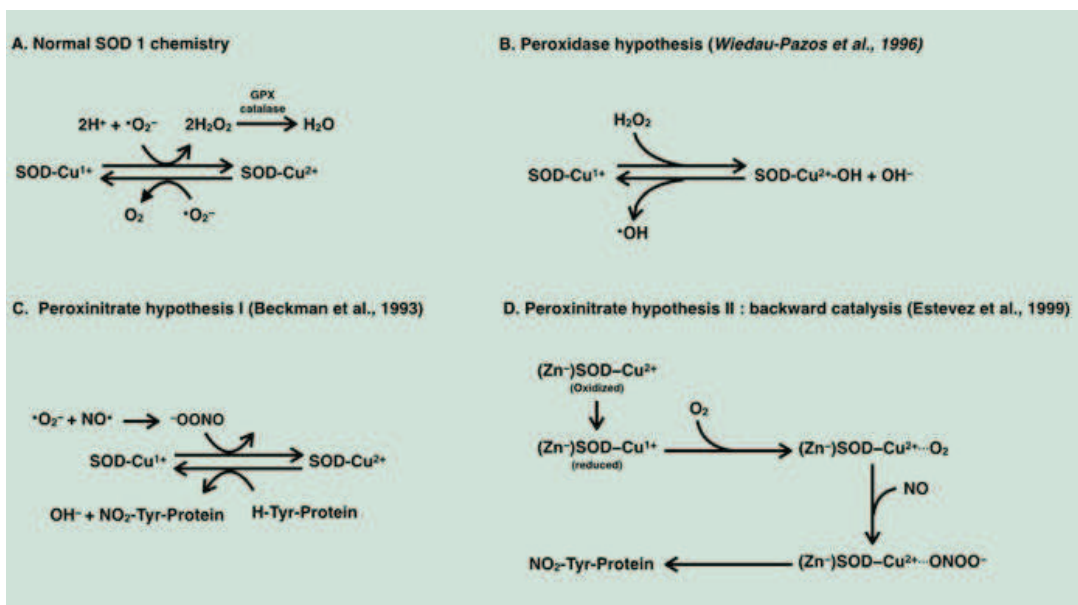


**Figure 2.1. Chemistry of mSOD1 toxicity** (adapted from Cleveland and Rothstein, 2001). A. SOD1 enzymatic function is that of scavenging superoxide free radicals, by dismutating  $\text{O}_2^-$  to  $\text{O}_2$  and peroxide. B-D. Point mutations of SOD1 gene, associated with ALS, change the chemistry of SOD1, conferring new toxic properties. Several chemical mechanisms of SOD1 toxicity have been proposed that arise from use of aberrant substrates, having as a result an increased in oxidative stress, rather than ROS scavenging.

All these proposed mechanisms revolve around the accumulation of peroxynitrite (Bruijn et al., 1997), which is strong oxidant compound that induces apoptosis in neuronal cells. However, deletion of nitric oxide synthase (NOS), aimed at reducing the levels of nitric oxide necessary for peroxynitrite production, has no effects *in vivo*, suggesting that these might not be the main toxic mechanism of mSOD1 (Facchinetti et al., 1999). Moreover, clinical attempts to reduce oxidative stress have been largely discouraging so far (Orrell et al., 2007).

## 2.2 PROTEIN AGGREGATES

The accumulation of toxic protein aggregates is a common feature for neurodegenerative diseases (AD, HD) and it has been showed that these aggregates are involved in neuronal apoptosis. But whether they are cause or consequence of disease, or even a protective mechanism, remains to be confirmed. This is also the case in ALS.

Protein aggregates positive for mSOD1 have been described in patients with SALS and FALS (Shibata et al., 1996) and animal models (Bruijn et al., 1998; Shibata et al., 1998; Watanabe et al., 2001). These aggregates have been described in motor neurons as well as astrocytes. As Bruijn and colleagues pointed out, the accumulation of SOD1-positive aggregates coincide with disease onset in mice. The authors argued that the aggregates might more easily explain the toxic function of misfolded SOD1, since overexpression of human WT SOD1 does not rescue neuronal death. If it were to be any of the oxidant mechanism described before, the WT would compete with the mutant and reduce erroneous oxidative reactions and the concentration of toxic products, which was not the case. However it has been pointed out that since aggregates do not appear before muscle weakness, it may not be a triggering factor, but on the contrary, that it could be an attempt

to protect the cell from toxic damage issued from the enzymatic activity of misfolded SOD1 (Brown et al., 1998).

Regardless of this debate, SOD1 aggregates entangle within proteins essential for cell function and protein control (Figure 2.2). For instance, several proteins involved in protein quality control and degradation have been showed to interact with mSOD1 from transgenic mice: proteasome, ubiquitin, Hsc70 (Watanabe et al., 2001) or Hsp 105 (Yamashita et al., 2007). Equally, SOD1 may interact with other members of the heat shock protein family Hsp70 and Hsp40 (Shinder et al., 2001) as it was shown in neuronal cell cultures expressing mSOD1. While most of the Hsp family members that are upregulated in transgenic animal models, some are downregulated. For instance, Hsp70 or Hsp105 (Yamashita et al., 2007) seem to have a protective role, preventing formation of aggregates and increasing cell viability when overexpressed in neuronal cell cultures expressing mSOD1.

SOD1 aggregates also contribute directly/physically to neuronal apoptosis. In fact the WT SOD1 has anti-apoptotic properties while mSOD1 promotes apoptosis, by binding incorrectly to the anti-apoptotic protein Bcl2 and forming aggregates in spinal cord mitochondria from G93A transgenic mice (Pasinelli et al., 2004). Therefore it seems that by sequestering the anti-apoptotic protein Bcl2, mSOD1 promotes apoptosis in motor neurons. In support of this, it is known that overexpressing the protective Bcl2 in transgenic animal considerably extends life span delaying neuronal degeneration (Kostic et al., 1997).

More than 20 years of accumulating evidence suggest that misfolded SOD1 has toxic functions that lead to the same course of disease every time. Independent of the position of the mutation, the result is invariably the same: destabilization of the tertiary structure of SOD1. This is reinforced by the fact that even non-genetic alterations of WT SOD1 leading to protein misfolding (oxidation, metal depletion) give toxic properties similar to those of mSOD1 that are selectively detrimental to motor neurons (Kabashi et al., 2007;

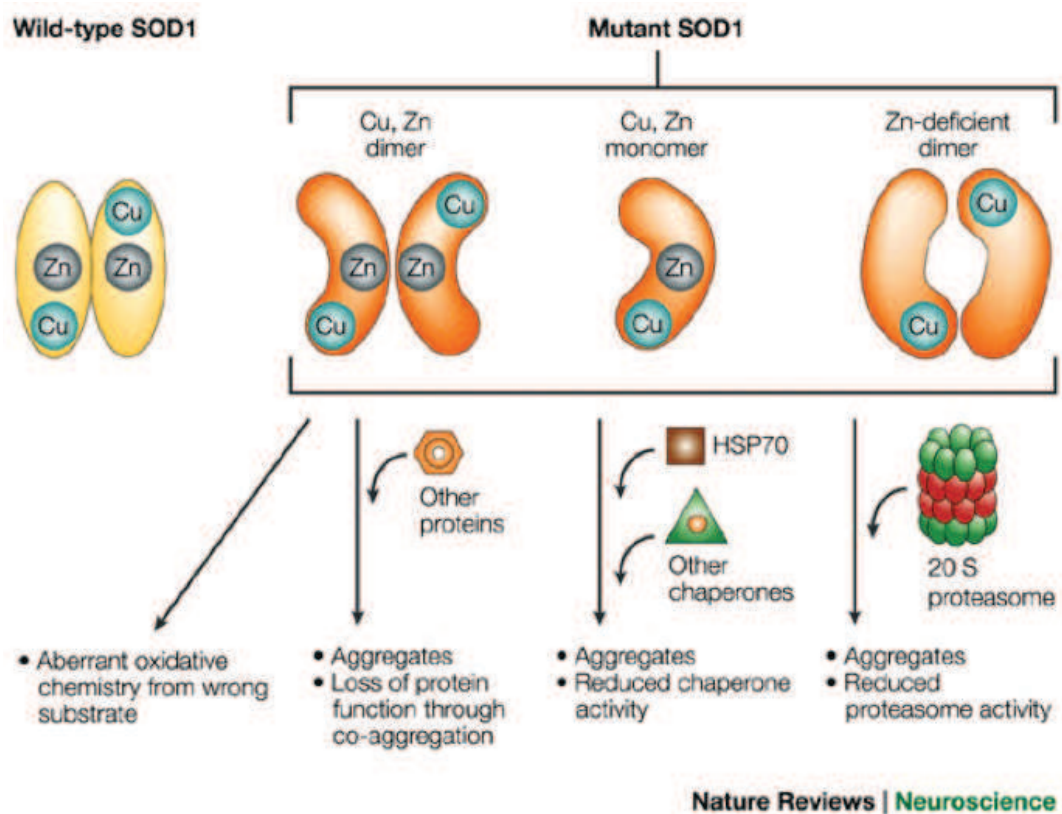


**Figure 2.2. Mechanisms of misfolded SOD1 toxicity** (from Cleveland and Rothstein, 2001). SOD1 point mutations associated with ALS alter the structural conformation of mSOD1. The loosely folded mSOD1 is prone to form aggregates, that entangle within several essential enzymes of the protein degradation pathway.

Rotunno & Bosco, 2013). Despite all efforts however, we have not yet been able to identify a clear toxic mechanism that is common to all mutant variants of SOD1 and that could trigger key pathogenic events in FALS and explain disease etiology.

## 2.3 MITOCHONDRIAL PATHOLOGY

Several pathological modifications in mitochondria from ALS patients have been described: ultrastructural changes like vacuolization and fragmentation, but also  $\text{Ca}^{2+}$  handling, and axonal transport (Cozzolino and Carri, 2012). Transferring mitochondrial DNA (mtDNA) from patients into mtDNA-depleted neuroblastoma cell line was enough to recapitulate ALS mitochondrial pathology (Swerdlow et al., 1998). Mitochondrial alterations are also very well documented in various ALS mouse models (Bendotti et al., 2001; Kong et al., 1998; Wong et al., 1995).

The ultrastructural changes (vacuolization and fragmentation) described, are related to alterations of mitochondrial fusion-fission dynamics, processes essential for mitochondrial renewal. An initial increase in both fusion and fission proteins is replaced by a decreased expression of fusion proteins in the pre-symptomatic stage of mSOD1 mice (Liu et al., 2013). The co-expression mSOD1 with a dominant negative of dynamin related protein 1 (DRP1), one of the fission proteins, prevented mitochondrial fragmentation and neuronal apoptosis *in vitro* (Song et al., 2013). The same effect was observed when co-expressing mSOD1 with mitochondrial metabolic regulators, Sirtuin 3 and Peroxisome Proliferator Activated Receptor  $\gamma$  Coactivator 1 $\alpha$  (PGC-1 $\alpha$ ).

The ultrastructural modifications are accompanied by alterations in mitochondrial function. Altered function of the respiratory electron chain, reduced ATP production together and increased ROS generation have been

described in patients and mouse models. Decreased activity of complex IV of the respiratory electron chain has been described in ventral horn motor neurons (Fujita et al., 1996) and muscle (Echaniz-Laguna et al., 2006; Echaniz-Laguna et al., 2002; Vielhaber, 2000) of SALS patients. Overexpression of mSOD1 in cultured motor neuron-like cells (NSC34) lead to decreased activity of complexes II and IV, and increased sensitivity to inhibition of glycolysis (Menziés, 2002). Detailed analysis of isolated mitochondrial from spinal cord of an ALS rat model revealed increased resting oxygen consumption correlating with increased ROS production, while state 3 respiration (oxidative phosphorylation) was significantly impaired (Panov et al., 2011).

$\text{Ca}^{2+}$  is essential signaling molecule for mitochondrial function, coupling ATP demand with synthesis (Jouaville et al., 1999). Dysfunction in mitochondrial  $\text{Ca}^{2+}$  handling was proposed to increase intracellular  $\text{Ca}^{2+}$  levels and to induce depolarization of mitochondrial membrane (Kawamata and Manfredi, 2010). Depolarized mitochondria are found at the level of neuromuscular junction, in nerve terminals (Nguyen et al., 2009) and in muscle fibers (Zhou et al., 2010). In mSOD1 mice increasing mitochondrial  $\text{Ca}^{2+}$  buffering capacity improved the ATP synthesis and preserved mitochondrial function in spinal cord. Moreover, this was accompanied by a decrease of astrogliosis, and significant reduction of motor neuron death (Parone et al., 2013). However, the improvement of mitochondrial  $\text{Ca}^{2+}$  buffering capacity did not prevent axonal degeneration and denervation, thus eliminated SOD1-mediated loss of  $\text{Ca}^{2+}$  buffering capacity as a primary contributor to ALS pathogenesis in these animal models.

The connection between mSOD1 and mitochondrial pathology are still under investigation, but it seems to be related to the localization, at least to some extent, of mSOD1 into the mitochondria (Carrì and Cozzolino, 2011). Increasing mSOD1 solubility in mitochondria, but not in cytoplasm, prevented mitochondrial fragmentation and neuronal apoptosis *in vitro*. Zinc seems to play an important role in mSOD1 mitochondrial toxicity. Expression of a zinc-

deficient SOD1 in *Drosophila melanogaster* induces vacuolization associated with inefficient ATP production and alterations in motor behavior (Bahadorani et al., 2013).

## 2.4 GLUTAMATE EXCITOTOXICITY

Glutamate is the major excitatory neurotransmitter in the CNS, with approximately 80-90% of synapses in the brain being glutamatergic. The post-synaptic cells are equipped with three main classes of ionotropic glutamate receptors (NMDA, AMPA and kainate receptors) and three main classes of metabotropic glutamate receptors (I, II and III). In the 70's, a series of experiments revealed that glutamate could act as a potent neurotoxin inducing neurodegeneration (Hassel and Dingledine, 2012). Since then, glutamate excitotoxicity has been associated with many pathological conditions like epilepsy, ischemic brain injury and several neurodegenerative disorders including ALS. The first report evidencing glutamate excitotoxicity in ALS, described an increase of 100 to 200% of glutamate and aspartate in the cerebrospinal fluid (CSF) of 18 ALS patients (Rothstein et al., 1990). This explained the potent toxic effect that the CSF from patients has on healthy neuronal cell cultures (Couratier et al., 1993).

This neurotoxic action of glutamate on neurons was explained by the deleterious effect that calcium ions exert when in high concentration. The glutamate excitotoxicity theory posits that under certain circumstances, glutamate is found in excess in the synaptic cleft leading to an over-stimulation of the glutamate receptors on the post-synaptic membrane. Specifically, AMPA and NMDA receptors, when over-stimulated, facilitate large quantities of Ca<sup>2+</sup> ions to enter into the cytoplasm.

The glutamate excitotoxicity was a particularly exciting theory for ALS and a promising therapeutic target for several reasons. Firstly, it is known that

motor neurons have low calcium buffering capacity. This makes them particularly vulnerable to calcium-mediated glutamate toxicity. Secondly, motor neurons express mainly glutamate receptors that are highly permeable to  $\text{Ca}^{2+}$ . Indeed, motor neurons are particularly vulnerable to AMPA-induced calcium toxicity. The experiments conducted by Couratier and colleagues in the early 90's clearly showed that AMPA but not NMDA antagonists could block the toxic effect of CSF from ALS patients on cultured motor neurons (Couratier et al., 1993). AMPA receptors are composed of 4 subunits (GluR1-4), out of which the GluR2, impermeable to  $\text{Ca}^{2+}$  ions and the most frequent in other neuronal populations in the CNS, is little expressed in human motor neurons (Kawahara et al., 2003; Williams et al., 1997). Mice lacking the GluR2 AMPA subunit do not present with motor neuron disease (Jia et al., 1996), however deleting the GluR2 subunit in a mouse line expressing the mutated G93A SOD1 accelerated the progression of the disease (Van Damme et al., 2005). Taken all together, these data indicate that glutamate excitotoxicity is a selective pathologic mechanism for motor neuron degeneration.

But what could explain the excess of glutamate present in the synaptic cleft in ALS? The fate of glutamate is under the control of astrocytes responsible for its clearance through glutamate transporters, critical for maintaining low concentrations of glutamate in the synaptic cleft. The absence of glutamate transporters, specifically Glut1/EAAT2 and GLAST leads to neurodegeneration and progressive paralysis (Rothstein et al., 1996). ALS patients present a dramatic loss of GLT-1/EAAT2 transporters compared to healthy patients, a decrease visible in both motor cortex and spinal cord (Rothstein et al., 1995). However, the overexpression of EAAT2 in transgenic SOD1 mice revealed a delay in motor neuron death but did not delay disease onset nor did it increase the life span of transgenic animals (Guo et al., 2003). Moreover, *Riluzole*, the only therapeutic molecule used as treatment for ALS, has been a major disappointment. *Riluzole* targets glutamate excitotoxicity and has been used with some success in transgenic models (Gurney et al., 1996; Gurney et al., 1998) but its administration extends patient life span for

about three months (Miller et al., 2012). While this approach did not give the expected results, it brought attention on one essential aspect: the involvement of astrocytes in pathological events in ALS.

As it is outlined in this section multiple mechanisms have been associated with SOD1 mutations but so far a clear-cut pathogenic mechanism is missing. Although it is evident that all these alterations, from oxidative stress to glutamate excitotoxicity are detrimental for neurons, some with a degree of selectivity for motor neurons, they do not stand out as causative factors, at least not by themselves. Blocking either one of them did not stop ALS in transgenic mice. For this reason the therapeutic approaches had extremely limited results. Understanding the chemistry of mSOD1 will probably be a big step in our understanding of mSOD1 related pathologic mechanisms and bring us closer to an efficient therapeutic approach.

### 3 MULTICELLULAR PATHOLOGY IN ALS

As it was originally defined, “ALS is solely a disease of motor neurons”, and for the last two decades scientists tried to understand why the disease is so selective for this neuronal population. Several theories have been postulated, as it was described in the previous section. Interestingly, some of the molecular and ultrastructural mSOD1-related modifications described above, were also found in cells other than motor neurons, like astrocytes and microglia. Moreover independent studies overexpressing different variants of mSOD1 specifically in motor neurons have demonstrated that motor neurons are not the sole participants to the pathogenesis and progression of ALS. Two initial studies showed that expression of mSOD1 in motor neurons does not induce motor neuron death, or an ALS-like pathology (Lino et al., 2002; Pramatarova et al., 2001). However, a subsequent study that used a different promoter reported a late onset ALS, with motor neuron degeneration and aggregates associate with muscular atrophy (Jaarsma et al., 2008). This late onset of disease in animal expressing mSOD1 specifically in motor neurons indicated that other cellular population might accelerate disease onset and/or progression, supporting the theory of non-cell autonomous mechanisms involved in ALS.

Nevertheless, the question of selectivity did not become obsolete, just more complicated. As Boillée et al. defined it, ALS is a disease of motor neurons and their non-neuronal neighbors (Boillée et al., 2006a). Different cellular populations surround the motor neuron and each of them has distinct roles in maintaining its integrity, like astrocytes and microglia. Astrocytes have an important metabolic function, supplying the substrate (lactate) for neuronal energy production. They form complex networks around neurons aimed at coupling the blood flow with the local energetic demands (Allaman et al., 2011). Microglia are the macrophages of the CNS and they play a major role in neurodegenerative diseases. They eliminate pathogens, dead and dying neurons, but also neuronal processes and live neurons that show sign of

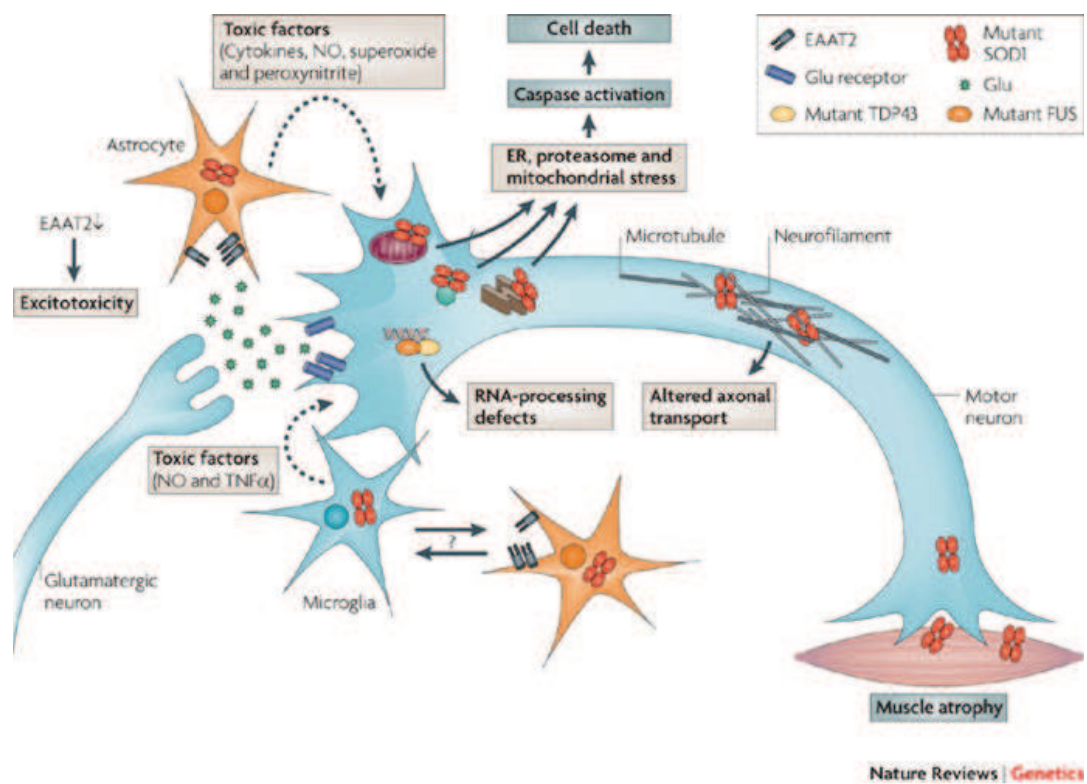


**Figure 3.1. Cell autonomous and non-cell autonomous pathogenic mechanisms in ALS** (from Dion et al., 2009). The mSOD1 pathology in ALS is the best characterized so far. Several cellular types present with mSOD1 aggregates: motor neurons, astrocytes, microglia and muscle. The mSOD1-related pathology in each of these cells contribute to motor neuron degeneration and disease progression.

stress (Brown et al., 2014). At the same time, muscle, so far considered as a simple victim of denervation, emerges as a target of mSOD1 toxicity (Dobrowolny et al., 2008). Muscle tissue pathology in ALS and its relevance for disease progression is probably the least understood so far. In order to design new efficient therapies for ALS we have to understand the participation of each of these cell types to the progressive deterioration and subsequent selective death of motor neurons (Figure 3.1).

### 3.1 ASTROCYTES

The astrocyte net is extremely important in maintaining extracellular and intracellular energy homeostasis in neurons. It controls pH and ion buffering, supplies metabolic substrates and clears waste products such as excess glutamate (Bélanger and Magistretti, 2009). It is noticeable that in spinal cord, astrogliosis is one of the hallmarks of ALS in patients and mouse models. As mentioned previously, in ALS, astrocytes came into the spotlight mainly due to their crucial role in protecting neurons from glutamate excitotoxicity through the astrocyte-specific glutamate transporter EAAT2. The expression of mSOD1 exclusively in this cell type proved to be detrimental to astrocytes, inducing hypertrophy and astrogliosis but did not induce motor neuron loss nor muscle atrophy (Gong et al., 2000). While not excluding a role for astroglia in ALS, the logical conclusion was that they do not initiate the disease. Reducing mutant SOD1 expression specifically in astrocytes did not affect disease onset, but significantly slowed disease progression and microglial activation (Yamanaka et al., 2008).

A series of elegant *in vitro* studies showed that astrocytes carrying SOD1 mutations induce apoptosis exclusively in motor neurons (when compared to other neuronal and non-neuronal lines) through soluble toxic factors (Cassina et al., 2005; Marchetto et al., 2008; Nagai et al., 2007). In these studies, the apoptotic mechanism seemed to be independent of

glutamate excitotoxicity, but rather dependent on the production of nitric oxide. Importantly, astrocyte toxicity seems to be a conserved mechanism in ALS, independent of the gene mutation involved. Astrocytes derived from patients with both FALS and SALS without SOD1 mutations had the same selective apoptotic effect on motor neurons (Haidet-Phillips et al., 2011). Interestingly, deleting WT SOD1 from these astrocytes prevented the neuronal death in this experimental setting.

In line of this evidence it became clear that astrocytes play an important part in neuronal degeneration. This role goes beyond glutamate excitotoxicity as other factors seem to be the crucial mediators of astrocyte-dependent neuronal damage.

## 3.2 MICROGLIA

Microglia are the macrophages of the nervous system. They become activated following neuronal injury, secreting several toxic molecules like reactive oxygen, nitrogen species and cytokines that are damaging for the surrounding cells. Inflammation accompanies neuronal injury in several degenerative diseases. It has also been described in ALS patients in affected areas (motor cortex, brainstem, corticospinal tract and spinal cord) (Kawamata et al., 1992). In animal models inflammation correlates with disease progression (Alexianu et al., 2001).

Several molecules that inhibit microglial activation were shown to have a beneficial effect on disease progression in animal models. Best results were obtained with the antibiotic and anti-inflammatory minocycline that delayed disease onset and extended survival by approximately 16% (Van Den Bosch et al., 2002; Zhu et al., 2002). The beneficial effect of minocycline seems to be mediated by the inhibition of *cytochrome c* release from the mitochondria, a potent activator of caspases 3 and 9. In order to completely isolate the role of microglia in the progression of the disease a transgenic mouse, expressing a

removable mSOD1, was created (Boillée et al., 2006b). By diminishing mSOD1 expression specifically in microglia disease onset was not significantly delayed. However, the mean survival was extended by more than 30%, suggesting that microglia are not pathogenic but they considerably modulate disease progression. It is important to note that in the experiments performed by Boillée and colleagues the activation of microglia and astrocytes was not reduced nor delayed, suggesting that factors other than inflammation-related molecules may be involved.

### 3.3 MUSCLE

The observation that the first event in disease progression is the retraction of nerve terminals and loss of neuromuscular synapses (Frey et al., 2000; Pun et al., 2006; Vinsant et al., 2013) turned the attention towards the distal end of the motor axis (Figure 3.2). From this perspective, ALS was proposed to be a distal axonopathy, with the dismantlement of the neuromuscular junction as a premier pathologic event, preceding denervation and any sign of motor neuron death (Fischer et al., 2004). Several series of experiments followed in support of this hypothesis attesting the fact that the neuronal cellular body is a late event and that rescuing the neuronal body is not enough to salvage the NMJ and prevent muscular atrophy (Gould et al., 2006; Rouaux et al., 2007).

These observations encouraged investigations of muscle pathology in ALS. The role of muscle tissue in disease pathogenesis and/or progression is probably the most debated. Muscle is considered a simple bystander merely reflecting the effects of denervation. For this reason mSOD1 pathology in muscle cells has not been extensively explored. Several mitochondrial defects have been described in muscles from patients (Echaniz-Laguna et al., 2006; Echaniz-Laguna et al., 2002) and animal models (Luo et al., 2013; Zhou et al., 2010). In animal models this defects consisting in reduced mitochondrial



dynamics, fragmentation and membrane depolarization that appear before disease onset. Moreover, targeting mSOD1 specifically to muscle mitochondria in healthy animals, induces the same type of mitochondrial defects (Luo et al., 2013). This suggests that these alterations are more likely related to mSOD1 toxicity than to the retraction of nerve endings. Equally, increased ROS production in non-symptomatic muscle of SOD1 mice has been shown to induce the over-expression of Ras-related associated with diabetes (*Rad*), a potent inhibitor of voltage-dependent calcium channels. *Rad* up-regulation correlates with disease severity in patients diagnosed with sporadic ALS (Halter et al., 2010). As it was mentioned earlier, protein quality control is altered due to SOD1 aggregates. While inclusions are not visible in muscle tissue, a robust activation of the protein quality control system and induction of autophagic response was evidenced in muscle from SOD1 mouse model. The activation was more important than in motor neurons (Crippa et al., 2013). This can be explained by differences in SOD1 chemistry according to cellular environment. In the muscle cell line C2C12 mSOD1 remains soluble without forming aggregates that affect the proteasome function. That allows a better clearance of misfolded mSOD1 than in the motor neuron cell line NSC34 (Onesto et al., 2011).

By applying the same strategy used to underpin the role of astrocytes and microglia, muscle came into the spotlight as a premiere target of SOD 1 toxicity. Two independent studies have showed that restricted expression of mSOD1 induces muscle atrophy and oxidative stress (Dobrowolny et al., 2008; Wong and Martin, 2010). The expression of mSOD1 specifically in muscle tissue recapitulates many aspects of the disease, including motor neuron death and glial activation (Wong and Martin, 2010).

Several lines of evidence suggest that muscle can play an active role in motor neuron degeneration. For instance the neurite outgrowth inhibitor *Nogo-A* was found to be upregulated in muscle tissue of patients and in pre-symptomatic SOD1 mouse model, in strong correlation with disease severity. For this reason *Nogo-A* was proposed to participate to the destabilization of

the NMJ and retraction of nerve terminals. The ablation of Nogo A in muscle of SOD1 mouse model extends survival by 10%, while overexpression in WT mice induces atrophy and denervation (Jokic et al., 2006). Altered muscle metabolism is another potential mechanism of muscle-induced denervation. Inducing a hypermetabolism in muscle by uncoupling mitochondrial respiration is enough to affect NMJ stability and function and to induce distal degeneration of motor neurons (Dupuis et al., 2009). Since mitochondrial defects come out as the most evident SOD1-related muscle defect in ALS, protection of mitochondria was another potential target. However, it has been shown that by rescuing muscle mitochondria through the upregulation of PGC-1 $\alpha$  atrophy is prevented but is not enough to prevent neuronal death in an ALS mouse model (Da Cruz et al., 2012).

The evidence available so far indicates an early muscle pathology that parallels the neuronal pathology. It is noticeable that targeting muscle opens therapeutic possibilities aimed at preventing muscle denervation and atrophy. It seems however that the mechanisms involved in mSOD1-related muscle pathology are different from those in neurons, since the chemical behavior of mSOD1 is different in the two cell types. Further characterization of muscle pathology in ALS is imperatively needed. Equally the cause-consequence relationship remains a matter of controversy. The experiments presented here proposed several potential pathways of muscle-nerve signaling that could participate to the destabilization of the NMJ. However, the extent to which muscle tissue may participate to disease progression and the potential mechanisms involved are less clear, the scientific literature remaining poor and inconclusive.

## 4 MUSCLE, METABOLISM AND ALS

Skeletal muscle is perfectly shaped to fulfill its function of transforming chemical energy into mechanic energy and movement. In order to do so continuous amounts of energy are needed, therefore it is not surprising that the muscular system consumes 30% of the overall body energetic supply at rest (Zurlo et al., 1990). In the same time, muscle fibers adapt perfectly to variations in energetic demands and nutrient supply just by tuning their metabolism. For instance, during periods of nutrient scarcity, muscle metabolism is tuned down in order to preserve energy for essential life supporting processes. Due to its intrinsic plasticity, muscle ultrastructure and metabolic profile are shaped by changes in activity, aging and disease. From this perspective muscle is a metabolic organ of high importance for whole body energy homeostasis.

### 4.1 MUSCLE STRUCTURE AND PHYSIOLOGY

From standing to running, from writing to boxing, skeletal muscles are designed to produce a diversity of movements with different energetic demands. Muscle fibers have the capacity of instantly providing high amounts of ATP for intense/acute activities, but also continuously providing ATP for longer periods of enduring physical activities. This is possible due to the structural and metabolic diversity of muscle fibers (Schiaffino and Reggiani, 2011).

Every muscle fiber is comprised of a multitude of protein complexes called myofibrils that are strings of smaller units called sarcomeres. The main sarcomeric proteins are the thick myosin filaments interposed by thin, shorter, actin filaments. The actin filaments slide during contraction over the thick filaments, toward the center of the sarcomere shortening the length of the

myofibrils and generating muscle contraction (Huxley, 1957). The number of aligned sarcomeres per area unit gives the force of one muscle.

The hexameric thick filament is a molecular motor. A thick filament consists of two myosin heavy chains of 220 kd (MyHCs), two myosin light chains of 20kd (MyLC<sub>20</sub>) and two myosin light chains of 17kd (MyLC<sub>17</sub>). The myosin heavy chain has an enzymatic function that consists in transforming the chemical energy stored in ATP molecules into mechanical energy through ATP hydrolysis. The mechanical function of myosin relies on conformational changes and binding of actin filaments through so-called cross-bridges or myosin heads. In fact a contraction is given by cyclic tightening and loosening of actin binding onto the myosin chain and this interaction requires ATP hydrolysis (Rayment et al., 1993). The MyLC<sub>17</sub> is involved in maintaining the structural stability of the cross-bridges, while the MyLC<sub>20</sub> has a regulatory function that is not well understood.

Muscle fibers are heterogeneous, and that is visible to the naked eye. The different muscle types can be distinguished by their color. The fact that muscle can be categorized into white and red is a known fact since the 19<sup>th</sup> century (Schiaffino and Reggiani, 2011). Advances in histochemical methods allowed the classification of muscle fibers using their enzymatic activity profile. The red slow-twitch muscles are rich in oxidative enzymes such as succinate dehydrogenase (SDH) and cyclooxygenase (COX), as opposed to white fast-twitch muscles that depend on glycolysis for fast ATP production (Burke et al., 1971; Edström and Kugelberg, 1968). Histochemical determination of enzymatic activities of such proteins is today a well-accepted method for fiber type characterization (SDH, COX or ATP-ases). Moreover, differences in size and mitochondrial content have equally been thoroughly characterized. The SDH positive fibers are generally smaller and have higher mitochondrial content than the bigger SDH-negative fibers (Schiaffino et al., 1970).

Today this classification has become more complex with the discovery of different myosin heavy chain (MyHC) isoforms that give the specificity of muscle fiber type. There are four main types of MHC isoforms: I, IIa, IIx and

Iib. The type I corresponds to slow oxidative fibers (SO or IA fibers), IIa and IIx for fast oxidative glycolytic (FOG or IIA and IIX fibers) and Iib for purely glycolytic fibers (FG or IIB fibers). A minority of fibers is hybrid, expressing more than one MyHC isoform. The ATP-ase activity differs between the different MyHC isoforms and that is reflected in the contractile properties of muscles. The rate of ATP hydrolysis is slower in type I fibers but the energetic cost of contraction is also lower (Bottinelli et al., 1994). That is why type I fibers are more suited for long duration but moderate activity. The glycolytic fibers are recruited for high intensity efforts but they fatigue quicker than the oxidative fibers because the capacity of providing enough energy at a sufficient rate is limited. That is due in part to the depletion glycogen stores, which are the main source of glucose during high intensity exercise. In the same time glycolytic metabolism induces acidosis through the accumulation of lactic acid, which seems to negatively affect the activity of several key enzymes involved in glycolytic ATP production (Sahlin et al., 1998).

From this rough characterization of muscle fiber types, it is obvious that between the MyHC isoforms present in one fiber, resistance to fatigue and fiber metabolism there is a strict correlation. This specialization is extended at the level of the entire motor unit, including the nerve terminals and the neuromuscular junction (Deschenes et al., 1994). Motor units are therefore classified according to their physiological properties in fast-fatiguable (corresponding to FG fibers), fast fatigue resistant (corresponding to FOG fibers) and slow fatigue resistant (corresponding to SO fibers) (Burke et al., 1971; Dum and Kennedy, 1980).

The neuromuscular junction is the synapse between a motor neuron and the muscle. One motor neuron branches and innervates a group of muscle fibers of the same type constituting a motor unit. The main neurotransmitter is acetylcholine, and specialized acetylcholine receptors (AChRs) coupled to ion channels are present on the sarcolemma of muscle fibers. At the synaptic level the muscle forms junctional folds, in order to enlarge the surface of the sarcolemma and enrich the expression of AChRs and voltage gated  $\text{Na}^{2+}$

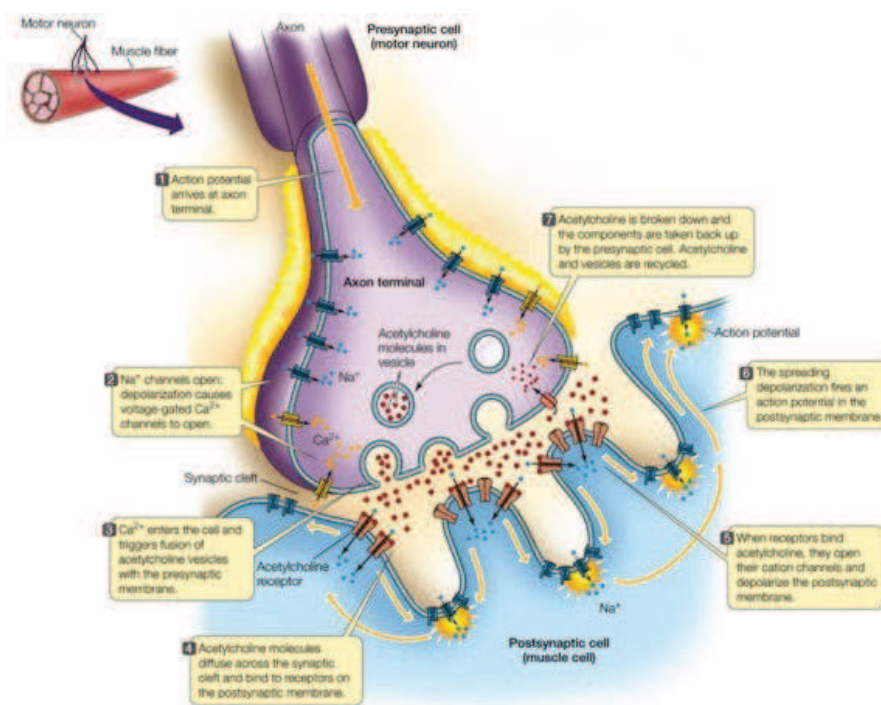


**Figure 4.1. Structure of neuromuscular junction** (from Sadava, 2010). The neuromuscular junction is the synapse between a motor neuron and the muscle. The sarcolemma of the muscle fibers present invagination named junctional folds, that increase the surface of interaction. The main neurotransmitter is acetylcholine, and specialized acetylcholine receptors (AChRs) coupled to ion channels are present on the sarcolemma of muscle fibers. Voltage gated  $\text{Na}^{+}$  channels present in the junctional folds help spreading the action potential along the postsynaptic membrane.

channels (Figure 4.1). Between the different types of fibers variations in the surface of the NMJ area but also density of AChRs (Sterz et al., 1983; Waerhaug and Lømo, 1994) and ion conductance (Milton et al., 1992) have been described. The NMJs of fast-twitch muscle necessitate a higher depolarization than the slow-twitch. This is accomplished through a higher degree of folding and higher density of AChRs and voltage gated  $\text{Na}^{2+}$  channels is higher (Hughes et al., 2006). Motor neurons innervating the different fiber types also present variations. Neurons innervating fast-twitch muscles are thicker and with bigger cell bodies and a complex dendritic ramification, which correlates with a higher conductance velocity (Henneman et al., 1965; Mendell, 2005).

## 4.2 METABOLIC REGULATORS OF MUSCLE FUNCTION AND FIBER TYPE

Physical exercise has been used as a tool in order to understand the dynamics between glucose and fat metabolism during exercise and the long-term effects of training on muscle metabolism. It was firstly observed that changes in intensity and duration of exercise employ differently the energy source for ATP production and mobilization of energy stores (Figure 4.2). During high intensity exercise less than half of energy comes from lipid breakdown. Carbohydrate metabolism prevails and inhibits fatty acids transport into the mitochondria (Holloszy et al., 1998; Wolfe, 1998). Lipolysis in the white adipose tissue and fatty acid uptake in muscle decrease with increased exercise intensity, while fatty acid oxidation is maximal during moderate prolonged exercise, and lower during low and high intensity exercise (Romijn et al., 1993).

During contraction changes in energetic homeostasis act as a signal in order to activate important pathways involved in preserving energy stores and ensuring substrate availability. Exercise increases translocation of

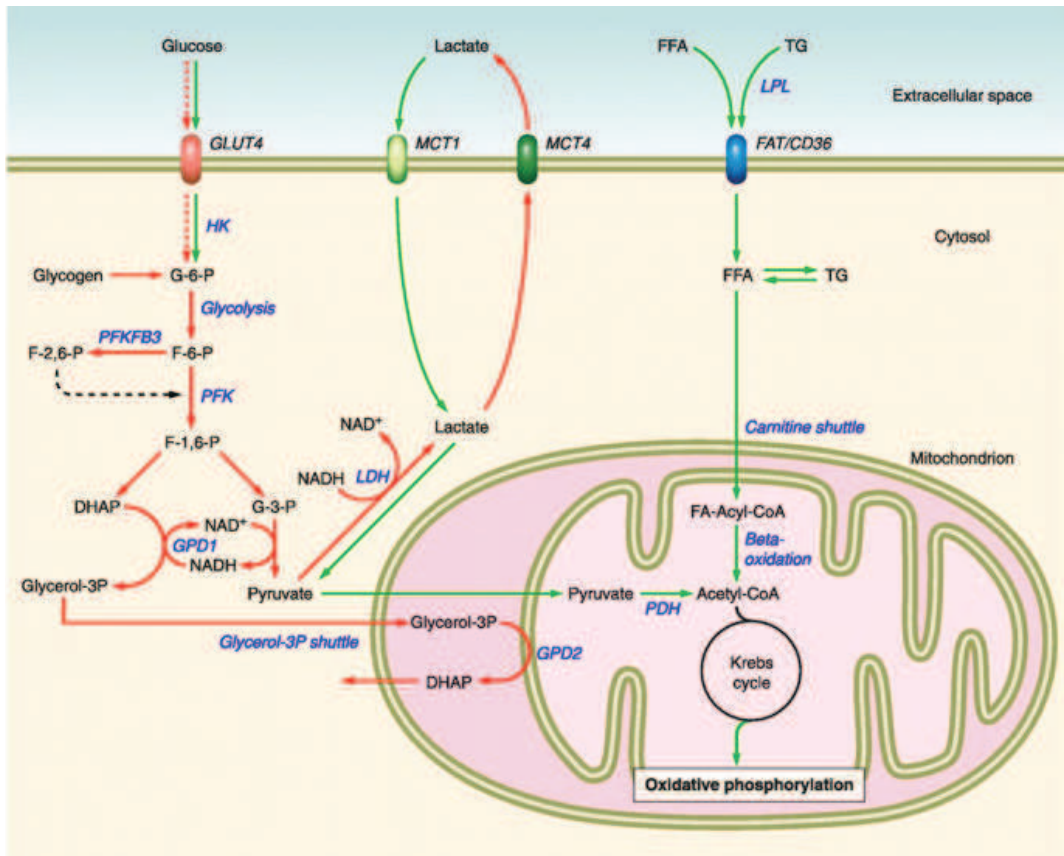


**Figure 4.2. Metabolic profile of the different types of muscle fibers** (from Schiaffino & Reggiani, 2011). According to intensity and duration of exercise, muscle fibers employ different energy sources for ATP production and mobilization of energy stores. Muscle fiber types are specialized in order to respond to different energetic demands. Fast glycolytic and fast oxidative glycolytic muscle fibers depend on glucose metabolism (in red) to produce ATP. Slow oxidative muscle fibers depend on lipid oxidation to produce the energy necessary for muscle contraction. Abbreviations: GLUT4-glucose transporter4; HK-hexokinase; G-6-P-glucose 6 phosphate; F-6-P-fructose 6 phosphate; F-2,6 (1,6)-P-fructose 2,6 (1,6) biphosphate; PFK-phosphofructokinase; DHAP-dihydroxyacetone phosphat; G-3-P-glyceraldehyde 3 phosphate; MCT (1,4)-monocarboxylate transport protein (1,4); LDH-lactate dehydrogenase; FFA-free fatty acid; TG-triglyceride; LPL-lipoprotein lipase; FAT/CD36-fatty acid transporter CD36; PDH-pyruvate dehydrogenase; GPD2-glycerol-3-phosphate dehydrogenase 2

sarcoplasmic glucose transporter GLUT4, fatty acids (FAs) transporter FAT/CD36 and induces substrate uptake and utilization. Several key metabolic regulators participate in concert to modulate these processes and ensure efficient energy production.

Contraction induces the opening of calcium pumps on the membrane of the sarcoplasmic reticulum and the release of calcium into the cytoplasm (Smith et al., 2013). Calcium signaling plays a central role in regulating muscle metabolism during contraction by activating calmodulin-dependent protein kinase (CaMK) in an intensity dependent manner (Egan et al., 2010). CaMK regulates muscle plasticity and activates mitochondrial biogenesis (Wu et al., 2002). It also upregulates glucose transport by enhancing GLUT4 exocytosis (Li et al., 2014) and lipid uptake and oxidation (Raney and Turcotte, 2008).

Increased ATP turnover (increased AMP/ATP ratio) activates AMP-activated protein kinase (AMPK). AMPK acts as a gatekeeper for metabolic equilibrium. During energy-deprived states, such as physical exercise, it switches off anabolic energy-consuming pathways and enhance substrate breakdown. Specifically, the primary role of AMPK during exercise is to reduce protein synthesis. Also it phosphorylates and inhibits glycogen synthase activity preventing glucose to be diverted to glycogen stores. Pharmacological up-regulation of AMPK with AICAR has also been shown to increase glucose uptake (Merrill et al., 1997) and lipid uptake and oxidation at rest (Raney et al., 2005). However its role in glucose and lipid utilization during exercise is not well understood (Jørgensen et al., 2006). It has been shown that FAT/CD36 and lipid uptake is not dependent on AMPK activity during contraction (Jeppesen et al., 2011). More likely it acts as a facilitator, by releasing inhibition exerted over lipid uptake pathway at rest (Catoire et al., 2014). Knock down of muscle AMPK *in vitro* reduces GLUT4 translocation in response to Ca<sup>2+</sup> entry following nervous stimulation (Li et al., 2014). However *in vivo* inactivation of this enzyme only partially reduced contraction-stimulated glucose uptake (Mu et al., 2001). Another important role of AMPK is the

activation of several other metabolic regulators essential for muscle activity and plasticity like PGC-1 $\alpha$ , class II histone deacetylases (class II HDACs) and class III histone deacetylases (sirtuins).

Physical activity modulates muscle fiber function, inducing changes in fiber-type specific contractile proteins, changes in enzymatic activity and mitochondrial content (Egan and Zierath, 2013). Training has long lasting effects on muscle function, reducing its capacity to use glucose for ATP production and increasing its respiratory capacity (Spina et al., 1996). This is reflected by an increased mitochondrial biogenesis (Hood et al., 1994) and increased activities of mitochondrial enzymes like citrate synthase, cytochrome c oxidase (Gollnick and Saltin, 1982; Murakami et al., 1994).

The most important intrinsic regulator of muscle function is Peroxisome Proliferator Activated Receptor  $\gamma$  Coactivator 1 $\alpha$  (PGC-1 $\alpha$ ). Initially PGC-1 $\alpha$  was characterized as a key element of adaptive thermogenesis, an important component of energy homeostasis. Upon exposure to cold PGC-1 $\alpha$  was found to up-regulate key genes encoding mitochondrial enzymes involved in respiration (ATP-synthase, cytochrome c oxidase, uncoupling protein 1) and induced mitochondrial biogenesis in brown adipose tissue (Puigserver et al., 1998). The role of PGC-1 $\alpha$  in muscle physiology was outlined later by overexpressing *Pgc-1 $\alpha$*  specifically in type II muscle fibers. The result was a potent induction of oxidative metabolic program together with a switch in fiber-specific protein content and increased fatigue resistance, white muscles becoming red (Lin et al., 2002). An essential aspect of this program of muscle fiber switch is that the induction of *Pgc-1 $\alpha$*  is activity- dependent. Physical activity was shown to induce its mRNA expression in muscle (Goto et al., 2000). Transcription and activity of *Pgc-1 $\alpha$*  is ensured by the upstream activity-sensitive elements CaMK and AMPK. The promoter region of *Pgc-1 $\alpha$*  includes myocyte enhancer 2 (MEF2) and c-AMP responsive element (CRE) binding regions. CaMK and AMPK activate MEF2 and CREB that in turn activate *Pgc-1 $\alpha$*  transcription (Egan et al., 2010). AMPK also regulates PGC-1 $\alpha$  activity through direct phosphorylation (Jäger et al., 2007). The regulation

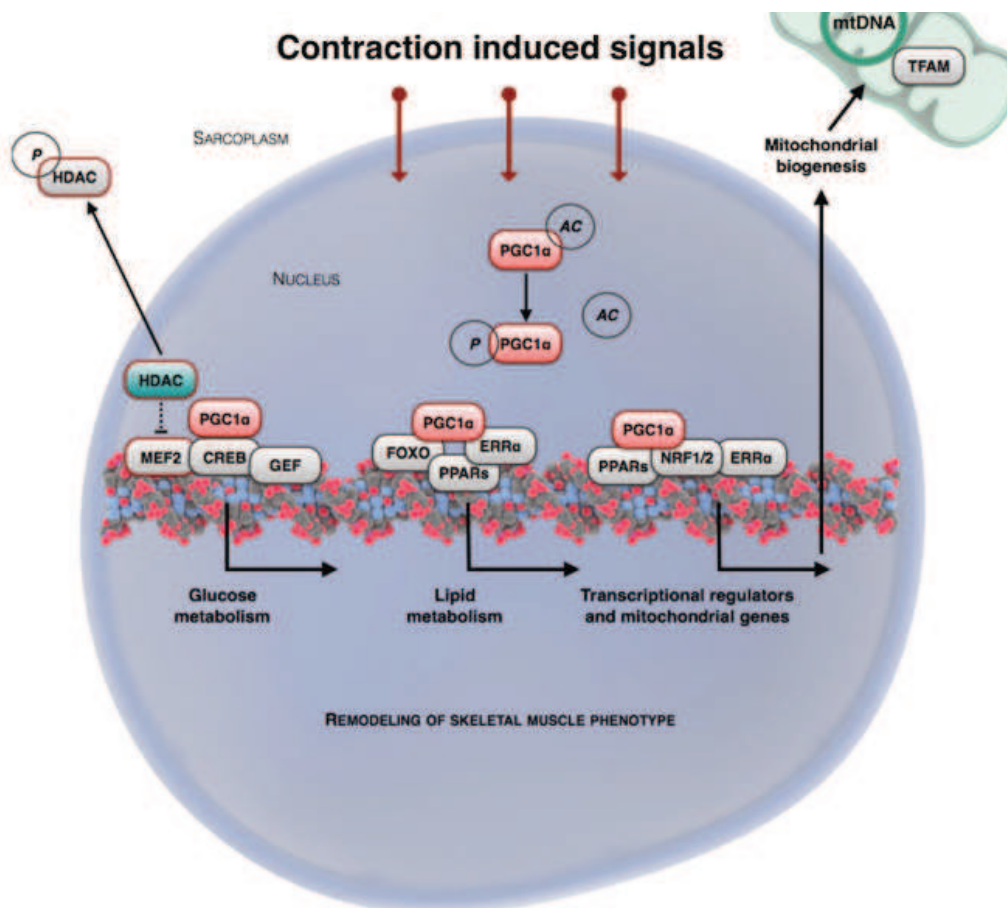


**Figure 4.3. Remodeling of skeletal muscle phenotype** (adapted from Egan & Zierath, 2013). Physical training induces metabolic and ultrastructural changes in muscle fibers, inducing a switch in muscle fiber type, from fast glycolytic to slow oxidative. This remodeling of skeletal muscle fibers is highly complex and necessitates the coordination of several pathways within the cell. The master regulator of skeletal muscle phenotype is PGC-1 $\alpha$ , that upregulates the oxidative metabolism, associated with increased mitochondrial biogenesis and respiration. Abbreviations: HDAC-hystone de-acetylase; PGC1 $\alpha$ -peroxisome proliferator-activated receptor  $\gamma$  coactivator  $\alpha$ ; MEF2-myocyte enhancer factor2; CREB-cAMP response element binding protein; GEF-Glut4 enhancer factor; FOXO-forkhead transcription factor, O box subfamily; ERR $\alpha$ -estrogen related receptor  $\alpha$ ; NRF1/2-nuclear respiratory factor 1&2; PPAR $\alpha$ -peroxisome proliferator-activated receptor  $\alpha$ ; mtDNA-mitochondrial DNA; TFAM-mitochondrial transcription factor A; P-phospho; Ac-acetyl

of muscle fiber type following training (Figure 4.3) is realized through a series of target genes for which PGC-1 $\alpha$  acts as a transcriptional factor as follows: several genes involved in mitochondrial biogenesis (nuclear respiratory factors *nrf1* and *2*, estrogen-related receptors *err*), lipid oxidation (peroxisome proliferator-activated receptors PPARs) but also genes involved in ROS scavenging (e.g. SOD) (Lin et al., 2005). Activation of ROS scavenging enzymes is of great importance because an increased mitochondrial respiration is usually accompanied by increased ROS production.

HDACs have an important regulatory role in muscle function, repressing the transcription of several genes involved in mitochondrial function and substrate utilization like PGC-1 $\alpha$ , hexokinase II (HKII), GLUT 4, carnitine palmitoyltransferase 1 (CPT1) and ATP-synthase (McGee and Hargreaves, 2011). Exercise alleviates HDACs inhibitory effect by translocating them from the nucleus into the cytoplasm (McGee et al., 2008). They have also been shown to repress MEF2, and in doing so they suppress the oxidative program and the formation of type I fibers (Potthoff et al., 2007). Some class II HDACS, like HDAC 4 and 5, are not even expressed in type I fibers (Potthoff et al., 2007), confirming their role in regulating fiber type specification. The class III HDACs, sirtuins, are another family of metabolic sensors, responding mainly to nutrient scarcity during states of energetic stress (caloric restriction, post-exercise recovery). Sirtuins are NAD<sup>+</sup> dependent deacetylases. After exercise the ratio NAD<sup>+</sup>/NADH is dramatically increased, reflecting an acute energetic stress. In this context, muscle fibers regulate their metabolism so that energetic stores are replenished. More specifically, after exercise, glucose utilization for energy production is diminished in order to replenish the glycogen reserves. Sirt1 de-acetylates and activates PGC-1 $\alpha$ , in an AMPK-dependent manner, being directly involved in increased transcription of mitochondrial genes, increased lipid usage and glucose sparing (Cantó et al., 2010).

Muscle metabolic network is highly complex, with tight connections and regulations between several metabolic sensors. This complexity ensures the

incredible capacity of muscle to rapidly adapt to changes in energy demands. However this equilibrium is fragile and anything from life style to aging and disease can compromise it, leading to muscle wasting and atrophy.

### 4.3 MUSCLE METABOLISM IN AGING AND DISEASE

Muscular disuse due to reduction in nervous and physical activity has dramatic effects on muscle function, muscle fiber type, and inevitably leads to muscular atrophy. This type of modifications can be seen in pathological conditions, such as denervation due to neurodegenerative disease or spinal cord injury, but also during aging. Equally, systemic diseases that affect whole body energetic homeostasis, like sepsis, diabetes and cancer-related cachexia are often accompanied by muscle atrophy. However, while the results are almost always the same, reduction in muscle mass and muscle weakness, the molecular modifications that the muscle is subjected to, are not similar between the different atrophy-inducing conditions.

All these pathologic conditions will affect preferentially certain fiber types more than others and are also accompanied by changes in fiber type. For instance disuse conditions such as immobilization or experimental sciatic nerve axotomy induce atrophy preferentially in type I muscle fibers and induce a switch of slow-to-fast fiber type. This situation can be seen in human pathologies like spinal cord injury and some muscular dystrophies. Other conditions like aging, diabetes or pathological conditions associated with glucocorticoids secretion (e.g. starvation and cancer cachexia), muscular atrophy is more pronounced in glycolytic type II fibers and accompanied by a fast-to-slow fiber type switch. This selectivity of the atrophic process and the differences between the different atrophic-inducing conditions are not yet understood.

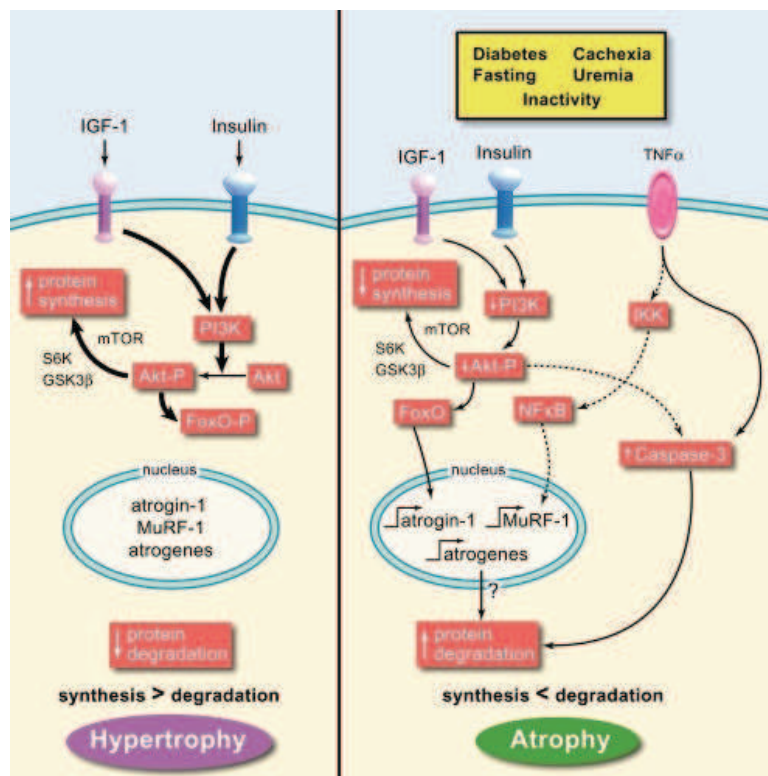


**Figure 4.4. Mechanisms regulating muscle mass** (from Rajan et al., 2007). Muscle mass depends on the balance between protein synthesis and protein degradation. Protein synthesis is mainly regulated by the activation of the Insulin-like Growth Factor 1 pathway (IGF1). In the absence of insulin signaling, two members of the ubiquitin ligase family are upregulated and induce muscle protein degradation and muscle wasting: muscle atrophy F-box/atrogen 1 and muscle RING-finger protein-1. Abbreviations: IGF-1-insulin-like growth factor 1; TNF1 $\alpha$ -tumor necrosis factor 1  $\alpha$ ; PI3K-phosphoinositide 3 kinase; Akt-protein kinase B; FoxO-forkhead transcription factor, O box subfamily; S6K-S6 kinase; GSK3 $\beta$ -glycogen synthase kinase 3  $\beta$ ; MuRF1- muscle RING finger protein-1; IKK-I kappa B kinase; P-phospho;

Muscle mass is the reflection of two antagonist processes: protein synthesis and protein degradation. Protein synthesis is mainly regulated by the activation of the Insulin-like Growth Factor 1 pathway (IGF1) (Schiaffino et al., 2013). Ablation of muscle IGF1 receptor leads to decreased number of muscle fibers and fiber area, but also to insulin resistance (Mavalli et al., 2010). Overexpression of muscle IGF1 specifically in muscle tissue induces muscle hypertrophy and prevents aging-related atrophy (Musarò et al., 2001). Activation of the IGF1 intervenes on two levels. Firstly, by stimulating Akt/Protein Kinase B (Akt/PKB) phosphorylation by Phosphoinositide 3 kinase (PI3K), it activates mammalian target of rapamycin (mTOR) and protein synthesis program (Bodine et al., 2001a; Latres et al., 2005). As Bodine and colleagues showed, overexpression of Akt can prevent muscle atrophy even after sciatic nerve axotomy through mTOR activation, highlighting the crucial role of Akt-mTOR pathway in muscle mass regulation. The second level of action of Akt is the inhibition of protein degradation pathway phosphorylation of FOXO (Figure 4.4).

Two members of the ubiquitin ligase family regulate muscle protein degradation during muscle wasting: muscle atrophy F-box/atrogin 1 (MAFbx/Atg-1) and muscle RING-finger protein-1 (MuRF1). These atrophic factors are induced in several atrophy models: denervation, immobilization, but also interleukin-1 and glucocorticoid treatments, making them the universal pathway for muscle protein degradation. Silencing MAFbx/Atg-1 and MuRF1 prevents muscle atrophy following sciatic nerve axotomy (Bodine et al., 2001b). In an *in vitro* model for muscle atrophy, IGF-1 counteracted the effect of the atrophy-inducing glucocorticoid dexamethasone, reducing the activation of both Atg-1 and MuRF1 (Sacheck et al., 2004). Equally *in vivo* local injection with IGF1 in muscles of animals treated with dexamethasone prevented muscle atrophy and upregulation of the atrophic genes (Stitt et al., 2004). Two concomitant studies revealed that the inhibitory effect of IGF1-Akt pathway on Atg-1 and MuRF1 is mediated by forkhead family of transcription factors FOXO (Sandri et al., 2004; Stitt et al., 2004). FOXO responds to

energetic and oxidative stress (Figure 4.5), conditions often associated with metabolic deregulations (e.g. starvation, diabetes and aging).

Maintenance of mitochondrial function is essential for preventing age-related muscular atrophy and AMPK-Sirt1-PGC axis is a potential protective mechanism (Johnson et al., 2013). PGC-1 $\alpha$  is a protective factor, preventing ROS accumulation and enhancing mitochondrial function (Figure. 4.5). In consequence, exercise, a potent activator of PGC-1 $\alpha$ , protects muscle and ensures a better adaptation to age-related atrophy (Mosole et al., 2014). Overexpression of PGC-1 $\alpha$  in skeletal muscle protects from sarcopenia, prevents oxidative damage and increases insulin sensitivity in aged mice (Wenz et al., 2009). PGC-1 $\alpha$  has been proposed as the basis of selectivity for type II fibers in atrophy, since it is more expressed in oxidative fibers compared to glycolytic fibers (Wang and Pessin, 2013). Exercise is essential in preventing life-style related metabolic disorders as well. For instance exercise is more effective in preventing type II diabetes than pharmacological intervention (Knowler et al., 2002). The relationship between muscle function and metabolism is two-sided: metabolic dysfunction has detrimental effects on muscle function, and muscle is a potential therapeutic target in preventing metabolic disease.

#### 4.4 METABOLIC ALTERATIONS IN ALS

As it was outlined in the previous sections, there is a tight connection between muscle function and integrity and whole body energy homeostasis. Unlike most other cell types, the adaptive response of muscle cells to increased energetic demands (e.g. exercise), depend on the interplay between lipid and glucose metabolism, external challenges leading to physiological modifications and changes in fiber type. Muscle modifications response to nutrient availability contributes to ensuring the organism's homeostasis in times of metabolic stress (e.g. high fat diet, caloric restriction).

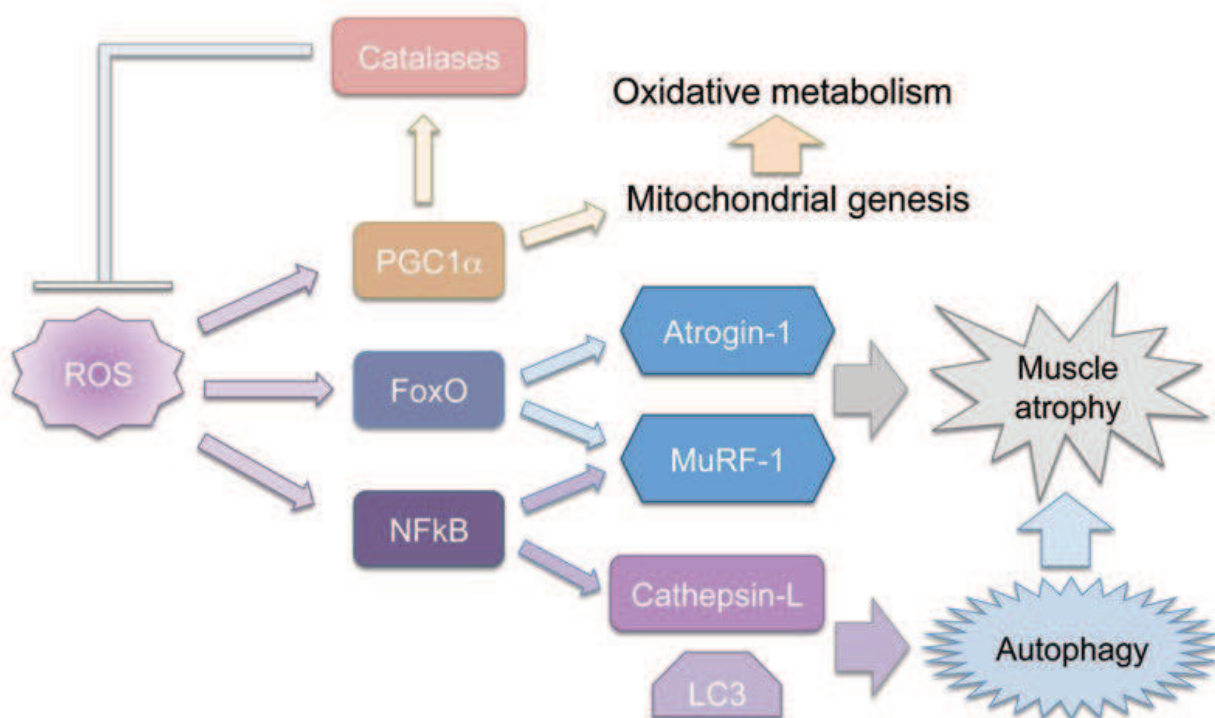


**Figure 4.5. ROS regulation of muscular atrophy** (from Vinciguerra, 2010). Increased ROS production is a hallmark of aging. ROS production was proposed to activate atrophy programs through activation of Foxo and NFkB. This in turn activate ubiquitin/proteasome and autophagy catabolic pathways. PGC-1a offers protection against atrophy by reducing ROS production. Abbreviations: ROS-reactive oxygen species; PGC1a-peroxisome proliferator-activated receptor  $\gamma$  coactivator  $\alpha$ ; FoxO-forkhead transcription factor, O box subfamily; MuRF1-muscle RING finger protein-1; LC3-Microtubule-associated protein 1A/1B-light chain 3;

However prolonged alterations of the energetic balance can have detrimental effects on muscle function and can induce muscular atrophy (e.g. diabetes, starvation).

ALS patients present with several metabolic alterations, reflecting profound impairments of the energetic balance (Dupuis et al., 2011). Alterations of the carbohydrate metabolism have long been associated with ALS, reflected in glucose intolerance and insulin resistance in patients diagnosed with ALS (Reyes et al., 1984; Pradat et al., 2010). Decreased weight and body mass index (BMI) have often been reported. The range of patients presenting with low BMI vary between 15% (Desport et al., 1999) and 55% (Mazzini et al., 1995), and constitute a negative prognostic factor for survival (Desport et al., 1999). Some of the causes that have been associated with this state of malnourishment in patients are swallowing difficulties, problems related to salivary secretion and inability to swallow saliva, constipation and physiological distress leading to anorexia (Desport et al., 2001). Low respiratory quotient ( $RQ=0.81\pm 0.03$ ), measured by indirect calorimetry ( $CO_2$  produced/ $O_2$  consumed), and decrease in body fat has also been reported (Kasarskis et al., 1996). A recent study, that used MRI technique for analyzing body fat distribution, characterized an altered fat distribution, with increase in visceral and decreased subcutaneous fat pads. The subcutaneous fat deposition positively correlate with disease progression, and is consistent with previous reports of glucose intolerance and increased circulating fatty acids (Lindauer et al., 2013). Taken all together, these data indicate a hypermetabolic state in ALS patients, where energy consumption exceeds energy intake. Hypermetabolism is now well documented in ALS patients, and the increase in resting energy expenditure negatively correlates with survival (Bouteloup et al., 2009; Desport et al., 2001).

Metabolic alterations have also been documented in ALS mouse models. Transgenic animals expressing mSOD1 are leaner, with decreased fat stores, increased corticosterone levels (the main glucocorticoid in rodents) and increased oxygen consumption ( $RQ<1$ ). More importantly, in animals these

alterations occur early, before disease onset (Dupuis et al., 2004). Taken altogether these data suggest increased lipid consumption and supplementing the lipid reserves with a high fat diet increases life span in ALS mice models. On the contrary, caloric restriction shortens life span, and exacerbates ROS production (Patel et al., 2010). Stress, which leads to increased corticosterone secretion, is another factor that was shown to accelerate disease onset and progression (Fidler et al., 2011). Moreover, the basal levels of corticosterone positively correlate with paralysis onset. The metabolic alterations in animal models appear as an early event with pathological significance, correlating with/aggravating disease progression.

As muscle is highly connected to the overall body metabolism, these early metabolic alterations are expected to have a major impact on muscle physiology. Changes in muscle fiber type have been described in patients and animal models. Overexpression of mSOD1 specifically in muscle triggers a switch from fast glycolytic to slow oxidative and activation of protein degradation pathways (Dobrowolny et al., 2008). Muscle has also been proposed as a contributor to the hypermetabolic profile, as the site of high substrate (glucose and lipid) uptake (Dupuis et al., 2004). Moreover, increased expression of the protein UCP3 was described in animal models and patients (Dupuis et al., 2003). UCP3 is a muscular isoform of the UCP family, mitochondrial proteins that separate oxidative phosphorylation from ATP production dissipating energy as heat. UCP3 responds to increase FFAs and has been proposed to have a role in fatty acid oxidation (Nabben and Hoeks, 2008). It was shown recently that UCP3 mild overexpression in skeletal muscle acts as an exercise mimetic, increasing fatty acid oxidation and increasing energy expenditure (Aguer et al., 2013). On the other hand mitochondrial uncoupling can have detrimental effects on neuromuscular junction stability. For example, it was shown that by overexpressing the brown adipose tissue isoform UCP1 specifically in muscle induces muscle hypermetabolism and age-dependent neuromuscular junction pathology and even late onset neuronal pathology (Dupuis et al., 2009).

Surprisingly, exercise, that is normally benefic for metabolism and muscle function, is considered as a risk factor in ALS. Several studies reported increased incidence of ALS/MND among professional athletes (Chiò et al., 2005) or people with an active life style (Scarmeas et al., 2002). A recent study reported a similar tendency towards an active life style but without a dose-dependent effect (Huisman et al., 2013). Therefore it was proposed that exercise itself does not constitute a risk factor, but more likely a genetic predisposition to physical fitness is associated with ALS (Turner, 2013). This association remains controversial, and several studies reported no association between physical activity, professional or leisure (Longstreth et al., 1998; Valenti et al., 2005). On the other hand, moderate aerobic exercise has been used in a few small clinical trials and improvement on the ALS functional rating scale have been reported (Dal Bello-Haas and Florence, 2013). In animal models the effect of exercise was proved to be beneficial, however choice of training protocol is crucial. Several studies reported neuroprotective effect of moderate exercise, accompanied by a delay in onset and disease progression (Deforges et al., 2009; Carreras et al., 2010). Exercise and IGF1 administration have a synergistic effect on SOD1 mouse model, extending survival, improving motor function and reducing neuronal apoptosis and motor neuron loss (Kaspar et al., 2005). High intensity endurance training had the opposite effect, hastening disease onset and shortening survival (Mahoney et al., 2004). However the detrimental effect remain somewhat controversial, as other studies using similar protocols no adverse effect of high intensity training was noted (Carreras et al., 2010).

Metabolic alterations in ALS (hypermetabolism) represent a negative prognosis factor, correlating with shorter lifespan. As proven by studies in animal models, these alterations are an early event, preceding disease onset, which indicates that it constitutes a separate pathologic event. However the origins of hypermetabolism are little understood. Several lines of evidence suggest that muscle can be a potential site of increased energy consumption.

However the relation between muscle pathology and metabolic pathology remains to be further investigated.

---

# OBJECTIVES

Muscle alterations, while yet not sufficiently described, emerge as an important aspect of ALS pathology, with potential therapeutic significance (Dobrowolny et al., 2008; Wong et al., 2010). First of all, delaying muscle atrophy could have an enormous impact on patient's quality of life. Secondly, the importance of muscle-nerve collaboration for NMJ stabilization has been indicated by several experimental approaches (Dupuis et al., 2009). For this reason therapeutic interventions targeting muscle could have a beneficial effect on NMJ, therefore delaying onset and potentially disease progression. At the same time, as previously shown in (Chapter 4.4), due to the tight relation between muscle and metabolism, it is possible to identify targets that could modulate whole body energy homeostasis and improve muscle function. Several interventions aimed at improving overall body metabolic status showed beneficial effects. For instance moderate exercise (Carreras et al., 2010) or high fat diet (Dupuis et al., 2004) increased survival and improved motor function in animal models. However, so far we do not have enough information and viable precise therapeutic targets are still lacking. The link between metabolism and ALS is still unclear. As muscle is an important metabolic tissue it is possible that understanding muscle pathology would provide some insight into this problematic.

One of the main objective of the studies presented here, was to better understand muscle pathology and its relation to the metabolic disequilibrium described in patients and animal models. In order to achieve this general goal, in the first paper we performed a detailed analysis of muscle metabolic profile. The goal was to identify potentially pathologic alterations that would appear before denervation and could account for the systemic metabolic imbalance and constitute potential therapeutic targets. In a second time, we evaluate the therapeutic potential of known metabolic regulators, histone deacetylases (HDACs) and sirtuins, by comparing their expression in both spinal cord and muscle, in two different animal models. These enzymes regulate important metabolic targets through de-acetylation and they have been previously proposed as potential targets, despite lack sufficient information. In the last part of the work presented here we sought investigating another essential

aspect of ALS-related muscle pathology, spasticity. Spasticity occurs in ALS patients from loss of inhibition from upper motor neurons. It consists of a velocity-dependent increase of muscle tone or stiffness of muscle, which might interfere with speech and movement, or be associated with discomfort or pain. Spasticity is also an aspect of ALS with great importance for managing quality of life of patients that present with such symptoms (McClelland et al., 2008). Spasticity has also received little attention so far and there are limited clinical interventions for the management of these symptoms.

**A metabolic switch towards lipid use in glycolytic muscle is an early pathologic event in a mouse model of Amyotrophic Lateral Sclerosis**

The metabolic changes characterized so far in ALS patients and animal models seem to point towards increased lipid consumption. The cause of this phenomenon and its pathological significance is still elusive. Since muscle tissue is an important metabolic organ, with an important role in whole body energy homeostasis, we hypothesized that muscle tissue could be affected by or participate to these systemic changes.

There are two important aspects that were considered in this study. In order to separate the events with a pathological significance, an early time point was considered, before apparent denervation or muscle weakness. Several techniques have been employed to thoroughly attest the absence of overt clinical manifestations at the selected time point (65 days of age). The second aspect was the choice of muscle studied. As it was shown previously in a different mouse model, glycolytic muscles seem to be the first affected during disease progression, while oxidative muscle are largely spared (Hegedus et al., 2007). This was the case in our animal model, the SOD1<sup>G86R</sup>, as well, and for this reason we chose to focus on the hind limb muscle *Tibialis anterior*, comprised mainly of glycolytic fibers.

Systemic metabolic alterations trigger metabolic inflexibility, which can reflect in a reduced physical capacity. Young SOD1<sup>G86R</sup> mice were tested for their capacity to adapt to physical exercise using two exercise paradigms: anaerobic versus aerobic capacity. Surprisingly, while their anaerobic capacity was reduced significantly, their aerobic capacity was significantly enhanced. These experiments pinpointed an early metabolic alteration in skeletal muscles, hinting towards an enhanced oxidative metabolism.

In order to understand the nature of this change in physical capacity, the main metabolic pathways, glycolytic and oxidative, were assessed. An increased expression of genes involved in lipid uptake and transport was evidenced. In the same time the glycolytic pathway was downregulated, as evidenced by the reduced enzymatic activity of PFK1, the rate limiting enzyme of the glycolytic pathway (Figure 4.2).

Untrained SOD1<sup>G86R</sup> acted as trained animals. However, the activation of the lipid pathway was not pendent of PGC-1 $\alpha$ , indicating a pathologic switch in fuel preference. Pyruvate dehydrogenase kinase 4 (*PDK4*) is known to be a primary signaling molecule during times of energetic stress (exercise/fasting/high fat diet) playing a key role in the regulation of muscle physiology and muscle fiber type in response to external stimuli (Spriet et al., 2004; Watt et al., 2004). *PDK4* accomplishes its role by regulating fuel selection through inhibition of pyruvate dehydrogenase complex (*PDC*), the enzyme responsible for coupling glycolysis to mitochondrial oxidation. While this is supposed to be a protective mechanism activated in times of nutrient scarcity aiming to preserve glucose for the central nervous system (as it is the case for exercise and fasting), under certain circumstances it becomes a non-adaptive response leading to metabolic inflexibility and reflects deeper pathological deregulations. *Pdk4*, together with the up-stream regulator PPAR $\delta$  were found upregulated in glycolytic muscles of young asymptomatic animals.

By inhibiting PDK4 activity with a pharmacological inhibitor, dichloroacetate (DCA) we sought restoring the metabolic equilibrium in glycolytic fibers. This treatment had several beneficial effects. The muscular strength was preserved until the end of the experiment, when non-treated transgenic animals already lost approximately 30% of their grip strength. Analyzing the expression of denervation markers, we also evidenced a delayed denervation of glycolytic muscle fibers. Interestingly, this was accompanied by increased expression of PGC-1 $\alpha$  and its main target genes, and a decreased expression of ROS-activated genes.

These results clearly indicate an early non-adaptive alteration of metabolic equilibrium in glycolytic muscle fibers, confirming the initial hypothesis. Targeting muscle metabolism has beneficial effects, delaying disease onset and improving muscle function.

## **A metabolic switch towards lipid use in glycolytic muscle is an early pathologic event in a mouse model of Amyotrophic Lateral Sclerosis.**

Lavinia Palamiuc<sup>1,2</sup>, Anna Schlagowski<sup>3,4</sup>, Aurelia Vernay<sup>1,2</sup>, Sylvie Grosch<sup>1,2</sup>, Anne-Laurence Boutillier<sup>5</sup>, Joffrey Zoll<sup>3,4</sup>, Shyuan T. Ngo<sup>6,7</sup>, Jean-Philippe Loeffler<sup>1,2,\*</sup>, Frédérique René<sup>1,2,\*</sup>

<sup>1</sup> INSERM, U1118, Mécanismes Centraux et Périphériques de la Neurodégénérescence, Strasbourg, France

<sup>2</sup> Université de Strasbourg, UMRS1118, Strasbourg, France.

<sup>3</sup> Equipe d'Accueil 3072, Mitochondrie, Stress oxydant et Protection Musculaire, Fédération de Médecine Translationnelle de Strasbourg, Université de Strasbourg, France.

<sup>4</sup> Service de Physiologie et d'Explorations Fonctionnelles, Pôle de Pathologie Thoracique Hôpitaux Universitaires, CHRU de Strasbourg, France.

<sup>5</sup> UMR7364 Laboratoire de Neurosciences Cognitives et Adaptatives, Université de Strasbourg-CNRS, GDR CNRS 2905, Faculté de Psychologie, Strasbourg, France.

<sup>6</sup> School of Biomedical Sciences, The University of Queensland, St Lucia, Queensland, Australia.

<sup>7</sup> University of Queensland Centre for Clinical Research, The University of Queensland, Herston, Queensland, Australia.

### **Corresponding authors:**

Frédérique René: phone (+33) 368 853 086; fax: (+33) 368 853 065

E-mail: frederique.rene@unistra.fr;

Jean-Philippe Loeffler: phone (+33) 368 853 081; fax: (+33) 368 853 065

Email: loeffler@unistra.fr

**Running title:** Early muscle metabolic changes in ALS

**Keywords:** amyotrophic lateral sclerosis, exercise, glucose, lipids, muscle

Character count (without bibliography and expended material): 65173

## ABSTRACT

Amyotrophic Lateral Sclerosis is the most common fatal motorneuron disease in adults. Numerous studies indicate that ALS is a systemic disease that affects whole body physiology and metabolic homeostasis. Using a mouse model of the disease (SOD1<sup>G86R</sup>), we investigated muscle physiology and motor behavior with respect to muscle metabolic capacity. We found that prior to denervation, SOD1<sup>G86R</sup> mice presented with improved endurance capacity associated with an early inhibition in the capacity for glycolytic muscle to use glucose as a source of energy and a switch in fuel preference towards lipids. Indeed, in glycolytic muscles we showed progressive induction of pyruvate dehydrogenase kinase 4 expression. Phosphofructokinase 1 was inhibited, and the expression of lipid handling molecules was increased. This mechanism represents a chronic pathologic alteration in muscle metabolism that is exacerbated with disease progression. Further, inhibition of pyruvate dehydrogenase kinase 4 activity with dichloroacetate delayed symptom onset while improving mitochondrial dysfunction and ameliorating muscle denervation. In this study, we provide the first molecular basis for the particular sensitivity of glycolytic muscles to ALS pathology.

## INTRODUCTION

Amyotrophic lateral sclerosis (ALS) is the most common adult motor neuron disease. Although historically defined as an age-related neurodegenerative disease specifically affecting upper and lower motor neurons, 145 years of research has now identified for ALS to be unquestionably more complex than initially described. In recent years, several non-neuronal cells including microglia (Boillée *et al*, 2006), astrocytes (Yamanaka *et al*, 2008), and skeletal muscle (Wong and Martin, 2010) have been proposed to influence the course of the disease. Moreover, mutations in an increasing number of genes have been associated with familial and sporadic forms of ALS (Chen *et al*, 2013). In accordance with this genetic heterogeneity, ALS has recently been redefined as a “syndrome”, regrouping complex and diverse pathophysiological and clinical manifestations that transgress the motor system (Andersen and Al-Chalabi, 2011; Hardiman *et al*, 2011).

Numerous studies indicate that ALS is a systemic disease that affects whole body physiology and energy homeostasis. In 2001, a systematic analysis of energy expenditure rates in a population of sporadic ALS patients revealed that two thirds of these patients were hypermetabolic (Desport *et al*, 2001). These observations were further confirmed and extended to familial ALS cases in follow-up reports (Desport *et al*, 2005; Bouteloup *et al*, 2009). ALS patients as well as mouse models of ALS present with weight loss and reduced fat mass, altered glucose and lipid handling, and increased resting energy expenditure (Dupuis *et al*, 2011). In mice, reduced lipid stores and increased resting energy expenditure precede motor symptoms (Dupuis *et al*, 2004). Interestingly, the burden of these metabolic alterations appears to affect the neurodegenerative process. Indeed, metabolic alterations correlate with duration of survival, and clinical data suggests that an imbalance in energy metabolism has a negative impact on the pathogenic process (Desport *et al*, 1999; Jawaid *et al*, 2010). Moreover, increased dietary lipid content offers neuroprotection and extends survival in mouse models of ALS (Dupuis *et al*, 2004; Mattson *et al*, 2007), while restricting calorie intake exacerbated motor symptoms in ALS mice (Pedersen and Mattson, 1999). Although the origin of metabolic dysfunction in ALS remains unclear, many of the metabolic modifications observed at the systemic level in ALS patients and related mouse models imply that skeletal muscle contributes to ALS progression.

At rest, skeletal muscle accounts for 20-30% of the total energy expenditure. Given that skeletal muscle plays a critical role in maintaining metabolic homeostasis, altered energy balance in this tissue over extended periods of time may represent a risk factor for the development of ALS. Interestingly, thorough mapping of neuromuscular junction (NMJ) denervation patterns in the SOD1<sup>G93A</sup> mouse model of ALS revealed increased susceptibility of glycolytic fibers to undergo denervation. The loss of fast fatigable

motor units composed of large motor neurons innervating type IIB fast glycolytic fibers before any apparent motor symptoms (Frey *et al*, 2000, Hegedus *et al*, 2008) suggests that the metabolic signature of glycolytic fibres may predispose them to NMJ dismantlement, one of the first pathologic events in the course of the disease (Fischer *et al*, 2004). Indeed, we have previously shown that promotion of muscle-specific hypermetabolism is sufficient to induce some hallmarks of ALS including destruction of the neuromuscular junction (NMJ) and the death of motor neurons (Dupuis *et al*, 2009). Collectively, these data suggest that metabolic changes in skeletal muscle could contribute to early destabilization of the NMJ in ALS.

In this study we investigated early muscle metabolic alterations that might account for the metabolic imbalance and early NMJ denervation observed in SOD1<sup>G86R</sup> mice. We report an early alteration in muscle metabolic homeostasis in SOD1<sup>G86R</sup> mice. The switch towards lipid use in glycolytic muscle precedes NMJ denervation detected by EMG and the increase in expression of denervation markers. By administering dichloroacetate (DCA) to SOD1<sup>G86R</sup> mice we reversed metabolic imbalance, improved metabolic function, and normalized the expression of denervation markers in SOD1<sup>G86R</sup> mice. Our results reveal an early metabolic pathology in skeletal muscle that contributes to the severity of the disease, and adds new insight into the already complex ALS syndrome.

## RESULTS

### Asymptomatic SOD1<sup>G86R</sup> mice have increased aerobic capacity

During ALS disease progression, a progressive shift in skeletal muscle fiber subtype from fast-twitch to slow-twitch would presumably result in a concomitant shift towards more oxidative metabolism (Dengler *et al*, 1990; Frey *et al*, 2000; Pun *et al*, 2006, Deforges *et al*, 2009). Thus, we aimed to determine whether SOD1<sup>G86R</sup> mice would have improved capacity to support endurance exercise. We compared anaerobic vs. aerobic capacities of 65 day old asymptomatic SOD1<sup>G86R</sup> mice using two exercise paradigms on a treadmill apparatus: an intense anaerobic exercise that recruits glycolytic fast-twitch fibers (Figure 1 A-C), and a low intensity endurance exercise that mobilizes slow-twitch oxidative muscle fibers (Figure 1 D-F). As shown in Figure 1A, when treadmill speed was progressively increased in the intense anaerobic exercise paradigm, 65 day old SOD1<sup>G86R</sup> mice had significantly poorer performance than their WT littermates; SOD1<sup>G86R</sup> mice ran on the treadmill for an average of 13.50min (median at 14.33), while their WT littermates spent an average of 15.78min (median at 15.50) on the treadmill (Figure 1B). Accordingly, SOD1<sup>G86R</sup> mice ran a total distance that was 17.6% shorter than the distance covered by their WT littermates (Figure 1C). By contrast, when challenged with a moderate exercise paradigm that is representative of an endurance workout (Figure 1D-F), SOD1<sup>G86R</sup> mice proved to have significantly greater endurance than their WT littermates (Figure 1D). In response to moderate exercise, SOD1<sup>G86R</sup> mice ran an average of 67.34min (median at 65.43) before reaching exhaustion, while their WT littermates ran an average of 46.10min (median at 59.33) prior to exhaustion (Figure 1D). Indeed, the resistance of SOD1<sup>G86R</sup> mice to reach

exhaustion when subjected to this exercise paradigm resulted in them running a total distance that was 36% greater than the distance covered by their WT littermates (Figure 1E).

Given that skeletal muscle possesses the capacity of adapt metabolically to physical and functional challenges (Constable *et al*, 1987, Bassel-Duby and Olson, 2006), the enhanced aerobic capacity and poor anaerobic capacity of SOD1<sup>G86R</sup> mice might occur as a consequence of muscle denervation. However, at 65 days of age SOD1<sup>G86R</sup> mice did not present with any sign of denervation, regardless of the metabolic capacity of muscle; grip strength muscles were comparable to that of WT littermates (Figure 2A), EMG profiles were normal (Figure 2B), and the mRNA expression of molecular markers of denervation (Figure 2C) and atrophy (Figure 2D) in glycolytic *tibialis anterior* or oxidative *soleus* muscles were similar to WT levels. By contrast, at 105 days when SOD1<sup>G86R</sup> mice are paralyzed and grip strength is decreased (Figure 2A), all SOD1<sup>G86R</sup> presented with increased spontaneous activity on their EMG profiles. Moreover, induction of denervation and atrophy markers were more pronounced in the *tibialis anterior* (TA) than in the *soleus*. These data support previous observations that in ALS, glycolytic muscles are more severely affected by disease pathology than oxidative muscles (Dengler *et al*, 1990, Frey *et al*, 2000, Pun *et al*, 2006). We therefore focused our subsequent analysis on the glycolytic TA.

## 2. Muscle glucose metabolism is inhibited in asymptomatic SOD1<sup>G86R</sup> mice

Glycolysis is the only metabolic pathway that provides a source of high-energy substrates for anaerobic exercise. Given that impaired glycolytic performance in SOD1<sup>G86R</sup> mice cannot be explained by denervation or atrophy, we hypothesized that reduced anaerobic performance was due to defective glucose utilization. In order to verify whether glucose metabolism is altered in SOD1<sup>G86R</sup> mice we first analyzed their response to glucose and insulin. The glucose tolerance test (Figure E1A) showed that at 65 days, SOD1<sup>G86R</sup> mice presented with higher blood glucose at 30 and 45min when compared to WT littermates, suggesting that initial glucose clearance is delayed in SOD1<sup>G86R</sup> mice. However, after 120min blood glucose levels were similar between WT and SOD1<sup>G86R</sup> mice, suggesting that there may be increased glucose uptake between 30 and 120 minutes in SOD1<sup>G86R</sup> mice. The response to insulin was also delayed in SOD1<sup>G86R</sup> mice when compared to WT littermates (Figure E1B). These data show an alteration in glucose handling in SOD1<sup>G86R</sup> mice at the asymptomatic stage of disease.

To determine whether altered glucose handling occurred at the level of skeletal muscle we assessed the activity of phosphofructokinase 1 (PFK1), the rate-limiting enzyme of glycolysis, in TA cytosolic homogenates. When compared to WT littermates, SOD1<sup>G86R</sup> mice had a significant 23% reduction in PFK1 enzymatic activity at 65 days of age. By the end-stage of disease (105 days of age), PFK1 activity was reduced by 88.8% in SOD1<sup>G86R</sup> mice when compared to WT littermates (Figure 3A). This was accompanied by a 5-fold down regulation in the expression of *Pfk1* mRNA in SOD1<sup>G86R</sup> mice (Figure E1C).

Glycolysis is regulated by a number of upstream and downstream components. Pyruvate is the end product of glycolysis and a downstream component in the glycolytic pathway that inhibits muscle PFK1 while glycogen synthase is a key enzyme that converts glucose to glycogen. Thus, we assessed pyruvate levels, glycogen synthase activity, and glycogen accumulation in the TA of SOD1<sup>G86R</sup> mice and WT littermates at the asymptomatic and symptomatic stages of disease. Pyruvate was 1.7 fold more concentrated in 65 days old SOD1<sup>G86R</sup> mice than in age-matched WT littermates (Figure 3B). By 105 days of age, symptomatic SOD1<sup>G86R</sup> mice had a significant reduction in pyruvate levels when compared to WT littermates. Changes in the expression of pyruvate levels in SOD1<sup>G86R</sup> mice occurred concurrently with altered activity of glycogen synthase and altered glycogen accumulation. At 65 days of age, SOD1<sup>G86R</sup> mice had decreased phosphorylation of glycogen synthase (Figure 3C) and a corresponding increase in glycogen accumulation (Figure 3D). By contrast, glycogen synthase phosphorylation in SOD1<sup>G86R</sup> mice at 105 days of age was dramatically increased, indicating the inhibition of its activity. The increased synthesis of glycogen and its subsequent accumulation was quantified in transverse sections of TA stained by periodic acid-Schiff (PAS) (Figure 3D).

### 3. Pyruvate dehydrogenase kinase 4 up-regulation in glycolytic muscle tissue is an early event

In skeletal muscle, pyruvate levels are primarily governed by pyruvate dehydrogenase complex (PDH) activity, which itself is inhibited when phosphorylated by pyruvate dehydrogenase kinase 4 (PDK4). Thus, we assessed the expression levels of *Pdk 4* mRNA by RT-qPCR. As shown in Figure 4A, at 65 days of age SOD1<sup>G86R</sup> mice had a 2.2-fold increase in *Pdk4* mRNA levels in TA when compared to WT mice (Figure 4A). At the end-stage of disease, *Pdk4* mRNA expression was 8.9-fold higher in SOD1<sup>G86R</sup> mice when compared to age-matched WT littermates. By contrast, *Pdk2* transcript levels were similar between SOD1<sup>G86R</sup> mice and WT littermates at 65 day of age, but decreased 2-fold in SOD1<sup>G86R</sup> mice at 105 days of age (Figure 4A).

PDK4 expression is stimulated by various parameters including skeletal muscle denervation, increased fatty acid (FA) use through  $\beta$ -oxidation (Jeong *et al*, 2012), and transcription factors peroxisome proliferator-activated receptors  $\beta/\delta$  (PPAR $\beta/\delta$ ) and forkhead Box O1A (FOXO1). Sciatic nerve axotomy-induced denervation in WT mice resulted in a 1.8-fold increase in *Pdk4* mRNA (Figure E2A), while in the *soleus* muscle of SOD1<sup>G86R</sup> mice, *Pdk4* expression was comparable to that of WT mice at 65 and 105 days of age (Figure E2B). These results clearly demonstrate that denervation is not the primary cause of *Pdk4* induction in TA muscle. Hence, we next conducted RT-qPCR analyses of genes involved in lipid handling. When compared to WT littermates, 65 days old SOD1<sup>G86R</sup> mice had a significant increase in the expression of genes encoding lipoprotein lipase (*Lpl*, 81.2%), Cd36 (18.7%), acylCoA synthetase (*Acsf2*, 50%), and carnitine palmitoyl-transferase 1B (*Cpt-1 $\beta$* , 70%) (Figure 4B). At the end-stage of disease, the expression of *Lpl* and *Cd36* in SOD1<sup>G86R</sup> mice was comparable to that of WT littermates, while *Acsf2* was decreased by 40% and *Cpt-1 $\beta$*  was increased by 45% (Figure 4B).

Increased expression of genes encoding an enzyme that hydrolyses triglycerides to facilitate the uptake of free fatty acids (LPL) (Mead *et al*, 2002), a membrane translocase that promotes FA entry into the cell (CD36), an enzyme that catalyses the conversion of FA to AcylCoA (ACSF2), and the rate-limiting enzyme for  $\beta$ -oxidation responsible for the FA transfer into the mitochondria (CPT-1B) (McGarry *et al*, 1983) in asymptomatic SOD1<sup>G86R</sup> mice suggests that an increase uptake of fatty acids into glycolytic muscle tissue when ALS occurs. Taken together with the increased expression of *Pdk4*, our data indicates that higher levels of  $\beta$ -oxidation exist in glycolytic muscle prior to denervation. Given that adenosine triphosphate (ATP) and reduced nicotinamide adenine dinucleotide (NADH) are two energetic substrates produced by  $\beta$ -oxidation and oxidative phosphorylation in the mitochondria that are known to stimulate PDK activity (for review see Harris *et al*, 2002), we measured the variation in these molecules in the TA of SOD1<sup>G86R</sup> mice and WT littermates at 65 and 105 days of age. We evidenced a significant increase in ATP and NADH levels (1.37- and 1.49-fold change respectively) in 65 day old SOD1<sup>G86R</sup> mice compared to WT while NAD<sup>+</sup> levels were comparable (Figure 4C). Interestingly, ATP and NADH levels were similar between SOD1<sup>G86R</sup> mice and WT littermates at 105 days of age while NAD<sup>+</sup> levels were increased 2.6-fold. Finally, mRNA levels of *Ppar $\beta/\delta$*  and *Foxo1* were increased in 65 day old SOD1<sup>G86R</sup> mice (Figure 5 A, B). Further, mRNA levels of citrate synthase, the first enzyme of the Krebs cycle, were comparable to WT at 65 days of age but significantly reduced at end-stage (Figure 5C). These data, together with the inhibition of glycolysis described in the previous section, clearly demonstrate that an early change in fuel preference from glucose toward lipids in glycolytic muscle fibers occurs before denervation in SOD1<sup>G86R</sup> mice.

#### 4. The metabolic switch in glycolytic muscle occurs independently of PGC-1 $\alpha$

The processes that promote the mobilization and use of fatty acids for ATP synthesis during moderate exercise are subjected to multiple regulatory steps. Typically, increased oxidative capacity and lipid use in muscle is accompanied by a switch in muscle fiber subtype, a phenomenon that is facilitated by Peroxisome Proliferator-Activated Receptor Gamma Co-activator 1-alpha (PGC1  $\alpha$ ), the master regulator of mitochondrial biogenesis and function (Wu *et al*, 1999; Lin *et al*, 2002). We thus analyzed the expression of PGC1  $\alpha$  in the TA of SOD1<sup>G86R</sup> mice. At 65 days of age *Pgc-1  $\alpha$*  mRNA and protein levels were similar between SOD1<sup>G86R</sup> and WT mice (Figure 5D, E) whereas they were significantly decreased at 105 days of age in SOD1<sup>G86R</sup> mice. Importantly, at the end-stage of the disease the decrease in PGC-1  $\alpha$  protein levels correlated with a decrease in the mRNA expression of the main target genes of PGC-1  $\alpha$  pathway, estrogen-related receptor  $\alpha$  (*ERR  $\alpha$* ), mitofusin 2 (*Mfn2*) and nuclear respiratory factor 1 (*Nrf1*) (Puigserver, 2005; Villena and Kralli, 2008) (Figure 5E). *ERR  $\alpha$*  mRNA expression was reduced by more than five-fold, *Mfn2* mRNA levels were decreased by two-fold and *Nrf1* were decreased by 30% in SOD1<sup>G86R</sup> mice when compared to WT animals at 105 days (Figure 5F). In addition, mitochondrial DNA quantification indicated a decreased number of mitochondria in TA of SOD1<sup>G86R</sup> mice towards the end-

stage of disease (Figure 6A). Interestingly this decrease in mitochondrial DNA was not observed in the *soleus* muscle. These data suggest that increased activation of the lipid oxidation pathways in skeletal muscle of SOD1<sup>G86R</sup> mice occurs independently of PGC1  $\alpha$ , and that this metabolic change does not have the support of the mitochondrial machinery of the cell. Presumably, this would have deleterious effects due to accumulation of  $\beta$ -oxidation by-products and ROS (Bonnard *et al*, 2008). Indeed, glutathione peroxidase 1 (*GPXI*), an important indicator of oxidative stress, was increased in the TA but not the *soleus* of SOD1<sup>G86R</sup> mice at end-stage of disease (Figure 6B).

### **5. Restoring metabolic equilibrium facilitates weight gain and delays the onset of motor symptoms and denervation in SOD1<sup>G86R</sup> mice**

In order to ascertain whether decreased glycolytic capacity in SOD1<sup>G86R</sup> mice significantly impacts weight loss (due to the mobilization of fat) and muscle function and pathology that is commonly observed in ALS (Dupuis *et al*, 2011), mice were treated with dichloroacetate (DCA), a halogenated organic acid that inhibits the activity of PDK and facilitates the entry of pyruvate into the Krebs cycle and the oxidation of glucose. By inhibiting PDK and preventing PDH phosphorylation, we aimed to force metabolism towards glucose oxidation (Abdel-aleem, 1996), thereby reversing the metabolic alterations observed in SOD1<sup>G86R</sup> mice, preventing weight loss, reducing the toxic effects of lipids on mitochondria, and delaying denervation in glycolytic muscle fibers. We administered DCA daily in drinking water from 60 days to 95 days of age. At the beginning of treatment (T<sub>0</sub>), SOD1<sup>G86R</sup> mice in both treated (DCA) and non-treated (CT) groups were significantly leaner than WT mice. Over five weeks of treatment, SOD1<sup>G86R</sup> mice that received drinking water (CT) maintained their initial weight. By contrast, SOD1<sup>G86R</sup> mice receiving DCA increased their initial weight by 10.8%, an increase that was similar to that observed in CT WT mice over the same treatment period. DCA has no effect on the weight gain of WT animals (Figure E3A, B).

Daily administration of DCA was able to reverse the changes in *Pdk4*, *Ppar $\beta/\delta$*  and *Foxo1* mRNA expression in SOD1<sup>G86R</sup> mice (DCA) when compared to non-DCA treated SOD1<sup>G86R</sup> mice (CT, Figure 7A, B, C). At the cessation of treatment, *Pfk1*, *Acsf2* and *citrate synthase* mRNA levels in DCA-treated SOD1<sup>G86R</sup> mice were comparable to DCA-treated WT mice (Figure 7D, E, F), indicating successful restoration of glycolysis and activation of the Krebs cycle. Importantly, CT SOD1<sup>G86R</sup> mice presented with significantly reduced *Pfk1* and *citrate synthase* expression when compared to DCA-treated SOD1<sup>G86R</sup> mice and/or CT WT mice. DCA treatment was also able to preserve the expression of *Pgc-1  $\alpha$*  and its target gene *Mfn2* in DCA-treated SOD1<sup>G86R</sup> mice at levels comparable to that seen in CT WT and DCA-treated WT mice (Figure 7G, H). The increase in the expression of genes involved in mitochondrial biogenesis was accompanied by a decrease in the expression of the *Gpx1* (Figure 7I). Notably, and in support of our results above, 95 day old CT SOD1<sup>G86R</sup> mice presented with a significant decrease in the expression of *Pgc-1  $\alpha$*  and *Mfn2* mRNA, and an increase in the expression of *Gpx1* mRNA (Figure 7G, H, I). Collectively, these

data suggest that DCA is able to restore glycolytic function whilst decreasing oxidative stress in glycolytic muscle of SOD1<sup>G86R</sup> mice.

At a functional level, DCA was able to almost completely preserve muscle strength. While CT SOD1<sup>G86R</sup> mice lost 30% of their grip strength, DCA-treated SOD1<sup>G86R</sup> mice only lost 8% of their grip strength when compared to initial grip force at the initiation of treatment (Figure 8A). Analysis of mRNA expression of muscle atrophy markers showed a more modest improvement (Figure 8B). *Murf-1* mRNA expression was reduced from a 1.6-fold increase in the non-treated CT SOD1<sup>G86R</sup> mice to 1.3-fold increase in DCA-treated SOD1<sup>G86R</sup> mice. Similarly, *Atg-1* mRNA expression was decreased from a 1.7-fold increase in CT SOD1<sup>G86R</sup> mice to a 1.4-fold increase in DCA-treated SOD1<sup>G86R</sup> mice. DCA treatment also prevented the increase in the expression of the denervation markers (Figure 8C). The increase in expression of *AChR α* mRNA in DCA-treated SOD1<sup>G86R</sup> mice was only 3.2-fold as compared to an 8.8-fold increase in CT SOD1<sup>G86R</sup> mice. *AChR γ* mRNA was increased by 3.9-fold in DCA-treated SOD1<sup>G86R</sup> mice as compared to a 15.87-fold increase in measured in CT SOD1<sup>G86R</sup> mice. Lastly, *MuSK* gene expression was also lower following treatment with DCA, decreasing from a 2-fold increase in CT SOD1<sup>G86R</sup> mice to a 1.3-fold increase in DCA-treated SOD1<sup>G86R</sup> mice. WT mice treated with DCA did not present with any modifications of these atrophy or denervation markers. Altogether, these results demonstrate that by facilitating the equilibrium between glucose and lipid oxidation through the administration of DCA, we are able to promote weight gain, restore mitochondrial gene expression, improve muscle strength, and decrease the expression of denervation markers in SOD1<sup>G86R</sup> mice.

## DISCUSSION

Here we provide evidence of a change in the metabolic capacity of glycolytic muscle in SOD1<sup>G86R</sup> mice. A switch from glucose metabolism to lipid metabolism occurs early in the disease process, and prior to any detectable NMJ denervation. By improving glycolytic capacity of SOD1<sup>G86R</sup> mice through administration of DCA, we promoted a delay in the onset of motor symptoms and amelioration of muscle denervation and atrophy. Thus, we demonstrate for the first time that an early switch to lipid metabolism in skeletal muscle may underlie early pathological mechanisms that lead to NMJ destabilization in ALS.

The decreased capacity for SOD1<sup>G86R</sup> mice to endure acute physical exercise that solicits anaerobic metabolism in muscle occurred before any measurable muscle weakness or denervation (Figure 1 and 2). This low resistance to intense exercise contrasted their enhanced endurance capacity during acute aerobic exercise. This observation suggests that SOD1<sup>G86R</sup> mice acquire new properties in skeletal muscle that enhance global aerobic capacity and promote endurance ability. It is plausible that altered glucose and insulin responses in SOD1<sup>G86R</sup> mice (Figure E1) might underlie this change in exercise capacity since insulin plays a critical role in driving glucose uptake into skeletal muscle for use as an energy substrate

(ref). Indeed, high incidences of glucose intolerance have been observed in patients diagnosed with sporadic ALS (Pradat *et al*, 2010). However, as basal glucose uptake in *extensor digitorum longus* (EDL: another glycolytic muscle) of the SOD1<sup>G93A</sup> mouse model of ALS is normal before denervation (Smittkamp *et al*, 2014), it would seem unlikely that altered insulin sensitivity underlies the metabolic changes observed in this study.

Endurance exercise is also supported by slow-twitch oxidative type I fibers while intense exercise requires movements involving strength and speed that are generated by fast-twitch glycolytic type IIb fibers (Bassel-Duby & Olson 2006). Given that a switch in fiber type from glycolytic to oxidative fibers has been described in ALS patient muscle biopsies (Telerman-Toppet & Coërs 1978), and in the SOD1<sup>G93A</sup> mouse model of ALS (Atkin *et al*, 2005, Hegedus *et al*, 2008, Deforges *et al*, 2009), the observed alteration in exercise capacity in SOD1<sup>G86R</sup> mice might also reflect a switch of muscle fiber type. In line with this, enhanced aerobic capacity is typically observed after endurance training, and this occurs concurrent with measurable changes in fiber type composition (Pette and Staron 2001).

PFK1 is the rate-limiting enzyme of the glycolysis, and an increase in glycogen synthase activity and glycogen accumulation in skeletal muscle is characteristic of muscle that is subjected to endurance training (Vestergaard, 1999). Thus, the increase in endurance capacity in SOD1<sup>G86R</sup> mice mirrors a profound alteration of fuel preference in muscle fibers. In accordance with this, we observed a progressive decrease of PFK1 activity, and an increase in glycogen synthase activity and glycogen accumulation in skeletal muscle. The initial decrease in PFK1 activity in SOD1<sup>G86R</sup> mice may be an adaptive response to the progressive accumulation of pyruvate and increased fatty acids uptake, two well-known potent inhibitors of PFK1 (Massao Hirabara *et al*, 2003). Furthermore, as the entry of glucose into muscle fibers in ALS mice is not affected early in disease (Dupuis *et al*. 2004; Smittkamp *et al*, 2013), our data suggests that glucose is rerouted towards glycogen stores rather than being used as an immediate energy source. By the end-stage of disease, reduced activities of PFK1 and glycogen synthase, together with an increase of glycogen stores and reduced levels of pyruvate demonstrate inhibition of the glycolytic pathway. Collectively, these observations suggests that glycolytic muscle is no longer able to mobilize glycogen stores to produce energy, and that the inhibition of glycolysis appears to originate downstream of PFK1 (Figure 9).

In contrast to inhibition of glycolysis in SOD1<sup>G86R</sup> mice, the lipid pathway was stimulated at 65 days of age, and remained functional until the end-stage of disease (Figure 4B, C). It is known that increased endurance should correlate with increased release of fatty acids from lipid stores, and enhanced uptake by muscle tissue (Talanian *et al*, 2010). Previous observations of decreased fat pad mass and respiratory quotient at an early stage in SOD1<sup>G86R</sup> mice (Dupuis *et al*, 2004), and increased lipid clearance in these mice (Fergani *et al*, 2007) are indicative of increased lipid use. Moreover, in patients diagnosed with sporadic ALS, Pradat and colleagues reported increased circulating free fatty acids (FFAs) (Pradat *et al*, 2010). Altogether, these observations indicate that muscle tissue of SOD1<sup>G86R</sup> is the potential site of abnormal lipid consumption. The question raised from these observations was whether the more “efficient” oxidation during exercise is due to a given group of muscles that work more efficiently, or whether other groups of muscles are

becoming oxidative to participate in the exercise task. The latter case appears to occur since fiber type switching towards more oxidative metabolism (Deforges *et al*, 2009), and increased expression of genes encoding enzymes involved in lipid metabolism (Dupuis *et al*, 2004, Fergani *et al*, 2007) is observed at later, symptomatic stages of disease in ALS mouse models. In line with this, we show an early increase in the gene expression of important components in lipid mobilization and uptake (*Lpl*, *Cd36*, *ACSF2* and *Cpt-1B*, Figure 4B), and increased  $\beta$ -oxidation by-products (ATP and NADH at 65 days) that activate PDK4 and inhibit PDH activity (Denton *et al*, 1975) in fast-twitch glycolytic muscle.

PDK4 appears to play a pivotal role in the switch in fuel preference by orchestrating substrate competition in SOD1<sup>G86R</sup> glycolytic muscle fibers. In skeletal muscle, PDK4 is the most highly expressed pyruvate dehydrogenase kinase isoform and is considered to be a critical regulator of pyruvate dehydrogenase (PDH) activity (Bowker-Kinley *et al*, 1998). By phosphorylating PDH, PDK4 completely inhibits the entry of pyruvate into the Krebs cycle, thus hampering glucose oxidation (for review, see Holness and Sugden, 2003). PDH and PDK4 are known to act as metabolic homeostats in response to energy imbalance. Indeed, PDK4 transcription is increased during prolonged exercise, after both short-term high-intensity and prolonged low-intensity exercise or during fasting, situations that represent metabolic states where the whole body glucose availability is in deficit (Spriet *et al*, 2004; Watt *et al*, 2004; Jeong *et al*, 2012). Its expression is controlled directly or indirectly by various transcription factors/transcriptional coactivators or stimuli including PPAR $\beta/\delta$ , FOXO1, PGC-1 $\alpha$ , ERR $\alpha$ , or FAs. In C2C12 mouse myoblasts, nutrient deprivation induces *Pdk4* gene expression (Furuyama *et al*, 2003). In rat muscle tissue, triglyceride infusion leads to increased plasma FA and increased expression of *Pdk4* mRNA (Kim *et al*, 2006). Moreover, it has been shown that in response to increased entry of FA in skeletal muscle or to fasting, induction of PPAR $\beta/\delta$  stimulates FOXO1 transcription, which in turn activates *Pdk4* expression (Nahle *et al*, 2008). Here, we show that *Pdk4* activation might occur in response to the increase in *Ppar $\beta/\delta$*  and *Foxo1* mRNAs, rather than via the classical transcription factors PGC-1 $\alpha$ /ERR $\alpha$ . If this were the case, then an increase of FA release due to the induction of *Lpl* and *Acsf2* would stimulate PDK4 expression via PPAR $\beta/\delta$  and FOXO1, which would in turn facilitate FA oxidation by conserving pyruvate for oxaloacetate formation to allow entry of acetyl-coA into the Krebs cycle (Figure 9).

Increased  $\beta$ -oxidation of fatty acids leads to the generation of lipid by-products that contribute to lipotoxicity and ROS production (Zhang *et al*, 2010). ROS accumulation in muscle tissue of SOD1<sup>G86R</sup> mice is an early event in the course of the pathology that precedes overt signs of denervation (Halter *et al*, 2010). Here we show an up-regulation of *Gpx1*, an indicator of ROS accumulation, in the TA but not in the *soleus* muscle of SOD<sup>G86R</sup> mice in the advanced stages of the disease. It is expected that this chronic/long term activation of lipid use would have toxic effects on mitochondria (Bonnard *et al*, 2008), which might explain the observed decrease of citrate synthase (Figure 5C), the decrease in the expression of genes responsible for mitochondrial dynamics, and the reduction in the quantity of mtDNA specific to glycolytic muscle (Figure 6). Indeed, rescuing muscle mitochondria in a mouse model for ALS through the

overexpression of muscle-specific PGC-1  $\alpha$  has been shown to prevent muscle atrophy and improve mitochondrial function (Da Cruz *et al*, 2012). Although PGC-1  $\alpha$  is often considered as the main “fiber type regulator” that contributes to muscle physiological plasticity under normal physiological conditions, PGC-1  $\alpha$  is down-regulated with disease progression in our SOD1<sup>G86R</sup> mice, and can therefore not account for the induction of *Pdk4*. Alternatively, muscle-specific over-expression of PPAR $\beta/\delta$  in skeletal muscle results in a greater number of oxidative type 1 fibers (Luquet *et al*, 2003), and over-expression of constitutively active PPAR $\beta/\delta$  results in mitochondrial biogenesis and a shift from fast twitch to slow twitch fibers (Wang *et al*, 2004). Thus, the early switch of fuel preference in ALS mice could be driven by the increased expression of PPAR $\beta/\delta$ . Altogether, these findings show that metabolic imbalance in muscle fibers of SOD1<sup>G86R</sup> mice is an early event. As glycolytic muscle fibers become progressively unable to use glucose as energy substrate, they switch to lipid use to maintain a sufficient amount of energy supply. Intriguingly this mechanism is specific to glycolytic muscle fibers as the deregulations observed in the TA differ from that seen in the oxidative *soleus* muscle.

Because PDK4 appears to be a key actor in the switch in fuel preference by suppressing glucose utilization, we used the halogenated carboxylic acid DCA, a specific inhibitor of PDK, to restore glucose metabolism and muscle metabolic plasticity. Indeed, maintaining PDH in its unphosphorylated active form will re-activate PDH function and recover glucose metabolism by restoring glucose oxidation (Whitehouse and Randle, 1973). In a model of statin-induced muscle atrophy, DCA treatment has been shown to increase glucose oxidation in type IIb muscle fibers and reduce the expression of markers of protein degradation (Mallinson *et al*, 2012). This is in line with the results presented here. Indeed, in this study, we demonstrate that DCA treatment exerts protective effects on muscle fibers in the SOD1<sup>G86R</sup> mice by restoring the ability of glycolytic muscle to use glucose as fuel. When compared to non-DCA treated SOD1<sup>G86R</sup> mice, those supplemented with DCA show a decrease in the mRNA expression of *Pdk4*, *Foxo1* and *Ppar $\beta/\delta$*  in parallel with an induction of *Pfk1* and *citrate synthase*. Moreover, DCA-treated SOD1<sup>G86R</sup> mice also had decreased expression of denervation and atrophy markers when compared to untreated SOD1<sup>G86R</sup> mice. At a functional level, this was reflected by a preservation of muscle strength. DCA treatment in SOD1<sup>G86R</sup> mice also exerted beneficial metabolic effects on the whole organism by stimulating weight gain during disease development, which is similar to what has been observed after DCA treatment of statin-induced myopathy in mice (Mallinson *et al*, 2012). It is important to note that DCA treatment improved mitochondrial function in SOD1<sup>G86R</sup> mice (Figure 7). We observed an up-regulation of mRNA expression of *Pgc-1  $\alpha$*  and *Mfn2*, a PGC-1 $\alpha$  target gene that is involved in mitochondrial dynamics. While DCA has not been shown to directly regulate the PGC-1  $\alpha$  pathway, it has been shown to reverse the inhibition of PGC-1  $\alpha$  and mitochondrial biogenesis that is induced in myotubes by chronic inhibition of glucose oxidation with pyruvate (Philp *et al*, 2010). The beneficial effects on mitochondrial metabolism following DCA treatment in SOD1<sup>G86R</sup> mice was also reflected by comparable levels of *Gpx1* in DCA-treated SOD1<sup>G86R</sup> mice and CT- and DCA-treated WT mice. Collectively, these data show that restoration of metabolic equilibrium in

glycolytic muscle fibers is able to protect muscle mitochondria and prevent oxidative stress, while also preventing denervation and atrophy.

DCA has previously been used in the SOD1<sup>G93A</sup> mouse model of ALS (Miquel *et al*, 2012). By limiting pyruvate turnover to lactate and facilitating the entry of pyruvate into the Krebs cycle, DCA reduced astrogliosis and motor neuron death (Miquel *et al*, 2012). This indicates that PDK activation may be a common mechanism in astrocytes and muscle. Interestingly, Miquel and colleagues also demonstrated that DCA-treated SOD1<sup>G93A</sup> mice presented with a marked improvement in the structure of NMJs in the *extensor digitorum longus* (glycolytic muscle fiber) but not *soleus* (oxidative muscle fiber). Taken together with our data showing an effect of DCA in restoring glycolysis in muscle, one can conclude that DCA treatment exerts its protective effects through stabilizing the NMJ. However, based on the action of DCA on both muscle and astrocytes, we cannot conclude whether the normalization of glycolytic muscle metabolism is sufficient in itself to maintain the positive effect observed at the NMJ. Collectively, these data provide convincing evidence that DCA treatment promotes the use of glucose as the preferred energy substrate (instead of lipids), thereby preventing denervation and maintaining function at NMJ.

In conclusion, our study provides compelling evidence to support a dramatic change in glycolytic muscle metabolism that specifically alters muscle metabolic plasticity in highly susceptible glycolytic fibers. Importantly these metabolic alterations occur very early in the course of the disease, before the onset of denervation, and prior to motor neuron death in SOD1<sup>G86R</sup> mice. These data, in combination with our sciatic nerve axotomy experiments suggest that glycolytic defects are not of neurogenic origin. Importantly, since altered metabolic plasticity might underlie the susceptibility of glycolytic fibers to denervation whilst limiting the capacity for muscle to become re-innervated, this would have detrimental effects on the rate of disease progression. By demonstrating the involvement of multiple cell types in ALS pathology and identifying a possible common metabolic thread between glycolytic muscle and astroglia in ALS pathogenesis, our work further exemplifies the complexity of ALS. Finally, our work has important therapeutic implications as we present evidence to suggest that by improving metabolic function in murine ALS animal models through DCA, it is possible to improve motor function, maintain muscular integrity and delay denervation.

## **MATERIALS AND METHODS**

### *Ethics statement*

All experiments followed current European Union regulations (Directive 2010/63/EU). They were approved by the regional ethics committee CREMEAS 35 under No. AL/01/20/09/12 and were performed by authorized investigators.

### *Animals*

FVB/N males overexpressing murine SOD1 with the G86R mutation were genotyped as described previously (Ripps *et al.*, 1995). Wild-type littermates were used as controls. Mice were housed in a temperature- and humidity-controlled environment at 23°C and under a 12 hours light/dark cycle. Mice had access to water and regular A04 chow *ad libitum*.

*Exercise paradigms:* The week before starting the experiment, all animals were acclimated to the treadmill exercise (Treadmill Control, Letica, Spain) by running at 25 cm/sec with a 5° inclination for 5 min for 3 days.

Intense anaerobic exercise : a maximal incremental test was carried out. The incline was set at + 10° and the speed at 40 cm/s and was maintained at this rate for 2 min. The speed was then increased by 3 cm/s every 90 sec until exhaustion of the animal. The speed at which each mouse stopped running was considered to be the maximal running speed (V<sub>max</sub>)

Low intensity endurance exercise: To determine maximal endurance capacity, a rectangular test was established. All mice ran at 80% of the V<sub>max</sub> attempt during the maximal incremental test. The incline was set at + 10°, after 2min of acclimation at 40cm/s, the speed was maintained at 80% of the V<sub>max</sub> until exhaustion.

The criterion for exhaustion was a time of 5 sec spent on the electrical grid without running. Blood samples from the tip of the tail were obtained immediately at the end of exercise to measure blood lactate using a lactate pro-LT device (Lactate Pro LT-1710, ARKRAY<sup>®</sup>, China).

### *Muscle grip strength*

Muscle grip strength was measured using a strength meter (Bioseb Grip test, Bioseb, France). Animals were placed over a metallic grid that they instinctively grab to stop the involuntary backward movement carried out by the manipulator until the pulling force overcomes their grip strength. Each animal was pulled over the entire length of the metallic grid until it lost its grip. Grip strength, expressed in Newton, was recorded over three trials for each animal in each test session. The maximal grip strength was obtained by averaging the three grip strength scores for each animal.

### *Electromyography*

All recordings were performed with a standard EMG apparatus (Dantec, Les Ulis, France) in accordance with the guidelines of the American Association of Electrodiagnosis Medicine (AAEM). Mice were anesthetized with 100 mg/kg ketamine chlorhydrate and 5mg/kg xylazine and maintained at 36°C over a thermostatic blanket. In order to minimize variability, all recordings were performed by the same experimenter. Recordings were monitored for 2min with a concentric needle electrode (9013S0011, diameter 0.3mm, Medtronic, USA) inserted into the *gastrocnemius* muscle. A monopolar needle electrode (9013R0312, diameter 0.3mm, Medtronic) was inserted into the tail of the mouse to ground the system.

Recordings showing voluntary activity were discarded. Spontaneous activity (mainly fibrillations) characteristic of muscle denervation was differentiated from voluntary activity (regular discharges which disappear with muscular relaxation) by visual and auditory inspection. Spontaneous activity with a peak-to-peak amplitude of at least  $50 \mu V$  was considered to be significant.

#### *Glucose tolerance test and insulin tolerance test*

Male transgenic and non-transgenic mice were fasted for 18 hours (starting at 6 PM) prior to the glucose tolerance test (GTT), or fasted for 4 hours (starting at 9AM) prior to the insulin tolerance test (ITT). Blood glucose levels were evaluated using a commercial FreeStyle Papillon InsuLinx glucometer (Abbot, France). Blood was drawn from a small incision at the tip of the tail. For GTTs, initial blood glucose was measured prior to an IP injection of 2g/kg body mass of glucose. For ITTs, insulin from bovine pancreas (Sigma Aldrich, USA) was injected IP (0.5U/kg body mass) after initial blood glucose was measured. Changes in blood glucose was followed for 120 minutes with measurements taken every 15 minutes for both GTTs and ITTs. For each mice, blood glucose was expressed as the percentage of initial blood glucose concentration (T0).

#### *Axotomy*

Axotomy of the sciatic nerve was performed on non-transgenic males. Mice were anesthetized by intraperitoneal (IP) injection of 100 mg/kg ketamine chlorhydrate and 5mg/kg xylazine. The sciatic nerve was exposed at mid thigh level and sectioned using microscissors. The skin incision was sutured, and mice were allowed to recover. Contralateral hind limbs served as non-axotomized controls. Mice were sacrificed by lethal injection of pentobarbital at 2 week following the surgical intervention.

#### *Dichloroacetate treatment*

The pharmacological treatment consisted in daily administration of Dichloroacetate (DCA, Sigma Aldrich) in drinking water at a concentration corresponding to a daily dose of 500mg/kg body mass as previously described (Miquel *et al*, 2012). The concentration was calculated based on a predicted water intake of 5ml/day/animal (Bachmanof *et al*, 2002). Water intake was carefully monitored throughout the duration of the experiment. Standard drinking water was used as control (CT). Mouse weights were monitored weekly.

#### *Quantitative RT-PCR*

Frozen muscle samples were homogenized in 1ml/100mg tissue Trizol reagent (Invitrogen, USA) together with a stainless bead. Two 3min homogenization cycles were performed in a TissueLyser (Qiagen, Germany) at 30Hz. RNA was extracted using chloroform/isopropyl alcohol/ethanol and stored at  $-80^{\circ}C$ . 1  $\mu g$  of total RNA was used to synthesize cDNA using Iscript reverse transcriptase (BioRad, USA) and oligo-dT primer as specified by the manufacturer. Gene expression was measured using the 2X SYBR green SsoAdvanced reagent (BioRad) according to the manufacturer's instructions on a BioRad iCycler.

PCR was performed under optimized conditions as follows: 95°C denaturation for 30sec, followed by 40 cycles of 10sec at 95°C and 30sec at 60°C. The extended list of primers (Eurogentec, Belgium) is provided in Table S1. Relative quantification was achieved by calculating the ratio between the cycle number (Ct) at which signal crossed a threshold set within the logarithmic phase of the gene of interest and that of TBP housekeeping gene. Ct values were means of duplicates.

#### *Quantification of mitochondrial DNA*

Snap frozen tissue was digested in KTT buffer (Tris 10mM pH 9, Triton X100 0.1%, KCl 50mM) with 2% proteinase K (Sigma Aldrich) overnight at 54°C under constant agitation. Proteinase K was inactivated at 100°C for 5 minutes. RNA was degraded with 0.3  $\mu$ g/ $\mu$ l RNAase for 1h at 37°C. Total DNA was extracted using a mix of Roti-Phenol reagent (Roth, USA), chloroform and isoamylalcohol (25/24/1). DNA was quantified using RT-qPCR (initial denaturation step at 98°C for 2min, followed by 40 cycles of 10sec at 98°C and 20sec at 62°C). The following pairs of primers were used for nuclear DNA quantification cyclophilin A: forward 5'-CTG-GTT-GCG-GAT-GGT-GGT-TA-3' and reverse 5'-CTT-CCC-AAA-GAC-CAC-ATG-CT-3'. The following pairs of primers were used for mitochondrial Cox1: forward 5'-TCC-ACT-ATT-TGT-CTG-ATC-CGT-ACT-3' and reverse 5'-AGT-AGT-ATA-GTA-ATG-CCT-GCG-GCT-A-3'. The relative mtDNA levels were calculated by normalizing the relative expression of mitochondrial Cox1 to the relative expression of the nuclear Cyclophilin A.

#### *Western blotting*

Snap frozen muscle tissue was pulverized in a TissueLyser (Qiagen) for 2 x 20sec under liquid nitrogen using stainless steel beads. Tissue powder was homogenized in RIPA lysis buffer (50mM Tris pH 7.4, 150mM NaCl, 1mM EDTA, 1% Triton 100X, 0.1% SDS, 0.5% Sodium Deoxycholate) at 1ml/100mg tissue containing 1:100 protease inhibitor cocktail (Calbiochem, USA) and phosphatase inhibitor cocktail 2 and 3 (Sigma Aldrich, Germany). Determination of protein concentration was carried out using a BCA Assay Reagent Kit (UP95424 Uptima, France). Protein was denaturated by boiling, resolved by sodium dodecyl sulfate–polyacrylamide gel electrophoresis and transferred to 2  $\mu$  m nitrocellulose membranes (BioRad, France) using a semi-dry Transblot Turbo system (BioRad, France). After using a chemiluminescent blocker (Millipore, France), membranes were probed with primary antibodies against Glycogen Synthase Rabbit mAb (3886, Cell Signaling, USA), Phospho-Glycogen Synthase Ser641 (3891, Cell Signaling, USA), PGC1  $\alpha$  (AB3242, Millipore, France) and total actin (A2103, Sigma Aldrich, France). Primary antibodies were detected with anti-rabbit HRP (BI2407, P.A.R.I.S, France). The protein bands were detected by chemiluminescence using ECL Lumina Forte (Millipore, France) and a chemiluminescence detector (Bio-Rad, France).

#### *Phosphofructokinase enzymatic activity*

For biochemical analysis, mice were sacrificed and tissues were quickly dissected, frozen in liquid nitrogen and stored at  $-80^{\circ}\text{C}$  until use. All chemicals were purchased from SIGMA. Frozen *tibialis anterior* muscles were pulverized with a mortar and pestle under liquid nitrogen. The powder was resuspended in 5 volumes (w/v) of extraction buffer containing 20mM Tris-HCl pH7.5, 0.15M NaCl and Protease Inhibitor Cocktail (Calbiochem, USA). Samples were homogenized by vortexing for 3min prior to incubation for 10min on roller at room temperature. After a final homogenization by vortexing for 2min, samples underwent centrifugation for 15min at 10000g at  $4^{\circ}\text{C}$ . The supernatant was used for the assay of PFK activity and determination of protein concentration as described above.

PFK activity was determined at  $25^{\circ}\text{C}$  in 96-well microplates in a total volume of  $240\ \mu\text{l}$ . An aliquot ( $10\ \mu\text{l}$ ) of tissue extract was added to  $200\ \mu\text{l}$  of reaction cocktail solution (50mM Tris-HCl pH8.0, 3mM  $\text{MgCl}_2$ , 3mM DTT, 0.1mM EGTA, 0.3mM NADH, 2mM Fructose-6-phosphate, 10IU Aldolase, 80IU Triose phosphate isomerase, 14IU Glycerol-3-phosphohydrogenase and  $10\ \mu\text{l}$  of distilled water. The reaction was started with the addition of  $20\ \mu\text{l}$  of 10mM ATP. PFK activity was measured every minute over 20min and calculated from the linear rate of change in absorbance at 340nm (Tristar LB 941 apparatus, Berthold Technologies, Germany). Calculations were based on the extinction coefficient of  $6.22 \times 10^{-3}\text{M}$  for NADH and corrected by the volume of the sample added, to obtain nmol of NADH oxidized/min/ $\mu\text{l}$  of sample. As one mole of NADH corresponds to one mole of PFK, the activity of PFK was calculated for each sample relative to the protein concentration of each sample.

#### *Intermediary metabolites*

All intermediary metabolites analyzed were extracted from fresh snap-frozen tissue. Quantification was performed using commercial colorimetric assays for pyruvate (K609-100 BioVision, USA) ATP (K354-100 BioVision, USA), and  $\text{NAD}^+$  and NADH (ab65348 Abcam, UK). Samples were deproteinized using 10kDa cutoff spin filters (ab93349 Abcam, UK) and assays were performed according to manufacturer's instructions. The optical densities for all assays were obtained using a Tristar LB 941 multimode plate reader (Berthold Technologies, France), and raw concentration values were calculated as indicated by the manufacturer.

#### *Histochemistry*

Glycogen deposition in muscle biopsies was determined using the standard periodic acid-schiff (PAS) stain. Transverse ( $10\ \mu\text{m}$ ) TA sections were obtained from snap frozen tissue embedded in TissueTek O.C.T. compound (Sakura, Japan) on a cryostat (Leica CM 3050S, Germany) at  $-24^{\circ}\text{C}$ . Freshly cut sections were briefly dried at  $37^{\circ}\text{C}$  for 30min. Sections were then incubated for 10min in Periodic Acid 1% (Roth, Germany), followed by 30min in Schiff Reagent (Roth, Germany) prior to a 5min counterstain in Mayer's solution (Roth, Germany). After thorough washing, slides were dehydrated with successive alcohol – toluene baths and mounted in Roti-Histokitt (Roth, Germany). Microphotographs were obtained at a

magnification of  $\times 100$  (Nikon, France). Counts were performed using National Institutes of Health IMAGE version 1.62 software (USA).

#### *Statistical analysis*

Unless otherwise indicated, data are expressed as the mean  $\pm$  SEM. PRISM version 5.0a software (GraphPad, USA) was used for statistical analysis. Tests are indicated in the legends under the figures. Differences with  $P$ -values  $\leq 0.05$  were considered significant.

## **AUTHOR CONTRIBUTIONS**

LP JZ JPL and FR conceived and designed the experiments and interpreted data; LP, AX, AV and SG performed the experiments; LP, AX, SG, ALB, JZ, STN, JPL and FR carried out the data analysis. LP, STN, JPL and FR wrote the manuscript.

## **FUNDING**

This work was supported by funds from "Association pour la Recherche sur la Sclérose Latérale Amyotrophique et autres Maladies du Motoneurone" (FR), "Association pour la recherche et le développement de moyens de lutte contre les maladies neurodégénératives" (AREMANE) (J.P.L.) André Combat la SLA (U1118 INSERM) and Euromotor (U1118 INSERM). LP is granted by "Association Française de lutte contre les Myopathies" and AV is granted by "Region Alsace" and INSERM. STN acknowledges the support of an Motor Neurone Disease Research Institute of Australia Bill Gole Fellowship, The University of Queensland, and The Australian Academy of Science. The funders had no role in study design, data collection and analysis, decision to publish, or preparation of the manuscript.

## **ACKNOWLEDGEMENTS**

We thank Annie Picchinenna and Marie José Ruivo for excellent technical assistance. We are also indebted to Drs. Floriane Imhoff-White and Bastien Fricker for their aid with part of the initial SOD1<sup>G86R</sup> mouse experiments.

## **THE PAPER EXPLAINED**

### **PROBLEM**

Amyotrophic lateral sclerosis is the most common adult motor neuron disorder characterized by motor neuron death and muscular atrophy, which ultimately leads to death. To date there is no efficient therapy for this fatal disease. Muscle denervation in disease progression seems to be a dynamic process of denervation and reinnervation that is different for the different muscle fibers types, with the glycolytic muscle fibers being the first affected. Moreover, as is the case for other pathological conditions accompanied by muscle atrophy, the severity of atrophy seems to be exacerbated in glycolytic muscle fibers. In the present work we investigated the potential mechanisms involved in this sensitivity of the glycolytic fibers in a mouse model for ALS.

### **RESULTS**

The most important findings of our study in this neuromuscular disease is an increase in endurance capacity during prolonged oxidative exercise associated with a switch in fuel preference in glycolytic muscle fibers towards lipid oxidation, prior to motor symptoms and denervation. The increased expression of genes involved in lipid handling is accompanied by a decrease in expression and activity of PFK1, the rate-limiting enzyme of glycolysis. Glycolysis inhibition is a bottom-to-top process, orchestrated by PDK4, a mitochondrial enzyme that blocks the entry of pyruvate, the end-product of glycolysis, into the TCA cycle. The increase in lipid use is not accompanied by an increase in mitochondrial biogenesis, but has deleterious effects on mitochondria and is associated with increased oxidative stress. We further show that it is possible to pharmacologically modulate this pathway and restore metabolic equilibrium. By doing so we were able to prevent denervation and muscular atrophy and improve metabolic profile in our ALS mouse model.

### **IMPACT**

We show for the first time that muscle tissue suffers metabolic alterations early in the course of disease development, alterations that influence the course of the pathology. These alterations are specific to glycolytic muscle fibers and therefore can explain the sensitivity of glycolytic fibers to atrophy and denervation. By exploring this mechanism we pinpoint the molecular components involved in these modifications and we identify a potential therapeutic target in this pathway.

## BIBLIOGRAPHY

Abdel-Aleem S (1996) Regulation of Fatty Acid Oxidation by Acetyl-CoA Generated from Glucose Utilization in Isolated Myocytes. *J Mol Cell Cardiol* 28: 825–833.

Andersen PM and Al-Chalabi A (2011) Clinical genetics of amyotrophic lateral sclerosis: what do we really know? *Nat Rev Neurol* 7: 603–615.

Atkin JD, Scott RL, West JM, Lopes E, Quah AK, Cheema SS (2005) Properties of slow- and fast-twitch muscle fibres in a mouse model of amyotrophic lateral sclerosis. *Neuromuscul Disord* 15: 377–388.

Bachmanov AA, Reed DR, Beauchamp GK, Tordoff MG (2002) Food intake, water intake, and drinking spout side preference of 28 mouse strains. *Behav Genet* 32(6):435-43.

Bassel-Duby R, Olson EN (2006) Signaling pathways in skeletal muscle remodeling. *Annu Rev Biochem* 75:19–37.

Boillée S, Yamanaka K, Lobsiger CS, Copeland NG, Jenkins NA, Kassiotis G, Kollias G, Cleveland DW (2006) Onset and progression in inherited ALS determined by motor neurons and microglia. *Science* 312: 1389–1392.

Bonnard C, Durand A, Peyrol S, Chanseaux E, Chauvin MA, Morio B, Vidal H, Rieusset J (2008) Mitochondrial dysfunction results from oxidative stress in the skeletal muscle of diet-induced insulin-resistant mice. *J Clin Invest* 118: 789–800.

Bouteloup C, Desport JC, Clavelou P, Guy N, Derumeaux-Burel H, Ferrier A, Couratier P (2009) Hypermetabolism in ALS patients: an early and persistent phenomenon. *J Neurol* 256: 1236–1242.

Bowker-Kinley MM, Davis WI, Wu P, Harris RA, Popov KM (1998) Evidence for existence of tissue-specific regulation of the mammalian pyruvate dehydrogenase complex. *Biochem J* 329:191-6.

Chen S, Sayana P, Zhang X, Le W (2013). Genetics of amyotrophic lateral sclerosis: an update. *Mol Neurodegener* 8: 28.

Constable SH, Favier RJ, McLane JA, Fell RD, Chen M, Holloszy JO (1987) Energy metabolism in contracting rat skeletal muscle: adaptation to exercise training. *Am J Physiol Cell Physiol* 253: C316–C322.

Da Cruz S, Parone P, Lopes VS, Lillo C, McAlonis-Downes M, Lee SK, Vetto AP, Petrosyan S, Marsala M, Murphy AN, Williams DS, Spiegelman BM, Cleveland DW (2012). Elevated PGC-1  $\alpha$  activity sustains mitochondrial biogenesis and muscle function without extending survival in a mouse model of inherited ALS. *Cell Metab* 15: 778–786.

Deforges S, Branchu J, Biondi O, Grondard C, Pariset C, Lécolle S, Lopes P, Vidal PP, Chanoine C, Charbonnier F (2009) Motoneuron survival is promoted by specific exercise in a mouse model of amyotrophic lateral sclerosis. *J Physiol* 587(Pt 14):3561-72.

Dengler R, Konstanzer A, Kuther G, Hesse S, Wolf W, Struppler A (1990) Amyotrophic lateral sclerosis: macro-EMG and twitch forces of single motor units. *Muscle Nerve* 13:545–550.

Denton RM, Randle PJ, Bridges BJ, Cooper RH, Kerbey AL, Pask HT, Severson DL, Stansbie D, Whitehouse S (1975) Regulation of mammalian pyruvate dehydrogenase. *Mol Cell Biochem* 9: 27–53.

Desport JC, PM Preux, TC Truong, JM Vallat, D Sautereau, P Couratier (1999) Nutritional status is a prognostic factor for survival in ALS patients. *Neurology* 53: 1059–1063.

Desport JC, Preux PM, Magy L, Boirie Y, Vallat JM, Beaufrère B, Couratier P (2001). Factors correlated with hypermetabolism in patients with amyotrophic lateral sclerosis. *Am J Clin Nutr* 74: 328–334.

Desport JC, Torny F, Lacoste M, Preux PM, Couratier P (2005) Hypermetabolism in ALS: correlations with clinical and paraclinical parameters. *Neurodegener Dis* 2: 202–207.

Dupuis L, Oudart H, René F, Gonzalez de Aguilar JL, Loeffler JP (2004) Evidence for defective energy homeostasis in amyotrophic lateral sclerosis: benefit of a high-energy diet in a transgenic mouse model. *Proc Natl Acad Sci U S A* 101: 11159–11164.

Dupuis L, Gonzalez de Aguilar JL, Echaniz-Laguna A, Eschbach J, René F, Oudart H, Halter B, Huze C, Schaeffer L, Bouillaud F, Loeffler JP (2009) Muscle mitochondrial uncoupling dismantles neuromuscular junction and triggers distal degeneration of motor neurons. *PLoS One* 4:e5390.

Dupuis L, Pradat PF, Ludolph AC, Loeffler JP (2011) Energy metabolism in amyotrophic lateral sclerosis. *Lancet Neurol* 10: 75–82.

Fergani A, Oudart H, Gonzalez De Aguilar JL, Fricker B, René F, Hocquette JF, Meininger V, Dupuis L, Loeffler JP (2007) Increased peripheral lipid clearance in an animal model of amyotrophic lateral sclerosis. *J Lipid Res* 48:1571-80.

Fischer LR, Culver DG, Tennant P, Davis AA, Wang M, Castellano-Sanchez A, Khan J, Polak MA, Glass JD (2004) Amyotrophic lateral sclerosis is a distal axonopathy: evidence in mice and man. *Exp Neurol* 185: 232–240.

Frey D, Schneider C, Xu L, Borg J, Spooren W, Caroni P (2000) Early and selective loss of neuromuscular synapse subtypes with low sprouting competence in motoneuron diseases. *J Neurosci* 20: 2534–2542.

Furuyama T, Kitayama K, Yamashita H, Mori N (2003) Forkhead transcription factor FOXO1 (FKHR)-dependent induction of PDK4 gene expression in skeletal muscle during energy deprivation. *Biochem J* 375:365-71.

Halter B, Gonzalez de Aguilar JL, René F, Petri S, Fricker B, Echaniz-Laguna A, Dupuis L, Larmet Y, Loeffler JP (2010) Oxidative stress in skeletal muscle stimulates early expression of Rad in a mouse model of amyotrophic lateral sclerosis. *Free Radic Biol Med* 48: 915–923.

Hardiman O, van den Berg LH, Kiernan MC (2011) Clinical diagnosis and management of amyotrophic lateral sclerosis. *Nat Rev Neurol* 7: 639–649.

Harris RA, Bowker-Kinley MM., Huang B, Wu P (2002) Regulation of the activity of the pyruvate dehydrogenase complex. *Adv Enzyme Regul* 42: 249–259.

Hegedus J, Putman CT, Tyreman N, Gordon T (2008) Preferential motor unit loss in the SOD1 G93A transgenic mouse model of amyotrophic lateral sclerosis. *J Physiol* 586: 3337–3351.

Holness MJ, Kraus A, Harris RA, and Sugden MC (2000) Targeted upregulation of pyruvate dehydrogenase kinase (PDK)-4 in slow twitch skeletal muscle underlies the stable modification of the regulatory characteristics of PDK induced by high-fat feeding. *Diabetes* 49: 775–781, 2000.

Holness MJ, Sugden MC (2003) Regulation of pyruvate dehydrogenase complex activity by reversible phosphorylation. *Biochem Soc Trans* 31 :1143-51.

Jawaid A, Murthy SB, Wilson AM, Qureshi SU, Amro MJ, Wheaton M, Simpson E, Harati Y, Strutt AM, York MK, Schulz PE (2010) A decrease in body mass index is associated with faster progression of motor symptoms and shorter survival in ALS. *Amyotroph Lateral Scler* 11(6):542-8.

Jeong JY, Jeoung NH, Park KG, Lee IK (2012) Transcriptional regulation of pyruvate dehydrogenase kinase. *Diabetes Metab J* 36(5):328-35.

Kim YI, Lee FN, Choi WS, Lee S, Youn JH (2006) Insulin regulation of skeletal muscle PDK4 mRNA expression is impaired in acute insulin-resistant states. *Diabetes* 55: 2311–2317.

Lin J, Wu H, Tarr PT, Zhang CY, Wu Z, Boss O, Michael LF, Puigserver P, Isotani E, Olson EN, Lowell BB, Bassel-Duby R, Spiegelman BM (2002) Transcriptional co-activator PGC-1 alpha drives the formation of slow-twitch muscle fibres. *Nature* 418: 797–801.

Luquet S, Lopez-Soriano J, Holst D, Fredenrich A, Melki J, Rassoulzadegan M, Grimaldi PA. (2003) Peroxisome proliferator-activated receptor delta controls muscle development and oxidative capability. *FASEB J* 17(15):2299-301.

Mallinson JE, Constantin-Teodosiu D, Graves PD, Martin EA, Davies WJ, Westwood FR, Sidaway JE, Greenhaff PL (2012) Pharmacological activation of the pyruvate dehydrogenase complex reduces statin-mediated upregulation of FOXO gene targets and protects against statin myopathy in rodents. *J Physiol* 590: 6389–6402.

Massao Hirabara S, de Oliveira Carvalho CR, Mendonça JR, Piltcher Haber E, Fernandes LC, Curi R (2003) Palmitate acutely raises glycogen synthesis in rat soleus muscle by a mechanism that requires its metabolization (Randle cycle). *FEBS Lett* 541: 109–114.

Mattson MP, Cutler RG, Camandola S (2007) Energy intake and amyotrophic lateral sclerosis. *Neuromolecular Med* 9: 17–20.

McGarry JD, Mills SE, Long CS, Foster DW (1983) Observations on the affinity for carnitine, and malonyl-CoA sensitivity, of carnitine palmitoyltransferase I in animal and human tissues. Demonstration of the presence of malonyl-CoA in non-hepatic tissues of the rat. *Biochem J* 214: 21–28.

Mead JR, Irvine SA, Ramji DP (2002) Lipoprotein lipase: structure, function, regulation, and role in disease. *J Mol Med (Berl)*. 80: 753–769.

Miquel E, Cassina A, Martínez-Palma L, Bolatto C, Trías E, Gandelman M, Radi R, Barbeito L, Cassina P (2012) Modulation of astrocytic mitochondrial function by dichloroacetate improves survival and motor performance in inherited amyotrophic lateral sclerosis. *PLoS One* 7: e34776.

Nahlé Z1, Hsieh M, Pietka T, Coburn CT, Grimaldi PA, Zhang MQ, Das D, Abumrad NA (2008) CD36-dependent regulation of muscle FoxO1 and PDK4 in the PPAR delta/beta-mediated adaptation to metabolic stress. *J Biol Chem* 283(21):14317-26.

Pedersen WA, Mattson MP (1999). No benefit of dietary restriction on disease onset or progression in amyotrophic lateral sclerosis Cu/Zn-superoxide dismutase mutant mice. *Brain Res.* 833, 117–120.

Pette D, Staron RS (2001) Transitions of muscle fiber phenotypic profiles. *Histochem Cell Biol* 115(5):359-72.

Philp A, Perez-Schindler J, Green C, Hamilton DL, Baar K (2010) Pyruvate suppresses PGC1alpha expression and substrate utilization despite increased respiratory chain content in C2C12 myotubes. *Am J Physiol Cell Physiol* 299: C240–50.

Pradat PF, Bruneteau G, Gordon PH, Dupuis L, Bonnefont-Rousselot D, Simon D, Salachas F, Corcia P, Frochot V, Lacorte JM, Jardel C, Coussieu C, Le Forestier N, Lacomblez L, Loeffler JP, Meininger V (2010). Impaired glucose tolerance in patients with amyotrophic lateral sclerosis. *Amyotroph Lateral Scler* 11: 166–171.

Puigserver P (2005) Tissue-specific regulation of metabolic pathways through the transcriptional coactivator PGC1- $\alpha$ . *Int J Obes (Lond)*. 29 Suppl 1: S5–9.

Pun S, Santos AF, Saxena S, Xu L, Caroni P (2006) Selective vulnerability and pruning of phasic motoneuron axons in motoneuron disease alleviated by CNTF. *Nat Neurosci* 9: 408–419.

Ripps ME, Huntley GW, Hof PR, Morrison JH, Gordon JW (1995) Transgenic mice expressing an altered murine superoxide dismutase gene provide an animal model of amyotrophic lateral sclerosis. *Proc Natl Acad Sci USA* 92: 689–693.

Smittkamp SE, Morris JK, Bomhoff GL, Chertoff ME, Geiger PC, Stanford JA (2014) SOD1-G93A Mice Exhibit Muscle-Fiber-Type-Specific Decreases in Glucose Uptake in the Absence of Whole-Body Changes in Metabolism. *Neurodegener Dis* 13(1):29-37.

Spriet LL, Tunstall RJ, Watt MJ, Mehan KA, Hargreaves M, Cameron-Smith D (2004) Pyruvate dehydrogenase activation and kinase expression in human skeletal muscle during fasting. *J Appl Physiol* 96: 2082–2087.

Talanian JL, Holloway GP, Snook LA, Heigenhauser GJF, Bonen A, Spriet LL (2010) Exercise training increases sarcolemmal and mitochondrial fatty acid transport proteins in human skeletal muscle. *Am J Physiol Endocrinol Metab* 299: E180–8.

Telerman-Toppet N, Coërs C (1978) Motor innervation and fiber type pattern in amyotrophic lateral sclerosis and in Charcot-Marie-Tooth disease. *Muscle Nerve* 1(2):133-9.

Vestergaard H (1999) Studies of gene expression and activity of hexokinase, phosphofructokinase and glycogen synthase in human skeletal muscle in states of altered insulin-stimulated glucose metabolism. *Dan Med Bull* 46(1):13-34.

Villena JA, Kralli A (2008). ERR $\alpha$ : a metabolic function for the oldest orphan. *Trends Endocrinol Metab* 19: 269–276.

Wang YX, Zhang CL, Yu RT, Cho HK, Nelson MC, Bayuga-Ocampo CR, Ham J, Kang H, Evans RM (2004) Regulation of muscle fiber type and running endurance by PPAR $\delta$ . *PLoS Biol* 2(10):e294.

Watt MJ, Heigenhauser GJF, LeBlanc PJ, Inglis JG, Spriet LL, Peters SJ (2004) Rapid upregulation of pyruvate dehydrogenase kinase activity in human skeletal muscle during prolonged exercise. *J Appl Physiol* 97: 1261–1267.

Whitehouse S, Randle PJ (1973) Activation of pyruvate dehydrogenase in perfused rat heart by dichloroacetate. *Biochem J* 134: 651–653.

Wong M, Martin LJ (2010) Skeletal muscle-restricted expression of human SOD1 causes motor neuron degeneration in transgenic mice. *Hum Mol Genet* 19(11):2284-302.

Wu Z, Puigserver P, Andersson U, Zhang C, Adelmant G, Mootha V, Troy A, Cinti S, Lowell B, Scarpulla R, Spiegelman BM (1999). Mechanisms controlling mitochondrial biogenesis and respiration through the thermogenic coactivator PGC-1. *Cell* 98: 115–124.

Yamanaka K, Chun SJ, Boillee S, Fujimori-Tonou N, Yamashita H, Gutmann DH, Takahashi R, Misawa H, Cleveland DW (2008) Astrocytes as determinants of disease progression in inherited amyotrophic lateral sclerosis. *Nat Neurosci* 11: 251–253.

Zhang L, Keung W, Samokhvalov V, Wang W, Lopaschuk GD (2010) Role of fatty acid uptake and fatty acid beta-oxidation in mediating insulin resistance in heart and skeletal muscle. *Biochim Biophys Acta* 1801(1):1-22.

## FIGURE LEGENDS

### **Figure 1: SOD1<sup>G86R</sup> mice have improved performance during endurance exercise.**

A-C: Exercise performance on a treadmill apparatus using an intense exercise, incremental speed paradigm that relies solely on anaerobic metabolism. D-F: Exercise performance on a treadmill apparatus using a moderate exercise, constant sub-maximal speed that relies on the recruitment of aerobic metabolism and that is representative of endurance exercise.

A and D. Kaplan-Meier curves representing values corresponding to the percentage of mice still running at a given time point.

B and E. Median values of the time that mice ran are represented in the min to max graphical representation; 15.5min for wildtype (WT) and 14.33min for SOD1<sup>G86R</sup> in B; 59.33min for WT and 65.43min for SOD1<sup>G86R</sup> in E.

C and F. Mean distance run  $\pm$  SEM by WT and SOD1<sup>G86R</sup> mice in C, and by WT and SOD1<sup>G86R</sup> mice in F. *Versus* WT,  $P=0.017$  in A (Mantel-Cox test);  $**P=0.0078$  in B,  $**P=0.008$  in C,  $P=0.036$  in D (Mantel-Cox test),  $**P=0.0078$  in E, and  $**P=0.0061$  in F,  $n \geq 10$ , Student's t test.

### **Figure 2. Decreased grip strength, increased denervation, and increased expression of denervation and atrophy markers throughout disease progression in SOD1<sup>G86R</sup> mice.**

A: Grip test was performed to measure mouse muscle strength at different time points during disease progression. Graph represents the mean of percentage from initial force measured at 11 weeks  $\pm$  SEM. At 13 weeks  $P=0.03$ , at 14 weeks  $P=0.06$ , at 15 and 16 weeks  $P=0.04$  ( $n \geq 5$ , Fisher's test).

B: Electromyography (EMG) recordings were performed weekly during disease development, starting from 9 weeks of age. Spontaneous electrical activity was considered as positive EMG only for peak-to-peak amplitudes  $> 50\mu\text{V}$ . The percentage of mice presenting with positive EMG in each age group are represented. Representative examples of negative (EMG -) and positive (EMG +) electromyography profiles are shown ( $n \geq 5$ ).

C: Relative mRNA levels of denervation markers AChR (subunits  $\alpha$  and  $\gamma$ ) and MuSK were evaluated by qPCR at the indicated ages (65 and 105 days) in *tibialis anterior* (upper panels) and *soleus* (lower panels) of WT and SOD1<sup>G86R</sup> mice. Graphs represent mean fold change  $\pm$  SEM from age-matched WT

(n>5). \*\*\**P*-values vs WT: <0.0001 for *AChRα*, *AChRγ* and *MuSK* in *tibialis anterior*, and \*\**P*-values vs WT: 0.001 for *AChRα*, and \*\*\**P*-values vs WT: 0.0007 for *AChRγ*, 0.0002 for *MuSK* in *soleus* (Fisher's test).

D: Relative mRNA levels of muscle atrophy markers MuRF1 and Atg-1 were measured by qPCR at the indicated ages (65 and 105 days) in *tibialis anterior* (upper panels) and *soleus* (lower panels). Graphs represent mean fold change ± SEM from age-matched WT for n≥5. \*\*\**P*-values vs WT: <0.0001 for MuRF1 and Atg-1 in *tibialis anterior* and \*\**P*-values vs WT: 0.007 for MuRF1 and *P*=0.006 for Atg-1 in *soleus* (Fisher's test).

**Figure 3. Phosphofructokinase 1 is inhibited in glycolytic muscle and glucose is rerouted towards glycogen stores.**

A: Enzymatic activity of phosphofructokinase in whole *tibialis anterior* muscle cytosolic homogenates is expressed as mean fold change ± SEM from age-matched WT at 65 days of age \* *P*=0.016 (n≥6, Fisher's test), and 105 days of age \*\*\* *P*<0.0001 (n=5, Fisher's test).

B: Pyruvate was measured in whole *tibialis anterior* muscle tissue homogenates. The mean fold change ± SEM compared to age-matched WT are represented with \* *P*=0.019 at 65 days of age, and \* *P*=0.041 at 105 days of age (n≥4, Fisher's test).

C: Left: Representative western blot showing glycogen synthase and phosphorylated glycogen synthase levels. Right: quantification represents the mean ratio of optical densities of glycogen synthase/glycogen synthase-P ± SEM. At 65 days of age \* *P*=0.0162, and at 105 days of age \* *P*=0.0163 (n≥5, Fisher's test).

D: Left: Representative microphotographs of PAS staining from WT and SOD1<sup>G86R</sup> *tibialis anterior* cross-sections at 65 and 105 days of age showing glycogen-negative (light pink) and glycogen-positive (dark pink) fibers. Scale bar: 200μm. Right: Quantification of glycogen-negative (-) and glycogen-positive (+) fibers at 65 and 105 days of age. For (-) fibers: \*\**P*-values vs WT: 0.0026 at 65 days and 0.0074 at 105 days, for (+) fibers: ##*P*-values vs WT: 0.0025 at 65 days and 0.0073 at 105 days (n=4-6, Student's t test).

**Figure 4. Altered fuel preference in glycolytic muscle of 65 day old, asymptomatic SOD1<sup>G86R</sup> mice.**

A: Relative mRNA levels of *Pdk4* and *Pdk2* evaluated by qPCR at the indicated ages in *tibialis anterior* of WT and SOD1<sup>G86R</sup> mice. Graphs represent mean fold change  $\pm$  from age-matched WT. *Pdk4*: \*\**P*-values vs WT: 0.014 at 65 days and 0.018 at 105 days; *Pdk2*: \*\*\**P*-value vs WT <0.0001 at 105 days (n $\geq$ 5, Fisher's test).

B: Relative mRNA levels of genes involved in lipid handling evaluated by qPCR at the indicated ages in *tibialis anterior* of WT and SOD1<sup>G86R</sup> mice. Graphs represent mean fold change  $\pm$  SEM from age-matched WT. *P*-values vs WT: *Lpl* \*\* *P*=0.0009, *Cd36* \* *P*=0.051, *Acsf2* \*\*\* *P*<0.0001 at 65 days, \*\* *P*=0.0059 at 105 days and *Cpt-1 $\beta$*  \*\* *P*=0.01 at 65 days and \* *P*=0.02 at 105 days (n $\geq$ 5, Fisher's test).

C: Relative levels of (left) ATP and (right) NADH and NAD<sup>+</sup> measured in total *tibialis anterior* homogenates of WT and SOD1<sup>G86R</sup> mice. Left: Graphs represent mean fold change  $\pm$  SEM in ATP from age-matched WT. \*\* *P*=0.002 (n $\geq$ 5, Fisher's test). Right: The amounts of NADH and NAD<sup>+</sup> relative to protein content in whole *tibialis anterior* homogenates are represented as mean  $\pm$  SEM. \* *P*=0.027 and \*\* *P*=0.001 (n=5, student's t test).

**Figure 5. Transcription factors, PGC-1 $\alpha$  and citrate synthase are differentially regulated in SOD1<sup>G86R</sup> mice.**

A-D: Relative mRNA levels of (A) *Ppar $\beta$ / $\delta$* , (B) *Foxo1*, (C) *citrate synthase*, and (D) *Pgc-1 $\alpha$*  were evaluated by qPCR at the indicated ages in *tibialis anterior* of WT and SOD1<sup>G86R</sup> mice. Graphs represent mean fold change  $\pm$ SEM from age-matched WT. *Ppar $\beta$ / $\delta$* : *P*-values vs WT: 0.0016 at 65 days; *P*-values vs WT: *Foxo1* \*\*\**P*=0.0001 at 105 days, *citrate synthase* \*\*\**P*<0.0001 at 105 days, *Pgc-1 $\alpha$*  \*\**P*=0.01 at 105 days (n $\geq$ 5, Fisher's test).

E: Representative western blot of PGC-1 $\alpha$  and respective actin that was used for normalization. PGC-1 $\alpha$  protein levels in *tibialis anterior* muscle tissue are represented as mean fold change  $\pm$  SEM from age-matched WT. *P*-values vs WT: 0.02 (n $\geq$ 5, Fisher's test).

F: Relative mRNA levels of *ERR $\alpha$* , *Mfn2* and *Nrf1* were evaluated by qPCR at the indicated ages in *tibialis anterior* of WT and SOD1<sup>G86R</sup> mice. Graphs represent mean fold change  $\pm$  SEM from age-matched WT. *P*-values vs WT: *ERR $\alpha$*  \*\*\* *P*<0.0001, *Mfn2* \*\* *P*=0.002 and *Nrf1* \*\* *P*=0.009 (n $\geq$ 5, Fisher's test).

**Figure 6. Altered mitochondrial function in glycolytic muscle of SOD1<sup>G86R</sup> mice.**

A: Mitochondrial DNA (mtDNA) was quantified using qPCR. Relative mtDNA levels are expressed as the ratio between mitochondrial encoded gene *Cox1* and the nuclear encoded gene *cyclophilin A*. Graphs represent mean fold change  $\pm$  SEM from age-matched WT for *tibialis anterior* (left panel) and *soleus* (right panel) of WT and SOD1<sup>G86R</sup> mice, bars represent standard errors. \*\*\*  $P < 0.0001$  ( $n \geq 4$ , Fisher's test).

B: Relative mRNA levels of *Gpx1* were measured by qPCR at the indicated ages in *tibialis anterior* (left panel) and *soleus* (right panel) of WT and SOD1<sup>G86R</sup> mice. Graphs represent mean fold change  $\pm$  SEM from age-matched WT. \*\*\*  $P < 0.0001$  ( $n \geq 5$ , Fisher's test).

**Figure 7. DCA treatment had beneficial effects on metabolism and mitochondrial function of SOD1<sup>G86R</sup> mice.**

Relative mRNA levels of (A) *Pdk4*, (B) *Ppar $\beta/\delta$* , (C) *Foxo1*, (D) *Pfk1*, (E) *Acsf2*, (F) *Citrate synthase*, (G) *PGC-1 $\alpha$* , (H) *Mfn2*, and (I) *Gpx1* were evaluated by qPCR in *tibialis anterior* of control (CT) or DCA-treated (DCA) WT and SOD1<sup>G86R</sup> mice. Graphs represent mean fold change  $\pm$  SEM from CT-WT group.  $P$ -values vs WT: *Pdk4* \*\*\* $P=0.002$  and <sup>##</sup> $P=0.0039$ , *Ppar $\beta/\delta$*  <sup>#</sup> $P=0.0178$ , *Foxo1* \*\* $P=0.0033$  and <sup>##</sup> $P=0.0038$ , *Pfk1* \*\*\* $P=0.0002$  and <sup>##</sup> $P=0.0080$ , *Acsf2* \* $P=0.0437$ , *citrate synthase* <sup>###</sup> $P=0.0004$ , *Pgc-1 $\alpha$*  \*\* $P=0.0084$  and <sup>###</sup> $P=0.0009$ , *Mfn2* \* $P=0.0272$ , <sup>S</sup> $P=0.0145$  and <sup>###</sup> $P=0.0002$  and *Gpx1* \*\*\* $P < 0.0001$  and <sup>###</sup> $P < 0.0001$  ( $n \geq 8$ , Fisher's test).

**Figure 8. DCA treatment had protective effects on muscle strength and prevented the expression denervation markers.**

A: Grip strength is represented as mean of percent from T<sub>0</sub> for each experimental group  $\pm$  SEM. <sup>##</sup> $P=0.0045$  and \*\*\* $P=0.0003$  ( $n \geq 8$ , Fisher's test)

B: Relative mRNA levels of muscular atrophy markers *Murf1* and *Atg-1* were measured by qPCR in *tibialis anterior* of control (CT) or DCA-treated (DCA) WT and SOD1<sup>G86R</sup> mice. Graphs represent mean fold change  $\pm$  SEM from CT-WT group. \*\* $P=0.0079$  and \*\*\* $P=0.0018$  ( $n \geq 8$ , Fisher's test).

C: Relative mRNA levels of denervation markers *AChR $\alpha$* , *AChR $\gamma$*  and *MuSK* were measured by qPCR in *tibialis anterior* of control (CT) or DCA-treated (DCA) WT and SOD1<sup>G86R</sup> mice. Graphs represent mean fold change  $\pm$  SEM from CT-WT group. \*\* $P=0.015$  for *AChR $\alpha$* , \* $P=0.028$  and \*\* $P=0.074$  for *AChR $\gamma$* , \* $P=0.042$  and \*\* $P=0.0029$  for *MuSK* ( $n \geq 8$ , Fisher's test)

**Figure 9: Schematic representation of the described metabolic imbalance in glycolytic muscle fibers of SOD1<sup>G86R</sup> mice.**

A: Under normal conditions in WT mice, both glucose and lipids enter the cell and are used as cellular fuels. In this situation, both pathways are used and are driven by PDK4 according to needs and fuel availability.

B: In the case of ALS, metabolic flexibility is lost because of chronically increased PDK4 and subsequent inhibition of PDH and PFK1 leading to glycogen accumulation. Increased lipid use through  $\beta$ -oxidation that can only function under aerobic conditions may underlie the greater endurance capacity in SOD1<sup>G86R</sup> mice. With time, the cell produces more reactive oxygen species, thereby inducing cellular damage. CD36: CD36 antigen/fatty acid translocase, CPT1: carnitine palmitoyl transferase 1, FAs: fatty acids, FA-CoA: acyl-fatty acids, GLUT4: glucose transporter 4, LPL: lipoprotein lipase, PDH: pyruvate dehydrogenase complex, PDK4: pyruvate dehydrogenase kinase 4, PFK1: phosphofructokinase 1, ROS: reactive oxygen species.

**Table E1: Sequences of primers used for qPCR.**

**Figure E1. Early changes in glucose handling changes in SOD1<sup>G86R</sup> mice.**

A: A glucose tolerance test was performed after 18 hours of fasting. Each point represents means  $\pm$  SEM of percentage from initial blood glucose concentration at T<sub>0</sub> over time. The significant differences observed correspond to  $P=0.032$  at 30 minutes and  $P=0.038$  at 45 minutes after glucose administration (n=7, multiple t tests).

B: An insulin tolerance test was performed after 4 hours of fasting. Values represent percent from initial blood glucose concentration at T<sub>0</sub> over time  $\pm$  SEM. The response to insulin presented a significant difference between the two groups at T<sub>30</sub> post-injection with  $P =0.034$ , (n $\geq$ 6, multiple t tests).

C: Relative mRNA levels of phosphofructokinase 1 (*Pfk1*) were measured by qPCR at the indicated ages (65 and 105 days) in *tibialis anterior* of WT and SOD1<sup>G86R</sup> mice. Graphs represent mean fold change  $\pm$  SEM from age-matched WT. \*\*\* $P<0.0001$  (n $\geq$ 5, Fisher's test).

**Figure E2: PDK4, PDK2 and FOXO1 expression in *tibialis anterior* after axotomy of WT mice or in *soleus* of WT and SOD1<sup>G86R</sup> mice.**

A (Left column): Relative mRNA levels of *Pdk4* (top panel), *Pdk2* (middle panel) and *Foxo1* (bottom panel) were measured by qPCR in *tibialis anterior* two weeks after axotomy (ipsi) or in the corresponding contralateral muscle (CT) of WT mice. Graphs represent mean fold change  $\pm$  SEM from CT-matched ipsi. *Pdk4*: \*\* $P=0.014$ ; *Pdk2*: \*\*\* $P<0.0001$ ; *Foxo1*: \* $P=0.0519$  ( $n=8$ , student's t test).

B (Right column): Relative mRNA levels of *Pdk4* (top panel), *Pdk2* (middle panel) and *Foxo1* (bottom panel) were measured by qPCR in *soleus* at the indicated ages. Graphs represent mean fold change  $\pm$  SEM from age-matched WT. *P*-values vs WT: *Pdk2*  $P=0.0023$  at 105 days; *Foxo1*  $P=0.0001$  at 105 days ( $n\geq 6$ , Fisher's test).

**Figure E3**

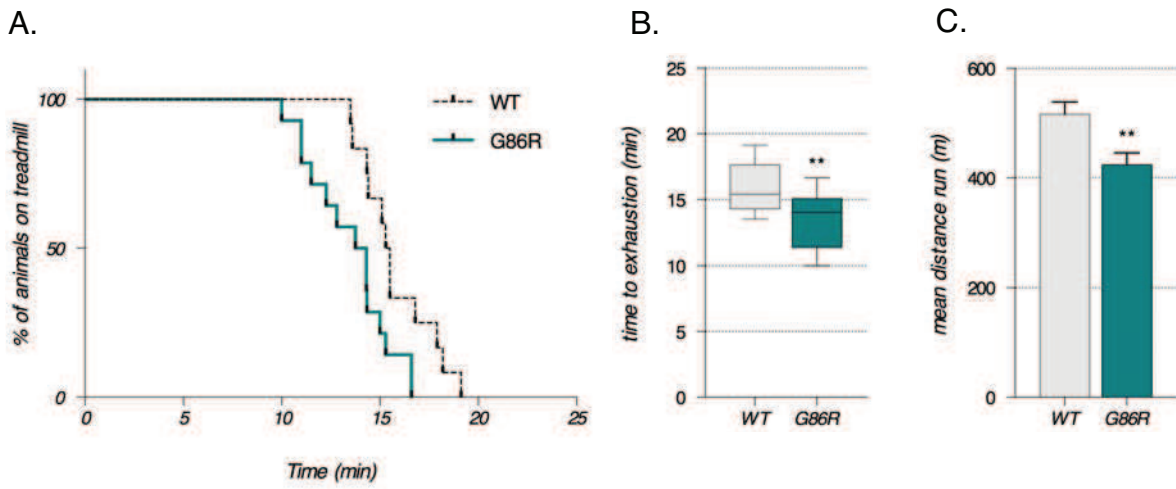
A: Weight over time in WT and SOD1<sup>G86R</sup> animals in CT and DCA treated groups. Each point represents mean weight  $\pm$  SEM at a given time point for a given group. At week 5 of treatment \* $P=0.011$  ( $n\geq 8$ , multiple t test between SOD1<sup>G86R</sup> CT vs DCA).

B: Weight gain at the end-point of treatment expressed means  $\pm$  SEM of percent from  $T_0$ ; \*\* $P=0.0013$  between WT CT and SOD1<sup>G86R</sup> CT groups, and <sup>##</sup> $P=0.0050$  between SOD1<sup>G86R</sup> CT and SOD1<sup>G86R</sup> DCA ( $n\geq 8$ , Fisher's test).

C: Relative transcript levels of *Pdk2* in WT and SOD1<sup>G86R</sup> animals in CT and DCA treated groups. Graphs represent mean fold change  $\pm$  SEM from age-matched CT WT. \*\*\* $P=0.0005$  between WT CT and SOD1<sup>G86R</sup> CT groups, and <sup>##</sup> $P=0.0069$  between SOD1<sup>G86R</sup> CT and SOD1<sup>G86R</sup> DCA ( $n\geq 8$ , Fisher's test).

Figure 1.

Intense exercise - incremental speed



Moderate exercise - constant speed

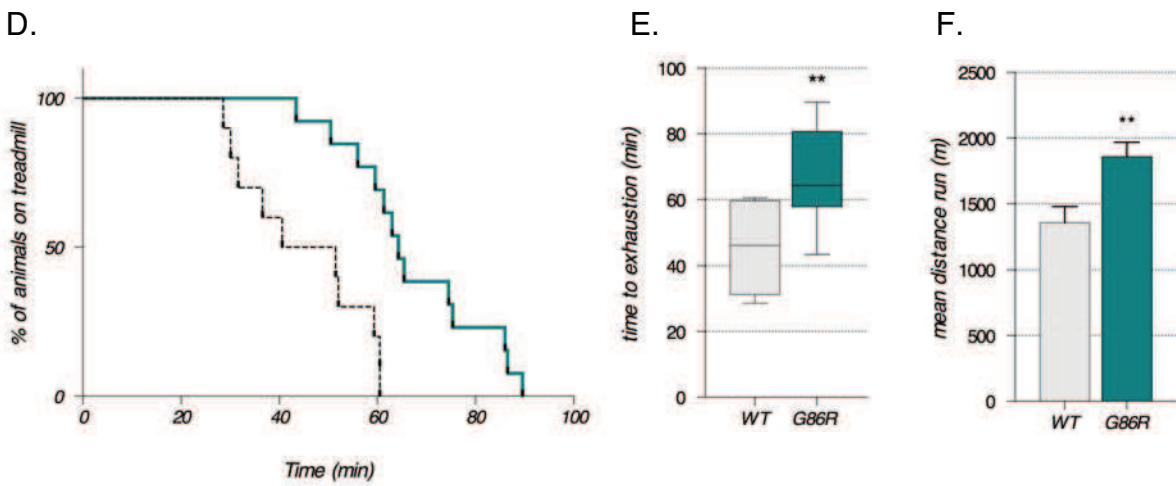
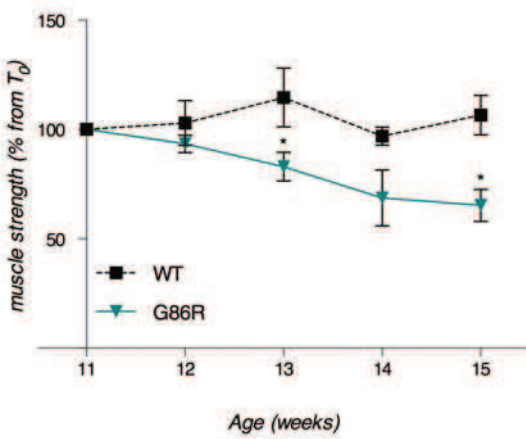
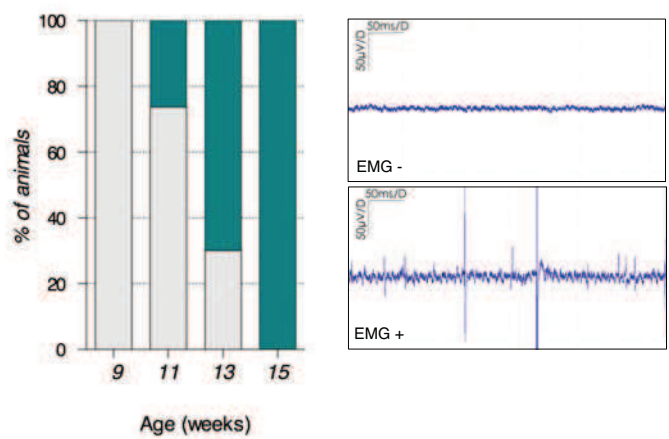


Figure 2.

A.

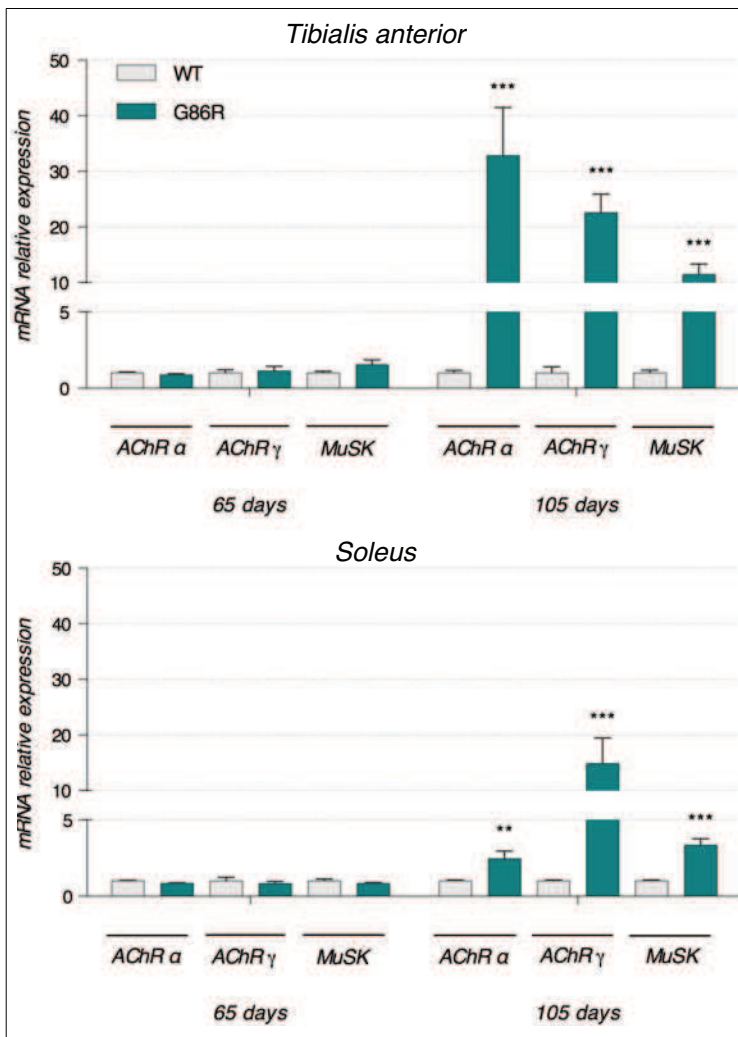


B.



C.

Denervation markers



D.

Atrophy markers

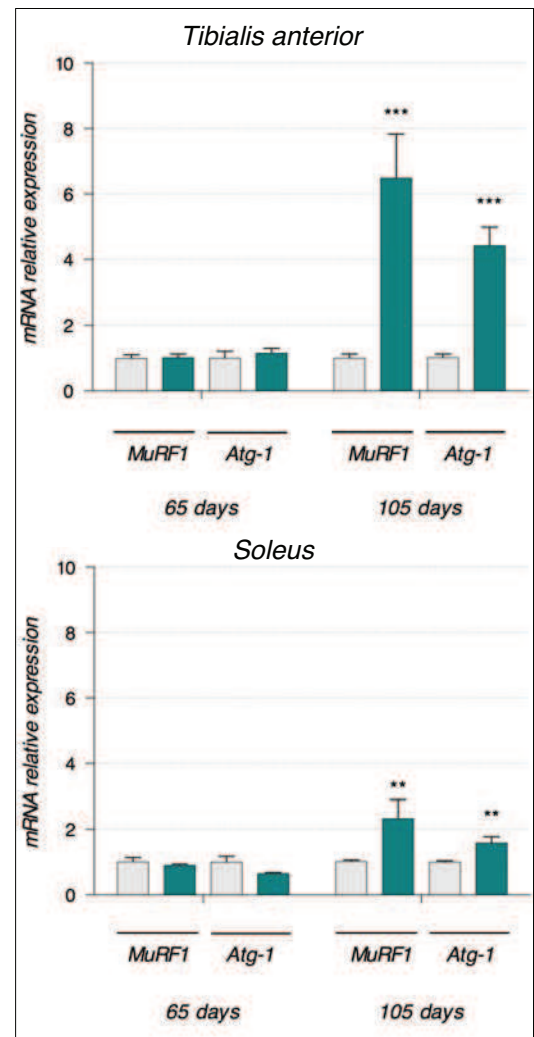


Figure 3.

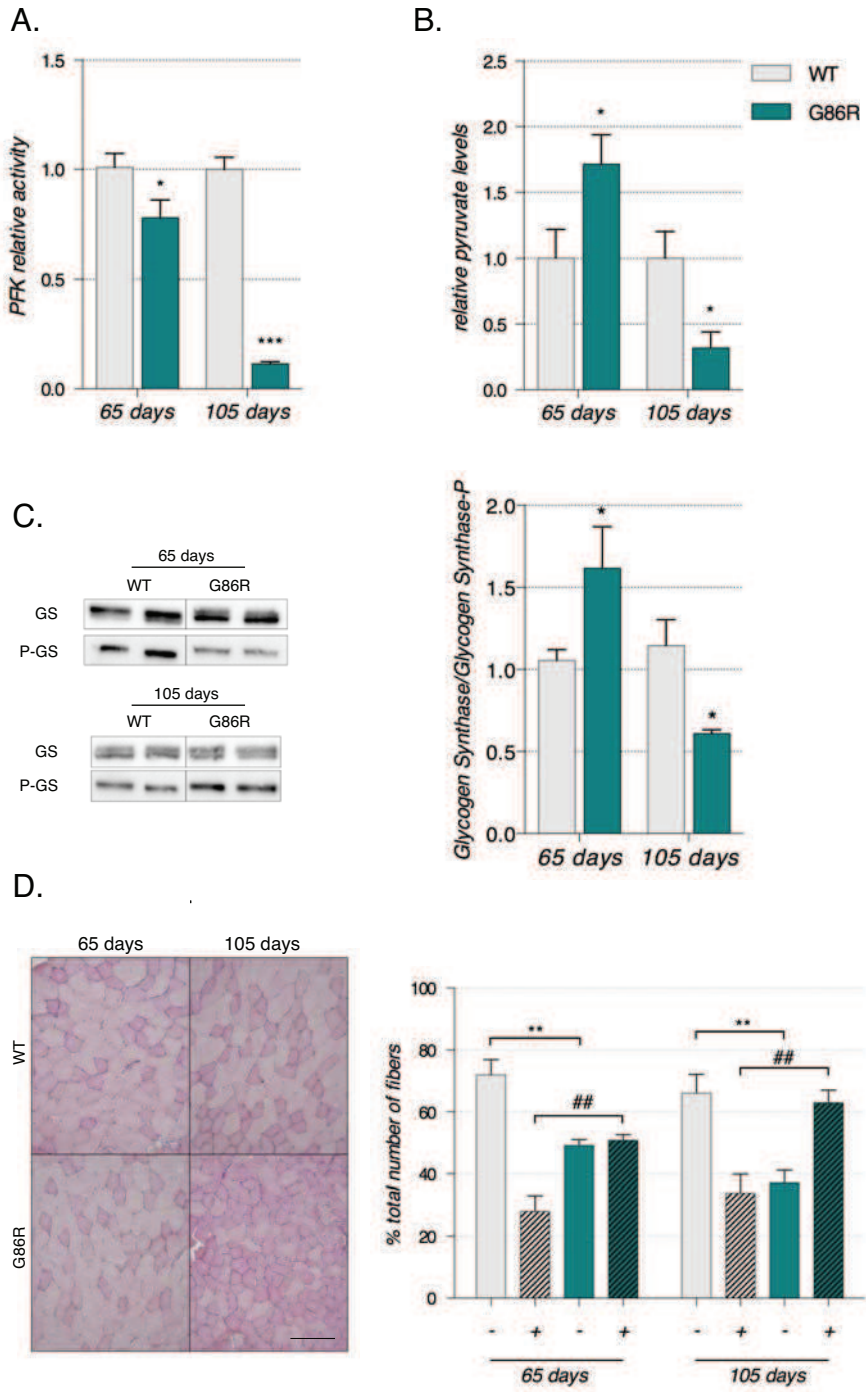
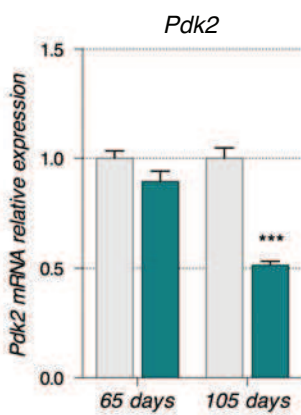
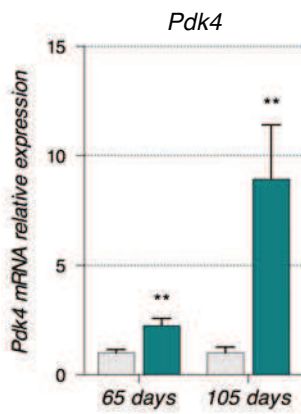
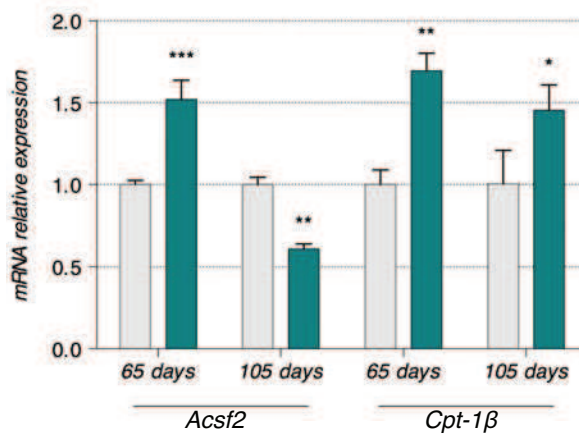
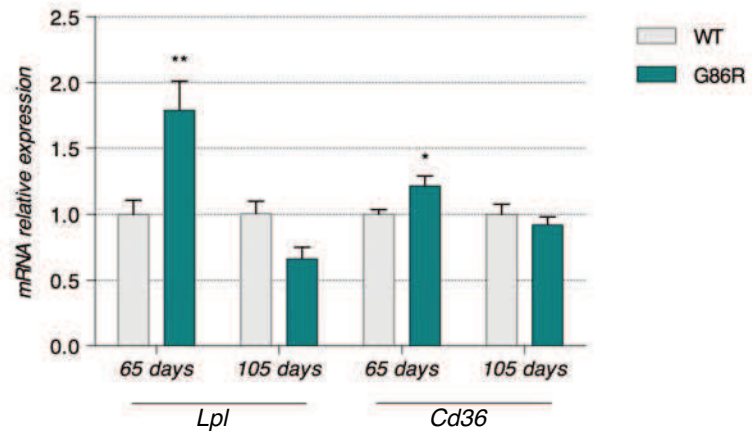


Figure 4.

A. Pdk isoforms



B. Lipid handling pathway



C. ATP and NAD levels

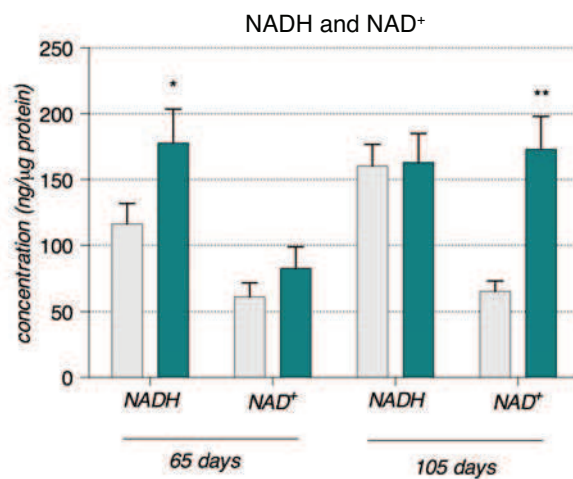
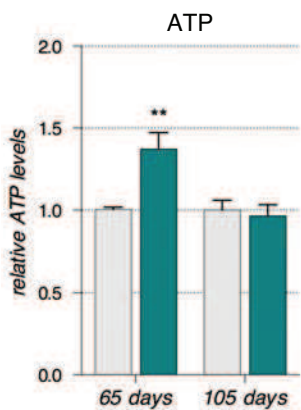


Figure 5.

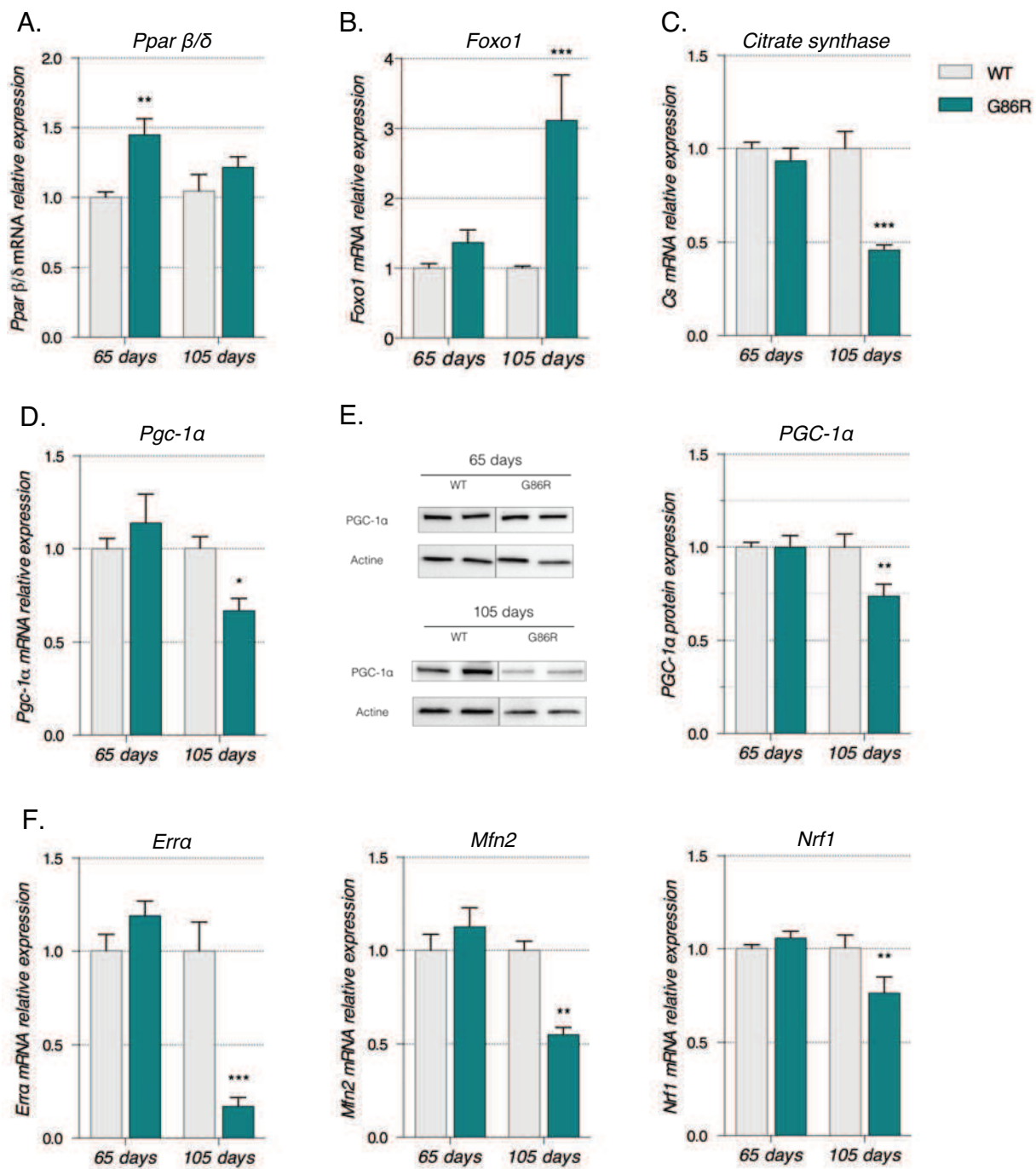
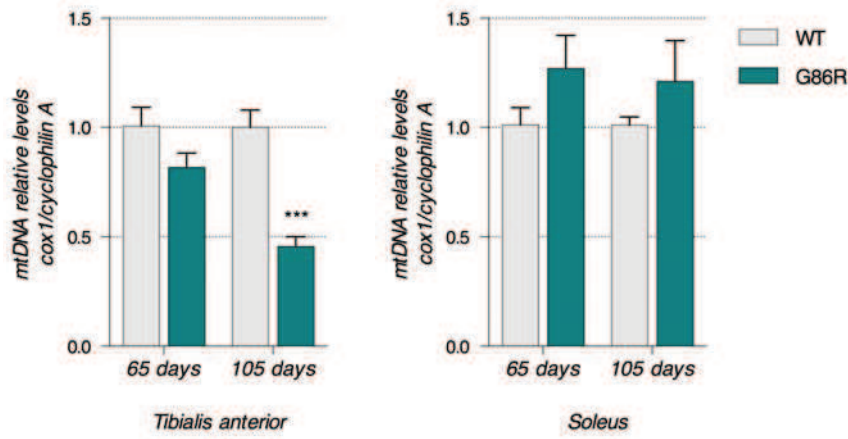


Figure 6.

A.

Mitochondrial DNA



B.

Glutathione peroxidase

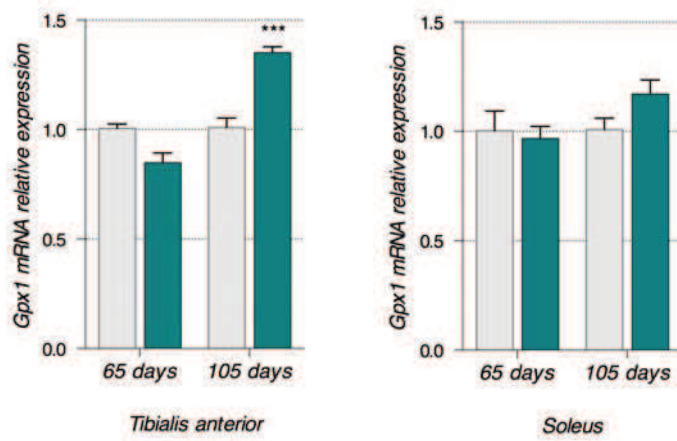


Figure 7.

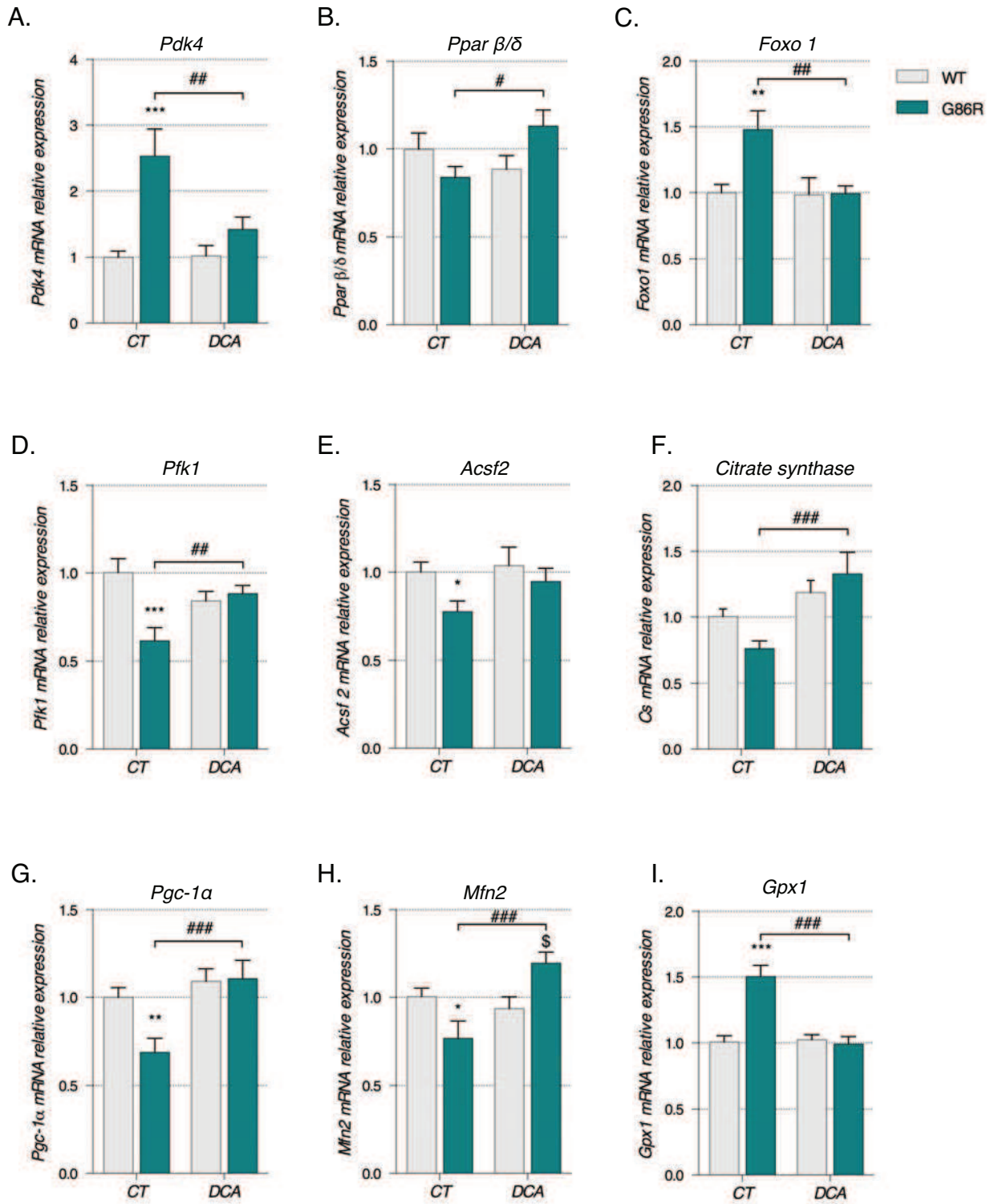


Figure 8.

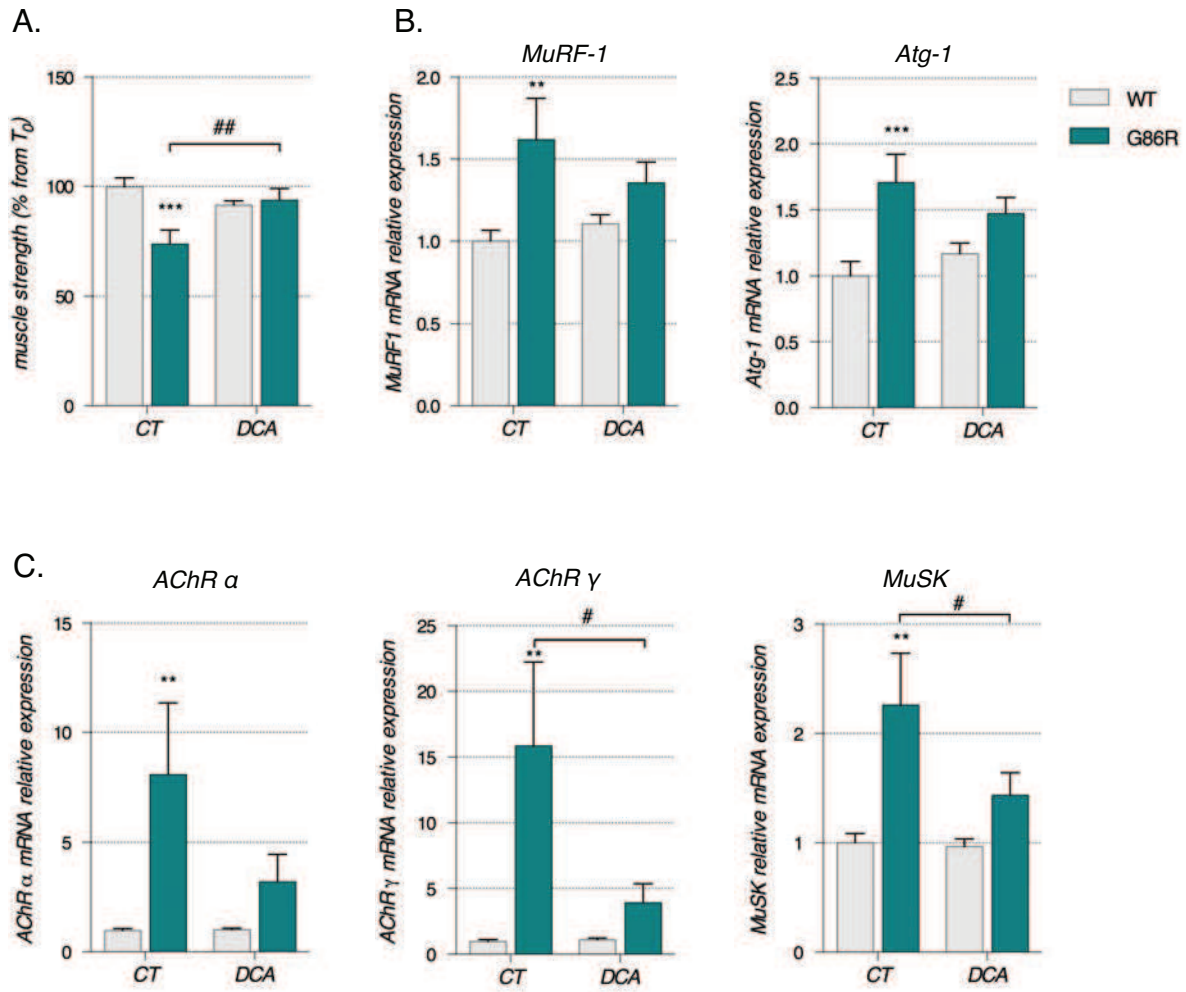


Figure 9.

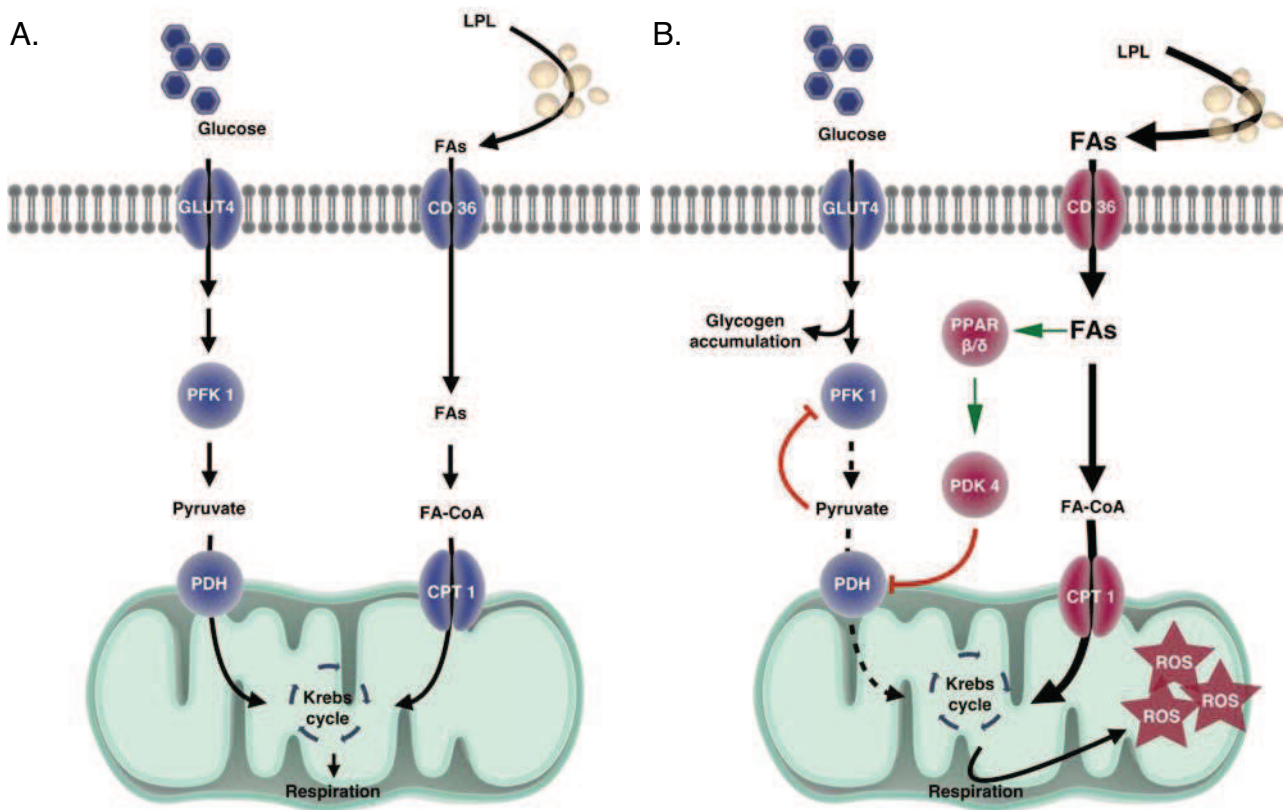
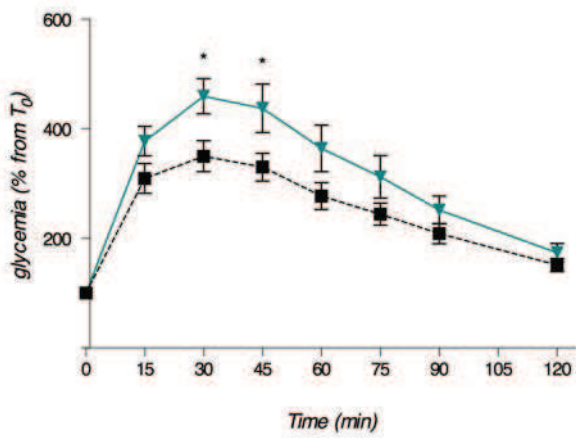


Table 1.

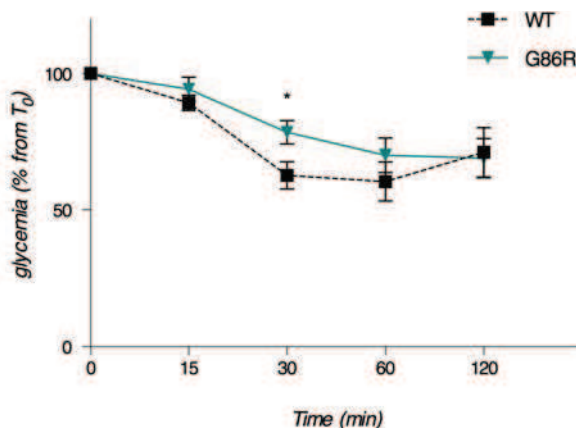
<i>Gene</i>	ID	5'-3'	3'-5'
<i>Acetylcholine receptor <math>\alpha</math></i>	<i>AChR <math>\alpha</math></i>	CCA-CAG-ACT-CAG-GGG-AGA-AG	AAC-GGT-GTGTGT-TGA-TG
<i>Acetylcholine receptor <math>\gamma</math></i>	<i>AChR <math>\gamma</math></i>	GAG-AGC-CAC-CTC-GAA-GAC-AC	GAC-CAA-CCT-CAT-CTC-CCT-GA
<i>Acyl-CoA synthetase family member 2</i>	<i>Acsf2</i>	CTC-TTT-CCC-ACC-ACA-ACA-TCG	TCT-GCA-GTC-TTT-GTG-GGC-A
<i>Atrogin1/F-box only protein 32</i>	<i>Atg-1/ Fbxo32</i>	AGT-GAG-GAC-CGG-CTA-CTG-TG	GAT-CAA-ACG-CTT-GCG-AAT-CT
<i>Carnitine palmitoyl transferase 1</i>	<i>Cpt-1<math>\beta</math></i>	GGC-TCC-AGG-GTT-CAG-AAA-GT	TGC-CTT-TAC-ATC-GTC-TCC-AA
<i>Citrate synthase</i>	<i>Cs</i>	TAG-CAA-ATC-AGG-AGG-TGC-TTG-T	TCT-GAC-ACG-TCT-TTG-CCA-AC
<i>CyclophilinA</i>	<i>Cypa</i>	CTG-GTT-GCT-GAT-GGT-GGT-TA	CTT-CCC-AAA-GAC-CAC-ATG-CT
<i>Cytochrome c oxidase subunit 1</i>	<i>Cox1</i>	TCC-ACT-ATT-TGT-CTG-ATC-CGT-ACT	AGT-AGT-ATA-GTA-ATG-CCT-GCG-GCT-A
<i>Estrogen related receptor <math>\alpha</math></i>	<i>Erra</i>	CCT-GGT-CGT-TGG-GGA-TGT	GGA-CAG-CTG-TAC-TCG-ATG-CTC
<i>Fatty acid translocase/CD36 antigen</i>	<i>CD36</i>	ATT-AAT-GGC-ACA-GAC-GCA-GC	TTC-AGA-TCC-GAA-CAC-AGC-GT
<i>Forkhead box O1</i>	<i>Foxo1</i>	GTG-AAC-ACC-AAT-GCC-TCA-CAC	CAC-AGT-CCA-AGC-GCT-CAA-TA
<i>Glutathione peroxidase 1</i>	<i>Gpx1</i>	CAC-CCG-CTC-TTT-ACC-TTC-CT	TCG-ATG-TCG-ATG-GTA-CGA-AA
<i>Lipoprotein lipase</i>	<i>Lpl</i>	GGG-CTC-TGC-CTG-AGT-TGT-AG	CCA-TCC-TCA-GTC-CCA-GAA-AA
<i>Mitofusin 2</i>	<i>Mfn2</i>	CGA-GGC-TCT-GGA-TTC-ACT-TC	CAA-CCA-GCC-AGC-TTT-ATT-CC
<i>Muscle specific ring finger protein 1</i>	<i>MuRF1/ Trim63</i>	GCA-GGA-GTG-CTC-CAG-TCG	TCT-TCG-TGT-TCC-TTG-CAC-AT
<i>Nuclear respiratory factor 1</i>	<i>Nrf1</i>	TGG-AGT-CCA-AGA-TGC-TAA-TGG	GCG-AGG-CTG-GTT-ACC-ACA
<i>Peroxisome proliferator-activated receptor <math>\beta/\delta</math></i>	<i>Ppar <math>\beta/\delta</math></i>	ATG-GGG-GAC-CAG-AAC-ACA-C	GGA-GGA-ATT-CTG-GGA-GAG-GT
<i>Peroxisome proliferator-activated receptor <math>\gamma</math> coactivator 1<math>\alpha</math></i>	<i>PGC1<math>\alpha</math></i>	TGC-TGC-TGT-TCC-TGT-TTT-C	CCC-TGC-CAT-TGT-TAA-GAC-C
<i>Phosphofructo-kinase 1</i>	<i>Pfk 1</i>	GCC-AAA-GGT-CAG-ATT-GAG-GA	CAG-GTT-CTT-CTT-GGG-GAG-AGT
<i>Pyruvate dehydrogenase kinase 2</i>	<i>Pdk 2</i>	TTC-AGC-AAT-TTC-TCC-CCG-TC	AGG-CAT-TGC-TGG-ATC-CGA-AG
<i>Pyruvate dehydrogenase kinase 4</i>	<i>Pdk 4</i>	GCT-GGA-TGT-TTG-GTG-GTT-CT	TGC-TTT-GAT-TCC-TCC-CAT-CC
<i>RNA Polymerase II polypeptide A</i>	<i>Polr2a</i>	AAT-CCG-CAT-CAT-GAA-CAG-TG	CA-TCC-ATT-TTA-TCC-ACC-ACC
<i>TATA box binding protein</i>	<i>Tbp</i>	CCA-ATG-ACT-CCT-ATG-ACC-CCT-A	CAG-CCA-AGA-TTC-ACG-GTA-GAT

Figure E1.

A. Glucose tolerance test



B. Insulin resistance test



C.

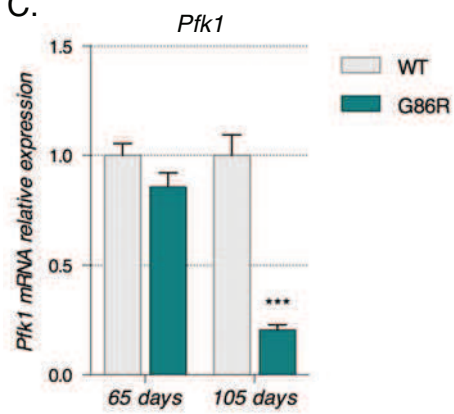
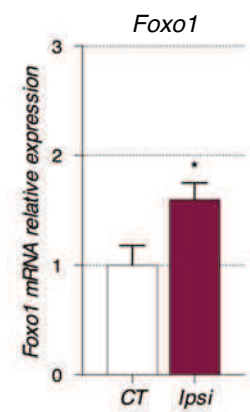
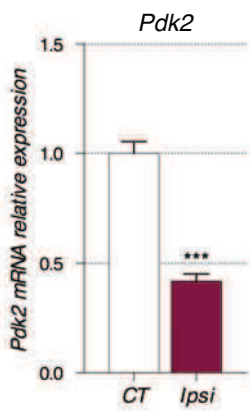
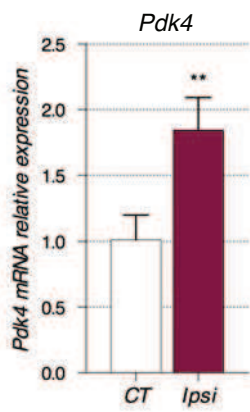


Figure E2.

A. Axotomy



B. Soleus

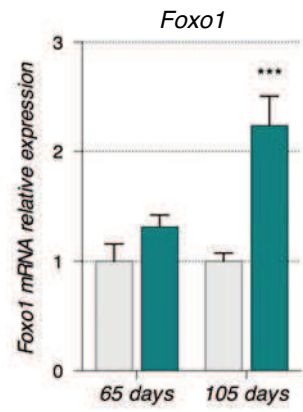
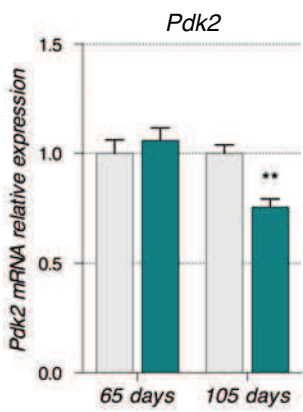
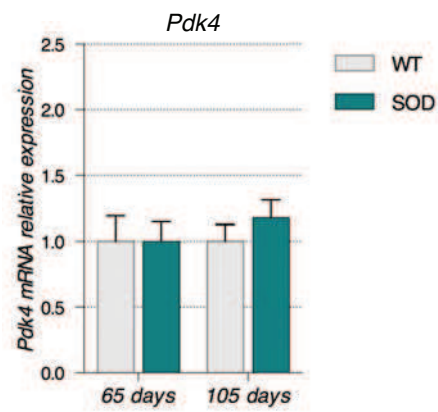
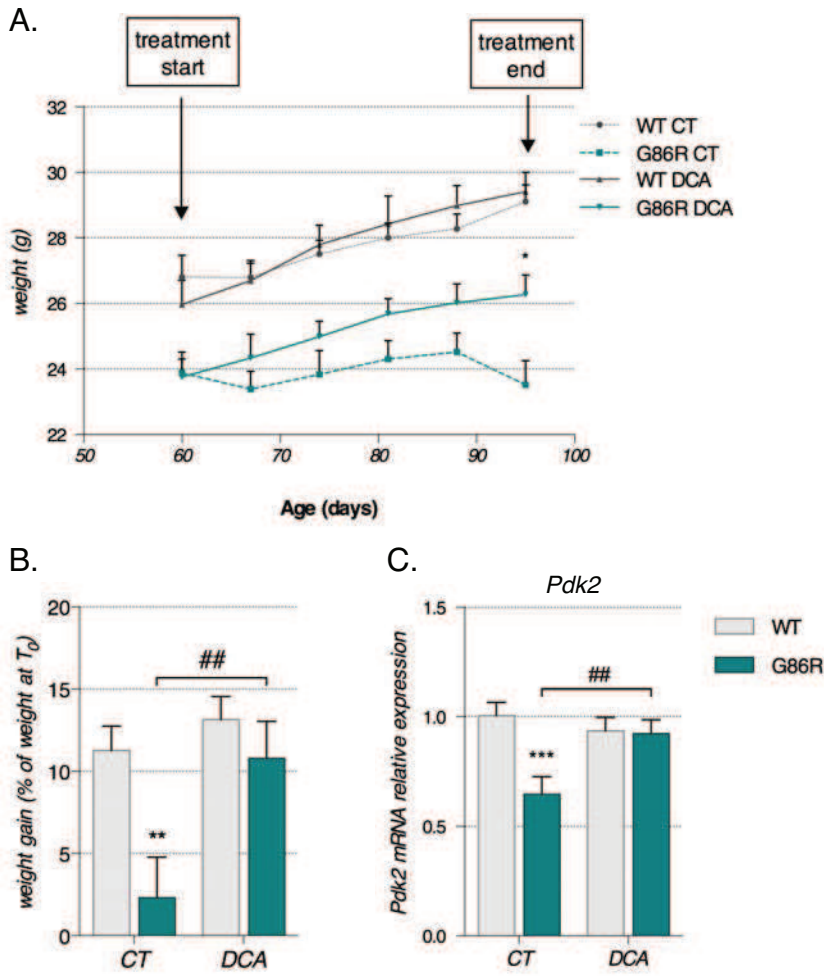


Figure E3.



### **Tissue specific deregulation of selected HDACs characterizes ALS progression in mouse models**

The numerous HDACs expressed in mammalian tissues are classified in four different classes. Classes I, II and IV are considered typical  $Zn^{2+}$ -dependent HDACs (from 1 to 11), while class III comprises  $NAD^+$ -dependent deacetylases also called sirtuins (from 1 to 7).

Globally, typical HDACs are considered as transcription inhibitors due to their role in histone deacetylation and chromatin condensation. In the past decade several studies indicated a protective effect of HDACs inhibitors on neurons (Chuang et al., 2009). Several positive results have also been obtained in SOD1 transgenic mice treated with 4-phenylbutyrate, either alone (Ryu et al., 2005) or in combination with other molecules (Petri et al., 2006; Del Signore et al., 2009). Valproate (Rouaux et al., 2007) or trichostatin A had more limited benefits (Yoo and Ko, 2011). Sirtuins, and especially Sirt1, occupy a special position amongst HDACs, due to the important role they have in controlling metabolism and extending life span (Guarente and Picard, 2005). Sirt1 is a highly conserved  $NAD^+$ -dependent deacetylase that acts as an energy sensor, orchestrating a series of adaptive response in times of nutrient deprivation (Bordone and Guarente, 2005). Sirt1 deacetylates and activates several important targets like PGC-1 $\alpha$ , FOXO, but it also inactivates the pro-apoptotic factor p53. Sirt1 activation has been documented as neuroprotective in animal models for Alzheimer's disease and ALS (Kim et al., 2007). In general, targeting HDACs in neurodegeneration shows some promising result. However due to the multitude of targets regulated by HDACs, undesired deleterious effects can sometimes accompany the beneficial effects and they should be used with consideration (Dietz and Casaccia, 2010). The aim of our study was to better characterize the expression of HDACs in two different mSOD1 ALS models (G93A and G86R), with emphasis on Sirt1 and Sirt2 as potential therapeutic targets.

In the spinal cord of both models mRNA and protein levels of Sirt1 were decreased, while Sirt2 was increased. The same trend was observed in neuroblastoma cell line SH-SY5Y expressing mSOD1<sup>G93A</sup>. However in this

setting, overexpression of mSOD1<sup>G93A</sup> had no effects on the acetylation levels of target proteins like PGC-1 $\alpha$ , acetyl-tubulin or p53. Using a Sirt1 specific activator (Sirt1720) did not rescue neurons expressing mSOD1<sup>G93A</sup>. Equally, inhibiting Sirt2 had no effect on neuronal survival. On the other hand using a known inhibitor of Sirt1, Ex527, we observed an increased in cell viability accompanied by a decrease in caspase 3 activation. The effect of Ex527 bypassed Sirt1, as no changes in acetylation of target proteins were observed. These puzzling results seemed to suggest that Sirt1 could not rescue neurons from apoptosis. This was further confirmed by overexpressing a constitutively active Sirt1 in neuronal cells expressing mSOD1<sup>G93A</sup> that did not rescue neurons from apoptosis.

The effects of mSOD1 on the two considered sirtuins are different in muscle tissue or in the myoblast cell line C2C12. Sirt2 expression does not change during disease progression, however an upregulation of both mRNA and protein expression of Sirt1 were observed at late stages of the disease. The same trend was observed in C2C12 overexpressing mSOD1<sup>G93A</sup>. As it was mentioned previously, Sirt1 plays an essential protective role in muscle metabolism, especially during times of energetic stress. The fact the mSOD1 can trigger Sirt1 activation in muscle C2C12 cell line, in absence of neuronal cells, is of outmost importance, underpinning the direct effect of mSOD1 on muscle metabolic homeostasis.

Taken altogether, these data show a different regulation of Sirt1 and 2 in spinal cord and muscle tissue. While Sirt1 emerges as an interesting potential target in muscle tissue, no beneficial effects of Sirt1 modulation were observed in differentiated motor neurons. For this reason future therapeutic approaches targeting Sirt1 should be carefully considered.

# Tissue-specific deregulation of selected HDACs characterizes ALS progression in mouse models: pharmacological characterization of SIRT1 and SIRT2 pathways

C Valle<sup>1,2</sup>, I Salvatori<sup>2,3</sup>, V Gerbino<sup>2,3</sup>, S Rossi<sup>2,3</sup>, L Palamiuc<sup>4,5</sup>, F René<sup>4,5</sup> and MT Carri<sup>\*,2,3</sup>

Acetylation homeostasis is thought to play a role in amyotrophic lateral sclerosis, and treatment with inhibitors of histone deacetylases has been considered a potential and attractive therapeutic approach, despite the lack of a thorough study of this class of proteins. In this study, we have considerably extended previous knowledge on the expression of 13 histone deacetylases in tissues (spinal cord and muscle) from mice carrying two different ALS-linked SOD1 mutations (G93A-SOD1 and G86R-SOD1). We have then focused on class III histone deacetylases SIRT1 and SIRT2 that are considered relevant in neurodegenerative diseases. SIRT1 decreases in the spinal cord, but increases in muscle during the progression of the disease, and a similar expression pattern is observed in the corresponding cell models (neuroblastoma and myoblasts). SIRT2 mRNA expression increases in the spinal cord in both G93A-SOD1 and G86R-SOD1 mice but protein expression is substantially unchanged in all the models examined. At variance with other sirtuin modulators (sirtinol, AGK2 and SRT1720), the well-known SIRT1 inhibitor Ex527 has positive effects on survival of neuronal cells expressing mutant SOD1, but this effect is neither mediated by SIRT1 inhibition nor by SIRT2 inhibition. These data call for caution in proposing sirtuin modulation as a target for treatment.

*Cell Death and Disease* (2014) 5, e1296; doi:10.1038/cddis.2014.247; published online 19 June 2014

Accumulating evidence indicates that altered acetylation homeostasis has a determinant role in the pathogenesis of amyotrophic lateral sclerosis (ALS), a late-onset neurodegenerative disorder characterized by progressive muscle atrophy and paralysis because of the death of upper and lower motoneurons.<sup>1</sup>

Acetylation is controlled by two classes of enzymes with opposite function: histone acetyltransferases (HATs) and histone deacetylases (HDACs). During neurodegeneration, the levels of acetylation in neurons are decreased globally<sup>2,3</sup> as a consequence of an imbalance in the acetylation apparatus because of general loss of HATs.<sup>4–6</sup> Once the balance is disturbed and the HAT/HDAC ratio shifts in favor of HDAC in terms of availability and enzymatic functionality, an altered transcription profile is observed, typically represented by the repression of pro-survival molecules and the derepression of several pro-apoptotic gene products.<sup>2,3</sup> Thus, in the past decade, the use of HDAC inhibitors has been considered a potential and attractive therapeutic approach.<sup>5,7–11</sup>

In mammals, 18 HDACs have been identified and classified based on cofactor dependency and sequence similarity. Two families have been described: the ‘classical’ HDACs with 11

members that require Zn<sup>2+</sup> for deacetylase activity, and the sir2-related HDACs called Sirtuins (silent information regulator (SIRT)) with 7 members that require NAD<sup>+</sup> as cofactor.

Up to date, little is known about the involvement of the individual HDAC isoforms in ALS onset and progression and a thorough survey of all isoforms has never been carried out.

Previous work on post-mortem ALS brain and spinal cord specimens indicates a reduction of HDAC11 mRNA and increased HDAC2 levels.<sup>12</sup>

A crucial role of muscle HDAC4 and its regulator microRNA-206 was suggested in the G93A-SOD1 mouse model of ALS<sup>13</sup> and, more recently, it has been observed that HDAC4 mRNA and protein levels in muscle are greater in patients with rapidly progressive ALS, and this negatively influences reinnervation.<sup>14</sup> These studies strongly suggest a negative role of muscle HDAC4 upregulation on the reinnervation process.

The role of HDAC6 is still debated, possibly because it catalyzes multiple reactions.<sup>15</sup> An *in vitro* interaction between TDP-43 and HDAC6 has been demonstrated, suggesting that the lack of activity of HDAC6 induced by TDP-43 may be a pathogenic factor in ALS.<sup>16</sup> More recently, Taes *et al.*<sup>17</sup> reported that the deletion of HDAC6 in an ALS mouse model

<sup>1</sup>Institute for Cell Biology and Neurobiology, CNR, Rome, Italy; <sup>2</sup>Fondazione Santa Lucia IRCCS, Rome, Italy; <sup>3</sup>Department of Biology, University of Rome Tor Vergata, Rome, Italy; <sup>4</sup>INSERM U1118, Laboratoire de Mécanismes Centraux et Périphériques de la Neurodégénérescence, Strasbourg, France and <sup>5</sup>Université de Strasbourg, Faculté de Médecine, UMRS1118, Strasbourg, France

\*Corresponding author: MT Carri, Department of Biology, University of Rome Tor Vergata, Via della Ricerca Scientifica, Rome 00133, Italy. Tel: +39 6 501703087; Fax: +39 6 501703323; E-mail: carri@Bio.uniroma2.it

**Abbreviations:** HDAC, histone deacetylase; HAT, histone acetyltransferase; ALS, amyotrophic lateral sclerosis; SOD1, Cu-Zn superoxide dismutase; SIRT, silent information regulator-sirtuin; RT-PCR, real-time PCR; UPL, universal probe library

Received 05.3.14; revised 22.4.14; accepted 23.4.14; Edited by A Verkhratsky

significantly extends survival and maintains motor axon integrity without affecting disease onset. This protective effect is associated with increased  $\alpha$ -tubulin acetylation. However, it has also been reported that HDAC6 knockdown increases mutant Cu–Zn superoxide dismutase (SOD1) aggregation in cultured cells and mutant G93A-SOD1 can modulate HDAC6 activity and increase tubulin acetylation.<sup>18</sup>

Some experimental evidence for a role of Sirtuins in ALS is also available. SIRT1 overexpression protects neurons against toxicity induced by mutant G93A-SOD1 in both cultured neurons and mouse brain.<sup>19</sup> SIRT1 is upregulated in the spinal cord of mutant G37R-SOD1 mice,<sup>19</sup> in the cortex, hippocampus, spinal cord and thalamus of G93A-SOD1 transgenic mice<sup>20</sup> and in spinal neurons from post-mortem patient samples,<sup>21</sup> whereas it is reduced in primary motor cortex.<sup>21</sup> Deletion of SIRT2 fails to affect the disease course, and also does not modify  $\alpha$ -tubulin acetylation in the G93A-SOD1 mouse,<sup>17</sup> whereas SIRT3 protects against mitochondrial fragmentation and neuronal cell death induced by mutant SOD1.<sup>22</sup>

Thus, the proposed neuroprotective/neurotoxic role of Sirtuins still remains debated.<sup>21</sup>

With the aim to better understand whether specific HDAC isoforms play a major role in ALS onset and progression and whether their modulation may rescue the ALS phenotype, in this work we analyzed the specific expression pattern of all HDACs in spinal cord and muscle from two ALS transgenic mice models (G93A-SOD1 and G86R-SOD1) and in neuronal and muscle cell cultures expressing mutant SOD1.

Only a few HDACs showed an altered expression profile in ALS tissues and therefore we focused our interest on the most extensively studied SIRT1 and on treatment with its known modulators.

## Results

**Expression of selected HDAC isoforms is modulated during progression of the disease in mice.** In order to get a complete picture of known HDACs in the course of ALS, we have performed an extended analysis of the expression of all HDACs by real-time PCR (RT-PCR) on mRNA extracted from the spinal cord of two well-characterized models for mutant SOD1-linked ALS. Both G93A-SOD1 and G86R-SOD1 transgenic mice essentially recapitulate the human form of the disease, although with a difference in age of onset and survival (see Materials and Methods). In this paper, we report data on all the 11 canonical class I–II–IV isoforms and two class III Sirtuins (SIRT1 and SIRT2). We have not been able to monitor SIRT4–7, possibly because of their low level of expression. Data on SIRT3 are the subject of a separate paper (C Valle *et al.*, manuscript in preparation). In the spinal cord, mRNA expression of most HDACs is not grossly affected (Supplementary Figure S1) during the course of the disease in both mice strains compared with age-matched nontransgenic littermates, with the notable exception of HDAC5 and SIRT1 that clearly decrease during progression and HDAC11 and SIRT2 that clearly increase in this tissue during progression of the disease (Figure 1). As observed in

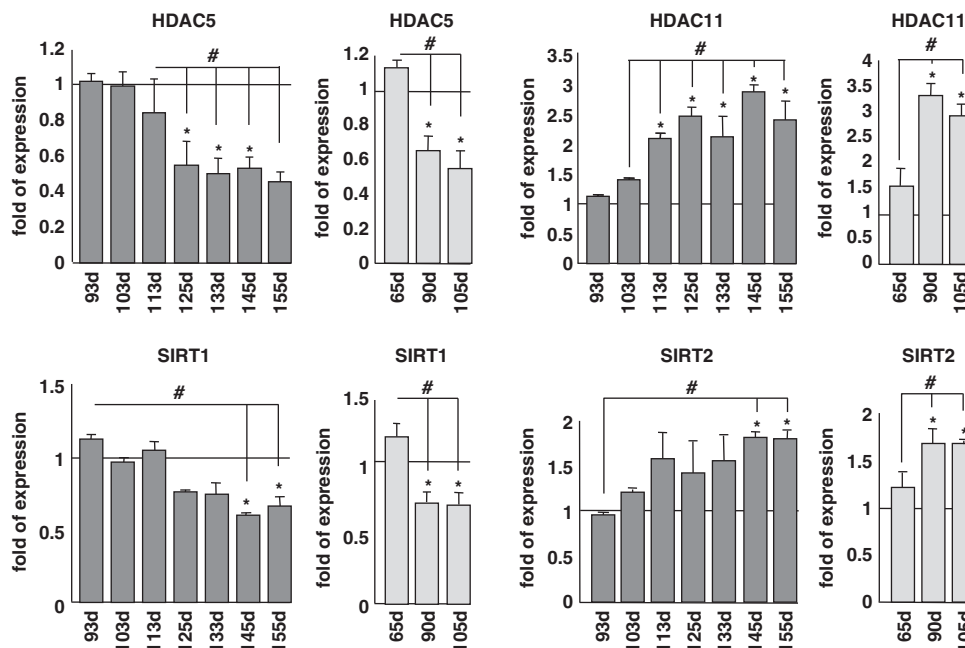


**Figure 1** Expression of selected HDACs in the spinal cord of ALS mice. The cDNAs obtained from total RNA extracted from spinal cord of G93A-SOD1 (dark bars) and G86R-SOD1 (light bars) transgenic mice and their nontransgenic littermates were analyzed by quantitative RT-PCR to assess mRNA expression of HDAC5, HDAC11, SIRT1 and SIRT2. Analysis was performed at different stages of disease starting from early presymptomatic to end stage. The mRNA levels from control mice are set as 1. Results were obtained from at least three different mice from each stage and are expressed as the ratio between the average of values, normalized to the average values of two different housekeeping genes, from nontransgenic and transgenic mice. \* $P < 0.05$  with respect to nontransgenic mice of the same age; # $P < 0.05$  with respect to presymptomatic or early symptomatic transgenic mice for G93A-SOD1 genotype, and with respect to presymptomatic or symptomatic transgenic mice for G86R-SOD1 genotype

western blot analysis from the same tissue, this trend is conserved at the level of immunoreactive protein for HDAC5, HDAC11 and SIRT1, although changes are slightly delayed in the course of the disease, whereas SIRT2 protein level is not significantly altered (Figures 2a–d and Supplementary Figure S2). Furthermore, expression of mutant SOD1 does not change the localization of SIRT1, which is mainly nuclear, and of SIRT2, which is mainly cytosolic, as in nontransgenic mice (Figure 2e). Interestingly, the expression pattern of SIRT1 and SIRT2 is not conserved in the muscle (*tibialis anterior*) from G93A-SOD1 transgenic mice, where SIRT1

increases and SIRT2 is not changed during the disease (Figures 3a and b).

The trend observed in mice tissues is reproduced quite faithfully in both corresponding cell models examined. In differentiated neuronal cells expressing mutant SOD1, protein levels are again decreased for HDAC5 and SIRT1 and increased for HDAC11 (Figures 4a and b). However, upon expression of mutant SOD1, there are no changes in the acetylation state of SIRT1 main targets p53 and PGC1 $\alpha$  (Figures 4a, c and d) or main target of SIRT2 tubulin (Figure 4a). Moreover, expression of mutant SOD1 does not

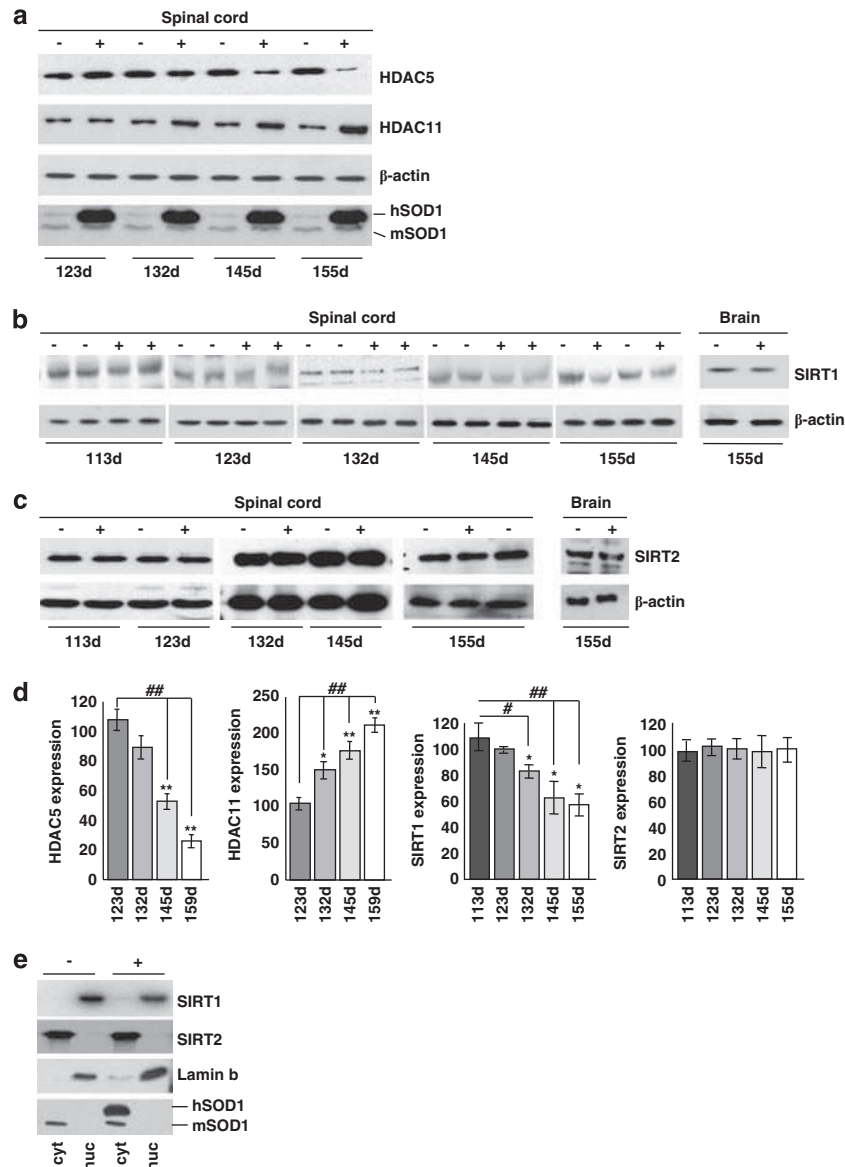


**Figure 2** HDAC protein expression in spinal cord of ALS mice. (a) Western blot analysis of 30  $\mu$ g of total protein extract from spinal cord of transgenic (+) and nontransgenic (–) G93A-SOD1 mice from symptomatic (123d) to end stage (155d) of disease using antibodies against HDAC5 and HDAC11,  $\beta$ -actin as a loading control and SOD1 to confirm genotypes. hSOD1 indicates exogenous human SOD1, and mSOD1 is endogenous mouse SOD1. (b and c) Same as (a) but starting from early symptomatic stage of disease (113d) using antibodies against SIRT1 and SIRT2. Total brain protein extract was used to confirm tissue specificity. (d) Densitometric analysis of data from  $n = 4$  G93A-SOD1 and  $n = 4$  nontransgenic mice from different experiments. \* $P < 0.05$  and \*\* $P < 0.01$  with respect to nontransgenic mice of the same age; ### $P < 0.01$  with respect to symptomatic transgenic mice. (e) Western blot analysis of cytosolic (cyt) and nuclear (nuc) protein extract from late symptomatic (145 days) G93A-SOD1 (G93A) and nontransgenic (–) mice using antibodies against SIRT1 and SIRT2. Fractions were controlled for the presence of the nuclear marker lamin B and the cytosolic marker SOD1

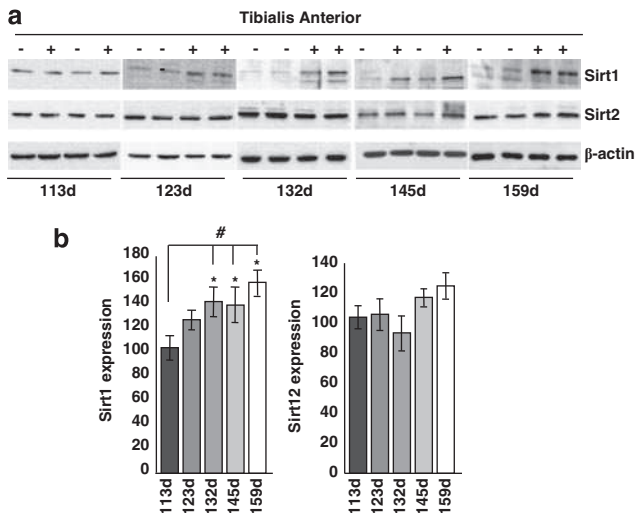


**Figure 3** SIRT1 and SIRT2 expression in the muscle of G93A-SOD1 mice. (a) Western blot analysis of 20  $\mu$ g of total protein extract from *Tibialis anterior* of transgenic (+) and nontransgenic (-) G93A-SOD1 mice from symptomatic (113d) to end stage (159d) of disease using antibodies against SIRT1 and SIRT2.  $\beta$ -Actin was used as loading control. (b) Densitometric analysis of  $n=4$  G93A-SOD1 and  $n=4$  nontransgenic mice from different experiments. Values significantly different from relative controls are indicated with \* $P < 0.05$  with respect to nontransgenic mice of the same age; # $P < 0.05$  with respect to early symptomatic transgenic mice

change the localization of these proteins as in differentiated SH-SY5Y cells, HDAC5, HDAC11 and SIRT1 are mainly nuclear whereas SIRT2 is cytosolic, as in control cells (Figure 4e). In addition, SIRT1 increases in C2C12 muscle cells expressing G93A-SOD1 (Figures 5a and b) where, at variance with SH-SY5Y cells, p53 is a target of SIRT1 (see below).

**Modulation of sirtuins and protection from cell damage.** SIRT1 is considered a pro-survival protein,<sup>23</sup> whereas the role of SIRT2 is still not clearly established.<sup>23</sup> Based on the results reported above, we further investigated whether known inhibitors or activators of SIRT1 are able to mimic the effects of G93A mutant SOD1 or to revert its toxicity in neurons. To this aim, we treated differentiated SH-SY5Y cells expressing Wt or mutant G93A-SOD1 with AGK2 (SIRT2 inhibitor), Ex527 (SIRT1 inhibitor), SIRTinol (SIRT1 and SIRT2 inhibitor) and SRT1720 (SIRT1 activator) (Figure 6a).

As shown in Figure 6, only Ex527 is able to restore viability in neuronal cells infected with viral vectors coding for the mutant protein (Figure 6b) and to prevent caspase-3 activation in a dose-dependent manner (Figure 6c). SIRTinol, which similarly to Ex527 efficiently inhibits SIRT1 activity, has no positive effect in preventing toxicity by mutant SOD1 and SRT1720, which efficiently increases SIRT1 activity, neither affects basal viability nor modulates SOD1 toxicity.

**G93A-SOD1 toxicity is not mediated by p53 acetylation state or by IRS-2/Ras/ERK1/2 pathway.** Overall, the above results suggest that Ex527 counteracts mutant SOD1 toxicity in neuronal cells independently from SIRT1 inhibition.

Indeed, by western blot analysis we could neither detect significant differences in the level of acetylated p53 (SIRT1 direct target) nor in the level of Erk1/2 and phospho-Erk1/2 in SH-SY5Y cells (Figures 7a and b). At the same time, the level of acetylated tubulin also remains unchanged (Figures 7a and b). Furthermore, the MEK1/2 inhibitor SL327, which is known to act immediately upstream of ERK1/2 in the IRS-2/Ras/Erk1/2 pathway, does not protect SH-SY5Y cells from G93A-SOD1 toxicity (Figure 7c). Similar results were obtained with MEK inhibitor UO126 (not shown). Interestingly, p53 is a target of SIRT1 acetylation in C2C12 cells (Figures 7d and e) but not in SH-SY5Y cells.

That the protective effect of Ex527 is independent from SIRT1 inactivation is further demonstrated by results reported in Figure 8. Constitutive overexpression of SIRT1 in SH-SY5Y cells (Figures 8a and b) efficiently increases SIRT1 activity (Figure 8c) but is not able to protect cells from mutant SOD1 toxicity in terms of viability (Figure 8d), caspase-3 activation (Figure 8e) and PARP cleavage (Figures 8f and g).

## Discussion

The use of HDAC inhibitors has been repeatedly suggested as a potential and attractive therapeutic approach for ALS treatment. However, in our opinion, the results in the literature and in this work should be pondered critically before any clinical attempt.

This consideration arises from the following observations:

(1) The pattern of expression of the various HDAC isoforms is not conserved between spinal cord and muscle of ALS mice. This suggests that systemic administration of any known modulator of these enzymes would have conflicting outcomes in different tissues and possibly bring no benefit to patients.

(2) Current knowledge of HDAC activity is still incomplete. For instance, data in this work suggest that p53 is not a molecular target of SIRT1 in neuronal cells, whereas it is SIRT1 dependent in muscle cells, at least in culture conditions where there is no neuron-muscle cross-talk. This implies that HDAC targets may be different in different cell types or tissues and may reflect a different role of these proteins in specific cell types, where they may exert a protective role or contribute to increase toxicity from the expression of G93A-SOD1. This is in line with a recent report<sup>17</sup> that tubulin is not a major target of SIRT2 in the nervous system.

(3) Current knowledge of HDAC modulators is still incomplete. Based on the observation that SIRT1 is down-regulated during progression of the disease in spinal cords of ALS mice, in this work we have focused on the possibility to activate SIRT1 as a neuroprotective strategy.

SIRT1 mediates heterochromatin formation through deacetylation of histones H1, H3 and H4,<sup>24,25</sup> and is also involved in the acetylation of nonhistone proteins, mainly transcription factors or coactivators, including p53, FOXOs, PGC1 $\alpha$ , p73, BCL6 and others.<sup>26-28</sup> Because of its ability to deacetylate a variety of substrates, SIRT1 is considered an important regulatory key in a broad range of physiological functions, including tumorigenesis,<sup>29</sup> metabolism,<sup>30</sup> aging<sup>31</sup> and neurodegeneration.<sup>32-34</sup>

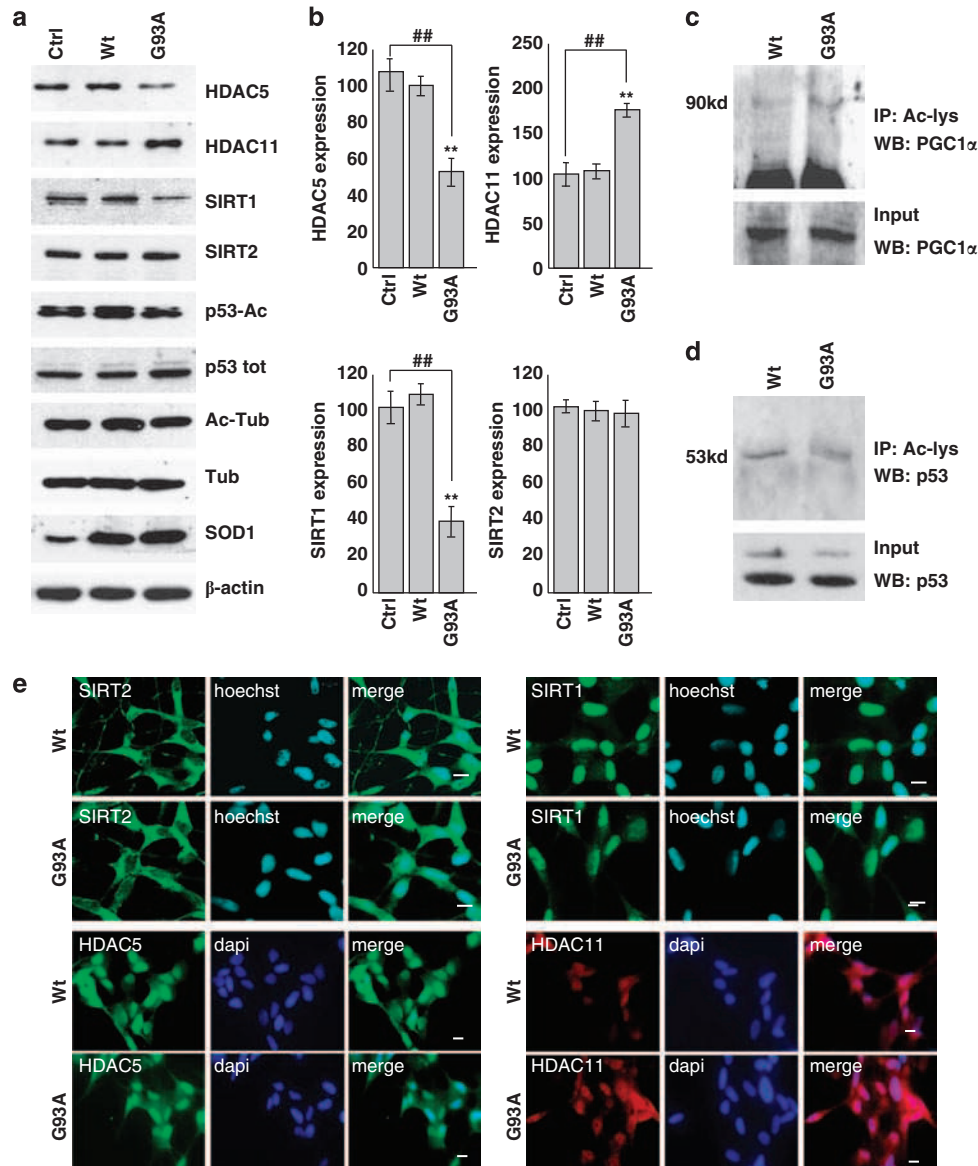


**Figure 4** Protein expression patterns of HDAC5, HDAC11, SIRT1 and SIRT2 in differentiated human SH-SY5Y neuroblastoma cells. SH-SY5Y cells were uninfected (Ctrl) or infected with adenoviral vectors coding for wild-type SOD1 (Wt) or G93A-SOD1 (G93A). (a) Western blot analysis of 20 µg of cell lysate using antibodies against HDAC5, HDAC11, SIRT1, SIRT2, p53-Ac and Ac-tubulin. β-Actin was used as loading control, SOD1 as infection control, and P-53 and tubulin to monitor the acetylation rate. (b) Densitometric analysis of  $n = 3$  experiments as in (a). Values significantly different from relative controls are indicated with \*\*,# $P < 0.01$ . (c and d) Western blot analysis to detect PGC1α and p53 acetylation, respectively, in the immunoprecipitate with anti Ac-lysine antibody. In the lower panel, 5% of input is shown. (e) Immunolocalization of HDAC5, HDAC11, SIRT1 and SIRT2. Panels show typical images observed in  $n = 3$  independent experiments. Scale bar: 5 µm

We analyzed the effects of different activators/inhibitors on SH-SY5Y cells infected with adenoviral vector coding for G93A-SOD1. Unexpectedly, SIRT1 inhibitor Ex527 is the only drug that is able to rescue the ALS phenotype in the neuronal cells expressing the mutant protein. Ex527 was originally described as a compound inhibiting the activity of SIRT1 in nanomolar concentration (and SIRT2 at micromolar concentrations). However, SIRTinol, which similarly to Ex527 efficiently inhibits SIRT1 activity, and AGK2, which inhibits SIRT2 activity, have no positive effect in this model. Furthermore, the beneficial effect of Ex527 seems to be independent of the known SIRT1 pathway in these cells and overexpression of SIRT1 *per se* does not counteract

mutant SOD1 toxicity. Interestingly, SRT1720 efficiently increases SIRT1 activity without affecting basal viability or modulating SOD1 toxicity. This supports that SIRT1 is not a pro-survival protein in the ALS context.

Finally, Ex527 efficiently stimulates p53 acetylation in muscle cells where SIRT1 is increased by mutant SOD1 expression whereas it has no effect on the same target in neuronal cells (Figure 7).

Overall, these data suggest that SIRT1 inhibitor Ex527 has other, previously unappreciated and possibly tissue-specific properties that should be further investigated. Understanding the mechanisms underlying the neuroprotective effects of Ex527 on neurons may offer new perspective to develop

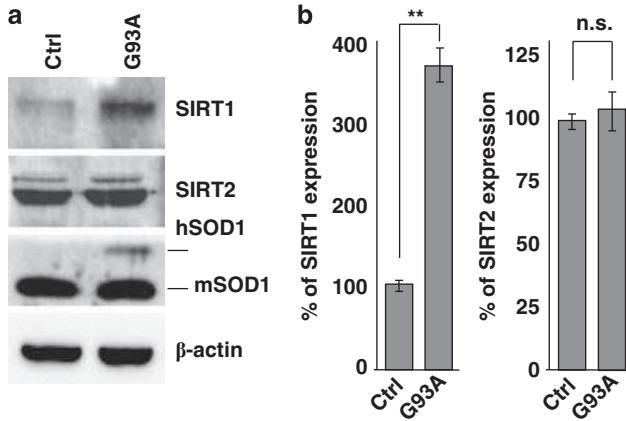


**Figure 5** Protein expression patterns of SIRT1 and SIRT2 in mouse myoblast C2C12 cells. Untransfected C2C12 (Ctrl) and C2C12 cells constitutively expressing G93A-SOD1 (G93A) were subjected to differentiation protocol to induce expression of the transgene under the myosin heavy chain promoter. (a) Western blot analysis of 20  $\mu$ g protein from cells lysates obtained 5 days after differentiation of C2C12 cells expressing G93A-SOD1 (G93A) or untransfected (Ctrl) using antibodies against SIRT1 and SIRT2. SOD1 was used to control genotype,  $\beta$ -actin as loading control. (b) Densitometric analysis of  $n=3$  experiments as in (a). Values significantly different from relative controls are indicated with  $**P<0.01$ ; n.s. indicates values that do not differ significantly

innovative strategies for treating ALS and neurodegenerative disorders.

#### Materials and Methods

**Antibodies and reagents.** The antibodies used in this study are: anti-HDAC1, anti-HDAC2, anti-SIRT2 and anti-PGC1 rabbit polyclonal (Santa Cruz Biotechnology, Dallas, TX, USA); anti-HDAC3, anti-HDAC6 and anti-lamin B goat polyclonal (Santa Cruz Biotechnology); anti-HDAC4 mouse polyclonal (Santa Cruz Biotechnology); anti-HDAC5 and anti-HDAC11 rabbit polyclonal (Abcam, Cambridge, UK); anti-HDAC7 rabbit polyclonal (Novus Biologicals, Littleton, CO, USA); anti-HDAC8 and anti-HDAC9 mouse monoclonal (Novus Biologicals); anti-HDAC10 rabbit polyclonal (Millipore, Burlington, MA, USA); anti-SIRT1 (mouse specific), anti-acetylated-lysine, anti-cleaved-PARP, anti-ERK1/2 and anti-Phospho-ERK1/2 rabbit polyclonal (Cell Signaling Technology, Beverly, MA, USA); anti-SIRT1 clone 10E4 mouse monoclonal (Millipore); anti-SIRT1 rabbit polyclonal (Millipore); anti-acetyl-p53 rabbit monoclonal (Millipore); anti-p53 mouse monoclonal (Abcam); anti-tubulin, anti-acetyl-tubulin and anti- $\beta$ -actin mouse monoclonal (Sigma-Aldrich, St. Louis, MO, USA); anti-SOD1 rabbit polyclonal (Enzo Life Science, Plymouth Meeting, PA, USA); anti-rabbit, anti-mouse and anti-goat peroxidase-conjugated secondary antibody (Amersham, Pittsburgh, PA, USA); and anti-rabbit, anti-mouse FITC or Cy3-conjugated secondary antibody (Sigma-Aldrich). All antibodies were used at the dilution recommended by the manufacturer's instructions.

AGK2, Ex527, Sirtinol, SRT1720 and SL327 were from Tocris Bioscience (Bristol, UK); all of them were resuspended in an appropriate volume of DMSO and kept stored at  $-80^{\circ}\text{C}$  before use.

All reagents used, unless otherwise specified, were from Sigma-Aldrich.

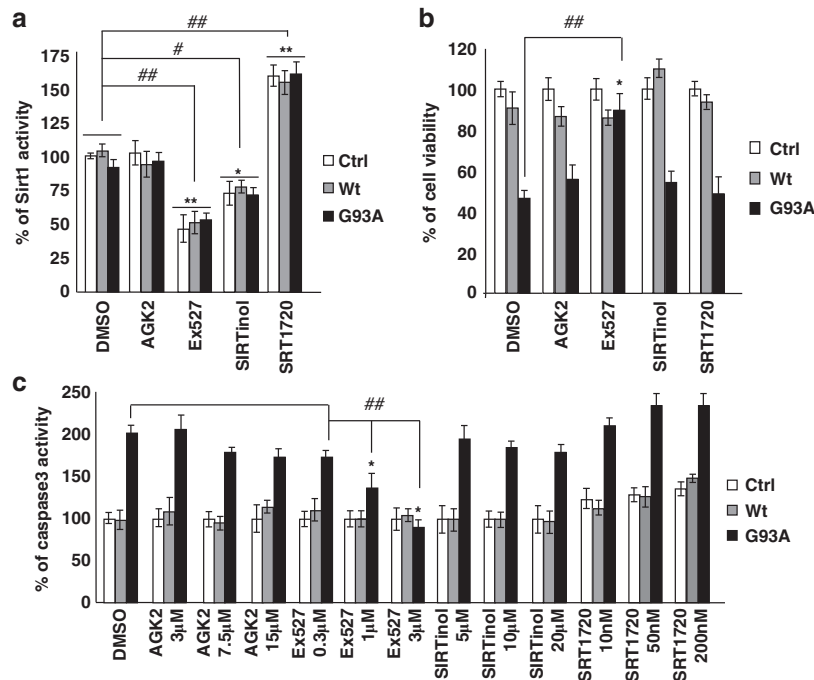


**Figure 6** Effect of SIRT1 and SIRT2 modulation in differentiated SH-SY5Y cells. (a) SIRT1 activity was measured by a fluorometric assay on 40  $\mu$ g of total protein extract from either uninfected (Ctrl) and cells infected with adenoviral vectors coding for Wt-SOD1 (Wt) and G93A-SOD1 (G93A) treated with one of the following: 15  $\mu$ M AGK2, 3  $\mu$ M Ex527 and 20  $\mu$ M Sirtinol that inhibit SIRT2, SIRT1 and both Sirtuins, respectively; and 10 nM SRT1720 that activates SIRT1. Activity is reported as percent of the relative uninfected DMSO-treated control and reported as the mean  $\pm$  S.D. of three independent experiments with each sample in triplicate. Values significantly different from relative controls are indicated with  $*P<0.05$  and  $**P<0.01$  with respect to Ctrl; and  $\#P<0.05$  and  $\#\#P<0.01$  with respect to DMSO-treated cells. (b) SH-SY5Y cells either uninfected (Ctrl) or infected with adenoviral vectors coding for Wt-SOD1 (Wt) and G93A-SOD1 (G93A) were treated with 15  $\mu$ M AGK2, 3  $\mu$ M Ex527, 20  $\mu$ M Sirtinol and 10 nM SRT1720. Cell viability was assessed by the MTS assay 48 h after infection and drug treatments. Absorbance at 490 nm are expressed as percent of the relative uninfected control cells and reported as the mean  $\pm$  S.D. of three independent experiments made in triplicate. Values significantly different from relative controls are indicated with  $*P<0.05$  with respect to Ctrl and  $\#\#P<0.01$  with respect to DMSO-treated cells. (c) Cells either uninfected (Ctrl) or infected with adenoviral vectors coding for Wt-SOD1 (Wt) and G93A-SOD1 (G93A) were treated with three increasing doses of AGK2, Ex527, Sirtinol or SRT1720. Cell protein extracts were assayed, 48 h after infection and drug treatment, for Caspase-3 activity by a fluorescence enzymatic assay and reported as percent of the relative uninfected control cells. Mean  $\pm$  S.D. of four independent experiments is given. Values significantly different from the relative controls are indicated with  $*P<0.05$  with respect to Ctrl and  $\#\#P<0.01$  with respect to DMSO-treated cells

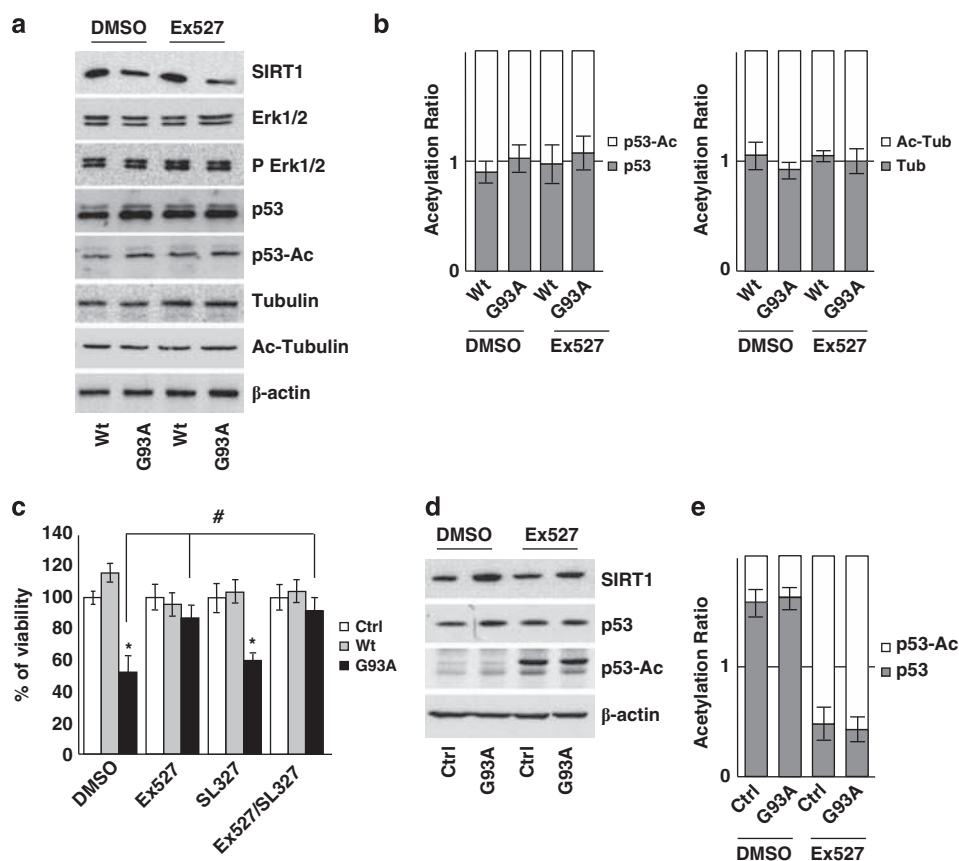


**Figure 7** G93A-SOD1 toxicity is not mediated by p53 acetylation state or by IRS-2/Ras/ERK1/2 pathway in SH-SY5Y cells. **(a)** Western blot analysis of 20  $\mu$ M of total protein extract from cells infected with adenoviral vectors coding for Wt-SOD1 (Wt) and G93A-SOD1 (G93A) and treated with 3  $\mu$ M Ex527 or DMSO. Antibodies against SIRT1, Erk1/2, pErk1/2, p53, p53-Ac, tubulin and Ac-tubulin were used.  $\beta$ -Actin was used as loading control. One representative blot is shown from three independent experiments giving comparable results. **(b)** Densitometric analysis of results as in **(a)**; data are expressed as acetylation ratio of p53 and tubulin. **(c)** Cells infected with adenoviral vectors coding for Wt-SOD1 (Wt) and G93A-SOD1 (G93A) were treated with 3  $\mu$ M Ex527 or with 3  $\mu$ M SL327 or both. Cell viability was assessed and reported for Figure 5a. Values significantly different from relative controls are indicated with \* $P < 0.05$  with respect to Ctrl and # $P < 0.05$  with respect to DMSO. **(d)** Western blot analysis of 20  $\mu$ M of total protein extract from C2C12 cells differentiated for 5 days and expressing G93A-SOD1 (G93A) or untransfected (Ctrl). Antibodies against SIRT1, p53 and p53-Ac were used.  $\beta$ -Actin was used as loading control. One representative blot is shown from three independent experiments giving comparable results. **(e)** Densitometric analysis of data as in **(d)**; data are expressed as acetylation ratio of p53

**Animals.** All animal procedures have been performed according to the European Guidelines for the use of animals in research (86/609/CEE) and the requirements of Italian and French laws (D.L. 116/92, Directive 2010/63/EU). The ethical procedure has been approved by the Animal welfare office, Department of Public Health and Veterinary, Nutrition and Food Safety, General Management of Animal Care and Veterinary Drugs of the Italian Ministry of Health (Application number 32/08 of 7 July 2008; Approval number 744 of 9 January 2009) and the regional ethics committee CREMEAS 35 (approval number AL/01/20/12). All the experiments were performed by authorized investigators.

All animals have been raised and crossed in the indoor animal house in a 12 h light/dark cycle in a virus/antigen-free facility with controlled temperature and humidity and have been provided with water and food *ad libitum*.

G93A-SOD1 mice B6.Cg-Tg(SOD1 G93A)1Gur/J were purchased from The Jackson Laboratory (Bar Harbor, ME, USA) and were on C57BL/6J background. In our animal house, these mice have an onset of disease at  $113 \pm 6$  days (determined as previously described<sup>35</sup>) and survival of  $156 \pm 8$  days.

G86R-SOD1 mice were initially obtained from Jon W Gordon (New York, NY, USA). In our animal house, these mice have an onset of disease at  $90 \pm 4$  days and survival of  $108 \pm 5$  days.

Mice compared in this study were all littermates and housed together to minimize environmental factors. Mice were genotyped using PCR protocols from The Jackson Laboratory or as previously described.<sup>36</sup> At the indicated time, mice were anesthetized with  $40 + 5$  mg/kg ketamine-xylazine, killed and dissected for the different experiments. All efforts were made to minimize suffering.

For the staging of the disease of transgenic mice we relied on previous studies from our laboratories.<sup>5,35,37</sup>

#### Cell culture, adenoviral infection and plasmid transfection.

Human neuroblastoma cells (SH-SY5Y, from European Collection of Cell Cultures, Salisbury, UK) and murine myoblasts (C2C12, either untransfected or transfected for the inducible expression of G93A-SOD1, a kind gift of Dr A Musarò) were grown in DMEM-Glutamax (Invitrogen, Carlsbad, CA, USA) supplemented with 10% FCS (Invitrogen) at 37°C in an atmosphere of 5% CO<sub>2</sub> in air.

Where specified, SH-SY5Y cells were subjected to a differentiation protocol as previously described.<sup>38</sup> Briefly, cells plated at the density of  $25 \times 10^3$  cells/cm<sup>2</sup> were washed with PBS and differentiated in DMEM-Glutamax supplemented with 1% N-2 (Invitrogen) without serum by the addition of 10  $\mu$ M retinoic acid for 3 days, after which with 100 ng/ml brain-derived neurotrophic factor was added to the medium and cells were kept for 3 more days in culture.

Myogenic differentiation of C2C12 cells at ~80% cell confluence was obtained by substituting the medium with fresh medium supplemented with 2% horse serum (EuroClone, Milan, Italy) to induce expression of mutant SOD1 under the myosin heavy chain promoter.<sup>39,40</sup>

Construction of recombinant adenoviruses expressing Wt-SOD1 as well as G93A-SOD1 was carried out in a previous work.<sup>37</sup> Infection of SH-SY5Y cells was carried out for 1 h in OPTIMEM (Invitrogen); after removal of the virus, cells were subjected to the differentiation protocol and grown for the indicated period of times before being used for further experimental manipulations.

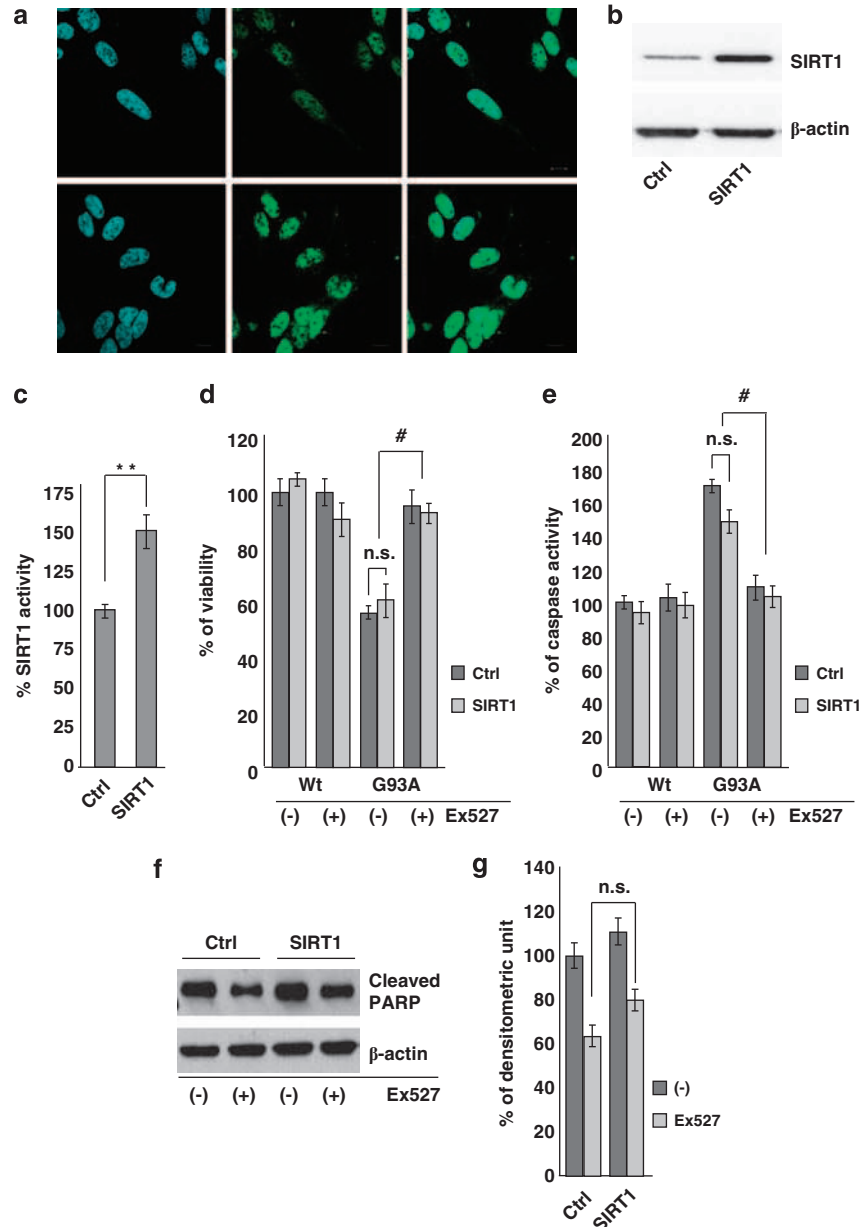


**Figure 8** Constitutive overexpression of SIRT1 does not protect differentiated SH-SY5Y neuroblastoma cells from G93A-SOD1 toxicity. **(a)** Immunofluorescence analysis on SH-SY5Y cells untransfected or stably transfected for SIRT1 overexpression using antibodies against SIRT1. Scale bar: 10  $\mu$ m. **(b)** Western blot analysis of 20  $\mu$ g of total protein extract from cells either untransfected (Ctrl) or stably transfected for SIRT1 overexpression (SIRT1) using antibodies against SIRT1 and  $\beta$ -actin as a loading control. One representative blot from three independent experiments giving comparable results is shown. **(c)** SIRT1 activity was measured by a fluorometric assay on 40  $\mu$ g of total protein extract from either untransfected (Ctrl) or stably transfected cells (SIRT1). Activity is reported as percent of control cells and as the mean  $\pm$  S.D. of three independent experiments with each sample done in triplicate. Values significantly different from relative controls are indicated with \*\* $P < 0.01$  with respect to Ctrl. **(d)** Cell viability of untransfected (Ctrl) and stably transfected (SIRT1) cells infected with adenoviral vectors coding for Wt-SOD1 (Wt) and G93A-SOD1 (G93A). Values are the mean  $\pm$  S.D. of three independent experiments in triplicate. Values that do not differ significantly are marked with n.s. **(e)** Total protein extracts from cells as in **(d)** and treated with 3  $\mu$ M Ex527 were assayed after 48 h for Caspase-3 activity. Data are reported as the mean  $\pm$  S.D. of three independent experiments. Values that do not differ significantly with respect to the relative control are marked with n.s.; # $P < 0.05$  significantly different with respect to DMSO. **(f)** Western blot analysis of cleaved PARP in 20  $\mu$ g of total protein extract from cells as in **(d)** and treated with DMSO (-) or 3  $\mu$ M Ex527 (+). Antibodies against  $\beta$ -actin were used as loading control. One representative blot is shown from three independent experiments giving comparable results. **(g)** Densitometric analysis of  $n = 4$  experiments as in **(f)**. n.s. indicates values that do not differ significantly

Human cDNA coding for SIRT1 (accession number AF083106) was cloned by reverse transcription-PCR from human SH-SY5Y neuroblastoma cell cDNA using the forward primer 5'-AAAAAGCTTATGGCGGACGAGCGGCC-3' and the reverse primer 5'-TTTCTCGAGCTATGATTGTTTGGATAG-3'. The resulting PCR

fragment was inserted into *HindIII/XhoI* restriction sites of pcDNA3 (Invitrogen). Plasmid construction was verified by automated sequencing. Transfection for either transient or stable expression of SIRT1 was obtained with Lipofectamine Plus reagent (Invitrogen) according to the manufacturer's instructions.

**Table 1** List of primers and probes used for Real Time PCR

Target	Forward primer (5'–3')	Reverse primer (5'–3')	UPL probe number
MmlHdac1	TGGTCTCTACCGAAAAATGGAG	TCATCACTGTGGTACTTGGTCA	73
MmlHdac2	AAAGGAGCAAAGAAGGCTAGG	GTCCTTGGATTTGTCTTCTTCC	94
MmlHdac3	TTCAACGTGGGTGATGACTG	TTAGCTGTGTTGCTCCTTGC	32
MmlHdac4	CACACCTCTGGAGGGTACAA	AGCCCATCAGCTGTTTTGTC	53
MmlHdac5	GAGTCCAGTGCTGGTTACAAAA	TACACCTGGAGGGGCTGTAA	105
MmlHdac6	CGCTGTGTGTCCTTTCAGG	CAGATCAATGTATTCCAGGCTGT	17
MmlHdac7	CCATGGGGGATCCTGAGT	GCAAACCTCTCGGGCAATG	71
MmlHdac8	GGTGATGAGGACCATCCAGA	TCCTATAGCTGCTGCATAGTCAA	5
MmlHdac9	TTGCACACAGATGGAGTGG	GGCCCATAGGAACCTCTGAT	32
MmlHdac10	TTCCAGGATGAGGATCTTGC	ACATCCAATGTTGCTGCTGT	60
MmlHdac11	GACGTGCTGGAGGGGAGAC	AAAACCACTTCATCCCTCTTCA	26
MmlSirt1	TCGTGGAGACATTTTTAATCAGG	GCTTCATGATGGCAAGTGG	104
MmlSirt2	CAAGGAAAAGACAGGCCAGA	GCCTTCTTGGAGTCAAAAATCC	10
MmlActβ	AAGGCCAACCGTGAAAAGAT	GTGGTACGACCAGAGGCATAC	56
MmlG6pdx	CAGCGGCAACTAAACTCAGA	TTCCCTCAGGATCCCACAC	53

For stable expression, after selection with 400  $\mu$ g/ml G418 (Gibco BRL, Grand Island, NY, USA), ~25 clones were isolated independently and analyzed in western blot with anti-SIRT1 antibodies. Three clones were chosen for equivalent expression of SIRT1 proteins and used for further analysis. All the clones analyzed gave consistent results and data from one clone are shown.

Conditions for treatments with Sirtuins modulators are given in the Figure legends. All drugs were added to the culture medium starting from infection/differentiation protocol and were maintained in all medium changes. Medium with or without experimental drugs was replaced every 3 days.

**RNA extraction, reverse transcription and RT-PCR.** Total RNA was extracted from spinal cord and muscle of transgenic mice and their nontransgenic littermates at different stages of disease using TRIzol reagent (Invitrogen). The SuperScript III First-Strand reverse transcription system (Invitrogen) was used to synthesize cDNA, with 1 mg of total RNA and random hexamers, according to the manufacturer's instructions. Appropriate negative controls were included (without reverse transcriptase) to determine the presence of genomic DNA contamination. Samples with genomic contamination were treated with DNase I, Amp Grade (Invitrogen) following the manufacturer's instructions.

RT-PCR analysis was performed on custom-designed plates from Roche (Hilden, Germany). Each well contained primers (see Table 1) and probes (UPL (Universal Probe Library) probe) specific for the genes of interest (all canonical HDACs and SIRT1 and SIRT2) designed to pair up within regions to be amplified. Each test was performed in duplicate. As a control for the efficiency of reverse transcription and RNA quality, some wells were prepared with specific oligonucleotides designed to amplify the 3', 5' and central regions of the template; in order to exclude genomic contamination, untranscribed RNA samples were loaded in two wells as negative controls. As housekeeping genes we chose  $\beta$ -actin and glucose-6-phosphate dehydrogenase (G6pdx); both were used for normalization of each sample through the dedicated software (see below). Finally, two wells contained the specific reagents for the human SOD1 in order to have a further control of mice genotype. RT-PCR was performed on G93A-SOD1, G86R-SOD1 and the corresponding nontransgenic control littermate mice. The plates were sealed with a sheet of adhesive plastic and the reaction was carried out in the thermal cycler LightCycler 480 (Roche).

Data analysis was made using LightCycler 480 SW1.5 software (Roche) and the subsequent analysis to make a comparison of different plates was made using LightCycler 480 Multiple Plate Analysis software (Roche).

**Tissue homogenates and cell lysis.** Total tissue homogenates were obtained by mechanical dissociation using a Teflon manual homogenizer for 30 s in ice in RIPA buffer (50 mM Tris-HCl, pH 8.0, 1% Triton X-100, 0.25% Na-deoxycholate, 0.1% SDS, 250 mM NaCl, 5 mM EDTA and 5 mM  $MgCl_2$ ) containing a 1:1000 dilution of protease inhibitor cocktail (Sigma-Aldrich). For *tibialis anterior* homogenates, samples had been previously incubated for 30 min in 0.25% Trypsin/EDTA (Invitrogen) at 37°C.

Cell lysates were obtained by resuspending pelleted cells in RIPA buffer.

A clear supernatant was obtained by centrifugation of tissue homogenates or cell lysates at 17 000  $\times$  g for 10 min and protein content was determined using the Bradford protein assay (Bio-Rad, Hercules, CA, USA). Nuclear and cytosolic

fractions from spinal cord were obtained using a low-salt buffer (10 mM Hepes, pH 7.4, 42 mM KCl, 5 mM  $MgCl_2$ , 0.5% CHAPS, 1 mM DTT, 1 mM PMSF and 1 mg/ml leupeptin) to homogenate samples; homogenates were then centrifugated at 2000  $\times$  g for 10 min, supernatants were collected and analyzed as cytosolic fractions in western blot with antibodies anti-SOD1, whereas pellets were lysed in high-salt buffer (50 mM Tris-HCl, pH 7.5, 400 mM NaCl, 1 mM EDTA, 1% Triton X-100, 0.5% Nonidet-P40, 10% glycerol, 2 mM DTT, 1 mM PMSF, protease inhibitor cocktail (Sigma-Aldrich)) for 30 min on ice. Nuclear lysates were then centrifuged at 20 000  $\times$  g, supernatants were collected and analyzed in western blot with antibodies anti-lamin B.

**Immunoblot analysis.** Protein samples were resolved on SDS-polyacrylamide gels and transferred to Hybond-P PVDF membranes (Amersham). Membranes were blocked for 1 h in TBS, 0.1% Tween 20 and 5% non-fat dry milk, followed by an overnight incubation with primary antibodies (see Materials and Methods) diluted in the same buffer. After washing with 0.1% Tween in Tris-buffered saline, the membrane was incubated with peroxidase-conjugated secondary antibody for 1 h, and then washed and developed using the ECL chemiluminescent detection system (Roche). Densitometric analyses were performed using ImageJ software program (National Institutes of Health, Bethesda, MD, USA; <http://imagej.nih.gov/ij/>) and normalized against the signal obtained by reprobating the membranes with mouse anti- $\beta$ -actin or anti-tubulin. The apparent molecular weight of proteins was determined by calibrating the blots with prestained molecular weight markers (Bio-Rad Laboratories, Richmond, CA, USA).

**Immunofluorescence analysis.** Cell cultures were grown on poly-L-lysine-coated glass slides, fixed in 4% paraformaldehyde for 10 min at room temperature, subsequently permeabilized with 0.1% Triton X-100 for 8 min and washed in PBS. Cells were blocked for 30 min in 2% horse serum in PBS and incubated for 1 h at 37°C with primary antibodies followed by fluorescein- or Cy3-conjugated secondary antibodies. After rinsing in PBS, cells were counterstained with 1  $\mu$ g/ml Hoechst 33342 and examined with a Zeiss LSM 510 Confocal Laser Scanning Microscope. Fluorescence images were processed using ZEN 2009 (Carl Zeiss, Milan, Italy) and Adobe Photoshop software (Adobe, San Jose, CA, USA).

**Immunoprecipitation.** Cell lysis was performed in RIPA buffer as described above, protein content was determined using Bradford protein assay (Bio-Rad) and 500  $\mu$ g of lysates were incubated at 4°C for 2 h with a rabbit polyclonal anti-acetyl-lysine antibody diluted 1:100. The immunocomplexes were collected by binding to protein A-Agarose beads (Roche), followed by three washes with lysis buffer and then directly resuspended in Laemmli sample buffer 1  $\times$ .

**Biochemical assays.** Caspase 3 activity was measured with a TruePoint Caspase 3 assay kit (PerkinElmer, Waltham, MA, USA), according to the manufacturer's instructions. Cell viability was assessed by a colorimetric assay using the 3-(4,5-dimethylthiazol-2-yl)-5-(3-carboxymethoxyphenyl)-2-(4-sulphophenyl)-2H-tetrazolium (MTS) assay (CellTiter 96 Aqueous One Solution Assay, Promega, Madison, WI, USA) according to the manufacturer's instructions. Absorbance at 490 nm was measured in a multilabel counter (Victor3-V, PerkinElmer).

The activity of SIRT1 was measured using the SIRT1 Fluorescent Activity Assay Kit (Enzo Life Science) according to the manufacturer's instructions using a fluorescent emission at 460 nm with excitation at 360 nm.

**Statistical analysis.** All data are expressed as means  $\pm$  S.D. of  $n \geq 3$  independent experiments. One-way analysis of variance (ANOVA) followed by Student's *t*-test was used for statistical evaluations. Values significantly different from the relative control are indicated with an asterisk, and values significantly different from another group are indicated with a hash. The level of significance was chosen as  $P < 0.05$ .

### Conflict of Interest

The authors declare no conflict of interest.

**Acknowledgements.** We thank Jean-Philippe Loeffler (INSERM U1118, Strasbourg, France) and Mauro Cozzolino (CNR, Rome, Italy) for critical reading of the manuscript and Monica Nencini (Fondazione Santa Lucia) for skilful technical assistance. Antonio Musarò kindly provided C2C12 cells expressing G93A-SOD1. This work was supported by an 'Association Française contre les Myopathies' grant to LP and an 'Association pour la Recherche sur la Sclérose Latérale Amyotrophique et autres Maladies du Motoneurone' grant to FR.

- Cozzolino M, Pesaresi MG, Gerbino V, Grosskreutz J, Carri MT. Amyotrophic lateral sclerosis: new insights into underlying molecular mechanisms and opportunities for therapeutic intervention. *Antioxid Redox Signal* 2012; **17**: 1277–1330.
- Schmalbach S, Petri S. Histone deacetylation and motor neuron degeneration. *CNS Neurol Disord Drug Targets* 2010; **9**: 279–284.
- Saha RN, Pahan K. HATs and HDACs in neurodegeneration: a tale of disconcerted acetylation homeostasis. *Cell Death Differ* 2006; **13**: 539–550.
- Rouaux C, Jokic N, Mbebi C, Boutillier S, Loeffler JP, Boutillier AL. Critical loss of CBP/p300 histone acetylase activity by caspase-6 during neurodegeneration. *EMBO J* 2003; **22**: 6537–6549.
- Rouaux C, Panteleeva I, René F, Gonzalez de Aguilar JL, Echaniz-Laguna A, Dupuis L *et al*. Sodium valproate exerts neuroprotective effects *in vivo* through CREB-binding protein-dependent mechanisms but does not improve survival in an amyotrophic lateral sclerosis mouse model. *J Neurosci* 2007; **27**: 5535–5545.
- Rouaux C, Loeffler JP, Boutillier AL. Targeting CREB-binding protein (CBP) loss of function as a therapeutic strategy in neurological disorders. *Biochem Pharmacol* 2004; **68**: 1157–1164.
- Ryu H, Smith K, Camelo SI, Carreras I, Lee J, Iglesias AH *et al*. Sodium phenylbutyrate prolongs survival and regulates expression of anti-apoptotic genes in transgenic amyotrophic lateral sclerosis mice. *J Neurochem* 2005; **93**: 1087–1098.
- Sugai F, Yamamoto Y, Miyaguchi K, Zhou Z, Sumi H, Hamasaki T *et al*. Benefit of valproic acid in suppressing disease progression of ALS model mice. *Eur J Neurosci* 2004; **20**: 3179–3183.
- Del Signore SJ, Amante DJ, Kim J, Stack EC, Goodrich S, Cormier K *et al*. Combined riluzole and sodium phenylbutyrate therapy in transgenic amyotrophic lateral sclerosis mice. *Amyotroph Lateral Scler* 2009; **10**: 85–94.
- Yoo YE, Ko CP. Treatment with trichostatin A initiated after disease onset delays disease progression and increases survival in a mouse model of amyotrophic lateral sclerosis. *Exp Neurol* 2011; **231**: 147–159.
- Garbes L, Riessland M, Wirth B. Histone acetylation as a potential therapeutic target in motor neuron degenerative diseases. *Curr Pharm Des* 2013; **19**: 5093–5104.
- Janssen C, Schmalbach S, Boeselt S, Sarlette A, Dengler R, Petri S. Differential histone deacetylase mRNA expression patterns in amyotrophic lateral sclerosis. *J Neuropathol Exp Neurol* 2010; **69**: 573–581.
- Williams AH, Valdez G, Moresi V, Qi X, McAnally J, Elliott JL *et al*. MicroRNA-206 delays ALS progression and promotes regeneration of neuromuscular synapses in mice. *Science* 2009; **326**: 1549–1554.
- Bruneteau G, Simonet T, Bauché S, Mandjee N, Malfatti E, Girard E *et al*. Muscle histone deacetylase 4 upregulation in amyotrophic lateral sclerosis: potential role in reinnervation ability and disease progression. *Brain* 2013; **136**(Pt 8): 2359–2368.
- d'Ydewalle C, Bogaert E, Van Den Bosch L. HDAC6 at the intersection of neuroprotection and neurodegeneration. *Traffic* 2012; **13**: 771–779.
- Fiesel FC, Schurr C, Weber SS, Kahle PJ. TDP-43 knockdown impairs neurite outgrowth dependent on its target histone deacetylase 6. *Mol Neurodegener* 2011; **6**: 64.
- Taes I, Timmers M, Hermus N, Bento-Abreu A, Van Den Bosch L, Van Damme P *et al*. Hdac6 deletion delays disease progression in the SOD1G93A mouse model of ALS. *Hum Mol Genet* 2013; **22**: 1783–1790.
- Gal J, Chen J, Barnett KR, Yang L, Brumley E, Zhu H. HDAC6 regulates mutant SOD1 aggregation through two SMIR motifs and tubulin acetylation. *J Biol Chem* 2013; **288**: 15035–15045.
- Kim D, Nguyen MD, Dobbin MM, Fischer A, Sananbenesi F, Rodgers JT *et al*. SIRT1 deacetylase protects against neurodegeneration in models for Alzheimer's disease and amyotrophic lateral sclerosis. *EMBO J* 2007; **26**: 3169–3179.
- Lee JC, Shin JH, Park BW, Kim GS, Kim JC, Kang KS *et al*. Region-specific changes in the immunoreactivity of SIRT1 expression in the central nervous system of SOD1(G93A) transgenic mice as an *in vivo* model of amyotrophic lateral sclerosis. *Brain Res* 2012; **1433**: 20–28.
- Körner S, Bösel S, Thau N, Rath KJ, Dengler R, Petri S. Differential sirtuin expression patterns in amyotrophic lateral sclerosis (ALS) postmortem tissue: neuroprotective or neurotoxic properties of sirtuins in ALS? *Neurodegener Dis* 2013; **11**: 141–152.
- Song W, Song Y, Kincaid B, Bossy B, Bossy-Wetzel E. Mutant SOD1G93A triggers mitochondrial fragmentation in spinal cord motor neurons: neuroprotection by SIRT3 and PGC-1 $\alpha$ . *Neurobiol Dis* 2013; **51**: 72–81.
- Donmez G, Outeiro TF. SIRT1 and SIRT2: emerging targets in neurodegeneration. *EMBO Mol Med* 2013; **5**: 344–352.
- Imai S, Armstrong CM, Kaeberlein M, Guarente L. Transcriptional silencing and longevity protein Sir2 is an NAD-dependent histone deacetylase. *Nature* 2000; **403**: 795–800.
- Vaquero A, Scher M, Lee D, Erdjument-Bromage H, Tempst P, Reinberg D. Human SirT1 interacts with histone H1 and promotes formation of facultative heterochromatin. *Mol Cell* 2004; **16**: 93–105.
- Pucci B, Villanova L, Sansone L, Pellegriani L, Tafani M, Carpi A *et al*. Sirtuins: the molecular basis of beneficial effects of physical activity. *Intern Emerg Med* 2013; **8**(Suppl 1): S23–S25.
- Nakagawa T, Guarente L. Sirtuins at a glance. *J Cell Sci* 2011; **124**(Pt 6): 833–838.
- Zhang F, Wang S, Gan L, Vosler PS, Gao Y, Zigmund MJ *et al*. Protective effects and mechanisms of sirtuins in the nervous system. *Prog Neurobiol* 2011; **95**: 373–395.
- Song NY, Surh YJ. Janus-faced role of SIRT1 in tumorigenesis. *Ann N Y Acad Sci* 2012; **1271**: 10–19.
- Li X. SIRT1 and energy metabolism. *Acta Biochim Biophys Sin (Shanghai)* 2013; **45**: 51–60.
- Belden WJ, Dunlap JC. Aging well with a little wine and a good clock. *Cell* 2013; **153**: 1421–1422.
- Donmez G. The neurobiology of sirtuins and their role in neurodegeneration. *Trends Pharmacol Sci* 2012; **33**: 494–501.
- Yang Y, Duan W, Li Y, Yan J, Yi W, Liang Z *et al*. New role of silent information regulator 1 in cerebral ischemia. *Neurobiol Aging* 2013; **34**: 2879–2888.
- Pasinetti GM, Bilski AE, Zhao W. Sirtuins as therapeutic targets of caprylic triglyceride in ALS therapy. *Cell Res* 2013; **23**: 1073–1074.
- Crosio C, Valle C, Casciati A, Iaccarino C, Carri MT. Astroglial inhibition of NF- $\kappa$ B does not ameliorate disease onset and progression in a mouse model for amyotrophic lateral sclerosis (ALS). *PLoS One* 2011; **6**: e17187.
- Ripps ME, Huntley GW, Hof PR, Morrison JH, Gordon JW. Transgenic mice expressing an altered murine superoxide dismutase gene provide an animal model of amyotrophic lateral sclerosis. *Proc Natl Acad Sci USA* 1995; **92**: 689–693.
- Pesaresi MG, Amori I, Giorgi C, Ferri A, Fiorenzo P, Gabanella F *et al*. Mitochondrial redox signalling by p66Shc mediates ALS-like disease through Rac1 inactivation. *Hum Mol Genet* 2011; **20**: 4196–4208.
- Encinas M, Iglesias M, Liu Y, Wang H, Muhaisen A, Ceña V *et al*. Sequential treatment of SH-SY5Y cells with retinoic acid and brain-derived neurotrophic factor gives rise to fully differentiated, neurotrophic factor-dependent, human neuron-like cells. *J Neurochem* 2000; **75**: 991–1003.
- Song KS, Scherer PE, Tang Z, Okamoto T, Li S, Chafel M *et al*. Expression of caveolin-3 in skeletal, cardiac, and smooth muscle cells. Caveolin-3 is a component of the sarcolemma and co-fractionates with dystrophin and dystrophin-associated glycoproteins. *J Biol Chem* 1996; **271**: 15160–15165.
- Tang Z, Scherer PE, Okamoto T, Song K, Chu C, Kohtz DS *et al*. Molecular cloning of caveolin-3, a novel member of the caveolin gene family expressed predominantly in muscle. *J Biol Chem* 1996; **271**: 2255–2261.



**Cell Death and Disease** is an open-access journal published by Nature Publishing Group. This work is licensed under a Creative Commons Attribution-NonCommercial-NoDerivs 3.0 Unported License. The images or other third party material in this article are included in the article's Creative Commons license, unless indicated otherwise in the credit line; if the material is not included under the Creative Commons license, users will need to obtain permission from the license holder to reproduce the material. To view a copy of this license, visit <http://creativecommons.org/licenses/by-nc-nd/3.0/>

Supplementary Information accompanies this paper on Cell Death and Disease website (<http://www.nature.com/cddis>)

### **Degeneration of serotonergic neurons in amyotrophic lateral sclerosis: a link to spasticity**

Upper motor neuron degeneration is often associated with spasticity of skeletal musculature. This is a debilitating painful condition, considerably affecting motility and voluntary strength, which contributes to the poor quality of life of PLS but also ALS patients (McClelland et al., 2008). Although spasticity is a neurogenic condition, most treatments applied in these cases target the periphery, nerves and skeletal muscle. In ALS the therapeutic approaches targeting spasticity are extremely limited. One study evidenced limited benefits after moderate daily exercise (Ashworth et al., 2012).

The mechanisms of muscle spasticity were mostly studied in spinal cord injury models, where the monoamine neurotransmitter serotonin (5HT) was found to play an important part in the development of this condition. Serotonin has multiple functions in the CNS, where it acts through 7 different types of receptors (5HT<sub>1-7</sub>) with 14 subtypes (Nichols and Nichols, 2008). In the motor system 5HT plays a modulatory role. Serotonergic projection from the brainstem into the spinal cord facilitate motor output increasing the excitability of motor neurons (Jacobs et al., 2002; Perrier et al., 2005). Following spinal cord injury, 5HT<sub>2B</sub> and 5HT<sub>2C</sub> receptors become constitutively active in spinal cord motor neurons. This is a mechanism of compensating for the reduced serotonergic input which ultimately contributes to the emergence of muscle spasms (Murray et al., 2011).

In the present work we describe degeneration of serotonergic neurons in the brainstem of a group of seven ALS patients. Although the loss of cellular bodies was heterogeneous amongst patients and the different serotonergic nuclei studied, there we found an obvious loss of serotonergic neurites. Also, we observed a massive systematic loss of serotonergic projections into spinal cord and hippocampus of ALS patients.

Next we sought validating our findings in the ALS mouse model expressing the mSOD1<sup>G86R</sup>. We showed decrease in mRNA of cellular markers of serotonergic neurons in brain stem of pre-symptomatic SOD1<sup>G86R</sup> mice. This is indirect evidence for an early degeneration of serotonergic neurons. This was further confirmed by a decreased in serotonin levels in

brain stem, spinal cord and cortex evident before symptom onset. At symptomatic stages, immunohistochemical analysis of serotonergic neurons in the brain stem of mSOD1 mice revealed shrinkage of neuronal bodies and neurite fragmentation.

To understand the relevance of this impairment of the serotonergic system, we further focused on spasticity. Spasticity is visible in the tail of mSOD1 mice at disease onset, but at this stage it is difficult to quantify due to the presence of voluntary movements. However, we were able to quantify spasticity in end stage mice by performing electromyography (EMG) of the tail muscles.

At this stage we found that mRNA levels of the 5HT<sub>2B</sub> receptor were significantly increased in lumbar spinal cord. By using two different inverse agonists of the 5HT<sub>2B/2C</sub> receptors (SB206553 and cyproheptadine) we were able to alleviate spasticity, as confirmed by EMG analysis. Since the levels of 5HT<sub>2C</sub> receptors were unchanged, spasticity in this ALS mouse model is most likely due to overexpression of constitutively active 5HT<sub>2B</sub> receptors, following the reduction of serotonergic input.

Our work brings evidence of a serotonergic pathology in ALS patients and in an ALS mouse model. We further outline a potential mechanism for spasticity, linked to the degeneration of serotonergic neurons. This has important implication for the alleviating spasticity in PLS and ALS patients, a debilitating condition for which limited clinical intervention is available so far.

# Degeneration of serotonergic neurons in amyotrophic lateral sclerosis: a link to spasticity

Christel Dentel,<sup>1,2,3</sup> Lavinia Palamiuc,<sup>1,2</sup> Alexandre Henriques,<sup>1,2</sup> Béatrice Lannes,<sup>2,4</sup>  
Odile Spreux-Varoquaux,<sup>5,6,7</sup> Lise Gutknecht,<sup>8,9</sup> Frédérique René,<sup>1,2</sup> Andoni Echaniz-Laguna,<sup>1,2,3</sup>  
Jose-Luis Gonzalez de Aguilar,<sup>1,2</sup> Klaus Peter Lesch,<sup>8,10</sup> Vincent Meininger,<sup>11,12</sup>  
Jean-Philippe Loeffler<sup>1,2</sup> and Luc Dupuis<sup>1,2,12,13</sup>

1 U692, INSERM, 67085 Strasbourg, France

2 Faculté de Médecine, Université de Strasbourg, 67000 Strasbourg, France

3 Département de Neurologie, Hôpitaux Universitaires de Strasbourg, 67000 Strasbourg, France

4 Département d'Anatomopathologie, Hôpitaux Universitaires de Strasbourg, 67000 Strasbourg, France

5 Département de pharmacologie, Faculté de Médecine Paris-Ile de France-Ouest, 78180 Paris, France

6 Université de Versailles Saint-Quentin-en-Yvelines, 78000, Versailles, France

7 Centre Hospitalier Versailles, 78150, Le Chesnay, France

8 Unit for Molecular Psychiatry, Department of Psychiatry, Psychosomatics and Psychotherapy, University of Würzburg, 97080, Würzburg, Germany

9 Department of Neurobiology, Functional Genomic Institute, CNRS /INSERM UMR 5203, University of Montpellier, 35000 Montpellier, France

10 Department of Neuroscience, School for Mental Health and Neuroscience, Maastricht University, 6229, Maastricht, The Netherlands

11 Département des maladies du système nerveux, Université Pierre et Marie Curie, 75000 Paris, France

12 Département des Maladies du Système Nerveux, Centre Référent Maladie Rare SLA Hôpital de la Pitié-Salpêtrière (AP-HP), 75000, Paris, France

13 Department of Neurology, Ulm University, 89081, Ulm, Germany

Correspondence to: Luc Dupuis,  
INSERM U692, Faculté de médecine,  
11 rue Humann,  
67085 Strasbourg, France  
E-mail: ldupuis@unistra.fr

Spasticity is a common and disabling symptom observed in patients with central nervous system diseases, including amyotrophic lateral sclerosis, a disease affecting both upper and lower motor neurons. In amyotrophic lateral sclerosis, spasticity is traditionally thought to be the result of degeneration of the upper motor neurons in the cerebral cortex, although degeneration of other neuronal types, in particular serotonergic neurons, might also represent a cause of spasticity. We performed a pathology study in seven patients with amyotrophic lateral sclerosis and six control subjects and observed that central serotonergic neurons suffer from a degenerative process with prominent neuritic degeneration, and sometimes loss of cell bodies in patients with amyotrophic lateral sclerosis. Moreover, distal serotonergic projections to spinal cord motor neurons and hippocampus systematically degenerated in patients with amyotrophic lateral sclerosis. In SOD1 (G86R) mice, a transgenic model of amyotrophic lateral sclerosis, serotonin levels were decreased in brainstem and spinal cord before onset of motor symptoms. Furthermore, there was noticeable atrophy of serotonin neuronal cell bodies along with neuritic degeneration at disease onset. We hypothesized that degeneration of serotonergic neurons could underlie spasticity in amyotrophic lateral sclerosis and investigated this hypothesis *in vivo* using tail muscle spastic-like contractions in response to mechanical stimulation as a measure of spasticity. In SOD1 (G86R) mice, tail muscle spastic-like contractions were observed at end-stage. Importantly, they were abolished by 5-hydroxytryptamine-2b/c receptors inverse agonists. In line with this, 5-hydroxytryptamine-2b receptor expression was strongly increased at disease onset. In all, we show that serotonergic neurons degenerate during amyotrophic lateral sclerosis, and that this might underlie spasticity in mice. Further research is needed to determine whether inverse agonists of 5-hydroxytryptamine-2b/c receptors could be of interest in treating spasticity in patients with amyotrophic lateral sclerosis.

**Keywords:** ALS; animal models; motor neuron; serotonin; spasticity

**Abbreviations:** ALS = amyotrophic lateral sclerosis; 5-HIAA = 5-hydroxyindoleacetic acid; 5-Ht = 5-hydroxytryptamine; Tph2 = tryptophan hydroxylase 2

## Introduction

Spasticity is a symptom of many motor diseases that consists of velocity-dependent increase in muscle tone and exaggerated muscle responses to stretching. Spasticity develops either after trauma, in particular spinal cord injury, or in the course of degenerative diseases such as amyotrophic lateral sclerosis (ALS), a fatal neurodegenerative disorder affecting upper and lower motor neurons (Kiernan *et al.*, 2011). Spasticity represents the major phenotype of the upper motor neuron predominant subtype of ALS called primary lateral sclerosis and might be under recognized in other patients with ALS, as the physiological basis for detecting spasticity is disrupted by the degenerative process involving motor neurons of all classes (Swash, 2012). Spasticity is a painful and disabling symptom, and treatment options remain limited, especially in patients with ALS and those with primary lateral sclerosis (Ashworth *et al.*, 2012).

Mechanisms of spasticity have been mostly studied after spinal cord injury. In the current view, spinal cord injury-associated spasticity arises from several mechanisms, a major one being injury to serotonergic axons. Indeed, serotonergic axons, descending from several brainstem serotonergic nuclei, densely innervate lower motor neurons and maintain motor neuron excitability through increased persistent calcium current (Heckman *et al.*, 2009). After spinal cord injury, the transection of serotonergic axons leads to transient hypoexcitability of lower motor neurons. After a few weeks, lower motor neurons compensate for loss of serotonin input through the production of constitutively active 5-hydroxytryptamine (5-Ht)-2b and 5-Ht2c receptors, leading to an intrinsic hyperexcitability and subsequent spasticity (Murray *et al.*, 2010, 2011).

In ALS, degeneration of upper motor neurons, whose axons form the corticospinal tract, is traditionally thought to cause spasticity as part of the 'upper motor neuron syndrome' (Ivanhoe and Reistetter, 2004), but direct evidence linking upper motor neurons and spasticity in ALS is lacking. Other hypotheses, in particular the implication of serotonergic neurons, have not been explored so far. Indeed, studies on serotonergic involvement in ALS are scarce and limited. Early studies focusing on the quantification of serotonin and its metabolites yielded inconsistent results, most likely owing to the very limited numbers of post-mortem brain tissues included (Bertel *et al.*, 1991; Sofic *et al.*, 1991; Forrest *et al.*, 1996). More recent imaging studies have shown decreased binding of serotonin 1A (5-HT<sub>1A</sub>) ligands in ALS raphe and cortex (Turner *et al.*, 2005, 2007). To address the potential involvement of serotonin in ALS, we recently measured levels of platelet serotonin in a cohort of 85 patients with ALS and a control group of 29 healthy subjects. We found that platelet serotonin levels were significantly decreased in patients with ALS, and that higher platelet serotonin levels were positively correlated with increased survival of the patients (Dupuis *et al.*, 2010), suggesting that

serotonin might influence the course of ALS disease. However, investigation of a direct involvement of central serotonin in ALS has not been performed until now. Here, we show that central serotonergic neurons degenerate during ALS. From a functional point of view, our animal studies also suggest that spasticity might arise from serotonergic loss, at least in animal models.

## Materials and methods

### Patient tissues

Autopsy samples from hippocampus, brainstem and spinal cord were obtained from seven patients with ALS and six control subjects. Patient 2 had familial history of ALS, but gene analysis demonstrated no pathogenic variations in the *SOD1* gene. Hippocampus and brainstem samples were available for all patients. Spinal cord specimens were available for all patients with ALS and control subjects. Patients and/or families had provided written informed consent. Clinical details are presented in Supplementary Tables 1 and 2. ALS diagnosis was obtained using El Escorial criteria (Brooks *et al.*, 2000) and was confirmed after autopsy. During autopsy, tissues were fixed in 4% formaldehyde and embedded in paraffin using standard protocols. Use of these tissues for research was declared at the French ministry for research and higher education (DC-2011-1433).

### Transgenic mice

Transgenic mice carrying the *SOD1* (G86R) mutation (Ripps *et al.*, 1995; Dupuis *et al.*, 2000) and their non-transgenic littermates on a FVB/N background were housed in our animal facility with unrestricted access to food and water. Mice were sacrificed at different stages of the disease to perform the studies using the following clinical scale: asymptomatic mice show normal gait and no paralysis and were scored 4. EMG is typically normal in these mice. Animals with a score of 3 showed a mildly abnormal gait or one hindlimb with paralysis. Score 3 typically occurs between 90 and 100 days of age, and is associated with already detectable EMG abnormalities, i.e. spontaneous muscle electrical activity, but no loss of motor neuron cell bodies (Halter *et al.*, 2010). Frank paralysis of one limb is scored 2 and of both hindlimbs is scored 1. Profound weight loss and kyphosis are typical of score 0, and mice are euthanized at this stage. In this study, asymptomatic mice used were all scored 4, and were 75 days old. Mice at disease onset were mice with a score of 3. These mice were followed daily and were sacrificed the second day on which they showed a score of 3. End stage mice used in the EMG studies were scored 1 and thus showed frank paralysis of both hindlimbs. For ethical reasons, we did not use mice scored 0 in experiments but proceeded to their euthanasia.

For histology, brains were fixed by immersion in 4% formaldehyde in phosphate buffer 0.1 M pH 7.4, and tissues were post-fixed 24 h before paraffin embedding. For molecular biology, brainstem and lumbar spinal cord tissues were snap frozen in liquid nitrogen. Animal experiments were performed under the supervision of

authorized investigators (L.D. and F.R.), and approved by the local ethical committee for animal experiments (CREMEAS, agreement N° AL/01/02/02/12).

## Histology

Paraffin embedded tissues were cut in 4 µm sections using a HM 340E Microtome (Microm). Luxol Fast blue/Cresyl violet stain was performed using a standard histological technique. Immunohistochemistry was performed in a Benchmark XT automate slide system using the Ventana NexES® software and EZ Prep Ventana Roche® reagent. Sections were heated, and endogenous peroxidases were inactivated using H<sub>2</sub>O<sub>2</sub> (Ventana Roche®). Primary and secondary antibodies were incubated for 2 h at 37°C. Staining was performed using ultraview DAB (Ventana Roche®). Human sections were counterstained with haematoxylin (Ventana Roche®). Primary antibodies were as follows: rabbit polyclonal anti-ubiquitin (Dakocytomation 1/200), rabbit polyclonal TDP-43 (Proteintech LTD, 1/800) and rabbit polyclonal tryptophan hydroxylase 2 (Tph2) [described in Gutknecht *et al.* (2009), 1/1000].

## Quantification of tryptophan hydroxylase 2 positive neurons in human samples

The number of Tph2-positive cell bodies in various regions of interest was evaluated semi-quantitatively in at least two sections of the considered nuclei identified as shown in Supplementary Fig. 1. Number of neurons per section: negative = 0–10, + = 11–20, ++ = 21–30, +++ = >30. We systematically compared sections stained in parallel in matched regions. Regions of interest were identified in adjacent sections using Luxol Fast blue/Cresyl violet staining, and counting of neurons were performed at ×20 magnification in a blinded manner, on two sections of each region of interest.

## Measurement of perikaryon size of tryptophan hydroxylase 2 positive neurons

Sagittal brain sections (4 µm) were cut in series starting from the midline. In each animal, one of every five serial sections was sampled for Tph2 immunostaining. Using the second edition of the mouse brain in stereotaxic co-ordinates atlas (Franklin and Paxinos, 1997), position of the dorsalis raphe nucleus was determined on each section (medio-lateral: 0 to +0.48 mm; antero-posterior: –4 to –5.3 mm from Bregma; dorso-ventral: +2.75 to +4 mm). Images of the dorsalis raphe nucleus were captured using a Nikon digital camera DXM1200 connected to a Nikon eclipse E800 microscope. Tph2-positive neurons were analysed in seven to nine sections per animal in each group. The cell body area of all Tph2-positive neurons with a visible nucleus in the dorsalis raphe nucleus was measured using the NIH Image analysis software (ImageJ, version 1.45r), and 200–800 neurons were measured per animal.

## Real-time quantitative polymerase chain reaction

Total RNA was extracted using TRIzol® (Invitrogen) and standard procedures. Real-time quantitative PCR was performed as previously described (Braunstein *et al.*, 2010) using BIO-RAD iScript™ cDNA Synthesis Kit, iQ™ qPCR mix and a CFX95 thermocycler (BioRad).

Data were normalized with the GeNorm software (Vandesompele *et al.*, 2002) using geometric averaging of three internal standards (18S ribosomal RNA, Tata-box binding protein and RNA polymerase II subunit).

## 5-Hydroxytryptamine-2c receptor mRNA editing

We used the quantitative PCR method developed by Lanfranco *et al.* (2009, 2010) to measure 5-HT<sub>2c</sub> messenger RNA editing. This method is based on the use of TaqMan® probes selective for the various edited isoforms. We used the DNA templates provided by Lanfranco *et al.* (2009, 2010) to check for selectivity and specificity of the measurements, and obtained quantitative PCR cycling conditions that discriminate fully between the different templates using the published TaqMan® probes.

## High-performance liquid chromatography

Serotonin and 5-hydroxyindoleacetic acid (5-HIAA) were measured on tissue extracts using high-performance liquid chromatography with coulometric detection using a technique similar to Alvarez *et al.* (1999). Results were standardized to initial wet weight of tissue.

## Electromyographical evaluation of spasticity

Spasticity in tail muscles was measured with percutaneous EMG wires inserted in segmental tail muscles at the midpoint of the tail, as described by Bennett *et al.* (2004) and adapted to mouse. During EMG recording, muscle spasms were evoked with mechanical stimulation of the tail skin, and the tail was free to move. EMG was sampled at 5 kHz, rectified and averaged for a 4-s interval starting 1 s after stimulation. EMG over 1 s before stimulation was averaged for measure of background signal.

## Statistical analysis

Statistical analysis was performed using GraphPad Prism software. For comparison between two groups, Student's *t*-test was used. For comparison between three or more groups, ANOVA followed by Newman–Keuls *post hoc* test was applied. Significance level was set at  $P < 0.05$ .

## Results

### Degeneration of serotonergic neurons in amyotrophic lateral sclerosis

We analysed autaptic brains from seven patients with ALS and six control subjects (Supplementary Tables 1 and 2). Three patients with ALS had a bulbar onset of symptoms, and four had spinal onset. We focused our studies on major serotonergic nuclei of the brainstem presented in Supplementary Fig. 1. Ubiquitin and TDP43 cytoplasmic aggregates, two pathological hallmarks of ALS (Neumann *et al.*, 2006; Kiernan *et al.*, 2011), were observed almost systematically in the raphe magnus and gigantocellular nuclei but more rarely in other nuclei studied (Supplementary Figs 2 and 3). One patient (Patient 5) showed extensive ubiquitin

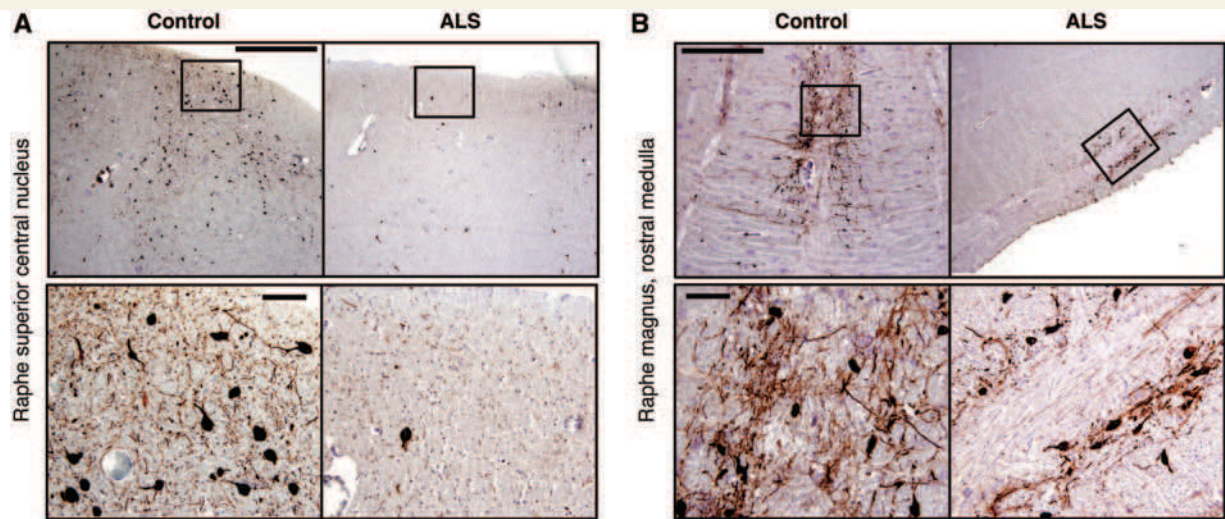


**Figure 1** Serotonergic neurons degenerate in patients with ALS. (A) Representative TPH2 immunohistochemistry in the raphe superior central nucleus of one control subject (control subject 3, left panels) and one ALS (Patient 3, right panel). Upper pictures show low magnification. Lower pictures show a magnification of the rectangle in upper picture. This ALS case exhibits extensive degeneration of TPH2-specific cell bodies in this serotonergic nucleus. (B) Representative TPH2 immunohistochemistry in the raphe magnus nucleus (rostral medulla) of one control subject (control subject 6, left panels) and one ALS (Patient 7, right panels). Upper pictures show low magnification. Lower pictures show a magnification of the rectangle in upper picture. Neuronal density of TPH2-positive cell bodies are similar in ALS and control subject, but that intense degeneration of TPH2-positive neurites is visible in the ALS patient.

**Table 1** Semi-quantitative analysis of Tph2-positive cell bodies in regions of interest in patients with ALS

	Case	Site of onset	Rostral pons		Caudal pons	Rostral medulla		Medulla (Inf. olive) RO
			RPF	RSCN	GCN	RM	RLN	
ALS	1	Bulbar	+++	+++	Neg	+++	+	
	2	Spinal	+++	+++	Neg	+++	++	
	3	Spinal	+++	Neg		+	Neg	+
	4	Spinal	+++	+++		+++	Neg	Neg
	5	Bulbar	+++	+++	+	+++	++	+
	6	Bulbar	+++	+	+	+	+	Neg
	7	Spinal	+++	+++		++	+++	+
Control	1				+			
	2		+++	+++		++	+++	+
	3		+++	+++		++	++	
	4				+			+
	5				+	++	++	
	6				+	+++	++	

Number of neurons per section: Negative (Neg) = 0–10, + = 11–20, ++ = 21–30, +++ = >30.

Empty cells = tissue not available; Inf = inferior; RPF = reticular pontine formation; RSCN = raphe superior central nucleus; GCN = gigantocellular nucleus; RM = raphe magnus; RLN = reticular lateral nucleus. Inf. olive: inferior olive.

and TDP43 pathology in all serotonergic nuclei studied. Serotonergic neurons were easily detected in the pons and rostral medulla nuclei of control patients using an antibody directed against TPH2, the rate limiting enzyme in central serotonin synthesis. Patients with ALS showed loss of TPH2-positive cell bodies in serotonergic nuclei (Fig. 1A), although these nuclei were not uniformly affected in patients with ALS. In many cases, cell bodies were still present, but loss of TPH2-positive neurites was obvious (Fig. 1B). Semi-quantitative analysis of TPH2-positive cell bodies showed a heterogeneous decrease in cell density in the studied serotonergic nuclei, irrespective of the site of onset of disease,

gender or age (Table 1). Patients 3 and 6 showed widespread serotonergic degeneration, whereas degeneration of serotonin cell bodies was more localized in Patients 1, 2 and 4. Patient 5, although displaying prominent ubiquitin and TDP43 pathology in these nuclei, and Patient 7 appeared to show preserved neuronal counts. Analysis of serial sections revealed that the cells displaying TDP-43 or ubiquitin-positive inclusions were not serotonergic neurons (not shown). Thus, serotonergic neurons suffer from a degenerative process with prominent neuritic degeneration, and sometimes cell body loss in patients with ALS, but do not show typical ALS pathology.

## Systematic degeneration of serotonergic projections in amyotrophic lateral sclerosis

We next sought to determine whether projections of serotonergic neurons degenerated in ALS. TPH2-labelled projections of serotonergic neurons were readily detectable in the hippocampus of control patients (Fig. 2A, left panel) but were almost absent in patients with ALS (Fig. 2A, right panel). In the spinal cord of Control 6, we observed spinal motor neurons densely innervated with TPH2-positive projections, as expected from the distribution of serotonin immunoreactivity in humans (Fig. 2B) (Perrin *et al.*, 2011). Contrasting with this, we occasionally observed isolated motor neurons with preserved serotonergic innervation, but neighbouring motor neurons were fully denervated (Fig. 2B). Even in Patients 5 and 7 with seemingly normal neuronal density, we barely observed motor neurons innervated by serotonergic axons. In all, we observed a massive and generalized reduction of TPH2-positive projections to spinal cord and hippocampus in patients with ALS.

## Degeneration of serotonergic neurons and early serotonin depletion in SOD1 (G86R) mice

Studies in patients are hampered by the inaccessibility to presymptomatic period. To determine whether serotonergic neuron degeneration precedes motor symptoms, we studied SOD1 (G86R) mice, a mutant mouse strain that over-expresses an ALS-linked mutant form of SOD1. This mouse strain and other similar models have

been shown to demonstrate ALS-like disease, with both lower and upper motor neuron degeneration (Gurney *et al.*, 1994; Ripps *et al.*, 1995; Ozdinler *et al.*, 2011). At disease onset (score of 3), messenger RNA levels of cell-specific markers of serotonergic neurons (Tph2, serotonin transporter, 5-Ht1a receptor) were lower in the brainstem of SOD1 (G86R) mice, indirectly suggesting degeneration of these neurons (Fig. 3A). Direct visualization of serotonergic neurons in the dorsalis raphe nucleus using Tph2 immunohistochemistry revealed similar features in SOD1 (G86R) mice at symptom onset (score 3) to patients with ALS. Semi-quantitative analysis revealed that the area of the cell body of Tph2-positive neurons was decreased of about one-third in this nucleus (Fig. 3B and C). We further observed fragmentation of Tph2-positive neurites of SOD1 (G86R) mice (Fig. 3B). Most importantly, levels of serotonin itself were decreased when compared with wild-type mice, not only in symptomatic (score 3) but also in non-symptomatic (score 4) SOD1 (G86R) brainstem (Fig. 4A), spinal cord (Fig. 4B) and cortex (Fig. 4C). The ratio between 5-HIAA, the major serotonin metabolite depending of mono-amine oxidase A activity, and serotonin represents an indirect measurement of local serotonin turnover (Shannon *et al.*, 1986). In SOD1 (G86R) mice, the 5-HIAA/serotonin ratio was unchanged before symptoms in all three tissues tested (Fig. 4D–F) and increased at disease onset in brainstem and cortex. This shows that serotonin depletion precedes increase in serotonin turnover, suggesting that early loss of serotonin is due to decreased supply rather than to increased turnover. Thus, the development of ALS is associated with an early and general impairment of central serotonin function in an animal model of the disease.

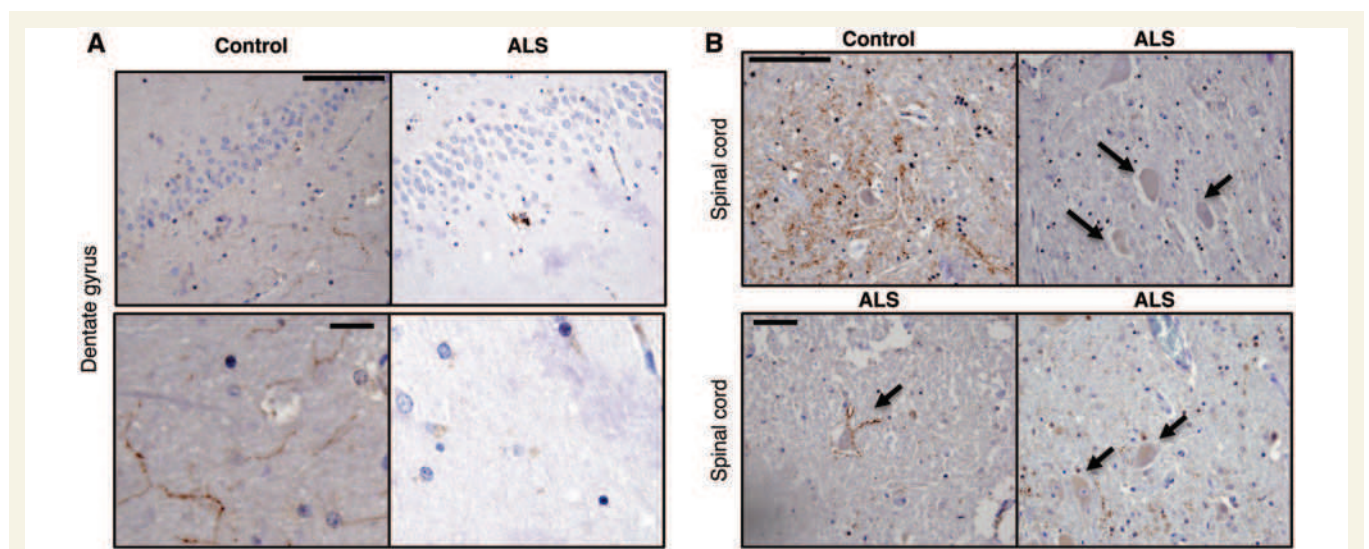


**Figure 2** Serotonergic projections degenerate in spinal cord and hippocampus of patients with ALS. (A) Representative TPH2 immunohistochemistry in the dentate gyrus of one control subject (Control 3, left panels) and one ALS (Patient 4, right panels). Upper pictures show low magnification. Lower pictures show a magnification of upper pictures. Note the almost complete absence of TPH2 immunoreactivity in the dentate gyrus of the patient with ALS. (B) Representative TPH2 immunohistochemistry in cervical spinal cord of one control subject (Control 6, upper left panel) and three patients with ALS (Patients 1, 3 and 7). Note the punctate TPH2 immunoreactivity surrounding motor neurons (arrows) in the control subject, but not in patients with ALS. A single motor neuron innervated by TPH2-positive serotonergic neuron terminals is shown in a patient with ALS (Patient 7, lower left panel).

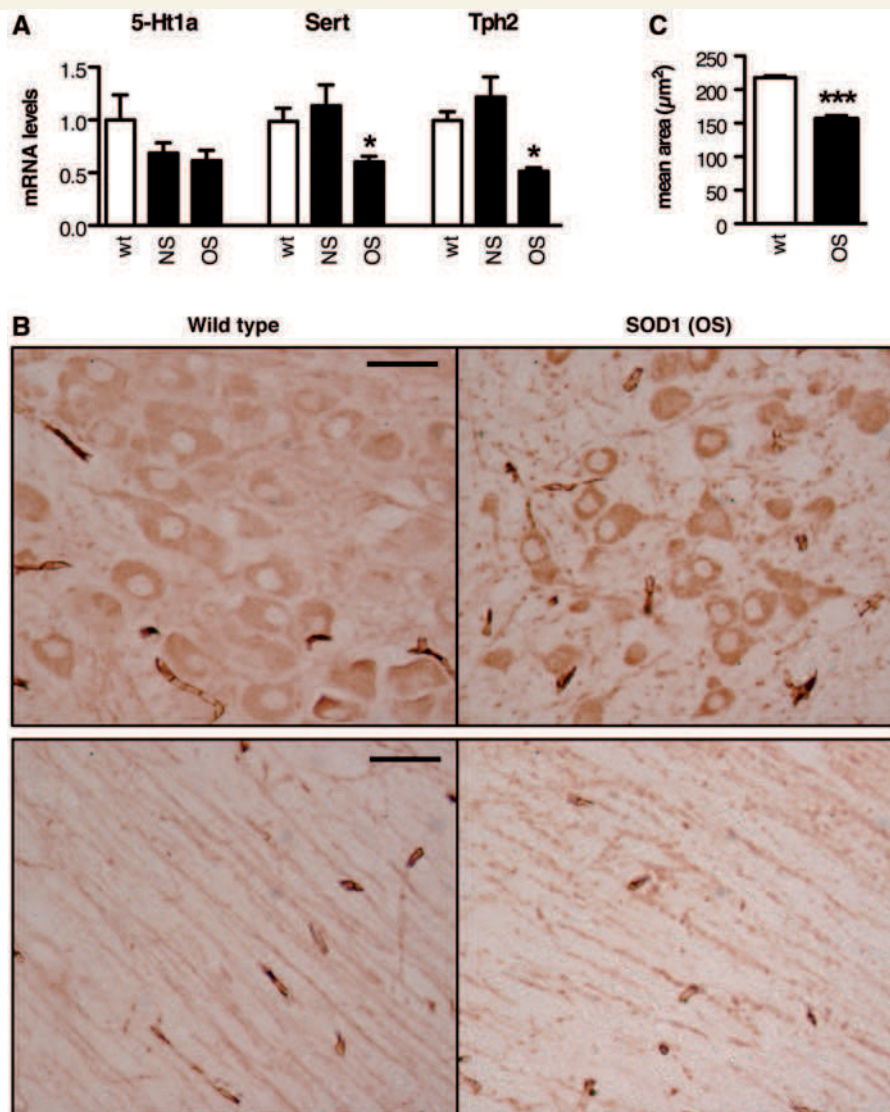


**Figure 3** Serotonergic neurons degenerate in SOD1 (G86R) mice. (A) Messenger RNA levels of 5-Ht1a receptor (5-Ht1a), serotonin transporter (Sert) and Tph2 in SOD1 (G86R) mice at 75 days of age (asymptomatic, NS) or at symptom onset (~100 days of age, OS) and wild-type litter mates (Wt). Note that serotonin transporter and Tph2 gene expression levels are downregulated at symptom onset.  $n = 7–10$  per group.  $*P < 0.05$  versus wild type, ANOVA followed by Newman–Keuls *post hoc* test. (B) Representative Tph2 immunohistochemistry in SOD1 (G86R) mice at disease onset (SOD1; OS) and wild-type littermates. Note the shrunken Tph2-positive cell bodies in SOD1 (G86R) mice (*upper right*) and neuritic degeneration (*lower right*).  $n = 3$  per group. (C) Mean area of Tph2-positive neurons in SOD1 (G86R) mice at disease onset (OS) and wild-type (Wt) littermates. The area of 200–800 neurons was measured per animal, with  $n = 3$  per group.  $***P < 0.0005$  versus wild type, Student's *t*-test.

### Spasticity develops in SOD1 (G86R) mice, and is alleviated by 5-hydroxytryptamine 2 b/c receptors inverse agonists

We sought then to characterize whether serotonin depletion occurring early in SOD1 (G86R) had pathogenic consequences on motor neurons. Serotonin modulates excitability of motor neurons by allowing sustained entry of calcium (Heckman *et al.*, 2009). In animal models of spinal cord injury, it was recently shown that serotonin depletion due to transection of serotonergic

axons was over-compensated by motor neurons. More specifically, motor neurons produce constitutively active 5-Ht2b and 5-Ht2c receptors through still poorly defined mechanisms, decreased editing of the 5Ht2c messenger RNA being one of these (Murray *et al.*, 2010). This constitutive activity of 5-Ht2b/c receptors is responsible for the occurrence of spasticity on spinal cord injury (Murray *et al.*, 2010). Other serotonin receptors, including 5-HT1A, 2A, 3, 4, 5, 6 and 7 appear to not be involved in this event (Murray *et al.*, 2011). By analogy, we reasoned that the chronic loss of serotonergic innervation of lower motor neurons in patients with ALS and SOD1 (G86R) mice could lead to spasticity. To explore this hypothesis, we used an electromyographical

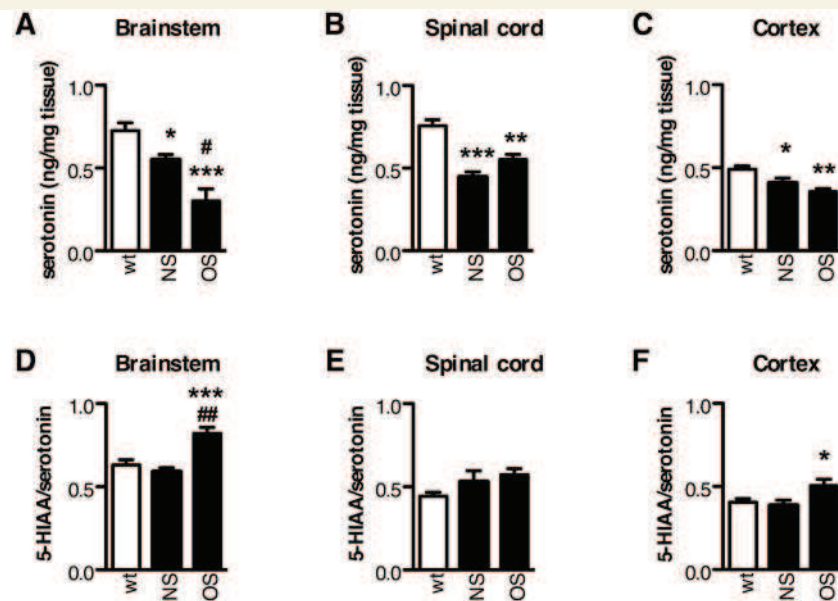


**Figure 4** Decreased levels of serotonin in SOD1 (G86R) mice. Serotonin (ng/mg tissue, A–C) and 5-HIAA/serotonin (D–F) in the brainstem (A and D), the spinal cord (B and E) and the cerebral cortex (C and F) of SOD1 (G86R) mice at 75 days of age (asymptomatic, NS) or at symptom onset (~100 days of age, OS) and wild-type littermates (Wt) as measured using high-performance liquid chromatography. \* $P < 0.05$  versus wild type, \*\* $P < 0.01$  versus wild type, \*\*\* $P < 0.001$  versus wild type, # $P < 0.05$  versus asymptomatic, ## $P < 0.01$  versus asymptomatic. ANOVA followed by Newman–Keuls *post hoc* test.  $n = 5–10$  per group.

protocol adapted from Bennett *et al.* (2004). This objective and quantitative electromyographical method appears correlated with clinical evaluation of spasticity (Bennett *et al.*, 2004) and facilitates the study of the effect of classical anti-spastic drugs such as baclofen or clonidine (Li *et al.*, 2004; Rank *et al.*, 2011). We visually observed spasticity in the tail of some animals at disease onset (score 3), but this was difficult to distinguish from voluntary contractions in these mice that are not yet paralysed. When disease progresses, however, spasticity of the tail was systematically observed and strong in end-stage (stage 1) mice. Thus, the mechanisms for spasticity are already present at disease onset, and might help with maintaining motor function, but are blurred by voluntary movements. For this reason, we used end-stage SOD1 (G86R) mice to adapt the EMG protocol initially developed for rats with spinal cord injury. Under this experimental set-up, spastic-like contractions of tail muscles were easily recorded (Fig. 5A), providing objective evidence of spasticity as a component of ALS disease in this mouse model. We further studied involvement of constitutive activity of 5-Ht2b/c receptors in this measure of spasticity and found that spasticity was strongly alleviated by injection of 5-Ht2b/c inverse agonists SB206553 (Fig. 5B and D) and cyproheptadine (Fig. 5C and D). In rats with chronic spinal cord injury, spasticity is associated with increased production of the unedited isoform of the 5-Ht2c messenger RNA leading to increased expression of the constitutively active INI-5-Ht2c receptor. In SOD1 (G86R) mice, we observed, however, decreased production of this specific isoform and normal levels of total messenger RNA and of other various edited isoforms (Fig. 5E and F) in the lumbar and sacral spinal cords at disease onset (score 3), i.e. the disease stage at which spasticity arises. Contrasting with this, we observed

a 10-fold increased expression of the 5-Ht2b receptor in the same animals (Fig. 5E). In all, our results suggest that serotonin depletion leads to over-expression of 5Ht2b receptors and subsequent constitutive activity of this receptor during development of spasticity. In turn, this constitutive activity likely leads to spasticity.

## Discussion

Here, we show that ALS is associated with degeneration of central serotonergic neurons, both in patients and animal model, and identify spasticity as a possible consequence of ALS-related serotonergic dysfunction.

The first major result of this study is that central serotonergic neurons degenerate in patients with ALS and in an animal model. We observed a major decrease in serotonergic innervation in target regions, such as the spinal cord and the hippocampus, along with obvious decreased density of serotonergic neurites in the serotonergic nuclei. In some nuclei, this was also accompanied by shrinkage and loss of cell bodies. We found limited ubiquitin and TDP-43 pathology in most serotonergic nuclei studied, but these inclusions were not in remaining cell bodies of serotonergic neurons. This might reflect either high intrinsic capacity in clearing protein aggregates in serotonergic neurons, or low production of aggregate-prone proteins in this neuronal type or, on the contrary, extreme sensitivity leading to degeneration of neurites, despite low levels of aggregates. Degeneration of serotonergic neurons could be either independent of lower motor neuron degeneration or be a secondary consequence of motor neuronal loss. However, we observed loss of serotonin in asymptomatic mice, as early as

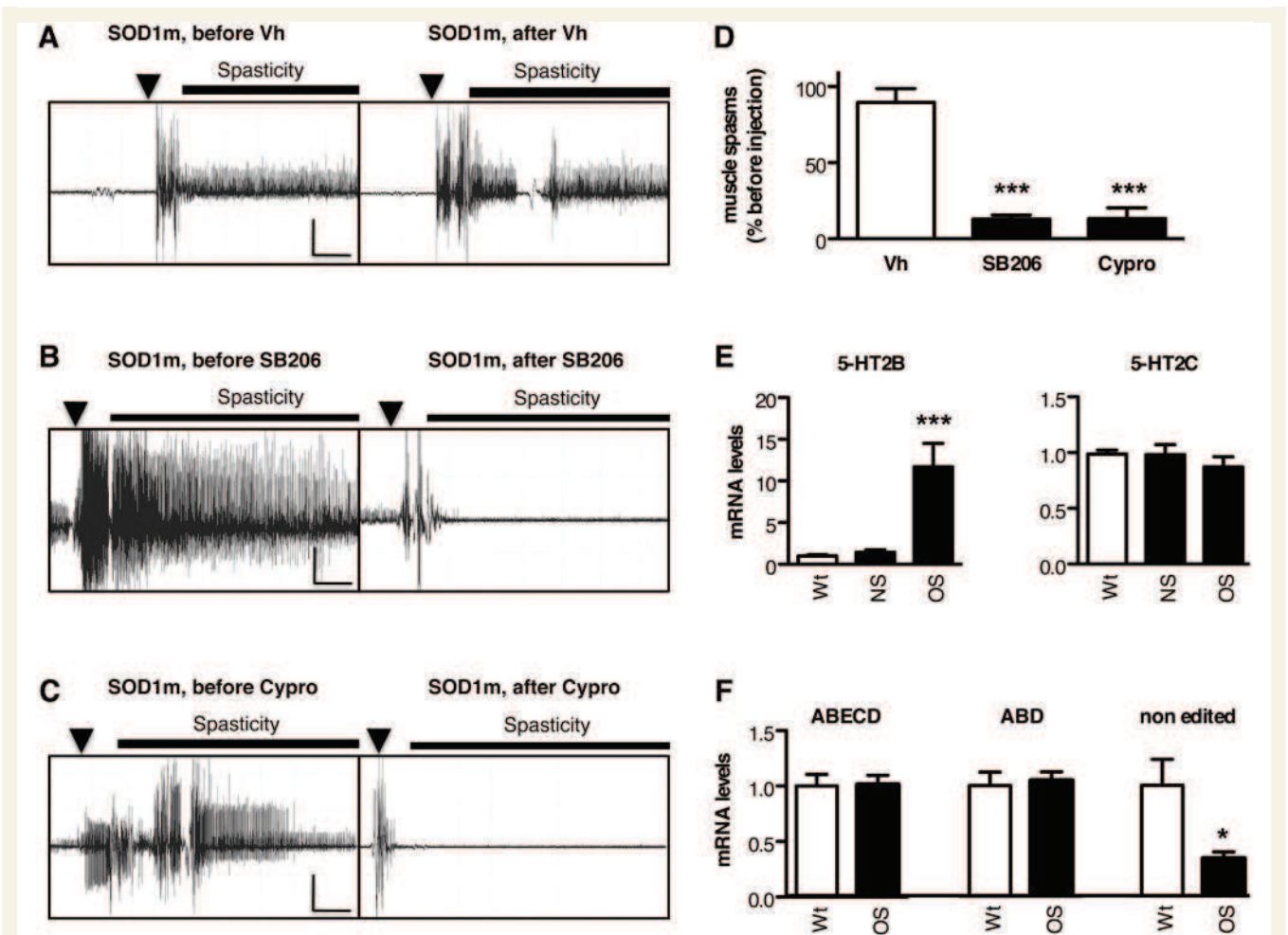


**Figure 5** Spasticity in SOD1 (G86R) mice is alleviated by 5-Ht2b/c inverse agonists. (A–C) Representative recording of long-lasting reflexes using tail EMG in one diseased SOD1 (G86R) mouse before (*left*) and after injections of vehicle (Vh, A), SB206553 (SB206, B) or cyproheptadine (Cypro, C). Spasticity was considered to be electrical activity above the baseline recorded 1 s after mechanical stimulation (arrowhead). (D) Quantitative analysis.  $n = 5–6$  mice per group and two to three EMGs were obtained before and after injection. We calculated a ratio between spasticity before and after injection and present the result as a percentage.  $*P < 0.05$  versus before injection, ANOVA followed by Newman–Keuls *post hoc* test. (E) Messenger RNA levels of 5-Ht2b (5-Ht2b), and 5-Ht2c (5-Ht2c) receptors in SOD1 (G86R) mice at 75 days of age (asymptomatic, NS) or at symptom onset (~100 days of age, OS) and wild-type littermates (Wt). 5-Ht2b gene expression levels are heavily upregulated at symptom onset.  $n = 12$  per group.  $***P < 0.001$  versus wild type, ANOVA followed by Newman–Keuls *post hoc* test. (F) Levels of editing variants of the 5-Ht2c messenger RNA in the spinal cord of SOD1 (G86R) mice at onset (OS) and wild-type littermates (Wt). ABECD (messenger RNA variant with full editing of A, B, E, C and D sites), ABD (messenger RNA variant edited at A, B and D sites) and the non-edited messenger RNA, which leads to the production of the constitutively active IN1 receptor, were measured by TaqMan<sup>®</sup> assays. Levels of the non-edited messenger RNA are decreased.  $n = 12$  per group.  $*P < 0.05$  versus wild type, Student's *t*-test.

75 days of age, an age that precedes from several weeks the onset of motor neuron degeneration. This suggests that degeneration of serotonergic neurons occurs independently of motor neuron death, at least in animal models.

The loss of serotonergic neurons causes loss of serotonin itself in regions of projections. In our animal model, serotonin levels are decreased in the brainstem and the spinal cord long before motor symptoms arise. Previous studies on serotonin and 5-HIAA in patients with ALS yielded conflicting results. Bertel *et al.* (1991) observed normal levels of serotonin and decreased levels of 5-HIAA in autopsy samples, whereas Forrest *et al.* (1996)

observed normal serotonin levels but increased 5-HIAA levels. However, serotonin is a labile molecule that might be significantly altered in post-mortem human samples with hours of delay before autopsy (Yoshimoto *et al.*, 1993). Our study overcomes this problem by studying serotonergic neurons using TPH2 immunostaining in fixed tissues. In asymptomatic animals, the loss of serotonin was associated with normal serotonin turnover (unchanged 5-HIAA/serotonin ratio), strengthening the idea that decreased serotonin was owing to decreased supply in serotonin rather than to increased degradation. Contrastingly, in end-stage mice, we observed an increased serotonin turnover (increased 5-HIAA/

serotonin ratio). This late increased serotonin turnover is likely to be due to increased release of serotonin by remaining nerve terminals. Indeed, this increased mobilization of residual serotonin in end-stage mice coincides with the loss of serotonin transporter expression, an event expected to limit serotonin reuptake and increase its turnover. Our studies are consistent with imaging studies using the PET scan ligand WAY100635 (Turner *et al.*, 2005, 2007). This compound binds to the 5-HT<sub>1A</sub> receptor, which is broadly expressed in serotonergic neurons, notably in brainstem and acts as an inhibitory somatodendritic autoreceptor in these neurons. The decreased binding potential of WAY100635 in the raphe of patients with ALS was hypothesized to be either owing to decreased sensitivity of 5-HT<sub>1A</sub> receptors to WAY100635 or to loss of neurons that express this receptor. As 5-HT<sub>1A</sub> receptor is strongly expressed in serotonergic neurons in the raphe, our current results argue for the latter view.

We next sought to delineate whether serotonin depletion had pathogenic consequences and focused on one of the potential consequences, the occurrence of spasticity. Spasticity had been previously shown to occur in spinal cord injury as a late consequence of transection of serotonergic axons (Murray *et al.*, 2010, 2011). Spasticity represents a symptom that is difficult to objectively measure in animals. We adapted an EMG technique measuring spastic-like contractions of tail muscles in response to a mechanical stimulation. Others had previously shown that this EMG method is clinically correlated with onset of spasticity in rats with spinal cord injury and sensitive to classical anti-spastic drugs (Bennett *et al.*, 2004; Li *et al.*, 2004; Rank *et al.*, 2011). This method thus represents a quantitative, observer-independent measurement of spasticity. In our model, we were able to almost abolish spasticity by the use of cyproheptadine, a broad 5-HT<sub>2</sub> inverse agonist, and SB206553, a much more selective compound known to target 5-HT<sub>2B</sub> and C (Kennett *et al.*, 1996), arguing for the involvement of one of these two receptors in ALS spasticity. Murray *et al.* (2010) observed increased production of the unedited 5-HT<sub>2c</sub> messenger RNA in rats with chronic spinal cord injury, whereas our result in mSOD1 mice was opposite. Recent work in another paradigm of spinal cord injury found unchanged levels of editing of the 5-HT<sub>2c</sub> messenger RNA in rats (Navarrett *et al.*, 2012). This discrepancy might be due to species differences (rats versus mice), to the different kinetics of serotonin loss [abrupt in spinal cord injury but much slower in SOD1 (G86R) mice]. We found a strong increase in spinal 5-HT<sub>2b</sub> receptor expression when spasticity was obvious, which could underlie the constitutive activity observed. Indeed, 5-HT<sub>2b</sub> receptor has intrinsic constitutive activity, and the increase of concentration of a G-protein coupled receptor is on its own sufficient to further increase any constitutive activity (Seifert and Wenzel-Seifert, 2002). For instance, a 7-fold over-expression of the 5-HT<sub>2b</sub> receptor in cardiomyocytes leads to a dramatic cardiac phenotype, suggesting that the over-expression of this receptor in the range we observed in SOD1 (G86R) mice is sufficient to induce strong constitutive activity (Nebigil *et al.*, 2003). Our mouse model of ALS is based on transgenic over-expression of mutant SOD1. Although these mouse models represent the only currently available model that display selective loss of both lower and upper motor neurons (Halter *et al.*, 2010; Ozdinler *et al.*, 2011), they only mimic the 20% of familial

cases that display mutations in the *SOD1* gene. Whether spasticity might also be alleviated by 5-HT<sub>2</sub> inverse agonists in other, non-SOD1 ALS cases represents an open question. In all, our animal study suggests that spasticity, at least in SOD1-linked ALS, is due to constitutive activity of the 5-HT<sub>2b</sub> receptor rather than 5-HT<sub>2c</sub>.

How far can these mechanistic results be compared with our pathology study in patients with ALS? Among the patients included in our study, only Patient 5 showed the complete picture of upper motor neuron signs, in particular spasticity, whereas the other patients exhibited either increased reflexes and/or Babinski signs, but not obvious spasticity (Supplementary Table 1). Patient 5, who displayed spasticity, showed strong loss of serotonergic terminals on motor neurons and thus appeared indistinguishable from the other patients with ALS in terms of loss of TPH2 projections. Interestingly, however, Patient 5 was the single case with ALS with widespread TDP43 pathology in serotonergic nuclei. Further work comparing autaptic material from patients with or without spasticity should be done to highlight potential correlations between serotonin loss and spasticity. Importantly, such a study could also investigate other phenotypes potentially related with serotonin such as weight loss, depression or dementia.

Our work has potential clinical implications for the management of spasticity in those patients presenting such a phenotype. This is especially true for patients with primary lateral sclerosis, a subtype of ALS with primary upper motor neuron involvement (Singer *et al.*, 2007; Gordon *et al.*, 2009). These patients develop prominent spasticity (Kuipers-Upmeijer *et al.*, 2001; Le Forestier *et al.*, 2001a, b) that is likely to be due to motor neuron hyperexcitability (Floeter *et al.*, 2005). Spasticity is also sometimes associated with ALS but difficult to detect clinically, as the tests used to assess spasticity rely on the integrity of alpha and gamma motor neurons, both degenerating during ALS (Swash, 2012). Spasticity in ALS and primary lateral sclerosis has been poorly studied, and few clinical trials have been performed to treat this symptom (Ashworth *et al.*, 2012). Only physical therapy was proven to be effective in a small trial (Drory *et al.*, 2001), and current guidelines of the European Federation of Neurological Societies state that other anti-spastic medications display class IV level of evidence of efficacy and 'may be tried' (Ashworth *et al.*, 2006). A rigorous clinical trial assessing cyproheptadine in ALS spasticity is thus needed, although treatment of spasticity might also lead to worsening of motor function as observed in spinal cord injury.

In conclusion, loss of serotonergic neurons is part of the degenerative process in ALS and may be involved in spasticity. Further research is needed to determine whether serotonergic degeneration has broader consequences on ALS pathophysiology.

## Acknowledgements

Annie PICCHINENNA (INSERM U692), Marie-Jo RUIVO (INSERM U692), Isabelle DROUET (Centre hospitalier de Versailles), Eliane SUPPER (Hopitaux Universitaires de Strasbourg) and Martine MUCKENSTURM (Hopitaux Universitaires de Strasbourg) provided technical support for this study.

## Funding

This work was funded in part by the Agence Nationale de la Recherche (ANR Jeune Chercheur Dynemit, to L.D.), Association pour la recherche sur la SLA et les autres maladies du motoneuron (ARSLA, to F.R. and J.P.L.), Thierry Latran Foundation (L.D., J.P.L.), Association pour la recherche et le développement de moyens de lutte contre les maladies neurodégénératives (AREMANE), the European Community's Health Seventh Framework Programme (FP7/2007-2013) under grant agreement No 259867 (J.P.L.), and Association française de lutte contre les myopathies (AFM, to J.P.L.). The generation of the Tph2 antibody was supported by the German Research Foundation (DFG) (SFB 581 and SFB TRR 58, to K.P.L.) and the European Community (NEWMOOD LSHM-CT-2003-503474, to K.P.L.). Collaboration between L.D. and V.M. is supported by a contrat d'interface INSERM/AP-HP. L.D. is supported by a Mercator Professorship (DFG, 2011-2012). A.H. is a research fellow receiving funding from FP7/2007-2013. J.L.G.D.A. is recipient of a Chaire d'excellence INSERM/Université de Strasbourg.

## Supplementary material

Supplementary material is available at *Brain* online.

## References

- Alvarez JC, Bothua D, Collignon I, Advenier C, Spreux-Varoquaux O. Simultaneous measurement of dopamine, serotonin, their metabolites and tryptophan in mouse brain homogenates by high-performance liquid chromatography with dual coulometric detection. *Biomed Chromatogr* 1999; 13: 293–8.
- Ashworth NL, Satkunam LE, Deforge D. Treatment for spasticity in amyotrophic lateral sclerosis/motor neuron disease. *Cochrane Database Syst Rev* 2006; 1: CD004156.
- Ashworth NL, Satkunam LE, Deforge D. Treatment for spasticity in amyotrophic lateral sclerosis/motor neuron disease. *Cochrane Database Syst Rev* 2012; 2: CD004156.
- Bennett DJ, Sanelli L, Cooke CL, Harvey PJ, Gorassini MA. Spastic long-lasting reflexes in the awake rat after sacral spinal cord injury. *J Neurophysiol* 2004; 91: 2247–58.
- Bertel O, Malessa S, Sluga E, Hornykiewicz O. Amyotrophic lateral sclerosis: changes of noradrenergic and serotonergic transmitter systems in the spinal cord. *Brain Res* 1991; 566: 54–60.
- Braunstein KE, Eschbach J, Rona-Voros K, Soyulu R, Mikrouli E, Larmet Y, et al. A point mutation in the dynein heavy chain gene leads to striatal atrophy and compromises neurite outgrowth of striatal neurons. *Hum Mol Genet* 2010; 19: 4385–98.
- Brooks BR, Miller RG, Swash M, Munsat TL. El Escorial revisited: revised criteria for the diagnosis of amyotrophic lateral sclerosis. *Amyotroph Lateral Scler Other Motor Neuron Disord* 2000; 1: 293–9.
- Drory VE, Goltzman E, Reznik JG, Mosek A, Korczyn AD. The value of muscle exercise in patients with amyotrophic lateral sclerosis. *J Neurol Sci* 2001; 191: 133–7.
- Dupuis L, de Tapia M, Rene F, Lutz-Bucher B, Gordon JW, Mercken L, et al. Differential screening of mutated SOD1 transgenic mice reveals early up-regulation of a fast axonal transport component in spinal cord motor neurons. *Neurobiol Dis* 2000; 7: 274–85.
- Dupuis L, Spreux-Varoquaux O, Bensimon G, Jullien P, Lacomblez L, Salachas F, et al. Platelet serotonin level predicts survival in amyotrophic lateral sclerosis. *PLoS One* 2010; 5: e13346.
- Floeter MK, Zhai P, Saigal R, Kim Y, Statland J. Motor neuron firing dysfunction in spastic patients with primary lateral sclerosis. *J Neurophysiol* 2005; 94: 919–27.
- Forrest V, Ince P, Leitch M, Marshall EF, Shaw PJ. Serotonergic neurotransmission in the spinal cord and motor cortex of patients with motor neuron disease and controls: quantitative autoradiography for 5-HT1a and 5-HT2 receptors. *J Neurol Sci* 1996; 139 (Suppl): 83–90.
- Franklin K, Paxinos G. The mouse brain in stereotaxic coordinates. San Diego: Academic Press; 1997.
- Gordon PH, Cheng B, Katz IB, Mitsumoto H, Rowland LP. Clinical features that distinguish PLS, upper motor neuron-dominant ALS, and typical ALS. *Neurology* 2009; 72: 1948–52.
- Gurney ME, Pu H, Chiu AY, Dal Canto MC, Polchow CY, Alexander DD, et al. Motor neuron degeneration in mice that express a human Cu,Zn superoxide dismutase mutation. *Science* 1994; 264: 1772–5.
- Gutknecht L, Kriegebaum C, Waider J, Schmitt A, Lesch KP. Spatio-temporal expression of tryptophan hydroxylase isoforms in murine and human brain: convergent data from Tph2 knockout mice. *Eur Neuropsychopharmacol* 2009; 19: 266–82.
- Halter B, Gonzalez de Aguilar JL, Rene F, Petri S, Fricker B, Echaniz-Laguna A, et al. Oxidative stress in skeletal muscle stimulates early expression of Rad in a mouse model of amyotrophic lateral sclerosis. *Free Radic Biol Med* 2010; 48: 915–23.
- Heckman CJ, Mottram C, Quinlan K, Theiss R, Schuster J. Motoneuron excitability: the importance of neuromodulatory inputs. *Clin Neurophysiol* 2009; 120: 2040–54.
- Ivanhoe CB, Reistetter TA. Spasticity: the misunderstood part of the upper motor neuron syndrome. *Am J Phys Med Rehabil* 2004; 83 (10 Suppl): S3–9.
- Kennett GA, Wood MD, Bright F, Cilia J, Piper DC, Gager T, et al. In vitro and in vivo profile of SB 206553, a potent 5-HT2C/5-HT2B receptor antagonist with anxiolytic-like properties. *Br J Pharmacol* 1996; 117: 427–34.
- Kiernan MC, Vucic S, Cheah BC, Turner MR, Eisen A, Hardiman O, et al. Amyotrophic lateral sclerosis. *Lancet* 2011; 377: 942–55.
- Kuipers-Upmeyer J, de Jager AE, Hew JM, Snoek JW, van Weerden TW. Primary lateral sclerosis: clinical, neurophysiological, and magnetic resonance findings. *J Neurol Neurosurg Psychiatry* 2001; 71: 615–20.
- Lanfranco MF, Anastasio NC, Seitz PK, Cunningham KA. Quantification of RNA editing of the serotonin 2C receptor (5-HT<sub>2C</sub>) ex vivo. *Methods Enzymol* 2010; 485: 311–28.
- Lanfranco MF, Seitz PK, Morabito MV, Emeson RB, Sanders-Bush E, Cunningham KA. An innovative real-time PCR method to measure changes in RNA editing of the serotonin 2C receptor (5-HT<sub>2C</sub>) in brain. *J Neurosci Methods* 2009; 179: 247–57.
- Le Forestier N, Maisonobe T, Spelle L, Lesort A, Salachas F, Lacomblez L, et al. Primary lateral sclerosis: further clarification. *J Neurol Sci* 2001a; 185: 95–100.
- Le Forestier N, Maisonobe T, Piquard A, Rivaud S, Crevier-Buchman L, Salachas F, et al. Does primary lateral sclerosis exist? A study of 20 patients and a review of the literature. *Brain* 2001b; 124 (Pt 10): 1989–99.
- Li Y, Li X, Harvey PJ, Bennett DJ. Effects of baclofen on spinal reflexes and persistent inward currents in motoneurons of chronic spinal rats with spasticity. *J Neurophysiol* 2004; 92: 2694–703.
- Murray KC, Stephens MJ, Ballou EW, Heckman CJ, Bennett DJ. Motoneuron excitability and muscle spasms are regulated by 5-HT<sub>2B</sub> and 5-HT<sub>2C</sub> receptor activity. *J Neurophysiol* 2011; 105: 731–48.
- Murray KC, Nakae A, Stephens MJ, Rank M, D'Amico J, Harvey PJ, et al. Recovery of motoneuron and locomotor function after spinal cord injury depends on constitutive activity in 5-HT<sub>2C</sub> receptors. *Nat Med* 2010; 16: 694–700.
- Navarrett S, Collier L, Cardozo C, Dracheva S. Alterations of serotonin 2C and 2A receptors in response to T10 spinal cord transection in rats. *Neurosci Lett* 2012; 506: 74–8.
- Nebigil CG, Jaffre F, Messaddeq N, Hickel P, Monassier L, Launay JM, et al. Overexpression of the serotonin 5-HT<sub>2B</sub> receptor in heart leads

- to abnormal mitochondrial function and cardiac hypertrophy. *Circulation* 2003; 107: 3223–9.
- Neumann M, Sampathu DM, Kwong LK, Truax AC, Micsenyi MC, Chou TT, et al. Ubiquitinated TDP-43 in frontotemporal lobar degeneration and amyotrophic lateral sclerosis. *Science* 2006; 314: 130–3.
- Ozdinler PH, Benn S, Yamamoto TH, Guzel M, Brown RH Jr, Macklis JD. Corticospinal motor neurons and related subcerebral projection neurons undergo early and specific neurodegeneration in hSOD1G(9)(3)A transgenic ALS mice. *J Neurosci* 2011; 31: 4166–77.
- Perrin FE, Gerber YN, Teigell M, Lonjon N, Boniface G, Bauchet L, et al. Anatomical study of serotonergic innervation and 5-HT(1A) receptor in the human spinal cord. *Cell Death Dis* 2011; 2: e218.
- Rank MM, Murray KC, Stephens MJ, D'Amico J, Gorassini MA, Bennett DJ. Adrenergic receptors modulate motoneuron excitability, sensory synaptic transmission and muscle spasms after chronic spinal cord injury. *J Neurophysiol* 2011; 105: 410–22.
- Ripps ME, Huntley GW, Hof PR, Morrison JH, Gordon JW. Transgenic mice expressing an altered murine superoxide dismutase gene provide an animal model of amyotrophic lateral sclerosis. *Proc Natl Acad Sci USA* 1995; 92: 689–93.
- Seifert R, Wenzel-Seifert K. Constitutive activity of G-protein-coupled receptors: cause of disease and common property of wild-type receptors. *Naunyn Schmiedebergs Arch Pharmacol* 2002; 366: 381–416.
- Shannon NJ, Gunnet JW, Moore KE. A comparison of biochemical indices of 5-hydroxytryptaminergic neuronal activity following electrical stimulation of the dorsal raphe nucleus. *J Neurochem* 1986; 47: 958–65.
- Singer MA, Statland JM, Wolfe GI, Barohn RJ. Primary lateral sclerosis. *Muscle Nerve* 2007; 35: 291–302.
- Sofic E, Riederer P, Gsell W, Gavranovic M, Schmidtke A, Jellinger K. Biogenic amines and metabolites in spinal cord of patients with Parkinson's disease and amyotrophic lateral sclerosis. *J Neural Transm Park Dis Dement Sect* 1991; 3: 133–42.
- Swash M. Why are upper motor neuron signs difficult to elicit in amyotrophic lateral sclerosis? *J Neurol Neurosurg Psychiatry* 2012; 83: 659–62.
- Turner MR, Rabiner EA, Al-Chalabi A, Shaw CE, Brooks DJ, Leigh PN, et al. Cortical 5-HT1A receptor binding in patients with homozygous D90A SOD1 vs sporadic ALS. *Neurology* 2007; 68: 1233–5.
- Turner MR, Rabiner EA, Hammers A, Al-Chalabi A, Grasby PM, Shaw CE, et al. [11C]-WAY100635 PET demonstrates marked 5-HT1A receptor changes in sporadic ALS. *Brain* 2005; 128 (Pt 4): 896–905.
- Vandesompele J, De Preter K, Pattyn F, Poppe B, Van Roy N, De Paepe A, et al. Accurate normalization of real-time quantitative RT-PCR data by geometric averaging of multiple internal control genes. *Genome Biology* 2002; 3.
- Yoshimoto K, Irizawa Y, Komura S. Rapid postmortem changes of rat striatum dopamine, serotonin, and their metabolites as monitored by brain microdialysis. *Forensic Sci Int* 1993; 60: 183–8.

---

## CONCLUSIONS AND PERSPECTIVES

As it is understood today ALS-related pathology is considerably more complex than originally envisaged. New pathologic events associated with mSOD1 in cellular populations other than motor neurons are coming into the spotlight (Boillée et al., 2006a). Throughout the works presented here, we bring new evidence that highlights the importance of two different cellular populations (muscle and serotonergic neurons) for disease progression and for development of future therapeutic approaches.

Muscle dysfunctions in ALS have received little attention so far, as its pathology was mostly considered a side effect of denervation. However several lines of evidence support the idea that the muscle is also a target of mSOD1 toxicity. Muscle is a tissue of great importance for whole body homeostasis. At the same time ALS has been associated with metabolic dysfunctions with undeniable clinical importance. Metabolic changes in ALS have a negative impact on disease progression and correlate with a bad prognosis (Dupuis et al., 2011). From this perspective we investigated the metabolic profile of muscle tissue in our mouse model for ALS, in order to establish whether there is a connection between muscle pathology and metabolic disequilibrium.

One exciting finding of our study showed that asymptomatic SOD1<sup>G86R</sup> mice have an increased resistance to moderate/aerobic exercise. This might provide an interesting explanation to the high prevalence of ALS amongst athletes, which has been a matter of debate for decades. In the same time these animals showed a lower performance during anaerobic/glycolytic exercise when compared to WT littermates. This indicated an alteration of the adaptability capacity in mSOD1<sup>G86R</sup> mice.

Indeed, the metabolic profile of glycolytic muscle fibers, that were the most affected by denervation and atrophy, presented deeper metabolic alteration that were evident at an early asymptomatic stage. We demonstrated that the increase in endurance capacity associated with the inability to support intense exercise mirrored a profound alteration of fuel preference in muscle

fibers consisting in an inhibition of glycolysis and an up-regulation of the lipid oxidation pathway. These alterations were identified in young asymptomatic animals, and they were specific to glycolytic muscle fibers. This is in agreement with previous findings indicating a switch in muscle fiber type, pinpointing muscle tissue as site of lipid usage and hypermetabolism. We identified PDK4 as the master regulator of this change in metabolic phenotype. In skeletal muscle, PDK4 is the major isoform of this kinase family expressed, and is considered as a critical regulator of pyruvate dehydrogenase (PDH) activity (Harris et al., 2002). By phosphorylating PDH, PDK4 inhibits the entry of pyruvate into the Krebs cycle and inhibits glucose oxidation (Sugden et al., 2000). This mechanism is activated mainly during periods of energetic crisis (e.g. starvation), and participates to a change in fiber type from glycolytic to oxidative. PDK4 was upregulated in glycolytic muscle fibers of young asymptomatic animals. The effect of PDK4 activation on glucose metabolism was evidenced by decreased enzymatic activity of phosphofructokinase, the rate-limiting enzyme of glycolysis. At this stage, glucose entry was not altered, as we observed an increase in glycogen that suggested that glucose is rerouted towards glycogen stores.

This switch towards increased lipid usage was independent of PGC-1 $\alpha$ , the main regulator of muscle metabolism. Moreover, PGC-1 $\alpha$  was inhibited with disease progression, and this correlates with a decreased expression of genes involved in mitochondrial biogenesis. This was reflected by a decreased expression of mtDNA especially evident at end stage. In this context, it is expected that the increased ROS production issued from lipid metabolism will add more pressure to an already fragile mitochondrial system.

Using dichloroacetate (DCA), a specific inhibitor of PDK4 we aimed at restoring the glycolytic pathway and metabolic equilibrium in muscle fibers. The attractiveness of this approach lies within the fact that PDK4 is not expressed in motor neurons, which helped us to relatively isolate the effects of our pharmacological treatment. Our results show clear benefits of DCA administration on disease progression, delaying symptom onset and denervation. Moreover this treatment had beneficial effects on mitochondrial

metabolism, restoring the expression of genes involved in glucose oxidation (citrate synthase), mitochondrial biogenesis (*Pgc-1α*, *mfn1*), and reducing the expression of genes involved in ROS scavenging (*Gpx*).

Our findings helped us isolate an interesting pathologic mechanism that participates to the hypermetabolic states of SOD1<sup>G86R</sup> mice. This brings new evidence supporting the involvement of muscle tissue in the progression of this disease, and supports the interest in further investigating metabolic targets for the development of future therapies.

In parallel we investigated the therapeutic significance of another important metabolic regulator, Sirt1. In muscle tissues Sirt1 has an important function regulating muscle adaptation to exercise, mainly by de-acetylating and activating PGC-1α. Sirt1 was found upregulated in muscle tissues of two different mouse models mainly at end stage. This correlates with an altered NAD<sup>+</sup>/NADH ratio that we have shown in the previous section and is probably the reflection an acute energetic distress. Targeting muscular Sirt1 in the early states of the disease could have beneficial effects, protecting mitochondria and protecting from energetic distress. However, in this work we showed a different expression of Sirt1 between muscle and spinal cord, where Sirt1 was inhibited. Activating Sirt1 (pharmacologically or genetically) in neuronal cells expressing mSOD1 did not have beneficial effects. Taken all these aspects into consideration, the therapeutic potential of Sirt1 remains elusive.

Another important aspect of muscle pathology that we explored was muscle spasticity, a debilitating condition that has a negative impact on patient's quality of life. We show for the first time pathological alterations of serotonergic system in ALS patients and an ALS mouse model. Further we bring evidence supporting a direct relationship between the degeneration of serotonergic projections and the development of spasticity in SOD1<sup>G86R</sup> mice. Activation of constitutively active serotonin receptors 5HT<sub>2B</sub> is the direct consequence of the loss of serotonergic projections to the motor neurons in the spinal cord. This is extremely relevant for management of spasticity in PLS and ALS patients presenting with such symptoms.

We show for the first time that muscle tissue suffers metabolic alterations early in the course of disease development, alterations that influence the course of the pathology. These alterations are specific to glycolytic muscle fibers and therefore can explain the sensitivity of glycolytic fibers to atrophy and denervation. Moreover, the mechanism described offers further understanding of the systemic metabolic alterations that accompany ALS. By exploring this mechanism we pinpointed the molecular actors involved in these modifications and we identified a potential therapeutic target on this pathway. Further we investigated the potential of specific therapeutic targets in the central nervous system that could improve muscle function and have beneficial effects on patient's quality of life. Altogether the work presented here brings new evidence supporting the importance of muscle pathology in ALS and its relevance for the design of new therapeutic approaches.

---

## SUMMARY IN FRENCH

## INTRODUCTION

La sclérose latérale amyotrophique (SLA) est une maladie neurodégénérative fatale caractérisée par une perte progressive et sélective des motoneurones. La dénervation musculaire associée à cette perte provoque une paralysie progressive des muscles squelettiques et une baisse de l'efficacité de la ventilation pulmonaire conduisant au décès du patient de 3 à 5 ans après la pose du diagnostic. La majorité des cas de SLA sont des cas sporadiques, et 5 à 10% d'entre eux sont d'origine familiale. A ce jour, une dizaine de gènes a été associée à cette pathologie. Parmi eux, le gène *sod1* codant pour la superoxyde dismutase 1 a été le premier identifié dans des formes familiales. Des mutations de ce gène sont retrouvées dans 20% des formes familiales et 2% des formes sporadiques. L'identification de ces mutations a permis de générer des souris transgéniques modèles de cette pathologie grâce auxquelles il est possible d'étudier les mécanismes cellulaires et moléculaires qui sous-tendent cette pathologie.

Jusque très récemment, la SLA était considérée comme une maladie intrinsèque du motoneurone, le premier événement visible dans la progression de la maladie étant une déstabilisation des jonctions neuromusculaires (JNM), points de contact fonctionnels entre les motoneurones et les muscles qu'ils innervent. Cependant depuis une quinzaine d'années, des travaux réalisés tant chez l'homme que dans des modèles murins montrent que la SLA est une maladie systémique qui affecte l'ensemble de l'organisme et s'accompagne d'importantes altérations de l'homéostasie énergétique. En effet, des altérations métaboliques (hypermétabolisme et dyslipidémie) et mitochondriales sont associées au développement de la pathologie et conduisent à un déficit énergétique chronique. Ces altérations métaboliques apparaissent précocement au cours de la maladie, bien avant que les motoneurones ne meurent et des arguments

expérimentaux suggèrent que des modifications métaboliques au niveau musculaire pourraient participer au développement de la pathologie. En effet, l'induction expérimentale d'un hypermétabolisme musculaire est suffisante à elle seule pour induire une dénervation musculaire et une perte de motoneurones. Ces travaux ont permis d'émettre de nouvelles hypothèses quant au point de départ de la pathologie et aux acteurs conduisant au démantèlement de la JNM et à la mort des motoneurones, mettant en avant le rôle actif potentiel du muscle dans cette pathologie.

## OBJECTIFS

Les modifications du métabolisme dans la SLA commencent à être perçues comme un aspect pathologique important, même si elles ne sont pas encore complètement définies. De nombreuses zones d'ombres persistent, mais il est déjà bien établi que l'état métabolique/énergétique dans la SLA a des effets directs sur la progression de la maladie et la survie. Un fort indice de masse corporelle est notamment associé à un meilleur pronostic clinique chez les patients SLA et une diète enrichie en lipides préserve les fonctions motrices des souris SOD1 et augmente leurs survies.

L'homéostasie générale d'un organisme a un effet direct sur l'activité métabolique musculaire. Certaines études montrent que l'exercice musculaire modéré est bénéfique dans les modèles animaux et pour les patients SLA. Il a également été démontré par diverses approches expérimentales que l'interaction nerf-muscle joue un rôle important dans la stabilité de la jonction neuromusculaire (JNM).

Le laboratoire a démontré que le métabolisme musculaire est altéré dans la SLA, et que ces altérations peuvent participer à la dénervation. A partir de ces observations, nous pouvons imaginer que des

interventions thérapeutiques ciblant le muscle seraient bénéfiques en préservant la fonctionnalité musculaire, l'intégrité de la JMN et en améliorant significativement la qualité de vie des patients.

L'hypothèse de ma thèse est qu'en disséquant la pathologie musculaire dans la SLA, nous gagnerons en compréhension dans cette maladie et que de nouvelles stratégies thérapeutiques pourront être proposées.

C'est dans ce contexte que se situe mon travail de thèse intitulé « Etudes des altérations métaboliques musculaires au cours de la sclérose latérale amyotrophique : rôle dans le développement de la pathologie. ».

Les objectifs de ce travail ont été doubles :

I- Caractériser précisément les modifications métaboliques précoces au niveau musculaire et comparer le décours de ces altérations dans deux types de muscles : les muscles glycolytiques, qui sont les muscles les plus touchés au cours de la SLA, et les muscles oxydatifs qui eux semblent plus résistants à la dénervation.

II- Evaluer les conséquences fonctionnelles de ces modifications par des approches pharmacologiques afin de comprendre si et comment ces altérations peuvent influencer la mise en place de la pathologie.

## METHODES

Ce travail a été réalisé dans le modèle de souris transgéniques SOD1<sup>G86R</sup> qui surexprime une mutation du gène codant pour la SOD1 et développent une maladie du motoneurone présentant le même tableau clinique que celui observé chez les patients. Dans ce modèle murin de SLA, le décours de la pathologie se décline en plusieurs stades : 65j stade asymptotique d'un point de vue des atteintes

motrices, 90j stade où les premiers déficits de motricité peuvent apparaître et où l'électromyogramme met en évidence une activité spontanée de dénervation des fibres musculaires chez certains animaux, et 105j stade auquel l'animal présente une paralysie avérée.

Pour mener à bien ces études portant sur la caractérisation et le rôle des altérations métaboliques musculaires précoces au cours de la SLA, j'ai utilisé des techniques complémentaires permettant d'une part une approche physiologique intégrée (exercice sur tapis roulant, test d'agrippement, électromyographie, traitement pharmacologiques) et d'autre part une approche à l'échelle cellulaire et moléculaire grâce à des techniques de biochimie et de biologie moléculaire (Western blot, mesures d'activités enzymatiques, dosages de métabolites, RT-qPCR), d'histologie, et d'immunohistochimie.

## RESULTATS

Dans un premier temps, j'ai réalisé une évaluation fonctionnelle de l'aptitude à l'exercice des souris SOD1<sup>G86R</sup> afin de tester les capacités physiques des souris SOD1<sup>G86R</sup> à 65j (âge où l'innervation est normale) en l'absence de tout entraînement et de déterminer si ces souris étaient capables de s'adapter à des conditions de stress énergétique de façon comparable à des souris contrôles (WT). Dans ce but, des souris ont été soumises à deux types d'exercice physique sur tapis roulant: 1) un protocole aigue à vitesse croissante qui sollicite principalement les fibres glycolytiques, 2) un protocole réalisé à une vitesse constante modérée correspondant à 80% de la vitesse maximale atteinte dans le protocole 1 et sollicitant les fibres oxydatives. Cette approche intégrée m'a permis de mettre en évidence une importante et surprenante différence entre les souris WT et les souris mutées : les souris SOD1<sup>G86R</sup> présentent des performances réduites lors d'un exercice intense alors qu'elles ont une endurance supérieure

aux souris WT lors d'une course à une vitesse modérée suggérant des capacités oxydatives accrues.

Pour comprendre l'origine de cette modification d'aptitude à l'exercice et de réponse à un stress énergétique, j'ai ensuite étudié en détail le métabolisme des fibres glycolytiques dans le *tibialis anterior* (TA) que j'ai comparé à celui de fibres oxydatives (soleus). Les muscles glycolytiques sont les premiers muscles touchés par la dénervation au cours de la maladie. Cela m'a permis de mettre en évidence l'existence d'altérations dynamiques entre le métabolisme glucidique et le métabolisme lipidique dans les muscles glycolytiques à un stade asymptotique du point de vue moteur.

Par des méthodes biochimiques et moléculaires j'ai mis en évidence une inhibition de la glycolyse reflétée par la réduction de l'activité de la phosphofructokinase 1 (PFK1). Cette inhibition est détectée dès 65j et augmente avec la progression de la pathologie. A cela s'ajoute une induction de l'expression de la pyruvate déshydrogénase kinase 4 (PDK4), une enzyme qui inhibe l'activité du complexe pyruvate déshydrogénase (PDH) empêchant ainsi l'oxydation du pyruvate en acétyl-CoA et son entrée dans le cycle de Krebs. Parallèlement à ce blocage de l'utilisation du glucose, il y a une surexpression des gènes impliqués dans la mobilisation et l'utilisation des lipides (LPL, FAT/CD36, CPT1) ainsi qu'une accumulation de NADH et d'ATP qui reflètent une augmentation du métabolisme lipidique. Ces molécules (NADH et ATP) peuvent à leur tour stimuler l'activité de la PDK4. Cette augmentation de la PDK4, qui s'amplifie avec l'âge, est indépendante du processus de dénervation et est spécifique des muscles glycolytiques. De plus, ces changements métaboliques s'accompagnent d'une répression de PGC1 $\alpha$  et de ses gènes cibles ainsi que d'une baisse de la quantité d'ADN mitochondrial, suggérant une perte progressive des mitochondries. Il est à noter qu'aucune des modifications mesurées dans le muscle glycolytique n'est retrouvée dans le muscle oxydatif.

Le dialogue entre ces deux voies métaboliques est essentiel pour la réponse adaptative du muscle. L'altération de celui-ci avec le blocage de l'utilisation du glucose peut conduire à une crise énergétique au sein de l'unité motrice et potentiellement induire la déstabilisation de la JNM.

Pour comprendre l'importance de ce dysfonctionnement métabolique précoce dans le développement de la SLA j'ai utilisée une approche pharmacologique systémique dans le but de normaliser les modifications observées. J'ai choisi de tester une molécule touchant une cible précise : la PDK4 qui est induite de manière précoce chez la souris SOD<sup>G86R</sup>. Pour cela j'ai utilisé le dichloroacétate (DCA), un inhibiteur de la PDK4. Le traitement a été initié à l'âge de 2 mois, âge auquel les souris présentent les premiers signes de dénervation ainsi qu'une perte de poids et une altération de la motricité, et pour une durée de 5 semaines. Le traitement a eu des effets bénéfiques ralentissant le processus de dénervation. Le traitement avec le DCA a normalisé l'expression de PDK4, augmenté l'expression des gènes impliqués dans le fonctionnement de la mitochondrie, prévenu la perte de poids associée à la progression de la maladie et augmenté la force musculaire. Ces expériences montrent que le dysfonctionnement métabolique est une composante importante de la pathologie et qu'en ciblant ces altérations métaboliques, il est possible de prévenir la dénervation et d'améliorer le métabolisme global des souris SOD1<sup>G86R</sup>.

## CONCLUSION

Telle qu'elle est comprise aujourd'hui, la SLA a un tableau clinique considérablement plus complexe que prévue initialement. Des nouvelles pathologies associées à la mSOD1 dans des populations cellulaires autres que les neurones moteurs sont mis en évidence. Tout au long des travaux présentés ici, nous apportons de nouveaux indices qui soulignent l'importance d'un autre type cellulaire (le muscle) dans la progression de la maladie.

Les dysfonctionnements musculaires dans la SLA ont reçu peu d'attention jusqu'à présent, comme la pathologie était surtout considérée comme un effet secondaire de la dénervation. Cependant plusieurs sources de données soutiennent l'idée que le muscle est également une cible de toxicité de la mSOD1. Le muscle est un tissu d'une grande importance pour l'homéostasie métabolique de l'organisme. En même temps, la SLA a été associée à des dysfonctionnements métaboliques ayant une importance clinique indéniable. La diminution de l'indice de masse corporel, et donc des réserves lipidiques, a un impact négatif sur la progression de la maladie et corrèle avec un mauvais pronostic. Dans cette perspective, nous avons étudié le profil métabolique du tissu musculaire dans notre modèle de souris pour la SLA, afin d'établir s'il existe un lien entre la pathologie musculaire et le déséquilibre métabolique.

La découverte majeure de notre étude est que les souris SOD1<sup>G86R</sup> asymptomatiques ont une résistance accrue à un exercice modéré / aérobic. Dans le même temps, ces animaux ont montré une performance inférieure pour un exercice anaérobic / glycolytique par rapport aux WT. Ceci indique une altération de la capacité d'adaptation chez la souris mSOD1<sup>G86R</sup>. Ces résultats peuvent fournir des éléments de réflexion pour l'étude des liens, actuellement débattus, entre l'activité physique et le développement de la SLA chez les patients.

En effet, le profil métabolique des fibres musculaires glycolytiques, qui sont en fait les plus touchés par la dénervation et l'atrophie, présente des profondes modifications métaboliques, évidentes à un stade asymptotique précoce. Nous avons démontré que l'augmentation de l'endurance associée à une capacité réduite pour un exercice intense reflète une altération profonde de l'utilisation de carburant dans les fibres musculaires des souris de 65 jours. Ces altérations consistent en une inhibition de la glycolyse et une hausse de la voie d'utilisation des lipides. Ces modifications ont été identifiées chez les animaux jeunes asymptotiques, et sont spécifiquement trouvés dans fibres musculaires glycolytiques. Ceci est en accord avec les résultats antérieurs indiquant un changement de type de fibre musculaire au cours de la maladie, et qui marque l'utilisation accrue des lipides par le muscle et son hypermétabolisme. Nous avons identifié PDK4 comme le régulateur de ce changement dans le phénotype métabolique. Ce mécanisme est activé principalement pendant les périodes de crise énergétique (par exemple, la restriction calorique), et participe à un changement de type fibre de glycolytique vers oxydatif. PDK4 est régulée à la hausse dans les fibres musculaires glycolytiques des jeunes animaux asymptotiques. L'effet de l'activation de PDK4 sur le métabolisme du glucose diminue de l'activité enzymatique de la phosphofructokinase, l'enzyme limitante de la glycolyse. A ce stade, l'entrée du glucose n'a pas été modifiée, comme nous avons observé une augmentation de glycogène qui suggère que le glucose est redistribué vers les réserves de glycogène.

Ce changement vers une utilisation accrue des lipides était indépendant de PGC-1 $\alpha$ , le principal régulateur du métabolisme musculaire. En outre, PGC-1 $\alpha$  est inhibée avec la progression de la maladie, ce qui est en corrélation avec une diminution de l'expression des gènes impliqués dans la biogenèse mitochondriale. Cela s'est traduit par une diminution de l'expression de l'ADNmt particulièrement évident au stade final. Dans ce contexte, il est attendu à ce que

l'augmentation de la production des ROS émis par le métabolisme lipidique ajoute plus de pression pour un système mitochondrial déjà fragilisé.

En utilisant le dichloroacétate (DCA), un inhibiteur spécifique de PDK4, nous avons cherché à restaurer la voie de la glycolyse et donc l'équilibre métabolique dans les fibres musculaires. L'attrait de cette approche réside dans le fait que PDK4 n'est pas exprimé dans les neurones moteurs, ce qui nous a aidé à isoler les effets de notre traitement pharmacologique. Nos résultats montrent des effets bénéfiques évidents de l'administration DCA de la progression de la maladie, ce qui retarde l'apparition des symptômes et la dénervation. En outre, ce traitement a des effets bénéfiques sur le métabolisme mitochondrial, la restauration de l'expression de gènes impliqués dans l'oxydation du glucose (citrate synthase), la biogenèse mitochondriale (PGC-1 $\alpha$ , mfn1), et la réduction de l'expression de gènes impliqués dans la neutralisation des ROS (GPX).

Nos résultats nous ont permis d'isoler un mécanisme pathologique intéressant qui contribue à l'état hypermétabolique de la souris SOD1<sup>G86R</sup>. Cela apporte une nouvelle preuve de la participation du tissu musculaire dans la progression de cette maladie, et soutient l'investigation des cibles métaboliques pour le développement de thérapies futures.

Mon travail de thèse a permis de montrer que dans un modèle murin de SLA il existe des altérations métaboliques précoces, spécifiques aux muscles glycolytiques qui sont les premiers atteints lors de la SLA, et d'identifier les mécanismes qui conduisent à l'inhibition de l'oxydation du glucose dans ces muscles. De plus il a permis de montrer que par des approches pharmacologiques, il est possible d'intervenir en limitant ces altérations permettant ainsi un maintien des unités motrices fonctionnelles.

---

# BIBLIOGRAPHY

- Aguer, C., Fiehn, O., Seifert, E.L., Bézaire, V., Meissen, J.K., Daniels, A., Scott, K., Renaud, J.-M., Padilla, M., Bickel, D.R., et al. (2013). Muscle uncoupling protein 3 overexpression mimics endurance training and reduces circulating biomarkers of incomplete  $\beta$ -oxidation. *FASEB J.* 27, 4213–4225.
- Alami, N.H., Smith, R.B., Carrasco, M.A., Williams, L.A., Winborn, C.S., Han, S.S.W., Kiskinis, E., Winborn, B., Freibaum, B.D., Kanagaraj, A., et al. (2014). Axonal transport of TDP-43 mRNA granules is impaired by ALS-causing mutations. *Neuron* 81, 536–543.
- Alexianu, M.E., Kozovska, M., and Appel, S.H. (2001). Immune reactivity in a mouse model of familial ALS correlates with disease progression. *Neurology* 57, 1282–1289.
- Allaman, I., Bélanger, M., and Magistretti, P.J. (2011). Astrocyte-neuron metabolic relationships: for better and for worse. *Trends Neurosci.* 34, 76–87.
- Almeida, S., Gascon, E., Tran, H., Chou, H.J., Gendron, T.F., Degroot, S., Tapper, A.R., Sellier, C., Charlet-Berguerand, N., Karydas, A., et al. (2013). Modeling key pathological features of frontotemporal dementia with C9ORF72 repeat expansion in iPSC-derived human neurons. *Acta Neuropathol.* 126, 385–399.
- Andersen, P.M., and Al-Chalabi, A. (2011). Clinical genetics of amyotrophic lateral sclerosis: what do we really know? *Nat. Rev. Neurol.* 7, 603–615.
- Armstrong, G.A.B., and Drapeau, P. (2013). Loss and gain of FUS function impair neuromuscular synaptic transmission in a genetic model of ALS. *Hum. Mol. Genet.* 22, 4282–4292.
- Ashworth, N.L., Satkunam, L.E., and Deforge, D. (2012). Treatment for spasticity in amyotrophic lateral sclerosis/motor neuron disease. *Cochrane Database Syst. Rev.* 2, CD004156.
- Bahadorani, S., Mukai, S.T., Rabie, J., Beckman, J.S., Phillips, J.P., and Hilliker, A.J. (2013). Expression of zinc-deficient human superoxide dismutase in *Drosophila* neurons produces a locomotor defect linked to mitochondrial dysfunction. *Neurobiol. Aging* 34, 2322–2330.
- Beckman, J.S., Carson, M., Smith, C.D., and Koppenol, W.H. (1993). ALS, SOD and peroxynitrite. *Nature* 364, 584.
- Beckman, J.S., Estévez, A.G., Crow, J.P., and Barbeito, L. (2001). Superoxide dismutase and the death of motoneurons in ALS. *Trends Neurosci.* 24, S15–S20.
- Bélanger, M., and Magistretti, P.J. (2009). The role of astroglia in neuroprotection. *Dialogues Clin. Neurosci.* 11, 281–295.
- Bendotti, C., Calvaresi, N., Chiveri, L., Prella, A., Moggio, M., Braga, M., Silani, V., and De Biasi, S. (2001). Early vacuolization and mitochondrial damage in motor neurons of FALS mice are not associated with apoptosis or with changes in cytochrome oxidase histochemical reactivity. *J. Neurol. Sci.* 191, 25–33.
- Bodine, S.C., Stitt, T.N., Gonzalez, M., Kline, W.O., Stover, G.L., Bauerlein, R., Zlotchenko, E., Scrimgeour, A., Lawrence, J.C., Glass, D.J., et al. (2001a). Akt/mTOR pathway is a crucial regulator of skeletal muscle hypertrophy and can prevent muscle atrophy in vivo. *Nat. Cell Biol.* 3, 1014–1019.
- Bodine, S.C., Latres, E., Baumhueter, S., Lai, V.K., Nunez, L., Clarke, B.A., Poueymirou, W.T., Panaro, F.J., Na, E., Dharmarajan, K., et al. (2001b). Identification of ubiquitin ligases required for skeletal muscle atrophy. *Science* 294, 1704–1708.

- Boillée, S., Vande Velde, C., and Cleveland, D.W. (2006a). ALS: a disease of motor neurons and their nonneuronal neighbors. *Neuron* *52*, 39–59.
- Boillée, S., Yamanaka, K., Lobsiger, C.S., Copeland, N.G., Jenkins, N.A., Kassiotis, G., Kollias, G., and Cleveland, D.W. (2006b). Onset and progression in inherited ALS determined by motor neurons and microglia. *Science* *312*, 1389–1392.
- Bordone, L., and Guarente, L. (2005). Calorie restriction, SIRT1 and metabolism: understanding longevity. *Nat. Rev. Mol. Cell Biol.* *6*, 298–305.
- Van Den Bosch, L., Tilkin, P., Lemmens, G., and Robberecht, W. (2002). Minocycline delays disease onset and mortality in a transgenic model of ALS. *Neuroreport* *13*, 1067–1070.
- Bottinelli, R., Canepari, M., Reggiani, C., and Stienen, G.J. (1994). Myofibrillar ATPase activity during isometric contraction and isomyosin composition in rat single skinned muscle fibres. *J. Physiol.* *481*, 663–675.
- Bouteloup, C., Desport, J.-C., Clavelou, P., Guy, N., Derumeaux-Burel, H., Ferrier, A., and Couratier, P. (2009). Hypermetabolism in ALS patients: an early and persistent phenomenon. *J. Neurol.* *256*, 1236–1242.
- Brown, R.H. (1998). SOD1 aggregates in ALS: cause, correlate or consequence? *Nat. Med.* *4*, 1362–1364.
- Brown, G.C., and Neher, J.J. (2014). Microglial phagocytosis of live neurons. *Nat. Rev. Neurosci.* *15*, 209–216.
- Bruijn, L.I., Beal, M.F., Becher, M.W., Schulz, J.B., Wong, P.C., Price, D.L., and Cleveland, D.W. (1997). Elevated free nitrotyrosine levels, but not protein-bound nitrotyrosine or hydroxyl radicals, throughout amyotrophic lateral sclerosis (ALS)-like disease implicate tyrosine nitration as an aberrant in vivo property of one familial ALS-linked superoxide di. *Proc. Natl. Acad. Sci. U. S. A.* *94*, 7606–7611.
- Bruijn, L.I., Houseweart, M.K., Kato, S., Anderson, K.L., Anderson, S.D., Ohama, E., Reaume, A.G., Scott, R.W., and Cleveland, D.W. (1998). Aggregation and motor neuron toxicity of an ALS-linked SOD1 mutant independent from wild-type SOD1. *Science* *281*, 1851–1854.
- Buratti, E., Dörk, T., Zuccato, E., Pagani, F., Romano, M., and Baralle, F.E. (2001). Nuclear factor TDP-43 and SR proteins promote in vitro and in vivo CFTR exon 9 skipping. *EMBO J.* *20*, 1774–1784.
- Burke, R.E., Levine, D.N., Zajac, F.E., Tsairis, P., and Engel, W.K. (1971). Mammalian Motor Units: Physiological-Histochemical Correlation in Three Types in Cat Gastrocnemius. *Science* (80- ). *174*, 709–712.
- Cantó, C., Jiang, L.Q., Deshmukh, A.S., Matak, C., Coste, A., Lagouge, M., Zierath, J.R., and Auwerx, J. (2010). Interdependence of AMPK and SIRT1 for metabolic adaptation to fasting and exercise in skeletal muscle. *Cell Metab.* *11*, 213–219.
- Carreras, I., Yuruker, S., Aytan, N., Hossain, L., Choi, J.-K., Jenkins, B.G., Kowall, N.W., and Dedeoglu, A. (2010). Moderate exercise delays the motor performance decline in a transgenic model of ALS. *Brain Res.* *1313*, 192–201.
- Carri, M.T., and Cozzolino, M. (2011). SOD1 and mitochondria in ALS: a dangerous liaison. *J. Bioenerg. Biomembr.* *43*, 593–599.
- Cassina, P., Pehar, M., Vargas, M.R., Castellanos, R., Barbeito, A.G., Estévez, A.G., Thompson, J.A., Beckman, J.S., and Barbeito, L. (2005). Astrocyte activation by fibroblast growth factor-1 and motor neuron apoptosis: implications for amyotrophic lateral sclerosis. *J. Neurochem.* *93*, 38–46.

- Catoire, M., Alex, S., Paraskevopoulos, N., Mattijssen, F., Evers-van Gogh, I., Schaart, G., Jeppesen, J., Kneppers, A., Mensink, M., Voshol, P.J., et al. (2014). Fatty acid-inducible ANGPTL4 governs lipid metabolic response to exercise. *Proc. Natl. Acad. Sci. U. S. A.* *111*, E1043–52.
- Chiò, A., Benzi, G., Dossena, M., Mutani, R., and Mora, G. (2005). Severely increased risk of amyotrophic lateral sclerosis among Italian professional football players. *Brain* *128*, 472–476.
- Chuang, D.-M., Leng, Y., Marinova, Z., Kim, H.-J., and Chiu, C.-T. (2009). Multiple roles of HDAC inhibition in neurodegenerative conditions. *Trends Neurosci.* *32*, 591–601.
- Cleveland, D.W., and Rothstein, J.D. (2001). From Charcot to Lou Gehrig: deciphering selective motor neuron death in ALS. *Nat. Rev. Neurosci.* *2*, 806–819.
- Conte, A., Lattante, S., Zollino, M., Marangi, G., Luigetti, M., Del Grande, A., Servidei, S., Trombetta, F., and Sabatelli, M. (2012). P525L FUS mutation is consistently associated with a severe form of juvenile amyotrophic lateral sclerosis. *Neuromuscul. Disord.* *22*, 73–75.
- Couratier, P., Hugon, J., Sindou, P., Vallat, J.M., and Dumas, M. (1993). Cell culture evidence for neuronal degeneration in amyotrophic lateral sclerosis being linked to glutamate AMPA/kainate receptors. *Lancet* *341*, 265–268.
- Cozzolino, M., and Carri, M.T. (2012). Mitochondrial dysfunction in ALS. *Prog. Neurobiol.* *97*, 54–66.
- Crippa, V., Boncoraglio, A., Galbiati, M., Aggarwal, T., Rusmini, P., Giorgetti, E., Cristofani, R., Carra, S., Pennuto, M., and Poletti, A. (2013). Differential autophagy power in the spinal cord and muscle of transgenic ALS mice. *Front. Cell. Neurosci.* *7*, 234.
- Crow, J.P., Sampson, J.B., Zhuang, Y., Thompson, J.A., and Beckman, J.S. (1997). Decreased zinc affinity of amyotrophic lateral sclerosis-associated superoxide dismutase mutants leads to enhanced catalysis of tyrosine nitration by peroxynitrite. *J. Neurochem.* *69*, 1936–1944.
- Da Cruz, S., Parone, P. a, Lopes, V.S., Lillo, C., McAlonis-Downes, M., Lee, S.K., Vetto, A.P., Petrosyan, S., Marsala, M., Murphy, A.N., et al. (2012). Elevated PGC-1 $\alpha$  activity sustains mitochondrial biogenesis and muscle function without extending survival in a mouse model of inherited ALS. *Cell Metab.* *15*, 778–786.
- Daigle, J.G., Lanson, N.A., Smith, R.B., Casci, I., Maltare, A., Monaghan, J., Nichols, C.D., Kryndushkin, D., Shewmaker, F., and Pandey, U.B. (2013). RNA-binding ability of FUS regulates neurodegeneration, cytoplasmic mislocalization and incorporation into stress granules associated with FUS carrying ALS-linked mutations. *Hum. Mol. Genet.* *22*, 1193–1205.
- Dal Bello-Haas, V., and Florence, J.M. (2013). Therapeutic exercise for people with amyotrophic lateral sclerosis or motor neuron disease. *Cochrane Database Syst. Rev.* *5*, CD005229.
- Van Damme, P., Braeken, D., Callewaert, G., Robberecht, W., and Van Den Bosch, L. (2005). GluR2 deficiency accelerates motor neuron degeneration in a mouse model of amyotrophic lateral sclerosis. *J. Neuropathol. Exp. Neurol.* *64*, 605–612.
- Deforges, S., Branchu, J., Biondi, O., Grondard, C., Pariset, C., Lécolle, S., Lopes, P., Vidal, P.-P., Chanoine, C., and Charbonnier, F. (2009). Motoneuron survival is promoted by specific exercise in a mouse model of amyotrophic lateral sclerosis. *J. Physiol.* *587*, 3561–3572.

- Deng, H., Hentati, A., Tainer, J., Iqbal, Z., Cayabyab, A., Hung, W., Getzoff, E., Hu, P., Herzfeldt, B., Roos, R., et al. (1993). Amyotrophic lateral sclerosis and structural defects in Cu,Zn superoxide dismutase. *Science* (80- ). *261*, 1047–1051.
- Deschenes, M.R., Covault, J., Kraemer, W.J., and Maresh, C.M. (1994). The neuromuscular junction. Muscle fibre type differences, plasticity and adaptability to increased and decreased activity. *Sports Med.* *17*, 358–372.
- Desport, J.C., Preux, P.M., Truong, T.C., Vallat, J.M., Sautereau, D., and Couratier, P. (1999). Nutritional status is a prognostic factor for survival in ALS patients. *Neurology* *53*, 1059–1059.
- Desport, J.C., Preux, P.M., Magy, L., Boirie, Y., Vallat, J.M., Beaufrère, B., and Couratier, P. (2001). Factors correlated with hypermetabolism in patients with amyotrophic lateral sclerosis. *Am. J. Clin. Nutr.* *74*, 328–334.
- Dietz, K.C., and Casaccia, P. (2010). HDAC inhibitors and neurodegeneration: at the edge between protection and damage. *Pharmacol. Res.* *62*, 11–17.
- Dobrowolny, G., Aucello, M., Rizzuto, E., Beccafico, S., Mammucari, C., Boncompagni, S., Boncompagni, S., Belia, S., Wannenes, F., Nicoletti, C., et al. (2008). Skeletal muscle is a primary target of SOD1G93A-mediated toxicity. *Cell Metab.* *8*, 425–436.
- Dum, R.P., and Kennedy, T.T. (1980). Physiological and histochemical characteristics of motor units in cat tibialis anterior and extensor digitorum longus muscles. *J. Neurophysiol.* *43*, 1615–1630.
- Dupuis, Pradat, P., Meininger, V., and Loeffler, J. (2003). sclerosis.
- Dupuis, L., Oudart, H., René, F., Gonzalez de Aguilar, J.-L., and Loeffler, J.-P. (2004). Evidence for defective energy homeostasis in amyotrophic lateral sclerosis: benefit of a high-energy diet in a transgenic mouse model. *Proc. Natl. Acad. Sci. U. S. A.* *101*, 11159–11164.
- Dupuis, L., Gonzalez de Aguilar, J.-L., Echaniz-Laguna, A., Eschbach, J., Rene, F., Oudart, H., Halter, B., Huze, C., Schaeffer, L., Bouillaud, F., et al. (2009). Muscle mitochondrial uncoupling dismantles neuromuscular junction and triggers distal degeneration of motor neurons. *PLoS One* *4*, e5390.
- Dupuis, L., Pradat, P.-F., Ludolph, A.C., and Loeffler, J.-P. (2011). Energy metabolism in amyotrophic lateral sclerosis. *Lancet Neurol.* *10*, 75–82.
- Echaniz-Laguna, A., Zoll, J., Ribera, F., Tranchant, C., Warter, J.-M., Lonsdorfer, J., and Lampert, E. (2002). Mitochondrial respiratory chain function in skeletal muscle of ALS patients. *Ann. Neurol.* *52*, 623–627.
- Echaniz-Laguna, A., Zoll, J., and Ponsot, E. (2006). Muscular mitochondrial function in amyotrophic lateral sclerosis is progressively altered as the disease develops: a temporal study in man. *Exp. ...* *198*, 25–30.
- Edström, L., and Kugelberg, E. (1968). Histochemical composition, distribution of fibres and fatiguability of single motor units. Anterior tibial muscle of the rat. *J. Neurol. Neurosurg. Psychiatry* *31*, 424–433.
- Egan, B., and Zierath, J.R. (2013). Exercise metabolism and the molecular regulation of skeletal muscle adaptation. *Cell Metab.* *17*, 162–184.
- Egan, B., Carson, B.P., Garcia-Roves, P.M., Chibalin, A. V, Sarsfield, F.M., Barron, N., McCaffrey, N., Moyna, N.M., Zierath, J.R., and O’Gorman, D.J. (2010). Exercise intensity-dependent regulation of peroxisome proliferator-activated receptor coactivator-1 mRNA abundance is associated with differential activation of upstream signalling kinases in human skeletal muscle. *J. Physiol.* *588*, 1779–1790.

- Estévez, A.G., Crow, J.P., Sampson, J.B., Reiter, C., Zhuang, Y., Richardson, G.J., Tarpey, M.M., Barbeito, L., and Beckman, J.S. (1999). Induction of nitric oxide-dependent apoptosis in motor neurons by zinc-deficient superoxide dismutase. *Science* 286, 2498–2500.
- Facchinetti, F., Sasaki, M., Cutting, F.B., Zhai, P., MacDonald, J.E., Reif, D., Beal, M.F., Huang, P.L., Dawson, T.M., Gurney, M.E., et al. (1999). Lack of involvement of neuronal nitric oxide synthase in the pathogenesis of a transgenic mouse model of familial amyotrophic lateral sclerosis. *Neuroscience* 90, 1483–1492.
- Fidler, J.A., Treleaven, C.M., Frakes, A., Tamsett, T.J., McCrate, M., Cheng, S.H., Shihabuddin, L.S., Kaspar, B.K., and Dodge, J.C. (2011). Disease progression in a mouse model of amyotrophic lateral sclerosis: the influence of chronic stress and corticosterone. *FASEB J.* 25, 4369–4377.
- Fischer, L.R., Culver, D.G., Tennant, P., Davis, A. a., Wang, M., Castellano-Sanchez, A., Khan, J., Polak, M. a., and Glass, J.D. (2004). Amyotrophic lateral sclerosis is a distal axonopathy: evidence in mice and man. *Exp. Neurol.* 185, 232–240.
- Frey, D., Schneider, C., Xu, L., Borg, J., Spooren, W., and Caroni, P. (2000). Early and Selective Loss of Neuromuscular Synapse Subtypes with Low Sprouting Competence in Motoneuron Diseases. *J. Neurosci.* 20, 2534–2542.
- Fujita, K., Yamauchi, M., Shibayama, K., Ando, M., Honda, M., and Nagata, Y. (1996). Decreased cytochrome c oxidase activity but unchanged superoxide dismutase and glutathione peroxidase activities in the spinal cords of patients with amyotrophic lateral sclerosis. *J. Neurosci. Res.* 45, 276–281.
- Gollnick, P.D., and Saltin, B. (1982). Significance of skeletal muscle oxidative enzyme enhancement with endurance training. *Clin. Physiol.* 2, 1–12.
- Gong, Y.H., Parsadanian, A.S., Andreeva, A., Snider, W.D., and Elliott, J.L. (2000). Restricted expression of G86R Cu/Zn superoxide dismutase in astrocytes results in astrocytosis but does not cause motoneuron degeneration. *J. Neurosci.* 20, 660–665.
- Goto, M., Terada, S., Kato, M., Katoh, M., Yokozeki, T., Tabata, I., and Shimokawa, T. (2000). cDNA Cloning and mRNA analysis of PGC-1 in epitrochlearis muscle in swimming-exercised rats. *Biochem. Biophys. Res. Commun.* 274, 350–354.
- Gould, T.W., Buss, R.R., Vinsant, S., Prevet, D., Sun, W., Knudson, C.M., Milligan, C.E., and Oppenheim, R.W. (2006). Complete dissociation of motor neuron death from motor dysfunction by Bax deletion in a mouse model of ALS. *J. Neurosci.* 26, 8774–8786.
- Guarente, L., and Picard, F. (2005). Calorie restriction--the SIR2 connection. *Cell* 120, 473–482.
- Guo, H., Lai, L., Butchbach, M.E.R., Stockinger, M.P., Shan, X., Bishop, G.A., and Lin, C.G. (2003). Increased expression of the glial glutamate transporter EAAT2 modulates excitotoxicity and delays the onset but not the outcome of ALS in mice. *Hum. Mol. Genet.* 12, 2519–2532.
- Gurney, M.E., Cutting, F.B., Zhai, P., Doble, A., Taylor, C.P., Andrus, P.K., and Hall, E.D. (1996). Benefit of vitamin E, riluzole, and gabapentin in a transgenic model of familial amyotrophic lateral sclerosis. *Ann. Neurol.* 39, 147–157.
- Gurney, M.E., Fleck, T.J., Himes, C.S., and Hall, E.D. (1998). Riluzole preserves motor function in a transgenic model of familial amyotrophic lateral sclerosis. *Neurology* 50, 62–66.

- Haeusler, A.R., Donnelly, C.J., Periz, G., Simko, E.A.J., Shaw, P.G., Kim, M.-S., Maragakis, N.J., Troncoso, J.C., Pandey, A., Sattler, R., et al. (2014). C9orf72 nucleotide repeat structures initiate molecular cascades of disease. *Nature* *507*, 195–200.
- Haidet-Phillips, A.M., Hester, M.E., Miranda, C.J., Meyer, K., Braun, L., Frakes, A., Song, S., Likhite, S., Murtha, M.J., Foust, K.D., et al. (2011). Astrocytes from familial and sporadic ALS patients are toxic to motor neurons. *Nat. Biotechnol.* *29*, 824–828.
- Halter, B., Gonzalez de Aguilar, J.-L., Rene, F., Petri, S., Fricker, B., Echaniz-Laguna, A., Dupuis, L., Larmet, Y., and Loeffler, J.-P. (2010). Oxidative stress in skeletal muscle stimulates early expression of Rad in a mouse model of amyotrophic lateral sclerosis. *Free Radic. Biol. Med.* *48*, 915–923.
- Ben Hamida, M., Hentati, F., and Ben Hamida, C. (1990). Hereditary motor system diseases (chronic juvenile amyotrophic lateral sclerosis). Conditions combining a bilateral pyramidal syndrome with limb and bulbar amyotrophy. *Brain* *113* ( Pt 2, 347–363.
- Hardiman, O., van den Berg, L.H., and Kiernan, M.C. (2011). Clinical diagnosis and management of amyotrophic lateral sclerosis. *Nat. Rev. Neurol.* *7*, 639–649.
- Harris, R.A., Bowker-Kinley, M.M., Huang, B., and Wu, P. (2002). Regulation of the activity of the pyruvate dehydrogenase complex. *Adv. Enzyme Regul.* *42*, 249–259.
- Hassel, B., and Dingledine, R. (2012). Glutamate and Glutamate Receptors. In *Basic Neurochemistry*, pp. 342–366.
- Hegedus, J., Putman, C.T., and Gordon, T. (2007). Time course of preferential motor unit loss in the SOD1 G93A mouse model of amyotrophic lateral sclerosis. *Neurobiol. Dis.* *28*, 154–164.
- Henneman, E., Somjen, G., and Carpenter, D.O. (1965). FUNCTIONAL SIGNIFICANCE OF CELL SIZE IN SPINAL MOTONEURONS. *J Neurophysiol* *28*, 560–580.
- Holloszy, J.O., Kohrt, W.M., and Hansen, P.A. (1998). The regulation of carbohydrate and fat metabolism during and after exercise. *Front. Biosci.* *3*, D1011–27.
- Hood, D.A., Balaban, A., Connor, M.K., Craig, E.E., Nishio, M.L., Rezvani, M., and Takahashi, M. (1994). Mitochondrial biogenesis in striated muscle. *Can. J. Appl. Physiol.* *19*, 12–48.
- Hughes, B.W., Kusner, L.L., and Kaminski, H.J. (2006). Molecular architecture of the neuromuscular junction. *Muscle Nerve* *33*, 445–461.
- Huisman, M.H.B., Seelen, M., de Jong, S.W., Dorresteyn, K.R.I.S., van Doormaal, P.T.C., van der Kooij, A.J., de Visser, M., Schelhaas, H.J., van den Berg, L.H., and Veldink, J.H. (2013). Lifetime physical activity and the risk of amyotrophic lateral sclerosis. *J. Neurol. Neurosurg. Psychiatry* *84*, 976–981.
- HUXLEY, A.F. (1957). Muscle structure and theories of contraction. *Prog. Biophys. Biophys. Chem.* *7*, 255–318.
- Jaarsma, D., Haasdijk, E.D., Grashorn, J.A., Hawkins, R., van Duijn, W., Verspaget, H.W., London, J., and Holstege, J.C. (2000). Human Cu/Zn superoxide dismutase (SOD1) overexpression in mice causes mitochondrial vacuolization, axonal degeneration, and premature motoneuron death and accelerates motoneuron disease in mice expressing a familial amyotrophic lateral sclerosis mutant SO. *Neurobiol. Dis.* *7*, 623–643.
- Jaarsma, D., Teuling, E., Haasdijk, E.D., De Zeeuw, C.I., and Hoogenraad, C.C. (2008). Neuron-specific expression of mutant superoxide dismutase is sufficient to induce amyotrophic lateral sclerosis in transgenic mice. *J. Neurosci.* *28*, 2075–2088.

- Jacobs, B.L., Martín-Cora, F.J., and Fornal, C.A. (2002). Activity of medullary serotonergic neurons in freely moving animals. *Brain Res. Brain Res. Rev.* *40*, 45–52.
- Jäger, S., Handschin, C., St-Pierre, J., and Spiegelman, B.M. (2007). AMP-activated protein kinase (AMPK) action in skeletal muscle via direct phosphorylation of PGC-1 $\alpha$ . *Proc. Natl. Acad. Sci. U. S. A.* *104*, 12017–12022.
- Jeppesen, J., Albers, P.H., Rose, A.J., Birk, J.B., Schjerling, P., Dzamko, N., Steinberg, G.R., and Kiens, B. (2011). Contraction-induced skeletal muscle FAT/CD36 trafficking and FA uptake is AMPK independent. *J. Lipid Res.* *52*, 699–711.
- Jia, Z., Agopyan, N., Miu, P., Xiong, Z., Henderson, J., Gerlai, R., Taverna, F.A., Velumian, A., MacDonald, J., Carlen, P., et al. (1996). Enhanced LTP in mice deficient in the AMPA receptor GluR2. *Neuron* *17*, 945–956.
- Johnson, M.L., Robinson, M.M., and Nair, K.S. (2013). Skeletal muscle aging and the mitochondrion. *Trends Endocrinol. Metab.* *24*, 247–256.
- Jokic, N., Gonzalez de Aguilar, J.-L., Dimou, L., Lin, S., Fergani, A., Ruegg, M.A., Schwab, M.E., Dupuis, L., and Loeffler, J.-P. (2006). The neurite outgrowth inhibitor Nogo-A promotes denervation in an amyotrophic lateral sclerosis model. *EMBO Rep.* *7*, 1162–1167.
- Jørgensen, S.B., Richter, E.A., and Wojtaszewski, J.F.P. (2006). Role of AMPK in skeletal muscle metabolic regulation and adaptation in relation to exercise. *J. Physiol.* *574*, 17–31.
- Jouaville, L.S., Pinton, P., Bastianutto, C., Rutter, G.A., and Rizzuto, R. (1999). Regulation of mitochondrial ATP synthesis by calcium: evidence for a long-term metabolic priming. *Proc. Natl. Acad. Sci. U. S. A.* *96*, 13807–13812.
- Kabashi, E., Valdmanis, P.N., Dion, P., and Rouleau, G.A. (2007). Oxidized/misfolded superoxide dismutase-1: the cause of all amyotrophic lateral sclerosis? *Ann. Neurol.* *62*, 553–559.
- Kasarskis, E., Berryman, S., Vanderleest, J., Schneider, A., and McClain, C. (1996). Nutritional status of patients with amyotrophic lateral sclerosis: relation to the proximity of death. *Am J Clin Nutr* *63*, 130–137.
- Kaspar, B.K., Frost, L.M., Christian, L., Umapathi, P., and Gage, F.H. (2005). Synergy of insulin-like growth factor-1 and exercise in amyotrophic lateral sclerosis. *Ann. Neurol.* *57*, 649–655.
- Kawahara, Y., Kwak, S., Sun, H., Ito, K., Hashida, H., Aizawa, H., Jeong, S.-Y., and Kanazawa, I. (2003). Human spinal motoneurons express low relative abundance of GluR2 mRNA: an implication for excitotoxicity in ALS. *J. Neurochem.* *85*, 680–689.
- Kawamata, H., and Manfredi, G. (2010). Mitochondrial dysfunction and intracellular calcium dysregulation in ALS. *Mech. Ageing Dev.* *131*, 517–526.
- Kawamata, T., Akiyama, H., Yamada, T., and McGeer, P.L. (1992). Immunologic reactions in amyotrophic lateral sclerosis brain and spinal cord tissue. *Am. J. Pathol.* *140*, 691–707.
- Kiernan, M.C., Vucic, S., Cheah, B.C., Turner, M.R., Eisen, A., Hardiman, O., Burrell, J.R., and Zoing, M.C. (2011). Amyotrophic lateral sclerosis. *Lancet* *377*, 942–955.
- Kim, D., Nguyen, M.D., Dobbin, M.M., Fischer, A., Sananbenesi, F., Rodgers, J.T., Delalle, I., Baur, J. a, Sui, G., Armour, S.M., et al. (2007). SIRT1 deacetylase protects against neurodegeneration in models for Alzheimer’s disease and amyotrophic lateral sclerosis. *EMBO J.* *26*, 3169–3179.

- Knowler, W.C., Barrett-Connor, E., Fowler, S.E., Hamman, R.F., Lachin, J.M., Walker, E.A., and Nathan, D.M. (2002). Reduction in the incidence of type 2 diabetes with lifestyle intervention or metformin. *N. Engl. J. Med.* *346*, 393–403.
- Kong, J., and Xu, Z. (1998). Massive mitochondrial degeneration in motor neurons triggers the onset of amyotrophic lateral sclerosis in mice expressing a mutant SOD1. *J. Neurosci.* *18*, 3241–3250.
- Kostic, V., Jackson-Lewis, V., de Bilbao, F., Dubois-Dauphin, M., and Przedborski, S. (1997). Bcl-2: prolonging life in a transgenic mouse model of familial amyotrophic lateral sclerosis. *Science* *277*, 559–562.
- Latres, E., Amini, A.R., Amini, A.A., Griffiths, J., Martin, F.J., Wei, Y., Lin, H.C., Yancopoulos, G.D., and Glass, D.J. (2005). Insulin-like growth factor-1 (IGF-1) inversely regulates atrophy-induced genes via the phosphatidylinositol 3-kinase/Akt/mammalian target of rapamycin (PI3K/Akt/mTOR) pathway. *J. Biol. Chem.* *280*, 2737–2744.
- Li, Q., Zhu, X., Ishikura, S., Zhang, D., Gao, J., Sun, Y., Contreras-Ferrat, A., Foley, K.P., Lavandero, S., Yao, Z., et al. (2014). Ca<sup>2+</sup> signals promote GLUT4 exocytosis and reduce its endocytosis in muscle cells. *Am. J. Physiol. Endocrinol. Metab.*
- Lin, J., Wu, H., Tarr, P.T., Zhang, C.-Y., Wu, Z., Boss, O., Michael, L.F., Puigserver, P., Isotani, E., Olson, E.N., et al. (2002). Transcriptional co-activator PGC-1 alpha drives the formation of slow-twitch muscle fibres. *Nature* *418*, 797–801.
- Lin, J., Handschin, C., and Spiegelman, B.M. (2005). Metabolic control through the PGC-1 family of transcription coactivators. *Cell Metab.* *1*, 361–370.
- Lindauer, E., Dupuis, L., Müller, H.-P., Neumann, H., Ludolph, A.C., and Kassubek, J. (2013). Adipose Tissue Distribution Predicts Survival in Amyotrophic Lateral Sclerosis. *PLoS One* *8*, e67783.
- Ling, S.-C., Polymenidou, M., and Cleveland, D.W. (2013). Converging mechanisms in ALS and FTD: disrupted RNA and protein homeostasis. *Neuron* *79*, 416–438.
- Lino, M.M., Schneider, C., and Caroni, P. (2002). Accumulation of SOD1 mutants in postnatal motoneurons does not cause motoneuron pathology or motoneuron disease. *J. Neurosci.* *22*, 4825–4832.
- Liu, W., Yamashita, T., Tian, F., Morimoto, N., Ikeda, Y., Deguchi, K., and Abe, K. (2013). Mitochondrial fusion and fission proteins expression dynamically change in a murine model of amyotrophic lateral sclerosis. *Curr. Neurovasc. Res.* *10*, 222–230.
- Logroscino, G., Traynor, B.J., Hardiman, O., Chiò, A., Mitchell, D., Swingler, R.J., Millul, A., Benn, E., and Beghi, E. (2010). Incidence of amyotrophic lateral sclerosis in Europe. *J. Neurol. Neurosurg. Psychiatry* *81*, 385–390.
- Longstreth, W.T., McGuire, V., Koepsell, T.D., Wang, Y., and van Belle, G. (1998). Risk of amyotrophic lateral sclerosis and history of physical activity: a population-based case-control study. *Arch. Neurol.* *55*, 201–206.
- Luo, G., Yi, J., Ma, C., Xiao, Y., Yi, F., Yu, T., and Zhou, J. (2013). Defective mitochondrial dynamics is an early event in skeletal muscle of an amyotrophic lateral sclerosis mouse model. *PLoS One* *8*, e82112.
- Mahoney, D.J., Rodriguez, C., Devries, M., Yasuda, N., and Tarnopolsky, M.A. (2004). Effects of high-intensity endurance exercise training in the G93A mouse model of amyotrophic lateral sclerosis. *Muscle Nerve* *29*, 656–662.

- Marchetto, M.C.N., Muotri, A.R., Mu, Y., Smith, A.M., Cezar, G.G., and Gage, F.H. (2008). Non-cell-autonomous effect of human SOD1 G37R astrocytes on motor neurons derived from human embryonic stem cells. *Cell Stem Cell* 3, 649–657.
- Mavalli, M.D., DiGirolamo, D.J., Fan, Y., Riddle, R.C., Campbell, K.S., van Groen, T., Frank, S.J., Sperling, M.A., Esser, K.A., Bamman, M.M., et al. (2010). Distinct growth hormone receptor signaling modes regulate skeletal muscle development and insulin sensitivity in mice. *J. Clin. Invest.* 120, 4007–4020.
- Mazzini, L., Corrà, T., Zaccala, M., Mora, G., Del Piano, M., and Galante, M. (1995). Percutaneous endoscopic gastrostomy and enteral nutrition in amyotrophic lateral sclerosis. *J. Neurol.* 242, 695–698.
- McClelland, S., Bethoux, F.A., Boulis, N.M., Sutliff, M.H., Stough, D.K., Schwetz, K.M., Gogol, D.M., Harrison, M., and Piro, E.P. (2008). Intrathecal baclofen for spasticity-related pain in amyotrophic lateral sclerosis: efficacy and factors associated with pain relief. *Muscle Nerve* 37, 396–398.
- McGee, S.L., and Hargreaves, M. (2011). Histone modifications and exercise adaptations. *J. Appl. Physiol.* 110, 258–263.
- McGee, S.L., van Denderen, B.J.W., Howlett, K.F., Mollica, J., Schertzer, J.D., Kemp, B.E., and Hargreaves, M. (2008). AMP-activated protein kinase regulates GLUT4 transcription by phosphorylating histone deacetylase 5. *Diabetes* 57, 860–867.
- Mendell, L.M. (2005). The size principle: a rule describing the recruitment of motoneurons. *J. Neurophysiol.* 93, 3024–3026.
- Menzies, F.M. (2002). Mitochondrial dysfunction in a cell culture model of familial amyotrophic lateral sclerosis. *Brain* 125, 1522–1533.
- Merrill, G.F., Kurth, E.J., Hardie, D.G., and Winder, W.W. (1997). AICA riboside increases AMP-activated protein kinase, fatty acid oxidation, and glucose uptake in rat muscle. *Am. J. Physiol.* 273, E1107–12.
- Miller, R.G., Mitchell, J.D., and Moore, D.H. (2012). Riluzole for amyotrophic lateral sclerosis (ALS)/motor neuron disease (MND). *Cochrane Database Syst. Rev.* 3, CD001447.
- Milton, R.L., Lupa, M.T., and Caldwell, J.H. (1992). Fast and slow twitch skeletal muscle fibres differ in their distribution of Na channels near the endplate. *Neurosci. Lett.* 135, 41–44.
- Mitchell, J.C., McGoldrick, P., Vance, C., Hortobagyi, T., Sreedharan, J., Rogelj, B., Tudor, E.L., Smith, B.N., Klasen, C., Miller, C.C.J., et al. (2013). Overexpression of human wild-type FUS causes progressive motor neuron degeneration in an age- and dose-dependent fashion. *Acta Neuropathol.* 125, 273–288.
- Morrison, B.M., Janssen, W.G., Gordon, J.W., and Morrison, J.H. (1998). Time course of neuropathology in the spinal cord of G86R superoxide dismutase transgenic mice. *J. Comp. Neurol.* 391, 64–77.
- Mosole, S., Carraro, U., Kern, H., Loeffler, S., Fruhmann, H., Vogelauer, M., Burggraf, S., Mayr, W., Krenn, M., Paternostro-Sluga, T., et al. (2014). Long-term high-level exercise promotes muscle reinnervation with age. *J. Neuropathol. Exp. Neurol.* 73, 284–294.
- Mu, J., Brozinick, J.T., Valladares, O., Bucan, M., and Birnbaum, M.J. (2001). A Role for AMP-Activated Protein Kinase in Contraction- and Hypoxia-Regulated Glucose Transport in Skeletal Muscle. *Mol. Cell* 7, 1085–1094.

- Murakami, T., Shimomura, Y., Fujitsuka, N., Nakai, N., Sugiyama, S., Ozawa, T., Sokabe, M., Horai, S., Tokuyama, K., and Suzuki, M. (1994). Enzymatic and genetic adaptation of soleus muscle mitochondria to physical training in rats. *Am. J. Physiol.* *267*, E388–95.
- Murray, K.C., Stephens, M.J., Ballou, E.W., Heckman, C.J., and Bennett, D.J. (2011). Motoneuron excitability and muscle spasms are regulated by 5-HT<sub>2B</sub> and 5-HT<sub>2C</sub> receptor activity. *J. Neurophysiol.* *105*, 731–748.
- Musarò, A., McCullagh, K., Paul, A., Houghton, L., Dobrowolny, G., Molinaro, M., Barton, E.R., Sweeney, H.L., and Rosenthal, N. (2001). Localized Igf-1 transgene expression sustains hypertrophy and regeneration in senescent skeletal muscle. *Nat. Genet.* *27*, 195–200.
- Nabben, M., and Hoeks, J. (2008). Mitochondrial uncoupling protein 3 and its role in cardiac- and skeletal muscle metabolism. *Physiol. Behav.* *94*, 259–269.
- Nagai, M., Re, D.B., Nagata, T., Chalazonitis, A., Jessell, T.M., Wichterle, H., and Przedborski, S. (2007). Astrocytes expressing ALS-linked mutated SOD1 release factors selectively toxic to motor neurons. *Nat. Neurosci.* *10*, 615–622.
- Nelson, L.M., Matkin, C., Longstreth, W.T., and McGuire, V. (2000). Population-based case-control study of amyotrophic lateral sclerosis in western Washington State. II. Diet. *Am. J. Epidemiol.* *151*, 164–173.
- Neumann, M., Sampathu, D.M., Kwong, L.K., Truax, A.C., Micsenyi, M.C., Chou, T.T., Bruce, J., Schuck, T., Grossman, M., Clark, C.M., et al. (2006). Ubiquitinated TDP-43 in frontotemporal lobar degeneration and amyotrophic lateral sclerosis. *Science* *314*, 130–133.
- Nguyen, K.T., García-Chacón, L.E., Barrett, J.N., Barrett, E.F., and David, G. (2009). The Psi(m) depolarization that accompanies mitochondrial Ca<sup>2+</sup> uptake is greater in mutant SOD1 than in wild-type mouse motor terminals. *Proc. Natl. Acad. Sci. U. S. A.* *106*, 2007–2011.
- Nichols, D.E., and Nichols, C.D. (2008). Serotonin receptors. *Chem. Rev.* *108*, 1614–1641.
- Okamoto, K., Kihira, T., Kondo, T., Kobashi, G., Washio, M., Sasaki, S., Yokoyama, T., Miyake, Y., Sakamoto, N., Inaba, Y., et al. (2007). Nutritional status and risk of amyotrophic lateral sclerosis in Japan. *Amyotroph. Lateral Scler.* *8*, 300–304.
- Onesto, E., Rusmini, P., Crippa, V., Ferri, N., Zito, A., Galbiati, M., and Poletti, A. (2011). Muscle cells and motoneurons differentially remove mutant SOD1 causing familial amyotrophic lateral sclerosis. *J. Neurochem.* *118*, 266–280.
- Orrell, R.W., Lane, R.J.M., and Ross, M. (2007). Antioxidant treatment for amyotrophic lateral sclerosis / motor neuron disease. *Cochrane Database Syst. Rev.* CD002829.
- Panov, A., Kubalik, N., Zinchenko, N., Hemendinger, R., Dikalov, S., and Bonkovsky, H.L. (2011). Respiration and ROS production in brain and spinal cord mitochondria of transgenic rats with mutant G93a Cu/Zn-superoxide dismutase gene. *Neurobiol. Dis.* *44*, 53–62.
- Parone, P.A., Da Cruz, S., Han, J.S., McAlonis-Downes, M., Vetto, A.P., Lee, S.K., Tseng, E., and Cleveland, D.W. (2013). Enhancing mitochondrial calcium buffering capacity reduces aggregation of misfolded SOD1 and motor neuron cell death without extending survival in mouse models of inherited amyotrophic lateral sclerosis. *J. Neurosci.* *33*, 4657–4671.
- Pasinelli, P., Belford, M.E., Lennon, N., Bacskai, B.J., Hyman, B.T., Trotti, D., and Brown, R.H. (2004). Amyotrophic lateral sclerosis-associated SOD1 mutant proteins bind and aggregate with Bcl-2 in spinal cord mitochondria. *Neuron* *43*, 19–30.
- Patel, B.P., Safdar, A., Raha, S., Tarnopolsky, M.A., and Hamadeh, M.J. (2010). Caloric restriction shortens lifespan through an increase in lipid peroxidation, inflammation and apoptosis in the G93A mouse, an animal model of ALS. *PLoS One* *5*, e9386.

- Perrier, J.-F., and Delgado-Lezama, R. (2005). Synaptic release of serotonin induced by stimulation of the raphe nucleus promotes plateau potentials in spinal motoneurons of the adult turtle. *J. Neurosci.* *25*, 7993–7999.
- Petri, S., Kiaei, M., Kipiani, K., Chen, J., Calingasan, N.Y., Crow, J.P., and Beal, M.F. (2006). Additive neuroprotective effects of a histone deacetylase inhibitor and a catalytic antioxidant in a transgenic mouse model of amyotrophic lateral sclerosis. *Neurobiol. Dis.* *22*, 40–49.
- Potthoff, M.J., Wu, H., Arnold, M.A., Shelton, J.M., Backs, J., McAnally, J., Richardson, J.A., Bassel-Duby, R., and Olson, E.N. (2007). Histone deacetylase degradation and MEF2 activation promote the formation of slow-twitch myofibers. *J. Clin. Invest.* *117*, 2459–2467.
- Pradat, P.-F., Bruneteau, G., Gordon, P.H., Dupuis, L., Bonnefont-Rousselot, D., Simon, D., Salachas, F., Corcia, P., Frochet, V., Lacorte, J.-M., et al. (2010). Impaired glucose tolerance in patients with amyotrophic lateral sclerosis. *Amyotroph. Lateral Scler.* *11*, 166–171.
- Pramatarova, a, Laganière, J., Roussel, J., Brisebois, K., and Rouleau, G. a (2001). Neuron-specific expression of mutant superoxide dismutase 1 in transgenic mice does not lead to motor impairment. *J. Neurosci.* *21*, 3369–3374.
- Puigserver, P., Wu, Z., Park, C.W., Graves, R., Wright, M., and Spiegelman, B.M. (1998). A Cold-Inducible Coactivator of Nuclear Receptors Linked to Adaptive Thermogenesis. *Cell* *92*, 829–839.
- Pun, S., Santos, A.F., Saxena, S., Xu, L., and Caroni, P. (2006). Selective vulnerability and pruning of phasic motoneuron axons in motoneuron disease alleviated by CNTF. *Nat. Neurosci.* *9*, 408–419.
- Rabizadeh, S., Gralla, E.B., Borchelt, D.R., Gwinn, R., Valentine, J.S., Sisodia, S., Wong, P., Lee, M., Hahn, H., and Bredesen, D.E. (1995). Mutations associated with amyotrophic lateral sclerosis convert superoxide dismutase from an antiapoptotic gene to a proapoptotic gene: studies in yeast and neural cells. *Proc. Natl. Acad. Sci. U. S. A.* *92*, 3024–3028.
- Raney, M.A., and Turcotte, L.P. (2008). Evidence for the involvement of CaMKII and AMPK in Ca<sup>2+</sup>-dependent signaling pathways regulating FA uptake and oxidation in contracting rodent muscle. *J. Appl. Physiol.* *104*, 1366–1373.
- Raney, M.A., Yee, A.J., Todd, M.K., and Turcotte, L.P. (2005). AMPK activation is not critical in the regulation of muscle FA uptake and oxidation during low-intensity muscle contraction. *Am. J. Physiol. Endocrinol. Metab.* *288*, E592–8.
- Rayment, I., Rypniewski, W.R., Schmidt-Bäse, K., Smith, R., Tomchick, D.R., Benning, M.M., Winkelmann, D.A., Wesenberg, G., and Holden, H.M. (1993). Three-dimensional structure of myosin subfragment-1: a molecular motor. *Science* *261*, 50–58.
- Reaume, A.G., Elliott, J.L., Hoffman, E.K., Kowall, N.W., Ferrante, R.J., Siwek, D.F., Wilcox, H.M., Flood, D.G., Beal, M.F., Brown, R.H., et al. (1996). Motor neurons in Cu/Zn superoxide dismutase-deficient mice develop normally but exhibit enhanced cell death after axonal injury. *Nat. Genet.* *13*, 43–47.
- Renton, A.E., Chiò, A., and Traynor, B.J. (2014). State of play in amyotrophic lateral sclerosis genetics. *Nat. Neurosci.* *17*, 17–23.
- Reyes, E.T., Perurena, O.H., Festoff, B.W., Jorgensen, R., and Moore, W. V (1984). Insulin resistance in amyotrophic lateral sclerosis. *J. Neurol. Sci.* *63*, 317–324.
- Romijn, J.A., Coyle, E.F., Sidossis, L.S., Gastaldelli, A., Horowitz, J.F., Endert, E., and Wolfe, R.R. (1993). Regulation of endogenous fat and carbohydrate metabolism in relation to exercise intensity and duration. *Am. J. Physiol.* *265*, E380–91.

- Rosen, D.R., Siddique, T., Patterson, D., Figlewicz, D.A., Sapp, P., Hentati, A., Donaldson, D., Goto, J., O'Regan, J.P., and Deng, H.X. (1993). Mutations in Cu/Zn superoxide dismutase gene are associated with familial amyotrophic lateral sclerosis. *Nature* *362*, 59–62.
- Rothstein, J.D., Van Kammen, M., Levey, A.I., Martin, L.J., and Kuncl, R.W. (1995). Selective loss of glial glutamate transporter GLT-1 in amyotrophic lateral sclerosis. *Ann. Neurol.* *38*, 73–84.
- Rothstein, J.D., Dykes-Hoberg, M., Pardo, C.A., Bristol, L.A., Jin, L., Kuncl, R.W., Kanai, Y., Hediger, M.A., Wang, Y., Schielke, J.P., et al. (1996). Knockout of glutamate transporters reveals a major role for astroglial transport in excitotoxicity and clearance of glutamate. *Neuron* *16*, 675–686.
- Rotunno, M.S., and Bosco, D.A. (2013). An emerging role for misfolded wild-type SOD1 in sporadic ALS pathogenesis. *Front. Cell. Neurosci.* *7*, 253.
- Rouaux, C., Panteleeva, I., René, F., Gonzalez de Aguilar, J.-L., Echaniz-Laguna, A., Dupuis, L., Menger, Y., Boutillier, A.-L., and Loeffler, J.-P. (2007). Sodium valproate exerts neuroprotective effects in vivo through CREB-binding protein-dependent mechanisms but does not improve survival in an amyotrophic lateral sclerosis mouse model. *J. Neurosci.* *27*, 5535–5545.
- Ryu, H., Smith, K., Camelo, S.I., Carreras, I., Lee, J., Iglesias, A.H., Dangond, F., Cormier, K.A., Cudkowicz, M.E., Brown, R.H., et al. (2005). Sodium phenylbutyrate prolongs survival and regulates expression of anti-apoptotic genes in transgenic amyotrophic lateral sclerosis mice. *J. Neurochem.* *93*, 1087–1098.
- Sabatelli, M., Conte, A., and Zollino, M. (2013). Clinical and genetic heterogeneity of amyotrophic lateral sclerosis. *Clin. Genet.*
- Sacheck, J.M., Ohtsuka, A., McLary, S.C., and Goldberg, A.L. (2004). IGF-I stimulates muscle growth by suppressing protein breakdown and expression of atrophy-related ubiquitin ligases, atrogin-1 and MuRF1. *Am. J. Physiol. Endocrinol. Metab.* *287*, E591–601.
- Sahlin, K., Tonkonogi, M., and Söderlund, K. (1998). Energy supply and muscle fatigue in humans. *Acta Physiol. Scand.* *162*, 261–266.
- Sandri, M., Sandri, C., Gilbert, A., Skurk, C., Calabria, E., Picard, A., Walsh, K., Schiaffino, S., Lecker, S.H., and Goldberg, A.L. (2004). Foxo Transcription Factors Induce the Atrophy-Related Ubiquitin Ligase Atrogin-1 and Cause Skeletal Muscle Atrophy. *Cell* *117*, 399–412.
- Sareen, D., O'Rourke, J.G., Meera, P., Muhammad, A.K.M.G., Grant, S., Simpkinson, M., Bell, S., Carmona, S., Ornelas, L., Sahabian, A., et al. (2013). Targeting RNA foci in iPSC-derived motor neurons from ALS patients with a C9ORF72 repeat expansion. *Sci. Transl. Med.* *5*, 208ra149.
- Scarmeas, N., Shih, T., Stern, Y., Ottman, R., and Rowland, L.P. (2002). Premorbid weight, body mass, and varsity athletics in ALS. *Neurology* *59*, 773–775.
- Schiaffino, S., and Reggiani, C. (2011). Fiber types in mammalian skeletal muscles. *Physiol. Rev.* *91*, 1447–1531.
- Schiaffino, S., Hanzlíková, V., and Pierobon, S. (1970). Relations between structure and function in rat skeletal muscle fibers. *J. Cell Biol.* *47*, 107–119.
- Schiaffino, S., Dyar, K.A., Ciciliot, S., Blaauw, B., and Sandri, M. (2013). Mechanisms regulating skeletal muscle growth and atrophy. *FEBS J.* *280*, 4294–4314.
- Shelkovnikova, T.A., Peters, O.M., Deykin, A. V, Connor-Robson, N., Robinson, H., Ustyugov, A.A., Bachurin, S.O., Ermolkevich, T.G., Goldman, I.L., Sadchikova, E.R., et al. (2013). Fused

in sarcoma (FUS) protein lacking nuclear localization signal (NLS) and major RNA binding motifs triggers proteinopathy and severe motor phenotype in transgenic mice. *J. Biol. Chem.* *288*, 25266–25274.

Shibata, N., Asayama, K., Hirano, A., and Kobayashi, M. (1996). Immunohistochemical study on superoxide dismutases in spinal cords from autopsied patients with amyotrophic lateral sclerosis. *Dev. Neurosci.* *18*, 492–498.

Shibata, N., Hirano, A., Kobayashi, M., Dal Canto, M.C., Gurney, M.E., Komori, T., Umahara, T., and Asayama, K. (1998). Presence of Cu/Zn superoxide dismutase (SOD) immunoreactivity in neuronal hyaline inclusions in spinal cords from mice carrying a transgene for Gly93Ala mutant human Cu/Zn SOD. *Acta Neuropathol.* *95*, 136–142.

Shinder, G.A., Lacourse, M.C., Minotti, S., and Durham, H.D. (2001). Mutant Cu/Zn-superoxide dismutase proteins have altered solubility and interact with heat shock/stress proteins in models of amyotrophic lateral sclerosis. *J. Biol. Chem.* *276*, 12791–12796.

Del Signore, S.J., Amante, D.J., Kim, J., Stack, E.C., Goodrich, S., Cormier, K., Smith, K., Cudkowicz, M.E., and Ferrante, R.J. (2009). Combined riluzole and sodium phenylbutyrate therapy in transgenic amyotrophic lateral sclerosis mice. *Amyotroph. Lateral Scler.* *10*, 85–94.

Smith, L.R., Meyer, G., and Lieber, R.L. Systems analysis of biological networks in skeletal muscle function. *Wiley Interdiscip. Rev. Syst. Biol. Med.* *5*, 55–71.

Song, W., Song, Y., Kincaid, B., Bossy, B., and Bossy-Wetzel, E. (2013). Mutant SOD1G93A triggers mitochondrial fragmentation in spinal cord motor neurons: neuroprotection by SIRT3 and PGC-1 $\alpha$ . *Neurobiol. Dis.* *51*, 72–81.

Spina, R.J., Chi, M.M., Hopkins, M.G., Nemeth, P.M., Lowry, O.H., and Holloszy, J.O. (1996). Mitochondrial enzymes increase in muscle in response to 7-10 days of cycle exercise. *J. Appl. Physiol.* *80*, 2250–2254.

Spriet, L.L., Tunstall, R.J., Watt, M.J., Mehan, K.A., Hargreaves, M., and Cameron-Smith, D. (2004). Pyruvate dehydrogenase activation and kinase expression in human skeletal muscle during fasting. *J. Appl. Physiol.* *96*, 2082–2087.

Stallings, N.R., Puttappathi, K., Luther, C.M., Burns, D.K., and Elliott, J.L. (2010). Progressive motor weakness in transgenic mice expressing human TDP-43. *Neurobiol. Dis.* *40*, 404–414.

Sterz, R., Pagala, M., and Peper, K. (1983). Postjunctional characteristics of the endplates in mammalian fast and slow muscles. *Pflugers Arch.* *398*, 48–54.

Stitt, T.N., Drujan, D., Clarke, B.A., Panaro, F., Timofeyeva, Y., Kline, W.O., Gonzalez, M., Yancopoulos, G.D., and Glass, D.J. (2004). The IGF-1/PI3K/Akt Pathway Prevents Expression of Muscle Atrophy-Induced Ubiquitin Ligases by Inhibiting FOXO Transcription Factors. *Mol. Cell* *14*, 395–403.

Sugden, M.C., Kraus, A., Harris, R.A., and Holness, M.J. (2000). Fibre-type specific modification of the activity and regulation of skeletal muscle pyruvate dehydrogenase kinase (PDK) by prolonged starvation and refeeding is associated with targeted regulation of PDK isoenzyme 4 expression. *Biochem. J.* *346 Pt 3*, 651–657.

Swerdlow, R.H., Parks, J.K., Cassarino, D.S., Trimmer, P.A., Miller, S.W., Maguire, D.J., Sheehan, J.P., Maguire, R.S., Pattee, G., Juel, V.C., et al. (1998). Mitochondria in sporadic amyotrophic lateral sclerosis. *Exp. Neurol.* *153*, 135–142.

Tsai, K.-J., Yang, C.-H., Fang, Y.-H., Cho, K.-H., Chien, W.-L., Wang, W.-T., Wu, T.-W., Lin, C.-P., Fu, W.-M., and Shen, C.-K.J. (2010). Elevated expression of TDP-43 in the forebrain of

mice is sufficient to cause neurological and pathological phenotypes mimicking FTLD-U. *J. Exp. Med.* *207*, 1661–1673.

Turner, M.R. (2013). Increased premorbid physical activity and amyotrophic lateral sclerosis: born to run rather than run to death, or a seductive myth? *J. Neurol. Neurosurg. Psychiatry* *84*, 947.

Valenti, M., Pontieri, F.E., Conti, F., Altobelli, E., Manzoni, T., and Frati, L. (2005). Amyotrophic lateral sclerosis and sports: a case-control study. *Eur. J. Neurol.* *12*, 223–225.

Vielhaber, S. (2000). Mitochondrial DNA abnormalities in skeletal muscle of patients with sporadic amyotrophic lateral sclerosis. *Brain* *123*, 1339–1348.

Vinsant, S., Mansfield, C., Jimenez-Moreno, R., Del Gaizo Moore, V., Yoshikawa, M., Hampton, T.G., Prevette, D., Caress, J., Oppenheim, R.W., and Milligan, C. (2013). Characterization of early pathogenesis in the SOD1(G93A) mouse model of ALS: part II, results and discussion. *Brain Behav.* *3*, 431–457.

Waerhaug, O., and Lømo, T. (1994). Factors causing different properties at neuromuscular junctions in fast and slow rat skeletal muscles. *Anat. Embryol. (Berl.)* *190*, 113–125.

Wang, Y., and Pessin, J.E. (2013). Mechanisms for fiber-type specificity of skeletal muscle atrophy. *Curr. Opin. Clin. Nutr. Metab. Care* *16*, 243–250.

Wang, H.-Y., Wang, I.-F., Bose, J., and Shen, C.-K.J. (2004). Structural diversity and functional implications of the eukaryotic TDP gene family. *Genomics* *83*, 130–139.

Watanabe, M., Dykes-Hoberg, M., Culotta, V.C., Price, D.L., Wong, P.C., and Rothstein, J.D. (2001). Histological evidence of protein aggregation in mutant SOD1 transgenic mice and in amyotrophic lateral sclerosis neural tissues. *Neurobiol. Dis.* *8*, 933–941.

Watt, M.J., Heigenhauser, G.J.F., LeBlanc, P.J., Inglis, J.G., Spriet, L.L., and Peters, S.J. (2004). Rapid upregulation of pyruvate dehydrogenase kinase activity in human skeletal muscle during prolonged exercise. *J. Appl. Physiol.* *97*, 1261–1267.

Wenz, T., Rossi, S.G., Rotundo, R.L., Spiegelman, B.M., and Moraes, C.T. (2009). Increased muscle PGC-1alpha expression protects from sarcopenia and metabolic disease during aging. *Proc. Natl. Acad. Sci. U. S. A.* *106*, 20405–20410.

Wiedau-Pazos, M., Goto, J.J., Rabizadeh, S., Gralla, E.B., Roe, J.A., Lee, M.K., Valentine, J.S., and Bredesen, D.E. (1996). Altered reactivity of superoxide dismutase in familial amyotrophic lateral sclerosis. *Science* *271*, 515–518.

Williams, T.L., Day, N.C., Ince, P.G., Kamboj, R.K., and Shaw, P.J. (1997). Calcium-permeable alpha-amino-3-hydroxy-5-methyl-4-isoxazole propionic acid receptors: a molecular determinant of selective vulnerability in amyotrophic lateral sclerosis. *Ann. Neurol.* *42*, 200–207.

Wolfe, R.R. (1998). Fat metabolism in exercise. *Adv. Exp. Med. Biol.* *441*, 147–156.

Wong, M., and Martin, L.J. (2010a). Skeletal muscle-restricted expression of human SOD1 causes motor neuron degeneration in transgenic mice. *Hum. Mol. Genet.* *19*, 2284–2302.

Wong, M., and Martin, L.J. (2010b). Skeletal muscle-restricted expression of human SOD1 causes motor neuron degeneration in transgenic mice. *Hum. Mol. Genet.* *19*, 2284–2302.

Wong, P.C., Pardo, C.A., Borchelt, D.R., Lee, M.K., Copeland, N.G., Jenkins, N.A., Sisodia, S.S., Cleveland, D.W., and Price, D.L. (1995). An adverse property of a familial ALS-linked SOD1 mutation causes motor neuron disease characterized by vacuolar degeneration of mitochondria. *Neuron* *14*, 1105–1116.

- Wu, H., Kanatous, S.B., Thurmond, F.A., Gallardo, T., Isotani, E., Bassel-Duby, R., and Williams, R.S. (2002). Regulation of mitochondrial biogenesis in skeletal muscle by CaMK. *Science* *296*, 349–352.
- Yamanaka, K., Chun, S.J., Boillee, S., Fujimori-Tonou, N., Yamashita, H., Gutmann, D.H., Takahashi, R., Misawa, H., and Cleveland, D.W. (2008). Astrocytes as determinants of disease progression in inherited amyotrophic lateral sclerosis. *Nat. Neurosci.* *11*, 251–253.
- Yamashita, H., Kawamata, J., Okawa, K., Kanki, R., Nakamizo, T., Hatayama, T., Yamanaka, K., Takahashi, R., and Shimohama, S. (2007). Heat-shock protein 105 interacts with and suppresses aggregation of mutant Cu/Zn superoxide dismutase: clues to a possible strategy for treating ALS. *J. Neurochem.* *102*, 1497–1505.
- Yang, C., Wang, H., Qiao, T., Yang, B., Aliaga, L., Qiu, L., Tan, W., Salameh, J., McKenna-Yasek, D.M., Smith, T., et al. (2014). Partial loss of TDP-43 function causes phenotypes of amyotrophic lateral sclerosis. *Proc. Natl. Acad. Sci. U. S. A.* *111*, E1121–9.
- Yoo, Y.-E., and Ko, C.-P. (2011). Treatment with trichostatin A initiated after disease onset delays disease progression and increases survival in a mouse model of amyotrophic lateral sclerosis. *Exp. Neurol.* *231*, 147–159.
- Zhou, J., Yi, J., Fu, R., Liu, E., Siddique, T., Ríos, E., and Deng, H.-X. (2010). Hyperactive intracellular calcium signaling associated with localized mitochondrial defects in skeletal muscle of an animal model of amyotrophic lateral sclerosis. *J. Biol. Chem.* *285*, 705–712.
- Zhu, S., Stavrovskaya, I.G., Drozda, M., Kim, B.Y.S., Ona, V., Li, M., Sarang, S., Liu, A.S., Hartley, D.M., Wu, D.C., et al. (2002). Minocycline inhibits cytochrome c release and delays progression of amyotrophic lateral sclerosis in mice. *Nature* *417*, 74–78.
- Zurlo, F., Larson, K., Bogardus, C., and Ravussin, E. (1990). Skeletal muscle metabolism is a major determinant of resting energy expenditure. *J. Clin. Invest.* *86*, 1423–1427.

## ÉTUDES DES ALTÉRATIONS MÉTABOLIQUES MUSCULAIRES AU COURS DE LA SCLÉROSE LATÉRALE AMYOTROPHIQUE

La sclérose latérale amyotrophique (SLA) est une maladie dégénérative neuromusculaire fatale. Elle est accompagnée par des altérations métaboliques, se manifestant précocement dans des modèles murins. L'objectif de cette thèse a été d'identifier les cibles moléculaires impliquées dans ces changements. Pour ce faire, nous avons étudié le muscle glycolytique, le premier touché par la dénervation au cours de la maladie dans un modèle de SLA, la souris SOD1<sup>G86R</sup>. Nous avons montré un déséquilibre entre les voies métaboliques glucidiques et lipidiques à un stade présymptomatique, avec une préférence pour la voie catabolique des lipides. Cette altération peut expliquer notre observation sur le changement des capacités à l'exercice des souris SOD1<sup>G86R</sup> présymptomatiques. Dans ce contexte, nous avons montré que l'inhibition pharmacologique de PDK4, un des principaux inhibiteurs de la glycolyse, est bénéfique, retardant l'apparition des symptômes. En prenant compte des spécificités métaboliques des différents éléments de l'axe neuromusculaire, ce travail ouvre des nouvelles pistes thérapeutiques pour le traitement de la SLA.

Mots-clés : ALS, métabolisme, exercice, muscle

Amyotrophic lateral sclerosis (ALS) is a fatal degenerative disease characterized by loss of upper and lower motor neurons, denervation and skeletal muscle atrophy. ALS is accompanied by metabolic alterations that are early events in mouse models for ALS. The main objective was to identify molecular targets responsible for these alterations. For this, we analyzed several metabolic regulators localized in presymptomatic glycolytic muscle tissue of an ALS mouse model, the SOD1<sup>G86R</sup>. We identified a pre-symptomatic alteration of metabolic equilibrium, showing an inhibition of glycolysis accompanied by an upregulation of lipid catabolic pathway. This alteration has functional significance, being reflected in a modified capacity of SOD1<sup>G86R</sup> mice to adapt to different types of exercise. Pharmacological inhibition of PDK4, one of the main inhibitors of glycolysis, delayed disease onset, underpinning the importance of metabolic equilibrium in disease progression. Taking into consideration the metabolic specificity of the different elements on the neuromuscular axis, this work opens towards new therapeutic approaches for ALS.

Key words : ALS, metabolism, exercise, muscle